



Characterising the role of Articular Cartilage Progenitor Cells in Osteoarthritis

Adam Esa (MB BCh)

Thesis submitted for the award of PhD,
June 2015



DECLARATION

This work has not been submitted in substance for any other degree or award at this or any other university or place of learning, nor is being submitted concurrently in candidature for any degree or other award.

Signed (candidate) Date

STATEMENT 1

This thesis is being submitted in partial fulfillment of the requirements for the degree of(insert MCh, MD, MPhil, PhD etc, as appropriate)

Signed (candidate) Date

STATEMENT 2

This thesis is the result of my own independent work/investigation, except where otherwise stated.

Other sources are acknowledged by explicit references. The views expressed are my own.

Signed (candidate) Date

STATEMENT 3

I hereby give consent for my thesis, if accepted, to be available online in the University's Open Access repository and for inter-library loan, and for the title and summary to be made available to outside organisations.

Signed (candidate) Date

STATEMENT 4: PREVIOUSLY APPROVED BAR ON ACCESS

I hereby give consent for my thesis, if accepted, to be available online in the University's Open Access repository and for inter-library loans **after expiry of a bar on access previously approved by the Academic Standards & Quality Committee.**

Signed (candidate) Date

Acknowledgments

Bismillah Al-Rahman Al-Rahim.

First of all, I would like to thank my supervisors Dr Clare Hughes and Prof Charlie Archer. Thanks to both of you for giving me this opportunity to study under your guidance. A special thanks to Clare for all the amazing supervision you provided me over the last 4 years. Also thanks to Professor Bruce Caterson for being an excellent exemplar of dedication to one's profession. I have learnt from you the highest work ethics and hope to follow it for the rest of my professional life.

I would like to thank my colleagues in Caterson, Duance, Mason, Archer and Blain's research groups. I have learnt a lot from you all during my PhD. A special thanks to my friend and mentor Dr Ahmed Ali for sharing with me this journey and often working together over many weekends and encouragements from the first day. Thank you to Drs Lawrence Glennon-Alty and Shane Wainwright for their encouragement.

I would like to thank my collaborators, Dr Ken Ewan for the assistance with the reporter assay work and Dr Gareth Willis for his assistance with the angiogenesis work. I was also lucky to have two talented undergraduate students to supervise namely Amo Sahota and Rob Aldridge, who were a pleasure to teach.

I would like to thank my clinical mentors during the years especially Professor Ashraf Rasheed for the amazing training I had and for allowing me to pursue a PhD study.

Last, I would like to thank my parents, siblings, Ismahan, Amira and my wife Hanna and the children for helping me. Thank you Hanna, this journey would not have happened without you! Sorry for neglecting my duties over the last few years and sorry for what to come!

This PhD study was kindly funded by the Medical Research Council.

Abstract:

Osteoarthritis (OA) is a chronic and highly prevalent degenerative disease of the synovial joint leading to cartilage destruction and bone remodelling. The current management of end-stage OA is joint replacement, however, this procedure is not suitable for a subset of patients hence there is a growing need for alternative treatments and technologies to address this limitation. One such approach to this problem is the application of cell-based therapies that regenerate areas of damaged cartilage. Recently discovered articular cartilage progenitor cells (CPC) have been hallmarked as a potential cell source for repair and/or regeneration of damaged articular cartilage.

Initial focus was on the characterisation of human CPC isolated from healthy donors and compared with OA derived CPC and patient matched OA Bone Marrow Mesenchymal Stem Cells (BM-MSCs). Comparison of all cell types showed similar morphology and proliferative capacity. In addition, all cell types isolated showed positive expression of the putative mesenchymal stem cell makers; CD-90, CD-105 and CD-166 while lacking expression of CD-34. All cell types investigated showed successful osteogenic, chondrogenic and adipogenic differentiation, hence providing evidence of the mesenchymal stem cell properties of isolated CPC.

A gene profiler array was used to identify the expression of Wnt pathway genes from RNA isolated from CPC cell lines originating from healthy and OA cartilage. Interestingly, the expression of Dkk-1 was observed to have the highest up-regulation in OA-derived CPC. The role of Dkk-1 was further studied in a number of CPC and chondrocyte cell lines from healthy and OA cartilage. It was found that normal CPC cell lines showed homogeneously low expression and secretion of Dkk-1, however, OA-derived CPC cell lines exhibited a heterogeneous expression and secretion of Dkk-1. In a pellet culture model of chondrogenic differentiation, CPC cell lines secreting high levels of Dkk-1 failed to undergo chondrogenic differentiation, measured by diminished expression of chondrogenic differentiation markers, Type II collagen, ACAN and Sox-9 at both molecular and protein levels.

Immunolocalisation of Dkk-1 in OA osteochondral plugs showed peri-cellular expression in chondrocytes located in all zones and around migratory endothelial cells

invading articular cartilage where there was a quantifiable increase of blood vessel invasion. This later observation was further studied through a series of experiments to investigate the role of Dkk-1 in relation to endothelial cell migration and angiogenesis using an in vitro model of angiogenesis and migration/invasion assays. A novel finding emerged from these studies, which provides evidence for a pro-angiogenic and pro-migratory role of Dkk-1 and to a lesser extent Dkk-2 in human endothelial cell lines.

A novel in vitro Transwell co-culture model was developed to study the interaction between chondrocytes and endothelial cells mimicking the osteochondral interface. A novel finding from these studies included the observation that normal or OA-derived chondrocytes appeared to induce an endothelial to mesenchymal transformation (EndMT) of the co-culture endothelial cells. This was assessed by a loss of the endothelial cobble stone morphology and a down-regulation of key factors implicated in endothelial cell phenotype, including VE-cadherin, Tie-2, e-NOS, PDGF-AA and PECAM-1. As endothelial cells lost their phenotype they adopted a spindle morphology and expressed mesenchymal cell markers including: Lumican, Snail, α -SMA, Vimentin and MMPs. Interestingly, this was also associated with an increase in Dkk-1 expression. To confirm a role for Dkk-1 in this process endothelial cells were cultured in the presence of Dkk-1 and were found to undergo EndMT when compared to the control.

In summary, this thesis has uncovered several interesting differences in CPC phenotype. In addition, my results suggest that Dkk-1 has potential as a biomarker of OA pathology. This thesis highlights further the complex role of the Wnt Pathway and in particular Dkk-1 may play a role in the pathogenesis of osteoarthritis.

Contents

| | |
|--|------------|
| Acknowledgments | iii |
| CHAPTER 1: GENERAL INTRODUCTION | 1 |
| 1.1 Synovial joint. | 1 |
| 1.1.1 Adult Articular Joint Anatomy..... | 2 |
| 1.1.2 Articular cartilage: Structure and Morphology..... | 3 |
| 1.1.3 Chondrocytes..... | 3 |
| 1.1.4 Zones of articular cartilage. | 4 |
| 1.1.5 Regions of extracellular matrix within articular cartilage..... | 7 |
| 1.2 Subchondral bone. | 7 |
| 1.2.1. Structure and Composition. | 7 |
| 1.2.2 Bone turnover and metabolism | 9 |
| 1.2.3. Osteoblasts..... | 10 |
| 1.2.4. Osteocytes..... | 11 |
| 1.2.5. Osteoclast..... | 12 |
| 1.3 Extracellular Matrix Molecules of cartilage. | 13 |
| 1.3.1 Collagens..... | 13 |
| 1.3.2 Proteoglycans. | 15 |
| 1.4. Maturation of articular cartilage and the skeletal system. | 18 |
| 1.5 Pathophysiology of OA. | 20 |
| 1.5.1 Mediators of Cartilage Degradation-Cytokines..... | 21 |
| 1.5.2 Aggrecanases (ADAMTS Proteinases)..... | 22 |
| 1.5.3 MMPs. | 23 |
| 1.5.4 Angiogenesis in Osteoarthritis..... | 23 |
| 1.6. The Wnt signalling pathway. | 24 |
| 1.6.1. The non-canonical Wnt signalling pathway..... | 24 |
| 1.6.2. The Canonical Wnt signalling pathway. | 26 |
| 1.6.3. Frizzled receptors (FZD) and co-receptors. | 27 |
| 1.6.4. Cytoskeletal role of the β -catenin family..... | 29 |
| 1.6.5. Modulators of the Wnt signalling pathways: Wnt ligands..... | 29 |
| 1.6.6. Alternate activators (ligands) of the Wnt Canonical pathway. | 30 |
| 1.6.7. Wnt antagonist proteins. | 31 |
| 1.7. The role of Wnt pathways in OA. | 32 |
| 1.8 Surgical treatment modalities for osteoarthritis. | 34 |
| 1.9 Overview of ACI and MSCs repair of cartilage defects. | 35 |

| | |
|---|-----------|
| 1.10. The role of the Wnt pathway in Chondrogenesis..... | 37 |
| 1.11 PhD hypothesis. | 39 |
| CHAPTER 2: GENERAL MATERIALS AND METHODS..... | 41 |
| 2.1 Materials | 41 |
| 2.2 Methods. | 44 |
| 2.2.1 Human Tissue material..... | 44 |
| 2.2.2 Isolation of human cartilage chondrocytes and cartilage progenitor cells (CPC). ... | 44 |
| 2.2.3. Isolation of human Bone marrow mesenchymal stem cells..... | 46 |
| 2.2.4. Passage of cell lines. | 47 |
| 2.2.5. Long-term storage and retrieval of cell lines..... | 48 |
| 2.3 Multipotency of derived CPC cell lines. | 49 |
| 2.3.1 Chondrogenic differentiation..... | 49 |
| 2.3.2 Osteogenic differentiation..... | 50 |
| 2.3.3 Adipogenic Differentiation. | 50 |
| 2.4 Cell Viability assay..... | 51 |
| 2.5 Endothelial cell culture | 52 |
| 2.5.1 Wound healing assay. | 52 |
| 2.5.2 Transwell-Invasion assay..... | 53 |
| 2.5.3 Tube formation assay..... | 54 |
| 2.6 Endothelial cells and chondrocytes co-culture assay. | 54 |
| 2.7 Histological analysis: | 55 |
| 2.7.1 Collection and preparation of tissue. | 55 |
| 2.7.2 Histological grading of cartilage tissue. | 56 |
| 2.7.3 Detection of Tartrate-resistant acid phosphatase (TRAP). | 57 |
| 2.8 Immunohistochemistry..... | 57 |
| 2.8.1 Immunofluorescence labelling. | 58 |
| 2.8.2 Peroxidase labelling..... | 58 |
| 2.9 Bromodeoxyuridine (BrdU) Assay..... | 60 |
| 2.10 Senescence associated β -galactosidase (SA β -Gal) staining..... | 61 |
| 2.11 Flow cytometry. | 61 |
| 2.12 Molecular analysis: | 63 |
| 2.12.1 RNA extraction from cells. | 63 |
| 2.12.2 Analysis of RNA using the Agilent 2100 Bioanalyzer. | 64 |
| 2.12.3 Gene expression analysis utilizing the RT ² Profiler™ PCR Array. | 65 |
| 2.12.4 Reverse Transcription of isolated RNA. | 67 |
| 2.12.5 Quantitative Real-Time PCR (qPCR). | 68 |

| | |
|---|------------|
| 2.13 Protein analysis:..... | 70 |
| 2.13.1 Cell lysis. | 70 |
| 2.13.2 Protein assay (BCA)..... | 70 |
| 2.13.3 Western blotting. | 71 |
| 2.13.4 Proteome Profiler Human XL Oncology Array. | 72 |
| 2.13.5 DKK-1 ELISA. | 73 |
| 2.14 T-Cell Factor (TCF) reporter assay. | 74 |
| 2.15 Statistical analysis. | 75 |
| CHAPTER 3: CHARACTERISATION OF CARTILAGE CHONDROPROGENITOR CELLS. | 76 |
| | |
| 3.1 Introduction..... | 76 |
| 3.2 Experimental Methods. | 79 |
| 3.3. Results. | 80 |
| 3.3.1. Analysis of the initial adhesion to fibronectin of isolated full-depth chondrocytes from OA and normal human articular cartilage. | 80 |
| 3.3.2. Analysis of the Colony Forming Potential of CPC isolated from OA and normal human articular cartilage. | 80 |
| 3.3.3 Comparison of the cell morphology of polyclonal CPC lines (from cartilage of normal and OA donors) and matched-Bone-marrow derived MSCs (from OA donors)..... | 83 |
| 3.3.4. Analysis of proliferating cells in CPC lines originating from cartilage of normal and OA donors and matched BM-MSCs from OA donors..... | 83 |
| 3.3.5. Analysis of senescent cells in CPC lines originating from cartilage of normal and OA donors and matched BM-MSCs from OA donors. | 86 |
| 3.3.6. Analysis of the expression of MSC cell surface markers in polyclonal CPC isolated from normal and OA donor cartilage with matched BM-MSCs from the OA donors. | 89 |
| 3.3.7. Characterisation of multi-lineage differentiation of CPC and BM-MSCs. | 94 |
| 3.4 Discussion. | 100 |
| CHAPTER 4: INVESTIGATING THE WNT SIGNALLING PATHWAY IN CLONAL PROGENITOR CELLS DERIVED FROM NORMAL AND OSTEOARTHRITIC DONORS. | 106 |
| | |
| 4.1 Introduction..... | 106 |
| 4.2 Experimental Methods. | 108 |
| 4.3 Results: | 110 |
| 4.3.1 Wnt signalling expression in human monoclonal CPC lines isolated from normal and osteoarthritic articular cartilage. | 110 |
| 4.3.2. Dkk-1 ELISA of conditioned media harvested from cultures of monoclonal N-CPC and OA-CPC lines..... | 115 |
| 4.4 The effect of CPC conditioned media on the modulation of β -catenin using the TCF-luciferase reporter assay. | 116 |

| | |
|--|------------|
| 4.5 Chondrogenic differentiation of high and low expressing Dkk-1 CPC cell lines isolated and culture expanded from normal and osteoarthritic articular cartilage..... | 127 |
| 4.5.1. Analysis of cell viability using the LDH assay. | 127 |
| 4.5.2. Analysis of Dkk-1 secretion post-differentiation. | 128 |
| 4.5.3 Analysis of mRNA expression of chondrogenic differentiated CPC. | 129 |
| 4.5.3.1. Analysis at time point zero..... | 129 |
| 4.5.3.2. Analysis at 7 days post-differentiation..... | 132 |
| 4.5.3.3. Analysis at 14 days post-differentiation. | 134 |
| 4.5.3.4. Analysis at 21 days post-differentiation. | 136 |
| 4.5.3.5. Comparison of patient matched Dkk-1 ^{high} and Dkk-1 ^{low} CPC during chondrogenic differentiation. | 138 |
| 4.6 Protein analysis of differentiated pellets. | 140 |
| 4.6.1. Histochemical analysis of chondrogenic differentiation of CPC. | 140 |
| 4.6.2. Immunohistochemical analysis of Dkk-1 in normal and osteoarthritic cartilage... | 143 |
| 4.7 Discussion. | 145 |
| CHAPTER 5: OSTEOCHONDRAL INTERFACE CHARACTERISATION OF CELLULAR INFILTRATION AND THE WNT ANTAGONIST DKK-1 | 153 |
| 5.1 Introduction..... | 153 |
| 5.2 Experimental methods. | 156 |
| 5.3 Results: | 157 |
| 5.3.1. Histological staining of osteochondral plugs..... | 157 |
| 5.3.2. Immunohistochemical labelling of Mesenchymal stem cell makers..... | 160 |
| 5.3.3. TRAP staining of osteochondral plugs: Involvement of osteoclast cells in cartilage invasion..... | 164 |
| 5.3.4. Microvessel density measurements. | 165 |
| 5.4 Characterisation of endothelial cells. | 169 |
| 5.4.1. Dkk-1 inhibits the nuclear translocation of β -catenin in cultured endothelial cells. | 171 |
| 5.4.2. Dkk-1 has an inhibitory effect on canonical β -catenin but does not alter its other catenin members. | 174 |
| 5.5 Dkk proteins stimulate endothelial tubule formation. | 174 |
| 5.6 Dkk-1 encourages endothelial cell migration and wound closure. | 177 |
| 5.7 Cell cycle analysis of endothelial cells treated with Wnt proteins. | 181 |
| 5.8 Discussion. | 184 |
| CHAPTER 6: AN <i>IN VITRO</i> MODEL TO STUDY THE INTERACTION OF CHONDROCYTES AND ENDOTHELIAL CELLS. | 190 |
| 6.1 Introduction..... | 190 |
| 6.2 Experimental Methods. | 192 |

| | |
|--|------------|
| 6.3 Results: | 193 |
| 6.3.1. Characterisation of chondrocytes and endothelial cells. | 193 |
| 6.3.2. Primary endothelial and chondrocytes co-culture promotes EnMT. | 195 |
| 6.3.3. Chondrocytes conditioned media resulted in endothelial cell alteration. | 200 |
| 6.3.4. Proteomic profiling of EnMT..... | 201 |
| 6.3.5. Dkk-1 influence MMP-13 expression and other markers of the EnMT-like transition in endothelial cells. | 205 |
| 6.3.6 Endothelial to mesenchymal transitions in human osteochondral tissues. | 208 |
| 6.3.6.1. Expression of Aggrecan. | 208 |
| 6.3.6.2. Expression of Alpha smooth muscle actin. | 210 |
| 6.3.6.3. Expression of vimentin staining..... | 212 |
| 6.3.6.4 Expression of Snail..... | 214 |
| 6.9 Discussion. | 215 |
| CHAPTER 7: GENERAL DISCUSSION | 223 |
| 7.1 General Discussion. | 223 |
| 7.2 Limitation and future work..... | 238 |
| Appendix: 1 | 240 |
| Appendix: 2 | 246 |
| Appendix 3: | 243 |
| Appendix 4: | 249 |
| Appendix 5: | 250 |
| Appendix 6: | 249 |
| Appendix 7: | 250 |
| Appendix 8: | 250 |
| References: | 255 |

List of figures:

Chapter 1:

| | |
|--|----|
| FIGURE 1. 1: A DIAGRAMMATIC REPRESENTATION OF A SYNOVIAL JOINT. | 2 |
| FIGURE 1. 2: ZONES OF HUMAN ARTICULAR CARTILAGE. | 5 |
| FIGURE 1. 3: DIAGRAM SHOWING COLLAGEN II: IX: XI HETEROFIBRIL. | 14 |
| FIGURE 1. 4: A DIAGRAM SHOWING THE STRUCTURE OF AGGREGAN. | 16 |
| FIGURE 1. 5: A DIAGRAM DEPICTING PROTEOGLYCANS PRESENT IN ARTICULAR CARTILAGE. | 18 |
| FIGURE 1. 6: THE NON-CANONICAL WNT SIGNALLING PATHWAY. | 25 |

Chapter 2:

| | |
|---|----|
| FIGURE 2. 1: SCHEMATIC DIAGRAM OF CHONDROPROGENITOR CELLS (CPC) ISOLATION PROCESS. | 46 |
| FIGURE 2. 2: REPRESENTATIVE IMAGE OF BIOANALYZER® GEL ELECTROPHORESIS OF TOTAL RNA. | 65 |
| FIGURE 2. 3: SCHEMATIC DESCRIPTION OF THE REPORTER CONSTRUCT STABLY TRANSFECTED IN EPITHELIAL HEK293-CELL LINE (7DF-3). | 75 |

Chapter 3:

| | |
|--|----|
| FIGURE 3. 1: IMAGE OF TIBIAL PLATEAUX ISOLATED FROM NORMAL (POST-MORTEM) AND OSTEOARTHRITIC (ARTHROPLASTY) DONORS. | 81 |
| FIGURE 3. 2: INITIAL ADHESION TO FIBRONECTIN AND COLONY FORMING EFFICIENCY. | 82 |
| FIGURE 3. 3: PHASE CONTRAST IMAGES OF CARTILAGE PROGENITOR CELLS AND BONE MARROW MSC. | 84 |
| FIGURE 3. 4: PERCENTAGE INCORPORATION OF BrDU (5-BROMO-2-DEOXYURIDINE). | 85 |
| FIGURE 3. 5: PERCENTAGE OF SENESCENT CELLS FROM NORMAL CPC AND OA-CPC AND BM-MSCs. | 88 |
| FIGURE 3. 6: BrDU LABELLING AND SENESCENCE ASSOCIATED B-GALACTOSIDASE ASSAY OF CPC AND BM-MSCs. | 89 |
| FIGURE 3. 7: PERCENTAGE BrDU UPTAKE BETWEEN MATCHED CPC AND MSCs. | 90 |
| FIGURE 3. 8: PERCENTAGE B-GALACTOSIDASE INCORPORATION IN MATCHED CPC AND MSCs. | 91 |
| FIGURE 3. 9: FLOW CYTOMETRY ANALYSIS OF MESENCHYMAL STEM CELLS MARKERS. | 93 |
| FIGURE 3. 10: CHONDROGENIC DIFFERENTIATION OF ISOLATED CPC AND MSCs. | 95 |
| FIGURE 3. 11: OSTEOGENIC DIFFERENTIATION OF ISOLATED CPC AND MSCs. | 97 |
| FIGURE 3. 12: ADIPOGENIC DIFFERENTIATION OF ISOLATED CPC AND MSCs. | 99 |

Chapter 4:

| | |
|--|-----|
| FIGURE 4. 1: SCATTER PLOT OF PCR ARRAY ANALYSE OF 84 GENES INVOLVED IN THE WNT SIGNALLING PATHWAY. . | 112 |
| FIGURE 4. 2: REAL-TIME QUANTITATIVE PCR OF DKK-1 mRNA EXPRESSION IN FULL-DEPTH CHONDROCYTES AND CPC. | 115 |
| FIGURE 4. 3: CONCENTRATION OF DKK-1 IN MEDIA FROM N-CPC AND OA-CPC LINES. | 116 |
| FIGURE 4. 4: EFFECTS OF CPC CONDITIONED MEDIA ON WNT TCF-LUCIFERASE REPORTER ASSAY. | 118 |
| FIGURE 4. 5: EFFECTS OF CPC CONDITIONED MEDIA ON WNT TCF-LUCIFERASE REPORTER ASSAY. | 120 |
| FIGURE 4. 6: EFFECTS OF CPC CONDITIONED MEDIA ON CELL VIABILITY. | 121 |
| FIGURE 4. 7: A SCATTER-PLOT FIGURE OF DKK-1 CONCENTRATION AND mRNA FOLD-CHANGE. | 123 |
| FIGURE 4. 8: A SCATTER-PLOT FIGURE OF TCF-LUCIFERASE ACTIVATION AND DKK-1 SECRETION. | 124 |

| | |
|---|-----|
| FIGURE 4. 9: A SCATTER-PLOT FIGURE OF TCF-LUCIFERASE ACTIVATION AND DKK-1 mRNA FOLD-CHANGE..... | 125 |
| FIGURE 4. 10: ASSESSMENT OF SECRETED LACTATE DEHYDROGENASE IN THE CONDITIONED MEDIA OF CPC..... | 127 |
| FIGURE 4. 11: EFFECT OF ENDOGENOUS DKK-1 LEVELS ON CHONDROGENIC DIFFERENTIATION OF CPC FROM HEALTHY AND OSTEOARTHRITIC DONORS (DAY 0)..... | 131 |
| FIGURE 4. 12: EFFECT OF ENDOGENOUS DKK-1 LEVELS ON CHONDROGENIC DIFFERENTIATION OF CPC FROM HEALTHY AND OSTEOARTHRITIC DONORS (DAY 7)..... | 133 |
| FIGURE 4. 13: EFFECT OF ENDOGENOUS DKK-1 LEVELS ON CHONDROGENIC DIFFERENTIATION OF CPC FROM HEALTHY AND OSTEOARTHRITIC DONORS (DAY 14)..... | 135 |
| FIGURE 4. 14: EFFECT OF ENDOGENOUS DKK-1 LEVELS ON CHONDROGENIC DIFFERENTIATION OF CPC FROM HEALTHY AND OSTEOARTHRITIC DONORS (DAY 21)..... | 137 |
| FIGURE 4. 15: EFFECT OF DIFFERENTIAL EXPRESSION LEVELS OF DKK-1 ON CHONDROGENIC DIFFERENTIATION OF CPC FROM THE MATCHED PATIENTS (DAY 21)..... | 139 |
| FIGURE 4. 16: HISTOCHEMICAL AND PHASE-CONTRAST IMAGES 3D CELL PELLETS FROM DKK-1LOW CPC AND DKK-1HIGH CPC CELL LINES SUBJECTED TO CHONDROGENIC DIFFERENTIATION. | 141 |
| FIGURE 4. 17: IMMUNOHISTOCHEMICAL ANALYSIS OF 3D CELL PELLETS FROM DKK-1LOW CPC AND DKK-1HIGH CPC CELL LINES SUBJECTED TO CHONDROGENIC DIFFERENTIATION. | 142 |
| FIGURE 4. 18: TOPOGRAPHICAL EXPRESSION OF DKK-1 IN NORMAL AND OSTEOARTHRITIC OSTEOCHONDRAL TISSUE. | 144 |

Chapter 5:

| | |
|---|-----|
| FIGURE 5. 1: HISTOCHEMICAL STAINING OF NORMAL AND OSTEOARTHRITIC OSTEOCHONDRAL TISSUES..... | 159 |
| FIGURE 5. 2: CONFOCAL IMAGES OF IMMUNOHISTOCHEMICAL ANALYSIS OF THE CD-105 PROTEIN IN OSTEOCHONDRAL TISSUES. | 162 |
| FIGURE 5. 3: CONFOCAL IMAGES OF IMMUNOHISTOCHEMICAL ANALYSIS OF THE CD-166 PROTEIN IN OSTEOCHONDRAL TISSUES. | 163 |
| FIGURE 5. 4: TRAP STAINING ASSAY OF OSTEOCHONDRAL TISSUES. | 165 |
| FIGURE 5. 5: REPRESENTATIVE IMMUNOHISTOCHEMICAL IMAGES OF SECTIONS TAKEN FROM OSTEOCHONDRAL PLUGS FROM DIFFERENT STAGES OF OA. | 167 |
| FIGURE 5. 6: REPRESENTATIVE CD-34 IMMUNOHISTOCHEMICAL STAINING OF SECTIONS TAKEN FROM NORMAL AND OA OSTEOCHONDRAL TISSUES. | 168 |
| FIGURE 5. 7: FLOW CYTOMETRY CHARACTERISATION OF ENDOTHELIAL CELL LINES (HECV)..... | 170 |
| FIGURE 5. 8: ASSESSMENT OF B-CATENIN NUCLEAR LOCALISATION IN RESPONSE TO EXOGENOUS TREATMENT OF SEVERAL CANONICAL WNT PATHWAY MODULATORS. | 172 |
| FIGURE 5. 9: B-CATENIN PROTEIN ANALYSIS IN RESPONSE TO EXOGENOUS TREATMENT OF SEVERAL CANONICAL WNT PATHWAY MODULATORS..... | 173 |
| FIGURE 5. 10: PLAKOGLOBIN (γ -CATENIN) PROTEIN ANALYSIS IN RESPONSE TO EXOGENOUS TREATMENT OF SEVERAL CANONICAL WNT PATHWAY MODULATORS. | 175 |
| FIGURE 5. 11: TUBULE FORMATION ASSAY OF ENDOTHELIAL CONTROL CELLS AND CELLS TREATED WITH VEGF, DKK-1 AND DKK-2 RECOMBINANT PROTEIN..... | 177 |
| FIGURE 5. 12: MIGRATORY CAPACITIES OF ENDOTHELIAL CELLS AFTER STIMULATION WITH SEVERAL CANONICAL WNT MODULATORS AS MEASURED BY THE SCRATCH WOUND CLOSURE ASSAY. | 178 |
| FIGURE 5. 13: TRANSWELL MIGRATION ASSAY..... | 180 |
| FIGURE 5. 14: EFFECT OF DIFFERENT MODULATORS OF THE CANONICAL WNT PATHWAY ON CELL CYCLE PROFILE OF AN ENDOTHELIAL CELL LINE. | 182 |

Chapter 6:

| | |
|--|-----|
| FIGURE 6. 1: MORPHOLOGICAL CHARACTERIZATION OF PRIMARY HUMAN UMBILICAL VEIN-DERIVED ENDOTHELIAL CELLS (EC) AND PRIMARY CHONDROCYTES ISOLATED FROM KNEE JOINT OF NORMAL DONORS. | 194 |
| FIGURE 6. 2: MORPHOLOGICAL CHANGES IN ENDOTHELIAL CELLS FOLLOWING CO-CULTURE WITH CHONDROCYTES. .. | 196 |
| FIGURE 6. 3: ENDOTHELIAL AND CHONDROCYTES CO-CULTURE INDUCED ENMT IN CO-CULTURE. | 198 |
| FIGURE 6. 4: WESTERN BLOT ANALYSIS OF ENMT MARKERS IN CO-CULTURE EXPERIMENTS. | 199 |
| FIGURE 6. 5: CHONDROCYTES INDUCED ENMT THROUGH SECRETORY FACTORS. | 201 |
| FIGURE 6. 6: PROTEIN ARRAY PROFILER OF ENDOTHELIAL TO MESENCHYMAL TRANSITION MARKERS. | 203 |
| FIGURE 6. 7: EFFECTS OF DKK-1 ON ENDOTHELIAL CELL PHENOTYPE. | 206 |
| FIGURE 6. 8: MMP-13, DKK-1 AND CD-34 CO-LOCALISATION IN INVADING OA-OSTEOCHONDRAL INTERFACE TISSUES. | 207 |
| FIGURE 6. 9: AGGREGAN IMMUNOLABELLING IN NORMAL AND OA OSTEOCHONDRAL TISSUES. | 209 |
| FIGURE 6. 10: A-SMA IMMUNOLABELLING IN NORMAL AND OA OSTEOCHONDRAL TISSUES. | 211 |
| FIGURE 6. 11: VIMENTIN IMMUNOLABELLING IN NORMAL AND OA OSTEOCHONDRAL TISSUES. | 213 |
| FIGURE 6.12: SNAIL IMMUNOLABELLING IN OA OSTEOCHONDRAL TISSUES. | 214 |

Chapter 7:

| | |
|--|-----|
| FIGURE 7. 1: PROPOSED MODEL OF THE ROLE OF DKK-1 IN THE OSTEOCHONDRAL TISSUES. | 237 |
|--|-----|

Appendices:

| | |
|---|-----|
| FIGURE 8. 1: CUMULATIVE POPULATION DOUBLINGS OF ISOLATED CPC AND MSCs. | 246 |
| FIGURE 8. 2: EFFECT OF CHONDROCYTES AND ENDOTHELIAL CELLS CO-CULTURE ON CELL VIABILITY WITH MEMBRANOUS FITC-ANNEXIN V/7-AAD STAINING AND THE STATISTICS BETWEEN CONTROL (ENDOTHELIAL CELLS) AND CO-CULTURE GROUP. | 248 |
| FIGURE 8. 3: FIGURE 8.3: CONFOCAL SCANNING IMAGES OF DKK-1 PROTEIN IN MONENSIN BLOCKED FULL-DEPTH OSTEOARTHRITIC CARTILAGE. | 248 |
| FIGURE 8. 4: SUMMARY OF CPC CHONDROGENIC DIFFERENTIATION EXPERIMENTS AT TIME POINTS 0, 7, 14& 21. | 249 |
| FIGURE 8. 5: EXAMPLE OF AMPLIFICATION, DISSOCIATION, THERMAL PROFILE SETUP AND STANDARD CURVE OF PCR REACTION. | 253 |
| FIGURE 8. 6: BRDU-INCORPORATED ASSAY WAS USED TO DETERMINATE THE CELL PROLIFERATION AFTER TREATMENT WITH WNT CANONICAL MODULATORS. | 254 |

List of tables:

Chapter 2:

| | |
|--|----|
| TABLE 2. 1: COMMERCIAL SOURCE OF REAGENTS AND MATERIALS USED. | 41 |
| TABLE 2. 2: CONJUGATED PRIMARY ANTIBODIES USED FOR FLOW CYTOMETRY. | 63 |
| TABLE 2. 3: WNT PCR-ARRAY PLATE LAYOUT..... | 67 |
| TABLE 2. 4: POLYMERASE CHAIN REACTION PRIMER SEQUENCE. ALL PRIMERS ARE SHOWN IN THE 5'-3' WITH ANNEALING TEMPERATURE AND SIZE. | 69 |
| TABLE 2. 5: REAGENTS USED TO MAKE UP RESOLVING AND STACKING GELS. | 71 |

Chapter 3:

| | |
|---|----|
| TABLE 3. 1: FLOW CYTOMETRY ANALYSIS OF MESENCHYMAL STEM CELLS MARKERS IN ISOLATED CPC AND BM-MSCs. | 94 |
|---|----|

Chapter 4:

| | |
|---|-----|
| TABLE 4. 1: TABLE SHOWING WNT PATHWAY GENES UP OR DOWN-REGULATED IN OA-CPC CELL LINES. | 113 |
| TABLE 4. 2: TABLE SHOWING DKK-1 mRNA AND PROTEIN EXPRESSION AND % ACTIVATION OF TCF-LUCIFERASE REPORTER ASSAY OF N-CPC AND OA-CPC CELL LINES. | 126 |
| TABLE 4. 3: QUANTITATIVE LEVELS OF DKK-1 SECRETED DURING CHONDROGENESIS..... | 128 |
| TABLE 4. 4: CUSTOM- PCR-ARRAY PLATE LAYOUT..... | 130 |

Chapter 5:

| | |
|--|-----|
| TABLE 5. 1: DISTRIBUTION OF ENDOTHELIAL CELLS BETWEEN CELL CYCLE PHASES IN CONTROL AND TREATED GROUPS. | 183 |
|--|-----|

Appendices:

| | |
|---|-----|
| TABLE 8. 1: SUMMARY OF PATIENT'S AGE, MANKIN SCORE AND CELL LINES ISOLATED. | 270 |
| TABLE 8. 2: SUPER ARRAY BIOSCIENCES WNT PATHWAY GENE EXPRESSION PCR ARRAY..... | 275 |

List of Abbreviations:

| | |
|--------|---|
| ACI | Autologous chondrocyte implantation |
| ADAMTS | A Disintegrin and Metalloproteinase Domain with Thrombospondin Motifs |
| ANOVA | Analysis of Variance |
| APS | Ammonium Persulphate |
| BCA | Bicinchoninic Acid |
| BMP | Bone Morphogenetic Protein |
| BMSCs | Bone Marrow-derived Stromal Cells |
| BrdU | Bromodeoxyuridine |
| BSA | Bovine Serum Albumin |
| CD | Cluster of Differentiation |
| cDNA | Complementary DNA |
| CFE | Colony Forming Efficiency |
| c-Fms | Colony Stimulating Factor 1 Receptor |
| CILP | Cartilage Intermediate-Layer Protein |
| COMP | Cartilage Oligomeric Matrix Protein |
| CPC | Chondroprogenitor cells (also known as cartilage progenitor cells) |
| CS | Chondroitin sulphate |
| DAB | 3,3'Diaminobenzidine |
| DAPI | 4',6-Diamidino-2-phenylindole |
| DKK | Dickkopf |
| DMEM | Dulbecco's Modified Eagle Medium |
| DMMB | Dimethylmethylene Blue |
| DMSO | Dimethyl sulfoxide |
| dNTP | Deoxyribonucleotide triphosphate |
| DS | Dermatan sulphate |
| DTT | Dithiothreitol |
| DZ | Deep Zone |
| ECM | Extracellular matrix |
| EDTA | Ethylenediaminetetraacetic acid |
| EMT | Epithelial to Mesenchymal Transition |
| EnMT | Endothelial to Mesenchymal Transition |
| FACIT | Fibril-Associated Collagen with an Interrupted Triple helix |
| FACS | Fluorescence-Activated Cell Sorting |
| FBS | Foetal Bovine Serum (also known as Foetal Calf Serum) |
| FGF | Fibroblast Growth Factor |
| FITC | Fluorescein Isothiocyanate |
| FZD | Frizzled |
| g | Gravity |
| GAGs | Glycosaminoglycans |

| | |
|----------------|--|
| GSK 3 β | Glycogen synthase kinase 3 β |
| HA | Hyaluronan |
| HHGS | Histological-Histochemical Grading System |
| HIF-1 α | Hypoxia Inducible Factor-1 α |
| HIF-2 α | Hypoxia Inducible Factor-2 α |
| HUVEC | Human Umbilical Cord Endothelial Cells |
| HECV | Human Umbilical cord Endothelial Cell line |
| HRP | Horseradish peroxidase |
| HS | Heparan sulfate |
| ICRS | International Cartilage Repair Society |
| IGD | Interglobular domain |
| IL-1 | Interleukin-1 |
| ISCT | International Society for Cellular Therapy |
| ITS | Insulin Transferring Selenium |
| KS | Keratan sulphate |
| LEF | Lymphoid Enhancer-binding Factor-1 |
| LPL | Lipoprotein Lipase |
| LRP5/6 | Low-density Lipoprotein Receptor-related Protein 5/6 |
| M | Molar |
| mM | Millimolar |
| nM | Nanomolar |
| MAPK | Mitogen Activated Protein Kinase |
| MMPs | Matrix Metalloproteinases |
| mRNA | Messenger ribonucleic acid |
| MSCs | Mesenchymal stem cells |
| MZ | Middle Zone |
| NBFS | Neutral buffered formalin solution |
| NF-kB | Nuclear factor kB |
| OA | Osteoarthritis |
| OCP | Osteochondral plug or tissue |
| PBS | Phosphate buffered saline |
| PBS-T | Phosphate buffered saline containing Tween™ 20 |
| PCNA | Proliferation Cell Nuclear Antigen |
| PCR | Polymerase Chain Reaction |
| PD | Population Doubling |
| PECAM-1 | Platelet Endothelial Cell Adhesion Molecule-1 |
| PI | Propidium Iodide |
| PS | Penicillin Streptomycin |
| RA | Rheumatoid arthritis |
| RNA | Ribonucleic acid |
| ROS | Reactive oxygen species |
| RPM | Revolutions per minute |
| R-Spo-1 | R-Spondin-1 |
| RT-PCR | Real Time Polymerase Chain Reaction |

| | |
|------------------|--|
| SA- β -Gal | Senescence associated β -Galactosidase |
| SCB | Subchondral bone |
| SD | Standard deviation |
| SDS-PAGE | Sodium dodecyl sulphate-polyacrylamide gel electrophoresis |
| SEM | Standard error of the mean |
| siRNA | Small interfering RNA |
| SLRPs | Small Leucine-Rich proteoglycan family |
| SZ | Superficial Zone |
| SZP | Surface Zone Protein |
| TBE | Tris Borate EDTA |
| TBS | Tris Buffered Saline |
| TBS-T | Tris Buffered Saline-Tween |
| TCF | T-cell factor |
| TEMED | Tetramethylethylenediamine |
| TGF- β | Transforming growth factor- β |
| TIMP | Tissue Inhibitors of Metalloproteinases |
| TKR | Total knee replacement |
| TM | Tidemark |
| TNF- α | Tumour necrosis factor - α |
| TP | Tibial plateaux |
| v/v | Volume per volume |
| w/v | Weight per volume |
| WIF | Wnt-inhibitory factor |
| WISP-1 | Wnt-1 induced secreted protein-1 |
| X-Gal | 5-Bromo-4-chloro-3-indolyl β -D-galactopyranoside |
| 3D | Three dimensional |

CHAPTER 1: GENERAL INTRODUCTION.

1.1 Synovial joint.

The synovial joint (diarthrosis) is the most common joint in mammals, allowing movement at the point of contact of two bones. It differs from other joints in the body as the two articulating surfaces are not in distinct contact but surrounded by a dense fibrous capsule within which is located a synovial cavity containing synovial fluid (Archer *et al.* 2003).

The synovial joint comprises several connective tissues including bone, ligament, synovium, and articular cartilage. The complex structural arrangement of these tissues allows the joint to provide frictionless motion and to transmit load to the underlying bone whilst allowing for free mobility of the joint (Aigner and Stove, 2003).

The synovial joint is normally subjected to mechanical forces throughout the human life-span and for the majority of physiological activities the joint can withstand such forces without damage. However, during the human life-span the synovial joint is susceptible to degenerative disease states the most common of which is osteoarthritis. Osteoarthritis (OA) is a chronic degenerative disease affecting synovial joints leading to articular cartilage destruction and inappropriate bone remodelling. It is the most common form of polyarthritis and its prevalence is on the rise especially in the Western World (Luyten *et al.*, 2009, Hollander *et al.*, 2010). It has been described as one of the most common forms of musculoskeletal diseases across the globe, leading to pain, disability and eventual whole dysfunction of the joint (Hollander *et al.*, 2010). Over 8 million people in the UK are affected by osteoarthritis (ARUK, 2013). The aetiology of OA is believed to be multi-factorial (Noth *et al.*, 2008). The disease

process involves pathological changes in many of the joint tissues but a major hallmark of the disease process is the destruction of the articular cartilage.

1.1.1 Adult Articular Joint Anatomy.

The central structural tissues of the adult diarthroidal joints comprise of bone and articular cartilage (meniscus in knees), ligaments, tendons and synovium and along with muscle facilitate the transmission of friction free joint articulation (Figure 1.1). Articular cartilage is maintained by the chondrocyte whilst bone is composed of three cell types, osteoblasts, osteoclasts and osteocytes. The composite of articular cartilage and bone (subchondral) is often referred to as an osteochondral plug and the study of this composite structure is key to our understanding of the structure and function of the articular joint in health and disease.

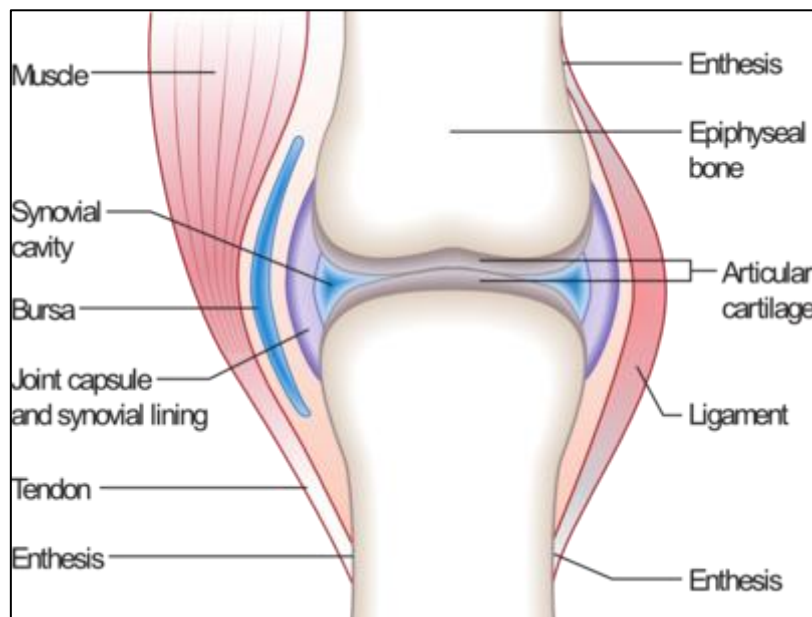


Figure 1. 1: A Diagrammatic representation of a synovial joint.
Adapted from www.mananatomy.com.

1.1.2 Articular cartilage: Structure and Morphology.

Articular cartilage comprises an extensive extracellular matrix in which a single cell type, the chondrocyte, is embedded. The tissue is described as avascular, aneural and alymphatic. These attributes have helped adapt the tissue to its purpose of transmitting and dissipating mechanical forces. Chondrocytes contribute less than 10% of the volume of mature articular cartilage; and the remaining volume are occupied by collagens, proteoglycans, a variety of non-collagenous proteins and water. The majority of articular cartilage comprises water molecules (around 60-70% of the tissue's wet weight), collagens (20%), proteoglycans (7%) and other proteins (around 1%). Generally, the thickness of mature human articular cartilage is between 1 and 7 mm and this variation is dependent upon the mechanical load experienced by the joint (Buckwalter, 1999).

1.1.3 Chondrocytes.

Chondrocytes are sparsely distributed within the extracellular matrix. Approximately 10µm in diameter they are unique cells that account for only 2-5% of the total tissue volume (Stockwell, 1978; Stockwell, 1979). Chondrocytes have many organelles (e.g. endoplasmic reticulum and Golgi apparatus) that are required to produce large quantities of essential matrix components. In addition, these cells have intracellular secretory vesicles, lysosomes and, intra-cytoplasmic filaments (Buckwalter, 1999). Cilia are present on the plasma membrane and may be responsible for detecting mechanical forces dissipated through the extracellular matrix (Poole *et al.* 1987; Poole *et al.* 1992). Chondrocytes also express cell surface integrin's including $\alpha 5\beta 1$, $\alpha 1\beta 1$, $\alpha 2\beta 1$, $\alpha 11\beta 1$ and $\alpha V\beta 3$ that recognise various molecules including fibronectin ($\alpha 5\beta 3$),

type II and VI collagen ($\alpha 1\beta 1$, $\alpha 2\beta 1$, $\alpha 11\beta 1$), laminin ($\alpha 6\beta 1$), osteopontin and vitronectin ($\alpha V\beta 3$) (Salter *et al.* 1992; van der Kraan *et al.*, 2002). In addition, chondrocytes express the trans-membrane receptor molecule CD44 that interacts with HA and is implicated in the maintenance of pericellular matrix homeostasis (Salter *et al.* 1996; van der Kraan *et al.*, 2002). Chondrocytes play a central role in the development and maturation of articular cartilage, as well as in the maintenance of the mature adult tissue.

1.1.4 Zones of articular cartilage.

Histological examination of articular cartilage shows the tissue to be divided into four distinct zones; the superficial zone, middle (transitional) zone, deep (radial) zone and the zone of calcified cartilage that anchors cartilage tissue to the underlying subchondral bone (Figure 1.2.A). Although there is no distinct boundary separating each zone, the four zones differ based on the distribution and shape of the chondrocytes and the composition of the extracellular matrix. Differences within these zones vary both between species and between joints of the same species (Buckwalter and Mankin, 1998; Buckwalter, 1999).

The superficial zone is the layer adjacent to the joint cavity and is defined by the lamina splendens (a semi-translucent membrane). Directly beneath the lamina splendens is a cellular region where chondrocytes assume a flattened morphology. Chondrocytes, in the superficial zone, secrete a matrix rich in collagen type II fibrils that run parallel to the surface of articular cartilage. This structure is thought to facilitate the transmission of mechanical forces along the joint. Chondrocytes in this zone also synthesise and secrete a specialized proteoglycan molecule known as

surface zone proteoglycan (SZP), which functions to lubricate the surface of the cartilage (Schumacher *et al.*, 1994, Flannery *et al.*, 1999) thus reducing friction between the articulating surfaces.

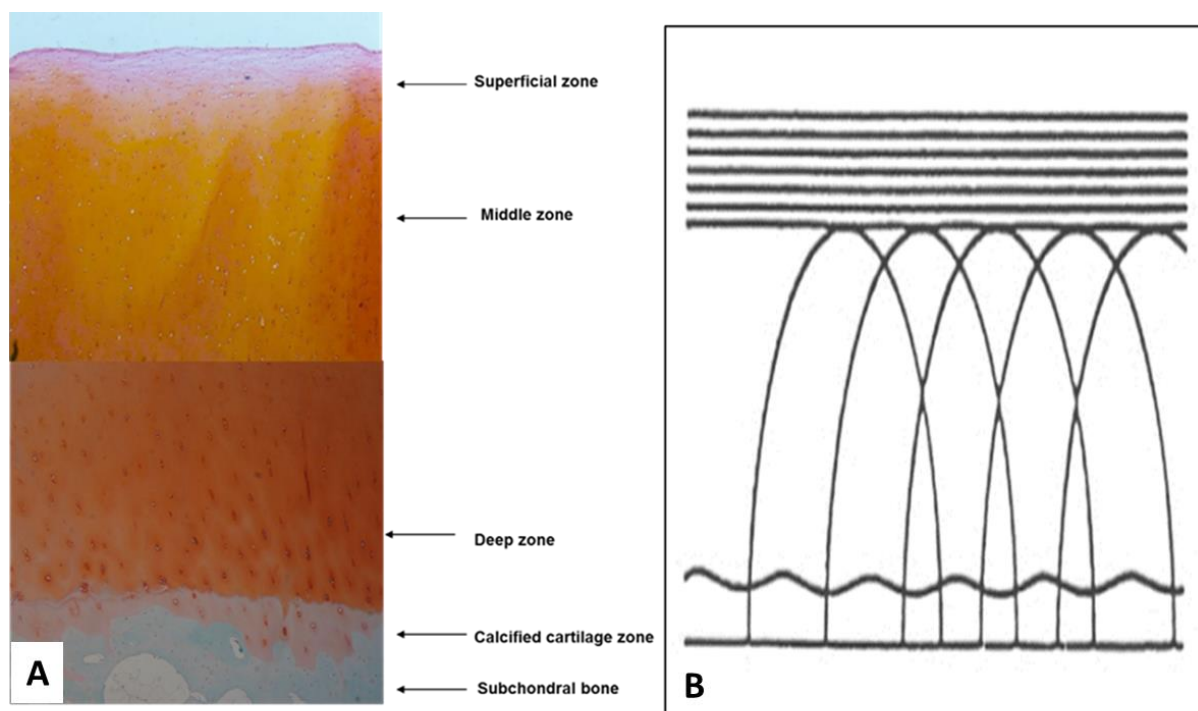


Figure 1. 2: Zones of human articular cartilage.

Image A is a tissue section of articular cartilage where chondrocytes are visible (blue/purple stain) throughout the depth of the tissue. Image B is a diagram of the collagen fibre orientation within the cartilage zones known as Benninghoff's arcades. Image 1.2.B is adapted from Landínez-Parra *et al.*, 2012.

Within the middle (transitional) zone, chondrocytes have a spherical morphology. Chondrocytes present in this zone are more metabolically active than those of other zones, as evidenced by their vast array of cellular organelles such as the Golgi apparatus and the endoplasmic reticulum. The transitional zone collagen fibres are wider in diameter but their arrangement is more disorganised than that seen in the superficial zone. There is also a higher proteoglycan concentration in comparison to

the superficial zone (Buckwalter, 1999). In addition, chondrocytes in this zone secrete a glycoprotein known as cartilage intermediate layer protein (CILP) which is unique to this zone and has been be implicated in the pathological processes of inflammatory arthritis (Lorenzo *et al.*, 1999, Bernardo *et al.*, 2011). The transitional zone accounts for up to 60% of the thickness of articular cartilage (Buckwalter, 1999).

The deep zone of articular cartilage is defined by the presence of chondrocytes with a spherical morphology that are arranged into nearly vertical columns of 3-6 cells. This arrangement of chondrocytes is due to the perpendicular orientation of the collagen fibres within the zone (Figure 1.2.B) (Eyre, 2002). This zone contains the highest concentration of proteoglycan but contains the least amount of water of all the zones (Buckwalter, 1999).

The calcified cartilage zone is above the subchondral bone and provides a site for attachment to the underlying bone (Oegema *et al.*, 1997). Type X collagen is present within the calcified cartilage and surrounds the cells of this region (Gannon *et al.*, 1991; Eyre, 2002). A 'tidemark' defines the area between the non-calcified and the calcified cartilage regions. It is an acellular basophilic region with the occasional presence of 'trapped' chondrocytes. Collagen fibrils extend into the tidemark from the non-calcified zone above (Buckwalter, 1999). The chondrocytes of the calcified cartilage zone are metabolically inactive, and consequently, have a limited number of organelles in their cytoplasm, although they do express alkaline phosphatase and Runx-2 (Schmid and Linsenmayer, 1985; Buckwalter, 1999; Enomoto-Iwamoto *et al.*, 2002).

1.1.5 Regions of extracellular matrix within articular cartilage.

The extracellular matrix comprises water, collagens, proteoglycans and non – collagenous proteins as well as glycoproteins. Interactions between these components of the extracellular matrix are responsible for the resilience and stiffness of articular cartilage (Buckwalter, 1999). The extracellular matrix can be divided into three regions depending on its distance from a chondrocyte and the components of the extracellular matrix. The matrix surrounding a chondrocyte is known as the pericellular region. The interterritorial region has been defined as the matrix furthest from the chondrocyte and, moreover, the territorial matrix has been defined as the matrix between the pericellular and interterritorial regions (van der Kraan *et al.*, 2002).

1.2 Subchondral bone.

1.2.1. Structure and Composition.

Bone is one of the most extensively studied and vital areas of human anatomy. The human skeleton is made up of five different types of bone: long bone, short bone, flat bone, sesamoid bones and irregular bones (Clarke 2008). The human skeleton not only provides shape, but also physical support for the systems contained within. Essentially, all bones are composed of bone marrow, blood vessels endothelial cells and nerves. Bone is a specialised form of dense connective tissue that comprises of three cell types; osteoblasts, osteocytes and osteoclasts, essential to the physiology of the bone, embedded within a specialised matrix made up of organic and inorganic components (Clarke 2008). Living bone contains 10 – 20% water. The bone matrix is mainly composed of type I collagen (Kadler *et al.* 1996). In addition, it has been

documented that bone matrix contains small amounts of collagen type III and type V (Keene *et al.* 1991), non-collagenous proteins including osteocalcin (BGLAP) bone sialoprotein and osteopontin (OPN) (Marie *et al.* 1989; Owen *et al.* 1990; McKee and Nanci 1996). Furthermore, there are many different types of non-collagenous proteins found in bone including albumin in addition to hyaluronan and other proteoglycans including fibromodulin and decorin (Fedarko *et al.* 1992). These organic components, mainly collagen fibres, give the bone its tensile properties that allow it to twist, compress and stress without breaking. The minerals strengthen the collagen composite, increasing the mechanical resistance of the tissue, and provide a source of calcium, phosphate and magnesium for systemic mineral homeostasis (Clarke 2008).

Long, short and sesamoid bones form part of the muscular skeletal system and aid in fulfilling the various roles of this system that includes support, protection, movement, production of blood cells and providing important endocrine roles and storage for a number of key minerals. The structure of long bone is optimised to provide a high tensile strength. Long bones (such as the femur) are made up of cortical bone and cancellous (trabecular) bone (Clarke 2008). Cortical bone (80% of the mass) forms a dense cylinder down the shaft of the bone (diaphysis) surrounding the central marrow cavity and gives the long bone its solid hard white exterior. Whereas, the cancellous or trabecular bone forms the end (epiphysis) of long bones (20% of the mass) and has an open honeycomb structure often termed the sponge-like area of the bone.

Cortical bone is composed of osteons, these are densely packed concentric lamellae (made mainly of collagen and hydroxyapatite crystals) each with a central Haversian canal containing a blood vessel. Osteocytes are embedded in lacuna within the osteons and at the outer end of each osteon is the cement line. Canaliculi are tiny

fluid like passageways that enable osteocytes cells within the mineralised matrix to communicate with other cells. Blood vessels in the central Haversian canal facilitate the exchange of nutrients and gases between osteocytes and the blood. Smaller Volkmann canals connect osteons and supply nutrients to all cells. The interior surface of the osteons are known as the endosteum and the exterior surface is the periosteum. The endosteum is the partition separating the cortical bone and the cancellous bone.

Trabecular bone, on the other hand, is present in some bones and resist compression. It has an open porous network with spaces that accommodate the bone marrow and hematopoietic stem cells. Osteocytes are particularly important in this area due to their local mechano-sensing properties (Bonewald and Johnson 2008).

1.2.2 Bone turnover and metabolism

In response to various physiological and mechanical (external) changes that occur in the human life cycle, the skeleton adjusts and accommodates to maintain its functions through the processes of bone modelling and remodelling. The process of bone remodelling occurs when the bone responds to factors that affect the bone density, structure and growth. This process involves the osteoclasts and osteoblasts that modulate the bone density, and resorb and rebuild, respectively.

Remodelling is orchestrated by osteoclasts anchored at the bone surface they create the 'sealed zone', producing an acidic environment that dissolves the bone mineral content of the matrix. Once this occurs, enzymes are released by the resident osteoclasts and remove the remaining collagenous matrix to complete the process of bone resorption. Following resorption, osteoblasts move to the resorption space and

start to produce osteons. This begins to create a scaffold where minerals like calcium phosphate and hydroxyapatite crystallise. Osteoblasts trapped in the matrix that they secrete either differentiate to become osteocytes, go through apoptosis or revert back to lining cells, which cover the bone surface (Raggatt and Partridge 2010).

1.2.3. Osteoblasts.

Osteoblasts are mononuclear mesenchymal bone cells found, in cluster form, along the bone surface. It covers 95% of cortical and 75% of the trabecular bone. Osteoblast have an extensive endoplasmic reticulum and enlarged Golgi complex all equipping them for synthesis of bone matrix (Franz-Odendaal., 2006) components which is the main function of these cells.

Key pathways crucial in osteoblastogenesis include the Wnt pathway and the TGF/BMP pathway. For example, Bone Morphogenetic Proteins (BMP) initiate the transformation process of MSCs undergoing osteoblastogenesis and this is marked by down-stream elevation of the osteoblast lineage transcriptional factor, Runt-related transcription factor x 2 (Runx-2) (Kern *et al.*,2001). Runx-2 expression in turn activates a variety of genes promoting osteoblast-lineage differentiation including Osterix (Osx) and collagen type I (Col1a1) (Harada *et al.*, 1999). Mature osteoblasts can further transform into osteocytes by becoming buried within the bone matrix, or occasionally undergo apoptosis but can also lie dormant as bone lining cells (Franz-Odendaal., 2006).

Osteoblasts also play a role in osteoclastogenesis through stimulating the release of key proteins and factors such as MCSF, receptor RANKL and OPG. Activation of these

key factors implicated in osteoclastogenesis result in osteoclast precursor cells undergoing differentiation into mature osteoclasts (Boyle *et al.*, 2003).

1.2.4. Osteocytes.

Osteocytes originate from mesenchymal stem cells and are star or dendritic shaped cells found in mature bone. Osteocytes reside in spaces called lacunae and canaliculi between the lamellae in bone and are responsible for maintaining homeostasis, oxygen and mineral levels. Osteocytes are mechano-sensor cells that control the production of osteoblasts and osteoclasts within the anatomic structure where bone remodelling occurs. Osteocytes support osteoclast formation for bone resorption by expressing the Receptor Activator of Nuclear factor Kappa-B Ligand (RANKL). In addition when clusters of osteocytes and osteoblasts bind, via their dendrites, it allows possible regulatory control of mineral homeostasis as well as control over both bone resorption and formation (Li *et al.*, 2003).

Osteocytes are an important regulator of bone mass as well as phosphate metabolism. SOST negatively regulates Wnt pathway signalling that is critical for osteoblast formation (Bonewald, 2008). Moreover, osteocytes are also able to remodel their own environment through the addition and removal of minerals within the lacunae and canaliculi. Through the expression of Dentin Matrix Protein 1 (DMP-1), MEPE and FGF-23, osteocytes control and regulate phosphate and mineral homeostasis (Yang *et al.*, 2005).

Furthermore, in response to micro-damage of the bone, osteocyte apoptosis occurs where pro-apoptotic factors are released in proximity to the damaged site (Teti, 2009). Osteocyte apoptosis is thought to occur due to lack of fluid flow or mechano-

transduction (Bonewald *et al.*, 2008; You *et al.*, 2009). Apoptotic osteocytes release apoptotic bodies expressing RANKL to recruit osteoclasts that begin the process of bone resorption.

1.2.5. Osteoclast.

Osteoclasts are multinucleated cells that are substantial in size and are highly specialised cells originated from haematopoietic stem cells lineage. Osteoclast is a type of bone cell that resorbs bone tissue. This function is critical in the maintenance and repair, and remodelling of bones. It does this when the hydroxyapatite mineral component of the bone dissolves and results in degrading the organic bone matrix. Furthermore, osteoclasts facilitate the expression of various key factors that aid in bone destruction such as Tartrate-Resistant Acid Phosphatase (TRAP).

In the early stages of bone resorption, osteoblasts release the transcription factor M-CSF that, when attached to its receptor c-Fms, helps in stimulating pathways that facilitate the production and survival of osteoclasts and their precursors. As this process starts and cells undergo osteoclastogenesis, RANK is expressed and this initiates the transformation of mono-nuclear pre-osteoclasts to undergo osteoclastogenesis (Yasuda *et al.*, 1998). RANK binding to its receptor RANKL that stimulates AP-1 and NF- κ B pathways, and this triggers cellular change that allows mononuclear pre-osteoclasts to fuse together with macrophages thus forming multinucleated mature osteoclasts (Franzoso *et al.*, 1997; Takayanagi *et al.*, 2002).

Conversely, to inhibit and hinder osteoclast differentiation, osteoblasts produce the protein osteoprotegerin (OPG) that when attached to RANKL prevents interaction with

RANK (Nakashima *et al.*, 2011). This occurs to stop bone resorption and allow bone to form or remodel naturally (Lacey *et al.*, 1998).

1.3 Extracellular Matrix Molecules of cartilage.

1.3.1 Collagens.

Collagens are a large family of triple helical proteins classified into a number of groups based upon function and domain homology (for review see Kadler *et al.* 2007).

There are various forms of collagen within mature articular cartilage. These include types I, V, VI, IX, X, XI, XII & XIV. The most abundant collagen is the fibril-forming type II collagen. Type II collagen contributes to the majority of the dry weight of cartilage. Type II collagen constitutes around 90% of collagen constituents in adult articular cartilage. Type II collagen comprises three identical α -chains, collectively forming a heterotrimer fibril molecules that are interconnected via intermolecular cross-links involving pyridinoline (Eyre and Wu 1995; Riesle *et al.*, 1998; Eyre 2002). The presence of these covalent intermolecular cross-links is much higher than in other connective tissues and provides the tensile strength of cartilage (Eyre and Wu 1995). Collagen type II is found as two splice variants (IIA, IIB) where IIA is expressed by immature chondrocytes while IIB is expressed in mature cartilage. Synthesis of type II collagen is similar to the majority of other collagen macromolecules as it is released from chondrocytes as pro-collagen and, ultimately, matures in the pericellular and inter-territorial matrix by protease cleaving of the C and N terminus pro-peptides.

Other fibril-forming collagens found in articular cartilage are types I, V, & XI. In addition, cartilage contains type X (a network-forming collagen) and type IX (FACIT collagen). Collagens function to elicit tensile and shear strength to the tissue. These

properties are increased by the formation of heterotypic collagen fibrils, in which type II collagen interacts with type IX and type XI collagen (see Figure 1.3).

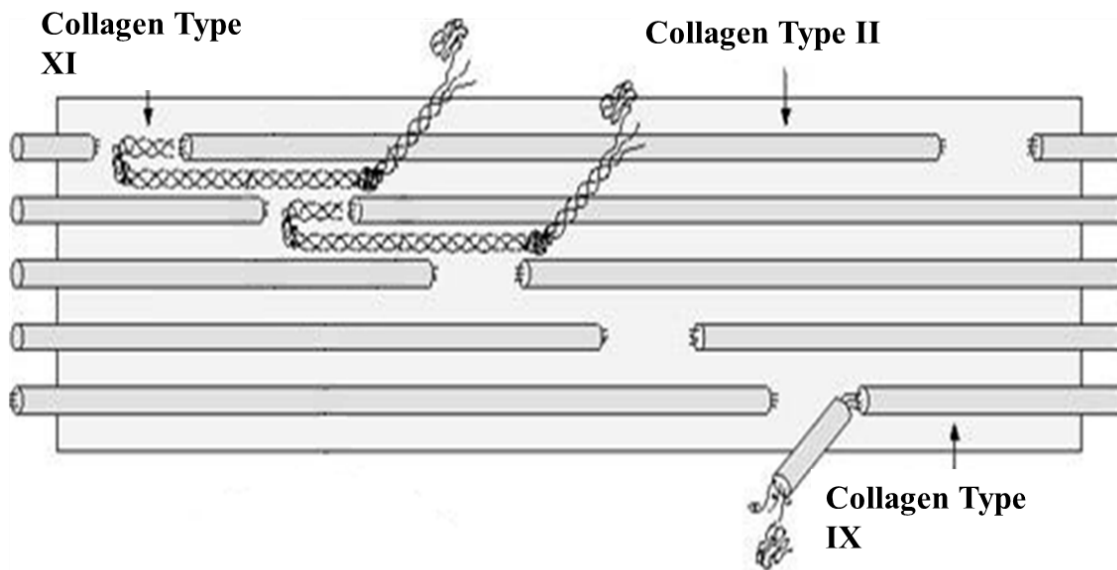


Figure 1. 3: Diagram showing collagen II: IX: XI heterofibril.
Adapted from Eyre, (2002).

Type IX collagen interacts predominantly with type II collagen and cross-linking studies have shown that there are at least six sites along the length of type II collagen that covalent bonds can form with corresponding type IX collagen (Svensson *et al.* 2001). Type (XI) collagen comprises three chains, $\alpha 1$ (XI), $\alpha 2$ (XI) and $\alpha 3$ (XI) and functions to restrict fibril diameter of type II collagen through retention of its N-pro peptide (Eyre and Wu., 1995; Duance and Vaughan-Thomas., 1999). This meshwork of collagen fibres acts to entrap negatively charged proteoglycans, resulting in the collagen network being under continual tension even when cartilage is unloaded (Eyre and Wu, 1995; Riesle *et al.*, 1998; Buckwalter and Mankin, 1998; Young *et al.*, 2000).

The orientation and diameter of the collagen fibres varies between the different cartilage zones (section 1.2.3). Benninghoff, (1925) coined the term "arcades" following his observation on the arrangement of collagen fibres from the deep zone to the superficial zone as arches or arcades (Figure 1.2). These arcades are arched extensions of radial fibres that are distributed within the transitional zone, and interact with fibres of the deep zone below (Clark, 1990; Eyre, 2002).

1.3.2 Proteoglycans.

Proteoglycans are a major component of articular cartilage, and comprise a core protein to which one or more glycosaminoglycans (GAG) are covalently attached (Knudson and Knudson, 2001). Glycosaminoglycans are un-branched polysaccharides formed by disaccharide repeats of an amino sugar (N-acetyl glucosamine, glucosamine that is variously N-substituted, or N-acetyl galactosamine) and an uronic acid (glucuronic acid or iduronic acid) or galactose. Glycosaminoglycans are classified into: heparin and heparan sulphate (HS), hyaluronan (HA), keratan sulphate (KS), chondroitin sulphate (CS) and dermatan sulphate (DS). Hyaluronan is the only GAG that is not found covalently linked to proteoglycans (Dudhia, 2005).

The major proteoglycan found in articular cartilage is the large aggregating proteoglycan, aggrecan, (Figure 1.4). Also present in lesser amounts are the non-aggregating small leucine rich proteoglycans such as, decorin, biglycan, lumican and keratocan. Aggrecan, the major proteoglycan of articular cartilage, functions to provide elasticity and resilience to the tissue and accounts for 90% of the proteoglycan present within articular cartilage. The core protein is approximately 230-250 kDa in size and comprises three globular domains, G1, G2 and G3. The inter-

globular domain separates the G1 and G2 domains and the KS domain and CS domains of the proteoglycan core protein separate the G2 and G3 domains. There are approximately 50 KS GAG chains attached within the KS domain of the protein core and 100 CS GAG chains attached within the CS domain of the protein core (Knudson and Knudson, 2001).

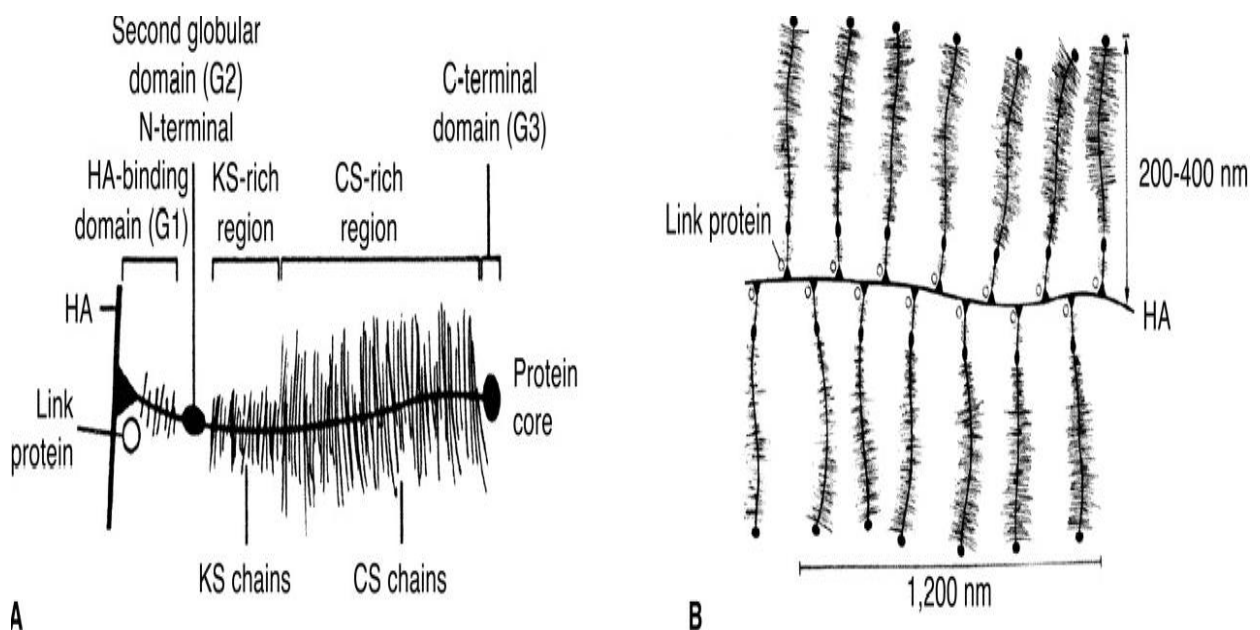


Figure 1. 4: A diagram showing the structure of aggrecan.

Adapted from Ulrich-Vinther et al., 2003 (Ulrich-Vinther et al., 2003)

The N terminal, G1 domain associates non-covalently with both link protein and hyaluronan and is also termed the hyaluronan binding region (HABR) (Knudson and Knudson, 2001). The functions of hyaluronan binding to aggrecan, is to allow the aggregation of aggrecan monomers into macromolecular complexes, which are stabilised by the non-covalent interaction with link protein (Spicer *et al.*, 2003). The aggrecan G1 domain binds to hyaluronan via the proteoglycan tandem repeat (PTR)

units, which are present as sub-domains. There are three sub-domains within the G1 PTR, which are A, B, and B' that are essential for the non-covalent interactions with hyaluronan.

At the C-terminal, there is a G3 domain comprising several different domains. These domains include a C-type lectin module, a complement regulatory protein (CRP) module, and an EGF module (Knudson and Knudson, 2001). The quantity of aggrecan monomers that possess the G3 domain decreases with age, resulting from extracellular proteolytic degradation (Knudson and Knudson, 2001; Dudhia, 2005).

Along with the large aggregating proteoglycans within articular cartilage, small leucine-rich proteoglycans, basement membrane proteoglycans and, cell surface/membrane bound proteoglycans are also present (Figure 1.5). Small leucine-rich proteoglycans include decorin, biglycan, fibromodulin and lumican. Each has a core protein with variable types and numbers of GAG side-chains of dermatan, chondroitin and keratan sulphate. Their distribution within the cartilage extracellular matrix also varies. Decorin (one chondroitin or dermatan side-chain) is located within the inter-territorial matrix whereas, biglycan (2 chondroitin or dermatan side chains) is present within the pericellular matrix (Knudson and Knudson, 2001). These smaller proteoglycans function to interact with specific collagen molecules and, alternatively, are involved in the regulation of collagen fibril diameter. The basement membrane proteoglycan, perlecan, has been located in the pericellular matrix of adult articular cartilage (Knudson and Knudson, 2001). Also present within articular cartilage are cell surface proteoglycans, such glypican and syndecan.

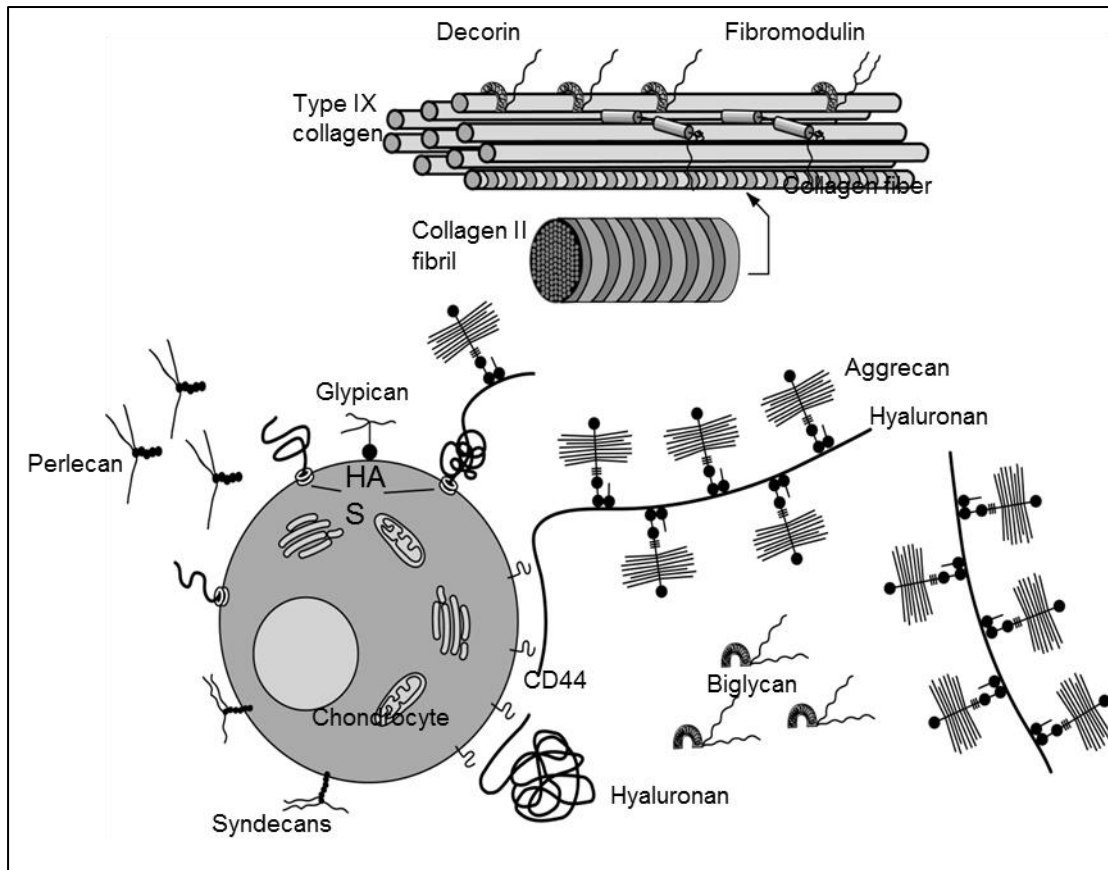


Figure 1. 5: A diagram depicting proteoglycans present in articular cartilage. Adapted from Knudson et al., 2000 (Knudson and Knudson, 2001).

1.4. Maturation of articular cartilage and the skeletal system.

The maturation of articular cartilage and growth of the skeletal elements is due to a combination of cell proliferation, cell hypertrophy and matrix secretions that have been shown to develop via an appositional growth mechanism (Hayes *et al.*, 2001). This tightly regulated mechanism has been proven to be controlled by chondrocytes in the surface zone of articular cartilage (Ward *et al.*, 1999; Hayes *et al.*, 2001).

Early studies by Hayes *et al.* (2003), using the proliferating cell marker bromodeoxyuridine (BrdU), identified a cohort of slow-cycle progenitor cells within the articular surface of *Monodelphis Domestica*. Using the cell-tracking agent 5-bromo-2-deoxyuridine (BrdU), which is incorporated during the S-phase of the cell cycle as a

thymidine analogue, this study showed that transitional zone chondrocytes retained BrdU staining for up to four days and thereafter lost labelling. This result indicated a transient amplifying population of cells within this zone. However, surface zone chondrocytes retained BrdU labelling for the duration of the experiment indicating that newly-formed cells, produced at the articular surface, expanded within the transitional zone and then finally undergo terminal differentiation within deeper cartilage zones. As the cartilage develops there is alteration in the structure from immature tissue, which is isotropic and features as a disorganised cellular arrangement then develops into an anisotropic tissue, which has a highly organised cellular arrangement (Hayes *et al.*, 2001; Archer *et al.*, 2003).

Further studies led to the identification of a population of chondrocytes that have stem-progenitor cell properties referred to as Cartilage Progenitor Cells (CPC). The first report of CPC was by Dowthwaite *et al.* (2003) in which immunohistochemical studies for Notch-1 localised a sub-population of chondrocytes staining positive in the superficial zone of immature bovine cartilage (Dowthwaite *et al.*, 2004). Further studies by Williams *et al.* (2010) resulted in the isolation of these stem-progenitor cells from cartilage using a classical fibronectin adhesion assay. They confirmed that sub-populations of chondrocytes possess properties of mesenchymal stem cells and are able to differentiate into a number of different cell lineages. In addition fibronectin isolated CPC sorted by FACS, using Notch antibodies, further demonstrated that Notch positive CPC when compared with Notch negative CPC had a higher colony-forming ability. These data demonstrate the stem cell/progenitor nature of chondrocytes and the role Notch plays in controlling the growth and development of articular cartilage.

1.5 Pathophysiology of OA.

Osteoarthritis is thought to be largely a degradative disease mainly affecting articular cartilage and subchondral bone. However, this somewhat simplistic concept of the pathophysiology of OA is constantly challenged, as there is a shifting paradigm where the disease is now considered to be a disease of an organ (the synovial joint). With this shifting paradigm, OA is now believed to be a disease of multiple tissues within the synovial joint including, the synovial lining, fat pads, cartilage and bone (Lewis *et al.*, 2011).

In normal adult articular cartilage there is an equilibrium between catabolism and anabolism, maintaining homeostasis and ensuring the extracellular matrix is maintained both structurally and functionally throughout the life-span of individual (Goldring and Goldring, 2004). In the development of OA, the balance is altered in favour of catabolism resulting in a net degradation of cartilage extracellular matrix that can progress to advance stages of the disease. The mechanisms of cartilage degradation are well understood: early osteoarthritis is characterised by aggrecanases (ADAMTS) induced proteoglycan loss, whereas late stage disease is characterised by subsequent degradation of the collagen network. This is induced by various matrix metalloproteinases (MMPs), which cause irreversible collagen depletion and, ultimately compromises the tissue's functional ability of mechanical force dissipation (Maroudas *et al.*, 1992; Maroudas *et al.*, 1998).

In addition to alterations of the extracellular constituents, OA is also accompanied by aberrant chondrocyte function, resulting in the formation of chondrocyte clusters that are thought to indicate attempted repair of the tissue. Further evidence for reparative

processes include:- increased expression of proliferative markers in these chondrocyte clusters such as Proliferating Cell Nuclear Antigen (PCNA) and Syndecan-3 (Pfander *et al.*, 2001). In addition, over the last decade, convincing studies conducted by several research groups have linked the pathogenesis of osteoarthritis to activation of key developmental pathway implicated in regulation of cell proliferation, homeostasis and fate determination including Wnt signalling pathway (Goldring and Goldring 2004; Luyten *et al.*, 2009; Shen *et al.*, 2014).

In addition to changes seen in the articular cartilage, there are alterations in the subchondral bone evident as subchondral sclerosis, as well as changes in the structure of the subchondral bone marked by osteophyte formation and appearance of subchondral cysts and tidemark duplication and breaching. Histologically, tidemark duplications and breaching are correlated with an increase in vascular invasion of the articular cartilage (Petersson *et al.*, 1998; Lajeunesse *et al.*, 2003; Martel-Pelletier and Pelletier 2010). This alteration in subchondral bone is often associated with reduced mineralisation and increase in stiffness of underlying bone therefore increasing joint stress (Grynpas *et al.*, 1991).

1.5.1 Mediators of Cartilage Degradation-Cytokines

Cytokines are intracellular messenger molecules that are either pro-inflammatory mediators or anti-inflammatory mediators and, binding to specific cytokine receptors on the cell surface induces their actions. Pro-inflammatory cytokines include IL-1 β and TNF- α (Fernandes *et al.*, 2002). IL-1 cytokine receptors are IL-1 receptor type1 (IL-1R1) and IL-1RII (Slack *et al.*, 1993; Kobayashi *et al.*, 2005). TNF- α receptors include p55 (TNFR1) and p75 (TNFR2) and are localised to the cell surface of chondrocytes

(Kobayashi 2005). These cytokines induce the synthesis and activation of proteolytic enzymes, e.g. MMPs and aggrecanases, which degrade extracellular matrix generating progressive cartilage damage and, via an autocrine mechanism, increase their own production and the production of other pro-inflammatory cytokines e.g. IL-6 and IL-8 (Martel-Pelletier *et al.*, 1999; Fernandes *et al.*, 2002; Martel-Pelletier and Pelletier 2010; Bonnet *et al.*, 2013).

There are elevated levels of IL-1 present within OA synovial fluid (Kobayashi *et al.*, 2005). TNF α has also been shown to have elevated protein expression in OA synovial fluid. Experimental evidence shows TNFR1 receptor expression to be present on chondrocytes in OA tissue at locations of proteoglycan loss (Goldring, 2000; Kobayashi *et al.*, 2005).

1.5.2 Aggrecanases (ADAMTS Proteinases).

Members of the ADAMTS family of proteinases (a disintegrin and metalloproteinase with thrombospondin type 1 motif), most notably ADAMTS4 and TS5 are responsible for the initial degradation of the large aggregating proteoglycan in articular cartilage (Arner *et al.*, 1998; Patwari *et al.*, 2005). Loss of this matrix molecule results in a loss of compressive resistance of articular cartilage that ultimately compromises the tissue (Arner *et al.*, 1998; Patwari *et al.*, 2005; Wieland *et al.*, 2005). ADAMTS mediated degradation of aggrecan occurs at several sites within both the chondroitin-sulphate region and the inter-globular domain (Sandy *et al.*, 1991; Aydelotte *et al.*, 1992; Arner *et al.*, 1998; Kobayashi *et al.*, 2005).

1.5.3 MMPs.

MMPs also play a role most notable in the later stages of the disease. There are 21 human MMPs that cleave a variety of ECM molecules (Egeblad and Werb 2002). Under normal conditions these endo-proteases are expressed at relatively low concentrations and play a role in tissue development, reproduction, and tissue homeostasis. Altered levels of expression are implicated in several diseases contributing to heart disease, cancer metastasis and arthritis (Nagase and Woessner, 1999; Egeblad and Werb, 2002; Mix *et al.*, 2004).

MMP1 and MMP13 have been shown to degrade type II collagen between residues 775 (glycine) and 776 (leucine) (Kobayashi *et al.*, 2005) in the late stages of OA. These MMPs cleave the triple helical of type II collagen enabling further degradation by the gelatinases MMP-2 and -9 (Seltzer *et al.*, 1981; Duerr *et al.*, 2004). Tight regulation of MMP activity occurs via endogenous inhibitors including thrombospondin -2, α 2-macroglobulin and tissue inhibitors of matrix metalloproteinases (TIMPs) 1-4 (Egeblad and Werb, 2002; Skiles *et al.*, 2004).

1.5.4 Angiogenesis in Osteoarthritis.

Normal adult articular cartilage is an avascular tissue and healthy mature cartilage contains proteins and proteoglycans in addition to other factors that have been shown to be anti-angiogenic (thrombospondin-1) (Hsieh *et al.*, 2010). Furthermore, factors that are believed to be pro-angiogenic including matrix metalloproteinases are carefully regulated in healthy cartilage by their tissue inhibitors (TIMPS) (Kim *et al.*, 2011). However, in OA, the degradation of the extracellular matrix of articular cartilage is thought to increase the susceptibility of the tissue to invading endothelial

cells from the underlying subchondral bone resulting in the formation of invading blood vessels. This process of angiogenesis is poorly understood and recently several regulatory pathways have been implicated such as the Notch and Wnt pathways in this process (Gao *et al.*, 2013).

1.6. The Wnt signalling pathway.

The Wnt pathway is possibly the most studied pathway in mammalian systems and has been found to have wide biological roles in embryogenesis, cellular and tissue development and homeostasis in a healthy setting but also extend to playing a key role in the pathophysiology of several diseases including arthritis and cancer (Xu and Nusse, 1998; Niehrs, 2012; Clevers and Nusse, 2012).

Wnt proteins constitute a family of secreted signalling proteins that bind to their respective receptors and activate two sub-groups of the Wnt signalling pathways: namely the canonical and non-canonical pathways. The difference between these two pathways is that the canonical pathway involves the protein β -catenin whilst the non-canonical pathway is independent of it.

1.6.1. The non-canonical Wnt signalling pathway.

The non-canonical Wnt signalling pathway is regulated by several Wnt ligands via Frizzled receptors and co-receptors (Gao *et al.*, 2011). In mammals, so far three non-canonical Wnt pathways have been described in the literature; the Wnt/ Ca^{2+} pathway, the Wnt/PCP pathway and the Wnt/PKC pathway (Figure 1.6).

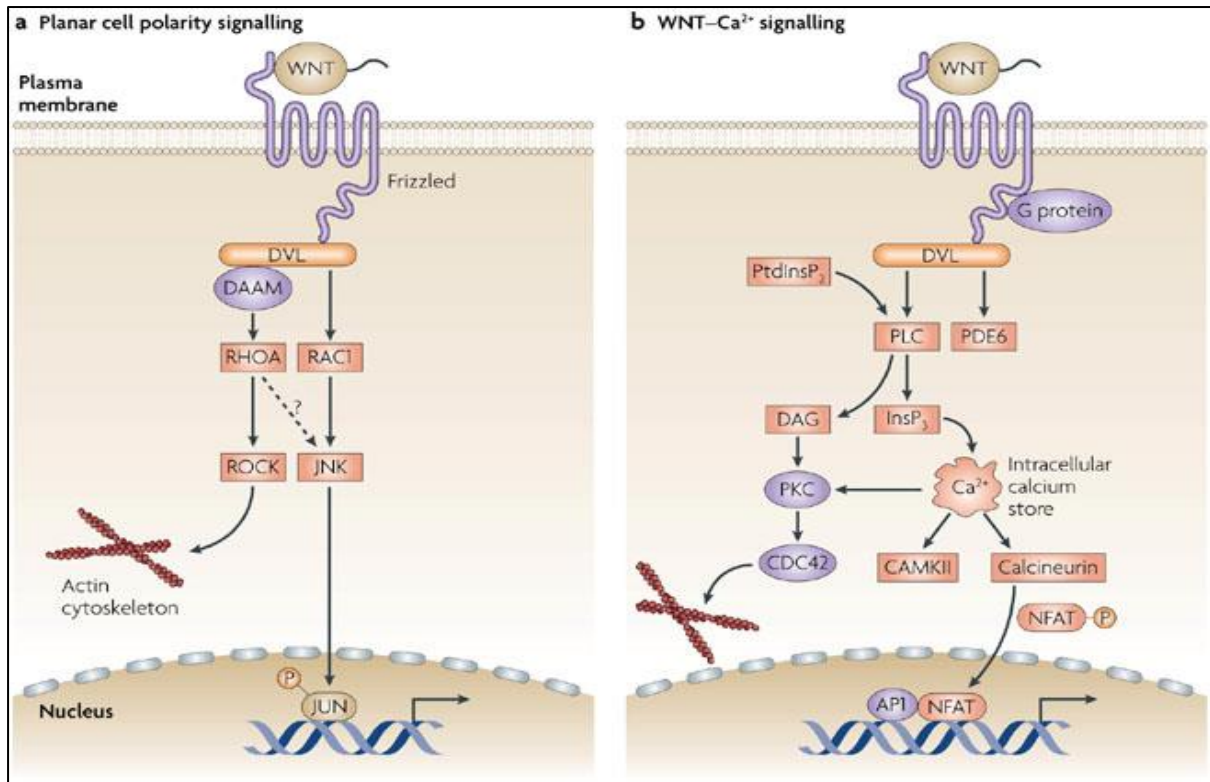


Figure 1. 6: The non-canonical Wnt signalling pathway.

Wnt ligands bind to FZD receptors and co-receptors to initiate the non-canonical Wnt pathway. Adapted from Staal *et al.*, 2015.

In addition to functioning independently of the transcriptional factor β -catenin, the non-canonical Wnt pathway does not require LRP5/6 as a co-receptor but, instead, acts via two co-receptors ROR 1/2 and RYK tyrosine kinases. However, the non-canonical pathway is still not completely understood and if the two sub-groups overlap (Hartmann, 2002; Niehrs, 2012).

The Wnt/Planar Cell Polarity (PCP) pathway has been implicated in the cell's cytoskeletal organisation by modulating actin through RhoA and c-Jun amino N-kinase (JNK). The Wnt/protein kinase C (PKC) pathway has been associated with muscle homeostasis through the activation of cyclic AMP (Staines *et al.*, 2012). In addition, the Wnt/Ca²⁺ pathway is implicated in the regulation of intracellular calcium

levels through phospholipase C and phosphodiesterase. The Wnt/Ca²⁺ pathway can also modulate the Canonical Wnt pathway through activating GSK3 β leading to β -catenin phosphorylation and its ubiquitin-proteasome degradation (Niehrs, 2012; Nusse, 2012).

1.6.2. The Canonical Wnt signalling pathway.

Of the two Wnt pathways, the canonical Wnt pathway is the more understood subgroup (Niehrs, 2012). The pathway causes the accumulation of β -catenin in the cytoplasm that eventually causes its translocation to the nucleus where it is able to act as a co-activator of the TCF/LEF family of transcription factors.

In the absence of Wnt signalling, phosphorylation of β -catenin leads to its degradation and this process is regulated by the β -catenin-destruction complex that includes the proteins: Axin, glycogen synthase kinase-3 β (GSK-3 β), casein kinase-1 (CK1) and adenomatosis polyposis coli (APC). The scaffold protein axin interacts with

GSK3 β and CK1a and this interaction results in the initial phosphorylation of β -catenin by CK1 at serine-45, followed by additional phosphorylation by GSK3 β at serine-33, serine-37 and threonine-41. The phosphorylation of β -catenin results in its degradation by β -Trcp through ubiquitination and proteasome degradation mechanism (Figure 1.7) (MacDonald *et al.*, 2009).

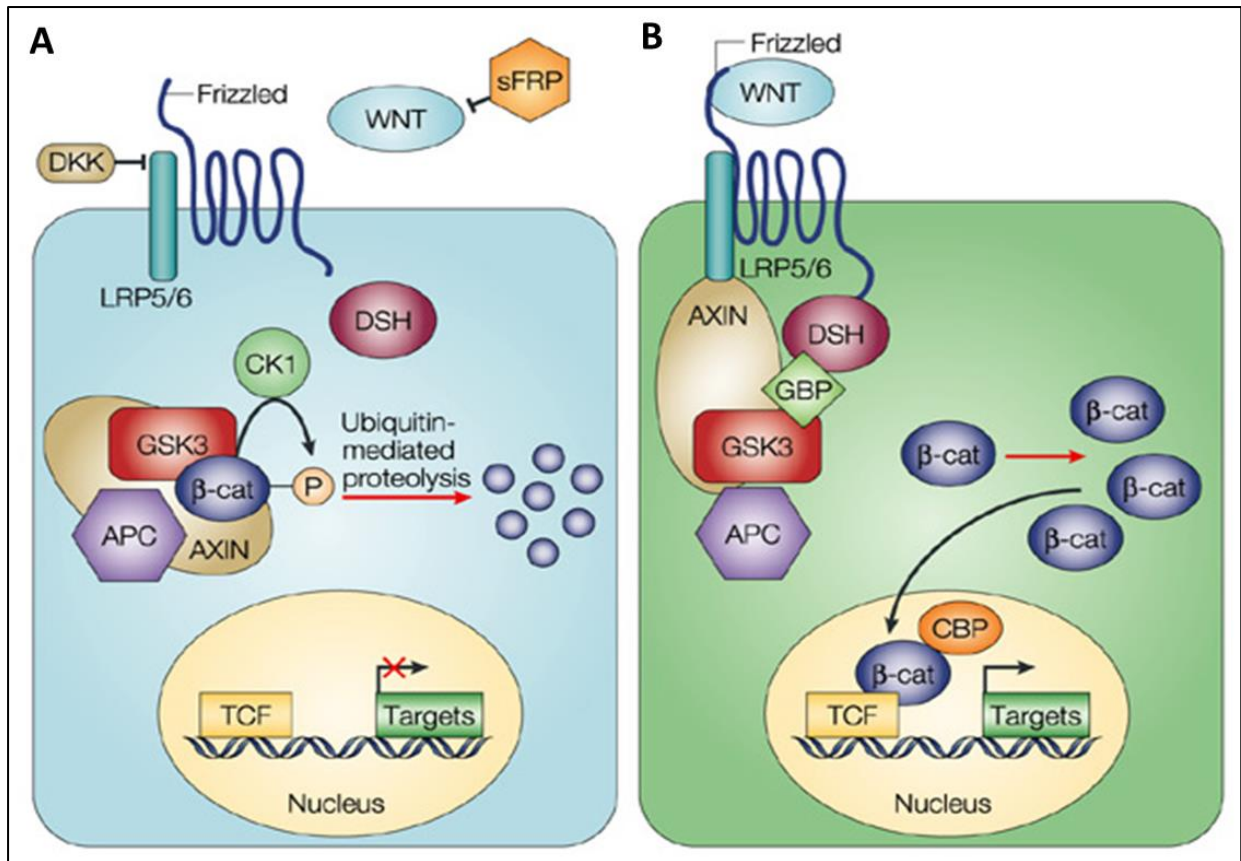


Figure 1. 7: Schematic diagram of the canonical Wnt signalling pathway.

Wnt ligands bind to FZD receptors and LRP5/6 co-receptors to initiate the canonical Wnt pathway. (A) In the absence of appropriate Wnt ligand binding, because of inhibitors such as sFRP and Dkk-1, GSK3 becomes phosphorylated. This, in turn, phosphorylates β -catenin. Phosphorylated β -catenin is subsequently targeted for ubiquitination and proteasome degradation. (B) Upon binding, Dishevelled is activated which in turn, inhibits GSK3 activity. This inhibition allows translocation of β -catenin to the nucleus where it activates the transcription of Wnt-associated genes. Adapted from Moon *et al.*, 2009.

1.6.3. Frizzled receptors (FZD) and co-receptors.

Wnt proteins are known to interact with FZD receptors and LRP 5/6 co-receptors to mediate the signalling cascades of the Canonical Wnt pathway. To date ten frizzled receptors have been discovered in humans (Nusse, 2012). Frizzled receptors are cell-surface trans-membrane receptors that all share a similar structural uniformity. They are comprised of an extracellular domain (N-terminus) with a highly conserved cysteine-rich region, seven trans-membrane domains, and an intracellular carboxyl

domain (Figure 1.8) (Niehrs, 2012). Of the already discovered Wnt co-receptors, low density lipoprotein receptor-related protein receptors 5 and 6 (LRP5/6) are the most studied. LRP5/6 is a single-span trans-membrane protein that is a key regulator of the Canonical Wnt pathway.

The interactions of LRP5/6 with FZD receptors in the presence of the ligand is thought to lead to LRP5/6 phosphorylation in the intracellular domain, which in turn, results in the internalisation of co-receptor-ligand complex (Xu and Nusse, 1998; Huang and Klein, 2004; Yamamoto *et al.*, 2008; Niehrs, 2012; Tauriello *et al.*, 2012).

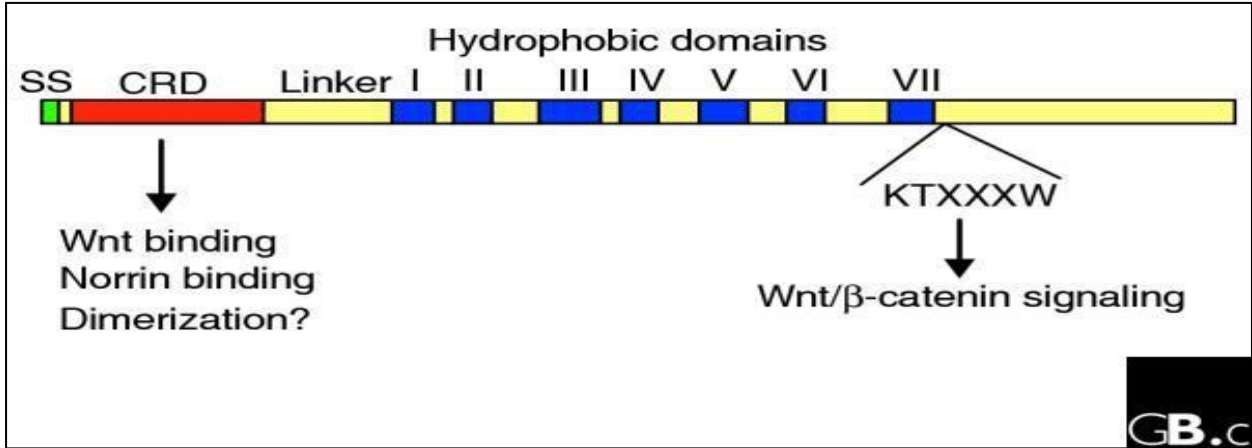


Figure 1. 8: A schematic diagram of the Frizzled receptor structure.

Adapted from Huang and Klein (2004).

Binding of the Wnt ligands to Frizzled (FZD) - LRP5/6 receptor complexes, at the cell surface, induces activation of the dishevelled scaffold proteins (Dsh) and subsequent phosphorylation-dependent recruitment of axin to LRP5/6 co-receptor. This leads to the disassembly of β -catenin from the axin complex. De-phosphorylation of axin subsequently leads to the activation of Dsh through phosphorylation of this protein (DIX and PDZ domains). This activation inhibits GSK3 activity resulting in the

accumulation of β -catenin in the cytoplasm and the translocation to the nucleus by a process yet to be elucidated (Figure 1.8B). This nuclear shuttling of β -catenin from the cytoplasm leads to the activation of the lymphoid enhancing factor (LEF) and T-cell factor (TCF) transcription factors. This, in turn, results in a wide range of downstream target gene activations, such as the activation of c-Myc, Cyclin D1 and Axin2 that regulate cell proliferation, differentiation, adhesion and migration (Tauriello *et al.*, 2012; Niehrs, 2012).

1.6.4. Cytoskeletal role of the β -catenin family.

In addition to this transcriptional role of β -catenin it is worth mentioning that β -catenin and other members of the catenin family, such as P120-catenin, α -catenin and γ -catenin (plakoglobin) are also involved in the cytoskeleton in association with cadherin and actin. Recently two tyrosine kinases (Fyn and Fer kinase) were noted to be able to phosphorylate β -catenin at amino acids Y-486 and Y-654 resulting in a release of β -catenin from its association with adherent junction proteins such as cadherin, catenin and actin. Cytoskeletal β -catenin phosphorylation at Y-486 and Y-654 is thought to result in free β -catenin accumulating in the cytoplasm. This results in the nuclear factor activation of TCF/LEF transcriptional activation hence by-passing the FZD-LRP-5/-6 surface receptors (Xu and Nusse, 1998; Tominaga *et al.*, 2008; Fujimori *et al.*, 2010).

1.6.5. Modulators of the Wnt signalling pathways: Wnt ligands.

Regulation of the Wnt signalling pathway is controlled by a group of secretory proteins (Wnt proteins) that can act in two distinctive and often opposing ways. One common feature associated with the two Wnt signalling pathway sub-groups is that

Wnt proteins directly interact with the cell-surface receptor frizzled proteins and associated co-receptors to propagate their cellular effect. The canonical and non-canonical pathways differ in the co-receptors used. The canonical pathway is dependent on interaction with the LRP5/6 co-receptor whilst the non-canonical pathway is dependent on interactions with co-receptors, Receptor RORS and RYK tyrosine kinase. So far at least 19 Wnt ligands have been identified and 7 of these have been associated with activation of the canonical Wnt pathway. Activation of either pathway has a wide range of effects on different tissues from being agonist as well as antagonist to key homeostatic functions (DeLise *et al.*, 2000; Niehrs, 2006; Niehrs, 2012).

1.6.6. Alternate activators (ligands) of the Wnt Canonical pathway.

There are now several new activators of the canonical Wnt/ β -catenin pathway, which include Norrin and Roof plate-specific Spondin (R-Spo) (de Lau *et al.*, 2012). The R-Spo family of proteins are members of a superfamily of thrombospondin type 1 repeat (TSR-1) proteins that are characterised by a TSR-1 domain in addition to the presence of two adjacent furin-like cysteine-rich repeats near the amino terminus of the mature protein. To date, there are four members of the R-Spo protein family (R-Spo 1-4) that have been described in literature (de Lau *et al.*, 2012). Despite R-Spo proteins being structurally dissimilar to the Wnt ligands they are able to activate the Wnt/ β -catenin pathway by either enhancing the activity of Wnt ligands or directly activating the Wnt/ β -catenin pathway. They achieve this by binding to leucine-rich repeat-containing G-protein coupled receptors (LGR 4-6) (Wen *et al.*, 2009; Carmon *et al.*, 2012; de Lau *et al.*, 2014).

1.6.7. Mechanism of inactivating the canonical Wnt pathway.

Inactivation of the canonical Wnt pathway can occur through the internalisation of the Wnt receptors (FZD) and co-receptor complex by Caveolin and Clathrin dependent endocytosis (Niehrs, 2012). In addition, interactions of the co-receptors Kremen-1 & -2 with the co-receptor LRP5/6 was shown to favour inhibition of the Wnt canonical pathway by increased endosome acidification leading to endocytosis of co-receptors. This interaction prevents the formation of the Wnt protein-Fzd-LRP5/6 complex required for β -catenin de-phosphorylation and accumulation in the cytoplasm and translocation to the nucleus (Mao *et al.*, 2001; Yamamoto *et al.*, 2008).

1.6.7. Wnt antagonist proteins.

Several classes of proteins have been noted to be involved in the modulation of the Wnt pathway. These Wnt modulators act either by directly binding to the frizzled receptors or co-receptors or binding to Wnt ligands, thereby inhibiting their mode of action. These known inhibitors include: secreted frizzled-related proteins (sFRPs), Wnt inhibitory factors (Wif), Wnt inhibitory secreted proteins (WISP), Sclerostin (SOST), and the Dickkopf proteins (Dkks) (Bafico *et al.*, 2001; Surmann-Schmitt *et al.*, 2009).

The Dkk family of secreted glycoproteins have protein cores ranging from 250-350 amino acids and molecular weights of 25-40 kDa (Niehrs, 2006). They consist of four members (1-4) that antagonise the Wnt signalling pathway by binding to the co-receptors LRP5/6, Wnt or Kremen-1/2. It is believed that the Dickkopf proteins only act on the canonical Wnt pathway. Studies have demonstrated that Dkk-1 forms a ternary complex with co-receptors LRP-6 and Kremen-1. This induces rapid endocytosis of the complex leading to β -catenin inhibition. Inactivation by Dkk results

in LRP-5/-6 receptor regulation via internalisation to the lysosomes. Once in the lysosome compartment the receptors are degraded. Alternatively, Dkk signalling can be modulated by ubiquitination of its frizzled receptors through ubiquitin ligase (Niehrs, 2006; Yamamoto *et al.*, 2008).

In the musculoskeletal system, SOST is mainly secreted by osteocytes. It interacts with LRP-5/6 co-receptors and is believed to be a key negative regulator of bone formation. This role is mediated by opposing the osteogenic role of growth factors such as BMP that is known to activate osteoblasts while favouring bone turnover by activating osteoclasts. Similar to Dkk proteins, SOST have preferential specificities to bind to the LRP5/6 co-receptors. More recently LRP-4, another member of the low-density lipoprotein family, was also noted to be a co-receptor for SOST in the bone tissue (Chan *et al.*, 2011; Staines *et al.*, 2012).

1.7. The role of Wnt pathways in OA.

Accumulating evidence is emerging, that the Wnt pathway plays a pivotal role in the homeostasis of many tissues including that of the skeletal system. Genome wide association studies of the genetics of OA have shown that several Wnt inhibitor genes have single nucleotide polymorphism mutations that predispose to OA (Hartmann, 2006; Luyten *et al.*, 2009). Recently, a number of human genome analyses studies on patients with osteoarthritis have identified a single nucleotide polymorphism mutation in the FRZB allele on chromosome 12. This mutation leads to the substitution of the amino acid Arg-200 in the FRZB to tryptophan and the amino acid Arg-324 to glycine. This substitution indicates that these changes may be a marker for predisposition to knee or hip osteoarthritis, respectively (Loughlin *et al.*, 2004; Lories *et al.*, 2007b ;

Rodriguez-Lopez *et al.*, 2007). Interestingly, knockout of the FRZB gene in mice did not exhibit degenerative joint changes (Lories *et al.*, 2007b). However, upon cytokine or surgical induction of joint damage, FRZB^{-/-} mice showed accelerated joint damage compared to their normal wild-type littermates. In addition to FRZB, other members of the secreted frizzled related proteins have been associated with development of osteoarthritis in *in vitro* and *in vivo* models. For example, sFRP-1, -2 and -4 have all been reported to be over-expressed in synovial tissue from osteoarthritic patients (Imai *et al.*, 2006; Luyten *et al.*, 2009; Staines *et al.*, 2012).

Polymorphisms of LRP-5 and LRP-6 have also been associated with increased risk of OA development in the spine (Luyten *et al.*, 2009). Up-regulation of LRP-5 in mice increased the expression of β -catenin and resulted in a down-stream activation of cartilage matrix degradation enzymes (i.e. ADAMTS & MMPs). Blocking of LRP-5 in human articular cartilage chondrocytes using siRNA resulted in a reduction of matrix metalloproteinase-13 levels and, therefore, might have a protective role against cartilage degradation (Papathanasiou *et al.*, 2010). In addition, the role of LRP-5 was found to be crucial in the development of the eye and skeletal system and mutational loss of function of LRP-5 in humans was found to cause osteoporosis pseudoglioma (Gong *et al.* 2001; Riancho *et al.* 2011). In mouse models of LRP-5 knockout, it was found that LRP-5 had a crucial role in the bone mineral density of the mouse (Cui *et al.* 2011)

The role of SOST, an inhibitor of the canonical Wnt signalling pathway, has been implicated in the homoeostasis of bone tissue. Its role in the pathogenesis of OA has been investigated by Chan *et al.* (2011). This study has found there was a decreased number of SOST-positive osteocytes in human OA patients.

Elevated biochemical serum levels of FRZB were associated with a reduction in radiographic hip osteoarthritis, while elevated levels of Dkk-1 were noted to be protective in radiographic hip osteoarthritis (RHOA) in humans (Lane *et al.*, 2007).

Wnt-1 induced secreted protein 1, a member of CCN family closely associated with Wnt-1, has been found to be present where osteoarthritis is diagnosed. WISP-1 is up-regulated in OA and using *in vitro* and *in vivo* models of WISP-1 over-expression, has revealed that WISP-1 cartilage degradation is mediated by down-stream activation of aggrecanase and matrix metalloproteases (Blom *et al.*, 2009).

1.8 Surgical treatment modalities for osteoarthritis.

Treatment modality of end-stage OA involves a surgical procedure known as joint arthroplasty. This procedure requires surgical resection of the damaged cartilage and underlying bone, as well as other associated soft tissues before a metallic prosthetic joint is implanted. Joint arthroplasty, despite being successful for end-stage OA, can have a number of drawbacks. These range from the technical complexity associated with the surgical procedure and the aftercare, to the limited life-span of the prosthetic device and ultimately, the need for surgical revisions thus requiring multiple operations during the patient's life-time which is necessitated by mechanical failure. Therefore, younger patients suffering from end-stage OA and requiring joint arthroplasty are discouraged from having joint replacement before their 6th decade. This is to avoid technical difficulties associated with multiple "surgical revisions" (Luyten *et al.*, 2009; Hollander *et al.*, 2010). In addition, joint replacement is contra-indicated in patients with other medical co-morbidities including cardiovascular diseases and obesity. These issues demonstrate why finding alternative and effective

treatment for a large number of excluded patients are paramount. The impact of this disease is felt throughout society and can be measured, for example, by the 36 million working days lost per-year which equates to a £3.2 billion loss for the UK economy (National Collaborating Centre for Chronic Conditions, 2008, Arthritis and Musculoskeletal Alliance, 2004).

1.9 Overview of ACI and MSCs repair of cartilage defects.

The current “gold” standard for repair of small cartilage defects is a cell-based therapy named autologous chondrocyte implantation (ACI). This involves invasive harvesting of chondrocytes from un-damaged areas, followed by *in vitro* expansion of the chondrocytes for several weeks. The cells are then seeded back into the symptomatic area beneath a periosteal flap covering the defect area or, alternatively, are embedded in a synthetic matrix plug to fill the defect (Brittberg *et al.*, 1994). Despite the success of this technique in alleviating symptoms, the resultant tissue is fibro-cartilaginous, which is inferior to the hyaline cartilage found in synovial joints (Diaz-Romero *et al.*, 2005; Khan *et al.*, 2009). Several studies, mainly using animal models, have been carried out to explore the potential use of autologous mesenchymal stem cells (MSC) as an alternative cell source for cartilage repair (Tuan *et al.*, 2003; Yan and Yu, 2007). Due to their inherent regenerative potential, chondroprogenitor cells and mesenchymal stem cells of multiple origins are of a significant interest in the field of orthopaedic medicine as they can be used for cartilage regeneration. In addition, MSCs have been noted to have an immune-modulatory response which enhances their regenerative potential (Petrie Aronin and Tuan, 2010)

Mesenchymal stem cells (MSC's) are multipotent cells that are capable of differentiating into the mesenchymal lineages; bone, cartilage and adipose tissue (Giordano *et al.*, 2007; Yang *et al.*, 2011). The classic source of adult MSCs, first described by Friedenstein, has been from bone marrow (Bianco *et al.*, 2001). However, in recent years adult mesenchymal stem cells have been isolated from numerous tissue sources including peripheral blood and adipose tissue. Several approaches were adopted in cartilage tissue engineering including injection of MSCs directly into the defect and placement of periosteal flap or lately embedding MSCs in a synthetic matrix plug to fill the defect. Despite the success of this technique in alleviating symptoms, the resultant tissue is cartilaginous tissue that is unstable and undergoes hypertrophic differentiation (McCarthy *et al.*, 2012). In 2001 Hayes *et al.* (2001) demonstrated that hyaline cartilage grew by apposition i.e. from the surface zone migrating downwards (Archer *et al.*, 1994; Hayes *et al.*, 2001). Building on this knowledge, Dowthwaite *et al.* (2004) isolated a rare cohorts of chondrocytes from immature articular cartilage which had higher expression of integrin expression and stem cells marker Notch-1, termed cartilage progenitor cells (CPC). These cells when further characterised were noted to have plasticity by being able to differentiate into cartilage, bone and adipose tissues as well as being able to retain their phenotype while undergoing extensive proliferation (Khan *et al.*, 2009; Williams *et al.*, 2010). These studies supported the notion that stem/progenitor cells, that are isolated from articular cartilage, could be suitable source for tissue regeneration of articular cartilage.

1.10. The role of the Wnt pathway in Chondrogenesis.

The most studied Wnt pathway ligand is thought to be Wnt3a. It has been shown to affect chondrogenesis by inhibiting the potential of mesenchymal precursor cells in chondrogenic differentiation. It is believed that Wnt-3a acts on the Wnt pathway via activating the canonical β -catenin. This activation leads to β -catenin nuclear translocation with widespread down-stream cellular activities, which affect cell fate, such as, cell proliferation, differentiation and activation of catabolic pathways. The inhibitory role of Wnt-3a on chondrogenesis of mesenchymal stem cells has been documented to favour osteogenic differentiation, in an *in vitro* setting (Hartmann; 2002; Goldring *et al.*, 2006; Hartmann, 2006).

The role of Wnt-3a has also been associated with BMP and Ihh as well as PTHrP-inducing chondrocyte hypertrophy and endochondral ossification. Similar to the role of Wnt-3a in chondrogenesis, other Wnt ligands were also shown to elicit a negative effect on chondrogenesis in *in vivo* experiments. For example, conditional over-expression of Wnt7a, which is localised to the developing limb bud and regulates dorsal-ventral patterning led to inhibition of chondrogenesis by affecting mesenchymal precursor cell condensation (Hartmann and Tabin, 2001; Goldring *et al.*, 2006; Spater *et al.*, 2006; Staines *et al.*, 2012). In addition, Wnt-1, Wnt-4, and Wnt-9a have a similar inhibitory role on chondrogenesis (Spater *et al.*, 2006; Hidaka and Goldring, 2008).

In addition to investigating the role of Wnt proteins, the role of Wnt antagonist proteins on chondrogenesis and limb development have also been investigated. For example, the effects of Wnt inhibitory factor-1 (Wif-1) and Wnt antagonist proteins on

chondrogenesis were investigated using chick embryos (Surmann-Schmitt *et al.*, 2009). They found that Wif-1 expression occurred during early chondrogenesis of the synovial joint of the chick. Levels of Wif-1 were sustained throughout chondrogenesis and in association with the chondrogenic transcriptional factor Sox-9. However, spatial expression of Wif-1 was confined to the superficial zone of the articular cartilage, hence preventing chondrocytes from undergoing terminal differentiation and hypertrophic maturation. This early expression of Wif-1 was thought to be counteracting Wnt-3a that is a potent canonical Wnt pathway agonist (Surmann-Schmitt *et al.*, 2009).

An *in vitro* chondrogenic model of a murine chondrocyte cell line demonstrated Wif-1 to promote cartilage nodule formation by blocking the inhibitory role of Wnt-3a. This inhibition was found to be dose dependent and, in the absence of the exogenous Wnt3a, Wif-1 still showed stimulation of cartilage nodule formation. This result might be explained by Wif-1 inhibiting endogenous Wnt3a levels (Surmann-Schmitt *et al.*, 2009; Luyten *et al.*, 2009; Staines *et al.*, 2012).

The role of the Wnt pathway also extends to hypertrophic differentiation and endochondral ossification of chondrocytes. Constitutive over-expression of the Wnt pathway components during *in vivo* experiments, involving mature chondrocytes from the chick sternum, has shown that over-expression of β -catenin leads to hypertrophic differentiation, evidenced by up-regulation of Runx-2 and collagen type X with concomitant reduction of collagen type II (Tamamura *et al.*, 2005; Dong *et al.*, 2006).

1.11 PhD hypothesis.

Articular cartilage contains a cohort of cells named chondrocyte progenitor cells (CPC) that have the selective advantage of long-term proliferation whilst maintaining their phenotype (Dowthwaite *et al.*, 2004; Khan *et al.*, 2009; Williams *et al.*, 2010). In immature bovine cartilage, CPC have been localised to the surface zone (Dowthwaite *et al.*, 2004; Hayes *et al.*, 2008). Recently, CPC's were also found in mature articular cartilage of several species including that of humans (Alsalameh *et al.*, 2004a; Fickert *et al.*, 2004; Koelling *et al.*, 2009; Williams *et al.*, 2010; McCarthy *et al.*, 2012).

Current literature indicates that the Wnt signalling pathway plays a vital role in the homeostasis and pathological changes affecting articular cartilage, subchondral bone, and surrounding soft tissues during osteoarthritis. These data convincingly suggests that the Wnt pathway may form a potential therapeutic target for OA. This approach might reduce synovial joint tissue degradation and, therefore, delay the need for more drastic surgical intervention. Both ligands and receptors of the Wnt signalling pathway have been localised within articular cartilage during development, hence, suggesting a role in controlling proliferation of articular cartilage chondrocytes.

The aim of this thesis is to further our understanding of the role that the Wnt pathway plays in the pathogenesis of OA. We hypothesise that in adult human cartilage, the Wnt signalling pathway may play a role in the pathogenesis of osteoarthritis through the regulation of the cartilage progenitor cell's fate and at the interface of articular cartilage and subchondral bone in mechanisms of a repair response. The experimental work in this thesis firstly, focuses on the unique population of mesenchymal progenitor cells isolated from normal and osteoarthritic human articular cartilage, herein named chondrocyte progenitor cells (CPC). Secondly,

the experimental work focuses on the interaction of cells within the cartilage-bone interface with a view to understanding the role of Wnt proteins in the breakdown and attempted repair of the tissue.

In order to achieve these aims, the objectives of this study are to:

1. Isolate and characterise human CPC and BM-MSCs from the knee joint of subjects undergoing knee arthroplasty.
2. Investigate the expression of Wnt proteins in CPC from normal and osteoarthritic articular cartilage.
3. Study the tissue distribution of the Wnt antagonists Dkk-1 in osteoarthritic tissue.
4. Examine the chondrogenic differentiation potential of CPC from normal and osteoarthritic articular cartilage and whether differences in the Wnt antagonist protein Dkk-1 expression has an effect on the 3D-pellet generated cultures.
5. Characterise the angiogenic properties of Wnt pathway proteins possibly thought to be involved in osteoarthritis.
6. Design a co-culture model system in order to investigate the possible interaction of chondrocytes and endothelial cells which might provide further insight in to cross-talk that occur during osteoarthritis.

CHAPTER 2: GENERAL MATERIALS AND METHODS.

2.1 Materials

The general reagents and materials used in this thesis are listed in table 2.1 below.

Table 2. 1: Commercial source of reagents and materials used.

| Material | Source |
|--|---|
| Agarose | Fisher Scientific, Loughborough, UK. |
| Amersham ECL Western Blotting Detection Reagent | Amersham GE Healthcare, Buckinghamshire, UK. |
| Amersham Hyperfilm ECL | Amersham GE Healthcare, Buckinghamshire, UK. |
| Ammonium persulfate (APS) | Fisher Scientific, Loughborough, UK. |
| Anti-mouse horseradish-peroxidase-linked IgG (source: sheep) | Amersham GE healthcare, Buckinghamshire, UK. |
| Anti-rabbit horseradish-peroxidase-linked IgG (source: donkey) | Amersham GE Healthcare, Buckinghamshire, UK. |
| Aprotinin | Sigma-Aldrich, Dorset, UK. |
| Acrylamide/bis-acrylamide (30% solution (v/v), 29:1 ratio) | Sigma-Aldrich, Dorset, UK. |
| Bovine Serum Albumin | R&D bio systems, Abingdon, UK. |
| Bromophenol blue | Sigma-Aldrich, Dorset, UK. |
| Cell culture medium | Sigma-Aldrich, Dorset, UK. |
| Cell Proliferation Reagent WST-1 | Roche Diagnostics, Burgess Hill, UK |
| Chondroitinase ABC from <i>Proteus vulgaris</i> | Sigma-Aldrich, Dorset, UK. |
| Cloning rings (6mm) | Sigma-Aldrich, Dorset, UK. |
| Cocktail of protease and phosphatase inhibitors | Sigma-Aldrich, Dorset, UK. |
| collagenase type II <i>Clostridium Histolyticum</i> | Worthington Biomedical, distributed by Lorne Laboratories Ltd, Reading, UK. |
| Cryotube™ vials (1.8ml, starfoot, round) | Nalgene, Nunc Int, Roskilde, Denmark |
| Dimethyl sulphoxide | Sigma-Aldrich, Dorset, UK. |
| Di-thiothreitol (DTT) | Promega, Southampton, UK. |

| | |
|---|--|
| dNTPs (dAPT, dCTP, dTTP, dGTP; 100 mM) | Promega, Southampton, UK. |
| Endothelial Cell Growth Medium (Basal medium + Growth supplements) | Promocell, Heidelberg, Germany. |
| Ethidium Bromide (EtBr) | Sigma-Aldrich, Dorset, UK. |
| Ethylene diamine tetraacetic acid | Sigma-Aldrich, Dorset, UK. |
| Foetal bovine Serum (FBS) | Sigma-Aldrich, Dorset, UK. |
| Glacial acetic acid | Fisher Scientific, Loughborough, UK. |
| Glycerol | Fisher Scientific, Loughborough, UK. |
| Glutaraldehyde (25%) | Agar Scientific, Stansted, UK. |
| GoTaq® Flexi DNA Polymerase kit | Promega, Southampton, UK. |
| Hydrochloric acid (HCL; 5M) | Fisher Scientific, Loughborough, UK. |
| Hyaluronidase from Streptomyces | Sigma-Aldrich, Dorset, UK |
| Indomethacin | Sigma-Aldrich, Dorset, UK |
| Low base DNA ladder | New England Biolabs, UK. |
| N,N,N',N'-tetramethylene-diamine (TEMED) | Sigma-Aldrich, Dorset, UK. |
| Notch-1 (M-20) antibody | Santa Cruz Biotech, USA distributed by Insight Biotechnology, Wembley, UK. |
| Novex® 12% Tris-Glycine Protein Gels | Life technologies, Paisley, UK. |
| pH calibration buffers tablets (pH 4, 7 and 10) | Fisher Scientific, Loughborough, UK. |
| Pierce™ BCA Protein Assay Kit | Thermofisher Scientific, Loughborough, UK. |
| Precision Plus Protein™ All Blue Standards (10-250kDa) | Bio-Rad Laboratories, Herts, UK |
| Pronase from Streptomyces griseus | Roche Diagnostics, Burgess Hill, UK |
| Random hexamers | Promega, Southampton, UK. |
| Recombinant RNase inhibitor | Promega, Southampton, UK. |
| RNase-free molecular water | Sigma-Aldrich, Dorset, UK. |
| SafeView Nucleic Acid Stain | NBS Biologicals, Huntingdon, UK. |
| Sodium dodecyl sulphate (SDS) | Sigma-Aldrich, Dorset, UK. |
| Sodium hydroxide (NaOH; 5M) | Fisher Scientific, Loughborough, UK. |
| Solvents (acetone, chloroform, ethanol, formaldehyde, isopropanol and methanol) | Fisher Scientific, Loughborough, UK. |
| Sterile bijoux tubes | Bibby Sterlin Ltd, Staffordshire, UK. |
| Sterile Falcon tubes (15 mL and 50 | Corning Inc., NY, USA |

| | |
|--|---|
| ml) | |
| Sterile phosphate buffered saline with ACE | Sigma-Aldrich, Dorset, UK. |
| Sterile syringe filters (0.2µm) | VWR, Soulbury, UK. |
| Sterile tissue culture plasticware (flasks, dishes and plates) | Corning life sciences distributed by Fisher Scientific, Loughborough, UK. |
| SuperScript™ III Reverse Transcriptase | Life technologies, Paisley, UK. |
| SYBR Green KicqStart Taq ReadyMix | Sigma-Aldrich, Dorset, UK. |
| TGFβ-2, FGF-basic, VEGF-A, Dkks recombinant proteins | PeproTech Ltd, London, UK. |
| Transwell filter insert (8 um, 0.2um) | Millipore distributed Fisher Scientific, Loughborough, UK. |
| TRI Reagent | Sigma-Aldrich, Dorset, UK. |
| Tris HCL | Sigma-Aldrich, Dorset, UK. |
| Triton X-100 | Sigma-Aldrich, Dorset, UK. |
| Trizma (Tris) base | Sigma-Aldrich, Dorset, UK. |
| Trypsin/EDTA 10x solution | Sigma-Aldrich, Dorset, UK. |
| TRyPLE | Life technologies, Paisley, UK. |
| Tween-20 | Sigma-Aldrich, Dorset, UK. |
| Ultra-low attachment spheroid Microplate | Corning life sciences distributed by Fisher Scientific, Loughborough, UK. |

2.2 Methods.

2.2.1 Human Tissue material.

Tibial plateaux and matched bone marrow aspirate (tibial plateaux), used in this study were obtained from clinically diagnosed OA patients undergoing total knee arthroplasty at the University Hospital Llandough, (n=10 mean age 56 yrs.; range 53-70). South East Wales Research Ethics Committee safety and ethical guidelines were followed in this study (Ethical codes 10/MRE09/28 and 09/WSE04/35). Written informed consents were obtained from each patient involved prior to sample acquisition. Tibial plateaux were obtained from healthy donors through Dr. Paul Rooney at the National Health Service Blood and Tissue Service, Liverpool (n=6, mean age=43, range=29-55).

2.2.2 Isolation of human cartilage chondrocytes and cartilage progenitor cells (CPC).

Cartilage was dissected from the tibial plateau of normal and OA donors (normal n=5, OA n=6), diced and digested with pronase (70 U /mL) in DMEM containing 5% (v/v) Foetal Bovine Serum (FBS) and penicillin/streptomycin (100 µg/mL) herein named DMEM-FBS-PS for 1hr at 37°C with constant agitation. Following removal of the pronase solution the tissue was further incubated overnight with collagenase (300 U /mL) in DMEM-FBS-PS for 3hrs at 37°C with constant agitation (Williams *et al.*, 2010). The cells were then filtered through a 40µm Nylon filter and the chondrocytes pelleted by centrifugation at 400 x g and re-suspended in 10 ml of DMEM containing penicillin/streptomycin herein named DMEM-PS. A cell count was taken using a bright light haemocytometer and isolated chondrocytes were either seeded into T75cm²

flasks at 0.5×10^6 cells/flask in DMEM containing 10% FBS and penicillin/streptomycin (100 $\mu\text{g}/\text{mL}$), herein named Basal Medium, or further subjected to the differential fibronectin adhesion assay to isolate cartilage progenitor cells (CPC) as described by Dowthwaite *et al.* (2004). Briefly, isolated chondrocytes were re-suspended at 1000 cells /mL in DMEM-PS and 1 ml of the cell suspension was seeded into each well (35 mm) of a 6 well cell culture plate pre-coated with fibronectin (10 $\mu\text{g}/\text{mL}$ in PBS containing 1mM MgCl_2 and 1mM CaCl_2 for 24 hours at 4°C). Seeded 6 well plates were incubated for 20 minutes at 37°C after which the medium containing the non-adherent cells was gently removed and discarded. The remaining adherent cells were then cultured in 2ml Basal medium overnight at 37°C in a humidified atmosphere of 5% CO_2 . After one day post-plating, medium was changed facilitating further removal of dead and non-adherent cells, and the number of adherent cells were counted and recorded as the initial cell adherence. Medium was changed every 4 days and at 10 days post-plating, the number of colonies (≥ 32 cells) formed were counted. The percentages of colony forming efficiency was calculated using the following formula:

$$CFE = \left(\frac{\text{Number of colonies at day 10} (>32 \text{ cells})}{\text{Number of the initial cells seeded}} \right) \times 100$$

Between 10 and 14 days of culture incubation on fibronectin coated plates, single colonies of cells (>32) were encircled using a sterile cloning ring (8mm, C7983, Sigma-Aldrich) to facilitate harvest of a population of cells derived from the descendants of one cell. These monoclonal CPC lines were transferred into individual wells of a 24 well plate and expanded as a population of cells from a single cell origin. In addition, colonies formed two weeks after initial plating were expanded without selection to generate a number of heterogeneous polyclonal CPC lines. Both cartilage progenitor cell lines (i.e. monoclonal and polyclonal) were maintained in Basal

medium containing 1 ng/mL transforming growth factor β 2 (TGF- β 2; PeproTech, UK) and 5 ng/mL fibroblast growth factor-2 (basic FGF₂; peproTech, UK), herein named CPC maintenance medium (Williams *et al.*, 2010). Medium was changed thrice weekly and passaged at approximately 70% confluence (2.2.4). Figure 2.1 presents an overview of the cell populations used in further studies.

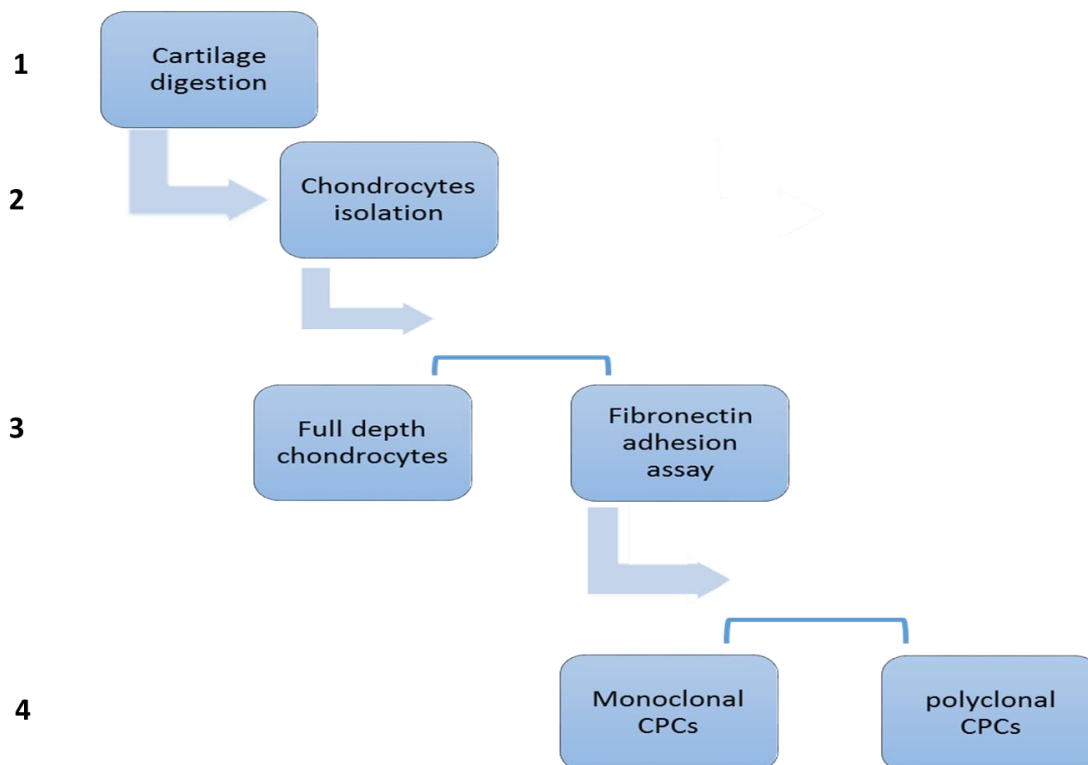


Figure 2.1: Schematic diagram illustrating the isolation procedure for chondroprogenitor cells (CPC) from articular cartilage.

2.2.3. Isolation of human Bone marrow mesenchymal stem cells.

For the isolation of bone marrow derived stem cells, bone marrow fluid aspirates (2–10 mls) were obtained from the medullary cavity of the tibial plateaux (n=5) and immediately mixed with 10 ml Basal medium. The resultant mix was layered gently on Ficoll-Paque PLUS (GE Healthcare Life Sciences, UK), 2 x 10 ml aliquots in 50 ml conical tubes. Tubes were centrifuged at 900 x g for 30 minutes at 18°C after which

the upper layer was removed leaving the mononuclear cell layer (buffy coat) undisturbed at the interface. This "buffy coat" containing the mononuclear cells was carefully harvested with a 19-gauge needle attached to a 5 mL syringe and transferred to a sterile 50 ml falcon-tube. The cells were washed by centrifugation (10 minutes at 750 x g) in Basal medium. A cell count was taken using a bright light haemocytometer and cells were re-suspended in an appropriate volume of Basal medium containing 5ng /mL fibroblast growth factor-2 (basic-FGF₂) for plating at a seeding density of 2 x 10⁶ per well (35 mm) in 6 well culture plates and incubated at 37°C in a humidified atmosphere containing 5% CO₂ (Murdoch *et al.*, 2007). Medium was replaced on day 1. On day 4 medium was removed and wells rinsed using DMEM-PS to remove non-adherent cells. The adherent cells were cultured using Basal medium containing 5ng /mL FGF₂. Medium was changed thrice weekly and at cells passaged at approximately 70% confluence (2.2.4).

2.2.4. Passage of cell lines.

All cell lines (monoclonal CPC's, polyclonal CPC and BMSC's) were passaged at 70-80% confluence. Spent medium was transferred to a sterile tube and centrifuged for 5 minutes at 400 x g to remove any debris or dead cells. This conditioned medium was stored at -20 °C until required. Cells were then washed twice using DMEM-PS to remove any remaining serum prior to addition of 5 mL of 0.05% Trypsin-EDTA solution. Flasks were returned to the incubator for 5-10 minutes at 37°C after which, cell detachment was assessed using an inverted microscope. The activity of the trypsin was inactivated by the addition of an equal volume (5 ml) of Basal medium. Dissociated cells were transferred to a sterile Falcon-tube and cells were centrifuged for 5 minutes at 400 x g. Pelleted cells were gently re-suspended in 1 ml Basal

medium and a cell count was taken using a bright light haemocytometer. Cells were split 1 in 4 and re-plated, or processed for long-term storage in Liquid Nitrogen (section 2.2.5)

The Growth kinetics of all CPC and BM-MSK cell lines were calculated at each passage as population doublings (PDs), from the following equation:

$$\text{PD} = [\log (N_1) - \log (N_0)] / 0.301$$

Where N_1 is the number of cells recovered at the end of the passage and N_0 is the number of cells initially plated (Williams *et al.*, 2010). For cumulative population doubling, see Appendix 4.

2.2.5. Long-term storage and retrieval of cell lines.

At passage, cell counts were calculated and cell suspensions were then pelleted by centrifugation at 400 x g for 5 minutes after which medium was aspirated and cell pellets re-suspended in freeze medium [90% (v/v) FBS and 10% (v/v) dimethyl sulphoxide (DMSO)] at 1×10^6 cells/ ml. Cells were transferred to cryovials and 1×10^6 cells were frozen at a rate of 1°C per minutes down to -80°C in a 'Mr Frosty Freezing Container' (Nalgene, USA). Two days later, cryovials were transferred to a liquid nitrogen cylinder for long-term storage.

When required, cell lines were recovered from liquid nitrogen storage by removing the cryovials from the container and rapidly thawing the cells in a 37°C water-bath for 1-2minutes. Once thawed, cells were removed to a sterile tube containing with 10 mls

Basal medium, cells were pelleted by centrifugation (400 x g for 5 minutes) and re-suspended in an appropriate volume of basal medium and conditioned medium (1:1 ratio) and transferred to a T75 tissue culture flask. Cells were placed overnight in an incubator at 37° C with 5% CO₂ and medium was changed 24 hrs later by decanting spent medium and replacing with 10 mls of appropriate medium (section 2.1). Cells were fed thrice weekly.

2.2.3 Multipotency of derived CPC cell lines.

Monolayer cultures of polyclonal CPC cell lines from normal donors (n=3), OA donors (n=3) and matched BM-MSCs (n=3) were trypsinized, washed and counted. Cells were either processed to assess their differentiation potential toward a chondrogenic, osteogenic and adipogenic lineage.

2.2.3.1 Chondrogenic differentiation.

Cell pellets were re-suspended in DMEM + Glutamax with, 100 mg/mL Gentamicin, 50 µg/mL ascorbic acid, 1% HEPES buffer, and supplemented with 1% insulin, transferrin, selenium (ITS), 0.1 µM dexamethasone and 10 ng/mL TGF-β₂ (chondrogenic medium) at 1.2 x 10⁶ cells / ml. Cells were seeded into Corning® 96 well Ultra low attachment spheroid Microplate at 100,000 cells per well (Yamashita *et al.*, 2010, Ball *et al.*, 2014) and incubated at 37°C in a humidified atmosphere containing 5% CO₂. CPC formed aggregates within the first 24 hrs and medium was changed thrice weekly for 3 weeks after which pellets were collected for mRNA isolation (section 2.12) for analysis of chondrogenic differentiation gene expression using RT-PCR (section 2.12.3) or fixed in 70 % (v/v) ethanol for Toluidine blue staining and Safranin-O staining.

2.2.3.2 Osteogenic differentiation.

Cell pellets were re-suspended at 0.2×10^6 cells/ml in medium consisting of DMEM containing 100 mg/mL Gentamicin, 10% (v/v) FBS, 50 μ M ascorbic acid 2-phosphate, 10 mM β -glycerol phosphate, 10 nM dexamethasone and 1% (v/v) HEPES buffer (osteogenic medium) and plated into 24 well tissue culture dishes at 50,000 cells per well (Williams *et al.*, 2010). Cells were cultured over a period of 21 days at 37°C in a humidified atmosphere containing 5% CO₂ and medium was changed three times a week. After 21 days of culture in osteogenic medium cell layers were washed briefly with PBS and either fixed using 4% (w/v) paraformaldehyde fixative solution (4°C for 20 minutes.) or mRNA was extracted as described in section 2.12 for analysis of osteogenic differentiation gene expression using RT-PCR (section 2.12.3).

Fixed cell layers were washed with PBS and then stained using Alizarin Red Stain solution (2 mg /mL, alizarin red in 0.5 M acetic acid pH 4.2 adjusted using 1 % (v/v) ammonium hydroxide) for 20 minutes at room temperature to detect for the presence of calcium deposits. Cells were washed five times with PBS to remove any unbound stain, and visualised and photographed using a Nikon TE-DH100w camera attached to a Nikon Eclipse TE300 microscope (Nikon, UK).

2.2.3.3 Adipogenic Differentiation.

Cell pellets were re-suspended at 0.2×10^6 cells/ml in an adipogenic differentiation medium consisting of DMEM containing 100 mg/mL Gentamicin, 10% (v/v) FBS, 0.5 mM isobutylmethyl xanthine (IBMX), 100 μ M indomethacin, 1 μ M dexamethasone, 10 μ g/ml insulin. Cells (50,000 cells per well) were maintained in adipogenic

differentiation medium for 1 week and medium was changed three times per week. After the experimental duration, cells were washed with PBS and either fixed with 4% (v/v) paraformaldehyde for 15 minutes at room temperature or mRNA was extracted as described in 2.15 for analysis of adipogenic differentiation gene expression using RT-PCR (section 2.12.3).

Freshly fixed cells were stained with Oil Red O (0.3% (v/v) Oil red-O in 60% isopropanol made from a freshly prepared stock solution of 0.5% (w/v) Oil red-O in 100% isopropanol) to detect the lipid droplets in the differentiated cells as per published protocol (Williams *et al.*, 2009). The stain was added to the plates for 1 hour at room temperature before being washed thoroughly in distilled water. Staining was visualised and photographed using a Nikon TE-DH100w camera attached to a Nikon Eclipse TE300 microscope (Nikon, UK).

2.2.4 Cell Viability assay.

Assessment of cell viability was measured by quantifying the amount of lactate dehydrogenase (LDH) released into the medium of cultured cells using the LDH based *in vitro* toxicology assay kit (Pierce, Thermo, UK). Briefly, 50 µl of cell supernatant was transferred to 96-well microplates and 50 µl of LDH assay reaction mix was added. The plate was covered with foil paper and incubated for 30 minutes in the dark at 37 °C. The reaction was terminated by addition of 50 µl of stop solution and the absorbance was measured at a wavelength of 490 nm. Data are shown as mean ± SEM.

2.2.5 Endothelial cell culture

Human umbilical cord endothelial cells (HUVEC) were purchased from GIBCO (Life technologies, UK). Cells were routinely cultured using endothelial cell growth medium (EGM-2, Promocell, Germany). Culture medium was changed three times a week and when the cells reached 70-80% confluency, they were passaged as described in 2.2.4. Cells were routinely frozen at each passage as described in 2.2.5. Cells were not maintained beyond passage 6. After passage 3, endothelial cells were characterised for endothelial markers (Table 2.2) using flow cytometry as described in section 2.11. In addition, isolated endothelial cells were seeded at 30,000 cells per well in chamber slides and the expression of PECAM-1 was studied using immunofluorescence (section 2.8.1). In addition, human umbilical cord derived endothelial cell lines were used for some of the analysis in chapter 5 only. These cells were a kind gift from Drs. Gareth Willis and Philip James (Institute of Molecular & Experimental Medicine, Cardiff School of Medicine). HECV cell lines were maintained in basal medium and without any additional growth factors.

2.2.5.1 Wound healing assay.

Endothelial cells were seeded into a 24-well plate at 1×10^5 cells/well in basal medium and after 24 hrs each confluent monolayer was scratched using a 200- μ L plastic pipette tip to create a wounded cell-free area and then washed twice with DMEM-PS while taking care not to dislodge cells. Cells were incubated at 37 °C with DMEM-PS containing the vehicle control of 0.01% BSA, or experimental treatments of recombinant Dkk-1(100 ng/mL), Dkk-2 (100 ng/mL), Wnt-3a (100 ng/mL), lithium chloride 10 μ M, or Dkk-1 (100 ng/mL). Cells were photographed at time 0 and after

24hr using an inverted microscope, (Nikon, Japan), equipped with a digital camera. The distance between the edges of the cell-free areas was measured using the imaging program (Wimasis, Germany).

2.2.5.2 Transwell-Invasion assay.

The Transwell migration assay was performed as per published protocol described in Mandelboimet *et al.* (2006) with a few modifications. Monolayer cultures of endothelial cells were serum starved for 24 hours, trypsinized (as described in section 2.2.4) and re-suspended in serum-free DMEM-PS at a concentration of 1×10^5 cells per ml. 100 μ l of the cell suspension was seeded onto the top of the Transwell insert (8 μ m pore size) previously coated with Matrigel™ (Becton Dickinson, UK) in serum-free DMEM-PS. 1 ml of medium comprising of DMEM-PS +/- Dkk-1 (100 ng/mL), or Dkk-1+ the Dkk-1 inhibitor WAY-262611 (1 μ M) was added to the outer chamber and the plate was maintained at 37°C in a humidified atmosphere with 5% CO₂ for 24 hrs. Medium was aspirated from the Transwell insert and outer chamber and fixative reagent (4% PFA) added to the Transwell insert and the outer chamber for 15 minutes at room temperature. 1 ml of 100% methanol was distributed to the insert and outer chamber and incubated for 15 minutes at room temperature. Methanol was removed and then PBS added to the insert and outer chamber. Following this the 1 ml of Giemsa solution (Sigma, UK) was distributed to the insert and outer chamber and incubated for 15 minutes at room temperature. The insert was removed and excess staining solution removed by submerging in 2 x PBS. Cells remaining in the insert were removed using cotton buds and cells that had invaded the Matrigel™ were imaged using an inverted microscope (Nikon Eclipse TS100, Japan). Images were

taken from each insert (n=3) using a Nikon E4500 camera with x10 objective magnification and the number of cells per view manually counted.

2.2.5.3 Tube formation assay.

The Tube formation assay was performed as published in the protocol by Arnaoutova and Kleinman, (2010). Briefly, 96-well plates were coated with 'Matrigel' (50 µl/well) and coated plate were allowed to polymerize at 37 °C under 5% CO₂ for 1hr. Endothelial cells were seeded at 2×10^4 cells/well in basal medium and incubated at 37 °C in 5% CO₂ for 1hr. Medium was removed carefully from each well ensuring not to pierce through the gel and replaced with DMEM+ 0.1% (w/v) BSA; DMEM + 0.1% (w/v) BSA + Dkk-1 (100 ng/mL); DMEM + 0.1% (w/v) BSA + Dkk-2 (100 ng/mL) DMEM + 0.1% (w/v) BSA + VEGF-C (10 ng/mL) to designated wells and incubated for 24 h. To assess tube formation, cells were imaged at 0 hr and 24 hrs and cell morphology and tube structures visualised using an inverted microscope (Nikon Eclipse TS100, Japan). Images were taken from each well (n=3 per group) using a Nikon E4500 camera (Nikon, Japan). Images were analysed using Wimasis imaging software (Wimasis, Germany) for tube formation. The circular images of the wells were divided into segments and the stimulation quantified by counting the number of branching points formed within each segment. Experiments were independently repeated twice.

2.2.6 Endothelial cells and chondrocytes co-culture assay.

Transwell co-culture experiments, to study the paracrine effect of culturing chondrocytes on endothelial cells, were conducted in a 24 well setup with a 0.4 µm PTFE membrane partitioning the chambers (Millipore, UK). Briefly, 5×10^4

chondrocytes were seeded in the upper chamber and 5×10^4 endothelial cells on the bottom of the lower chamber were maintained in maintenance medium containing 5% FBS and lacking any additional growth factors. For the control experiment both upper and lower chambers contained endothelial cells. Medium from the upper and lower compartments was changed three times a week and cells were cultured for 7 days before protein (section 2.13) and RNA was extracted (section 2.12) or cells were fixed for immunocytochemistry analysis (section 2.8).

For endothelial to mesenchymal (EnMT) induction using conditioned chondrocyte culture medium, seeded cells were grown on endothelial growth medium until 70% confluency. Cells were washed twice using serum free DMEM and incubated for 8hrs with serum free DMEM. Cells were incubated with control medium consisting of DMEM + 10% (v/v) FBS or conditioned chondrocyte medium (2 days culture period). Cells were incubated for 7 days at 37 °C in a humidified incubator with 5% CO₂ and medium was changed three times a week.

2.2.7 Histological analysis:

2.2.7.1 Collection and preparation of tissue.

Cartilage and osteochondral biopsies were dissected from the tibial plateaux of patients that had undergone total knee replacement surgery for OA (n= 10) and from normal donors (n=6). Tissues were fixed overnight in 10% neutral buffer formalin saline (NBFS). The following day the fixative agent was removed from cartilage samples and replaced with 70% (v/v) ethanol to minimize tissue hardening. Osteochondral biopsies were washed with phosphate buffer saline (PBS) before decalcification in 10% (w/v) EDTA, pH 7.5 at 4°C replaced twice a week for up to 6

weeks. Decalcification was checked by radiography at the Central Biotechnology Services, Cardiff University. Following decalcification, samples were washed in PBS, dehydrated using graded ethanol for 30 minutes at room temperature (70%, 95%, x2 100%). All samples were wax-embedded by the Histology Unit, Cardiff School of Biosciences, Cardiff University. Wax embedded tissue was sectioned at 10µm using a microtome (LKB BROMA 2218 microtome Historange) and mounted onto poly-L-lysine coated-slides.

Prior to processing sections were dewaxed using xylene (2 x 2 minutes) and rehydrated using a descending gradient of ethanol (100%, 90%, 70%, 1 x 2 minutes) with a final immersion in H₂O. Slides were circled using a hydrophobic pen (Dako, UK) and washed in PBS for 5 minutes.

2.2.7.2 Histological grading of cartilage tissue.

Cartilage sections were de-waxed and rehydrated prior to staining with Safranin-O, Fast Green and the nuclei counter-stain, Mayer's haematoxylin. This staining procedure enables the assessment of structural changes to the articular cartilage and the proteoglycan content in the extracellular matrix. First sections were stained with Mayer haematoxylin for 5 minutes, washed in running tap-water for 5 minutes and then transferred to a vessel containing 0.02% fast green solution for 5 minutes. Sections were washed with 1% v/v acetic acid solution for 15 seconds and transferred to a vessel containing 0.1% Safranin-O solution for 5 minutes after which they were washed in tap-water for 5 minutes. Sections were then dehydrated through an ethanol gradient (70%, 90%, 100%, 100% 1 x 2 minutes) and cleared using xylene (2 x 2 minutes) before mounting with coverslips using DPX mounting medium.

Stained slides were used to grade OA severity using the modified Mankin score; studying: zonal structure, cell density and Safranin-O staining, where the minimal score was 0 and the maximal score was 14, see Appendix 1.

2.2.7.3 Detection of Tartrate-resistant acid phosphatase (TRAP).

Tartrate-resistant acid phosphatase (TRAP) is an enzyme that is highly expressed by bone resorbing osteoclasts. Histochemical staining to visualize TRAP expression was performed on 10 µm osteochondral tissue sections from normal (n=5) and osteoarthritic donors (n=10) using the Acid Phosphatase, Leukocyte (TRAP) kit as per manufacturers protocol (Sigma). Briefly, dewaxed sections (2.10.1) were incubated in a solution of naphthol AS-BI phosphate (12.5 mg/mL naphthol AS-BI) at 37 °C for 1 hr, rinsed in distilled water for 5 minutes (room temperature) and counterstained with Mayer's haematoxylin (5 minutes) prior to rinsing in tap water, dehydrating through a gradient of ethanol and mounting with coverslips using DPX. TRAP-positive multinucleated cells containing three or more nuclei were imaged using Leitz DMRB light microscope (Leica, Germany).

2.2.8 Immunohistochemistry.

Cartilage sections were de-waxed and rehydrated (2.2.7.2) and for primary antibodies requiring epitope retrieval, (see Table 2.1) sections were either incubated with hyaluronidase (2U /mL in PBS) for 1 hr at 37 °C; citrate-buffer (Dako) for 3 minutes at 95 °C (DAKO, UK) or hyaluronidase (2U /mL) + C'ase ABC (0.1U /ml) in Tris acetate, pH 8.0 for 1 hr at 37 °C. Primary antibody was omitted and replaced with either relevant negative Ig sera or PBS to act as a negative control.

2.2.8.1 Immunofluorescence labelling.

Sections or fixed cells were blocked using goat serum (50 µg /mL) for 30 minutes at room temperature. The blocking serum was removed and primary antibody diluted in PBS containing 1 % BSA (Table 2.1) was added and sections were incubated overnight at 4°C. Sections were washed twice (5 minutes) in PBS-Tween and incubated with the appropriate secondary antibody (for mouse IgG primary antibody; goat anti mouse IgG Alexa Fluor 488, Alexa Fluor 594 or Alexa Fluor 647 was used. For polyclonal rabbit primary antibody; goat anti rabbit Alexa Fluor 633 was used and for mouse IgM primary antibody; goat anti mouse IgM Alexa Fluor 594 was used. All secondary antibodies were diluted to a final concentration of 10 µg/mL) for 1 hr at room temperature. Processed sections were mounted in Vectashield (Vector Labs, USA) containing 4, 6-diamidino-2-phenylindole (DAPI) or propidium iodide as a counterstain for cell nuclei and viewed using a Leica DM2500 confocal microscope or Leica DM6000 up-right confocal microscope (Leica, Germany).

2.2.8.2 Peroxidase labelling.

Sections or fixed cells were submerged in hydrogen peroxide (0.3% (v/v) in H₂O) for 30 minutes at room temperature to quench endogenous peroxidase activity. Sections were rinsed x 3 in PBS-Tween for 5 minutes and blocked using the R.T.U Vectastain Universal Quick Kit blocking serum (horse serum) for 30 minutes, excess serum was discarded and primary antibody diluted in PBS-T (Table 2.1) was directly applied to the sections and incubated at 4°C overnight.

Table 2. 1: Primary antibodies and dilution used for immunohistochemistry and Western blot.

| Antibody | Host species | Supplier | Optimum dilution |
|-------------------------|-----------------------|--|-------------------------|
| anti-BrdU | Mouse (IgG) | G3G4, DSHB | 1:40 |
| anti-CD105 | Mouse (IgG) | R&D | 1:100 |
| anti-CD166 | Mouse (IgG) | R&D | 1:100 |
| anti-DKK-1 | Mouse (IgG) | MAB10962, R&D | 1:500 |
| Anti- β -catenin | Mouse (IgG) | 610153, BD bioscience | 1:1000 |
| Anti- VE-cadherin | Mouse (IgG) | Clone BV9, Biolegend | 1:100 |
| Anti- CD-34 | Mouse (IgG) | QBEND-10, Abcam | 1:50 |
| Anti- SNAI1 | Rabbit (IgG) | H-130, Santa Cruz Kind gift of Dr. Rhian French | 1:200 |
| Anti-Vimentin | Mouse (IgG) | Clone V9, Sigma | 1:500 |
| Anti-SMA | Mouse (IgG) | Clone 1A4, Sigma | 1:500 |
| Anti-Aggrecan | Mouse (IgG) | 6B4 epitope, In-house antibody Generated by Prof. Caterson | 1:100 |
| Anti-collagen type II | Mouse (IgG) | CIICI, DSHB Kind gift of Prof. Duance | 1:50 |
| Anti-Sox9 | Rabbit (IgG) | H-90, Santa Cruz | 1:100 |
| Anti- MMP13 | Rabbit (IgG) | H-230, Santa Cruz | 1:500 |
| Anti- γ -catenin | Mouse (IgG) | 610253, BD bioscience | 1:1000 |
| Anti- β -actin | Mouse (IgG) | ab6276, Abcam | 1:10000 |
| Anti-Erk1/2 | Rabbit (IgG) | ADI-KAP-MA001-D, Enzo Life Sciences | 1:1000 |
| Anti-PECAM1 | goat polyclonal (IgG) | M-20, Santa Cruz | 1:1000 |
| Anti- CD-29 | Mouse (IgG) | Clone TS2/16, ebioscience | 1:100 |
| Anti-Stro1 | Mouse IgG | MAB1038, R&D | 1:100 |
| Anti-Notch1 | Mouse IgG | SC-6015, Santa Cruz | 1:100 |
| Anti- CD-44 | Mouse IgG | Clone BJ18, Biolegend | 1:100 |

Sections were subsequently washed thrice in PBS-Tween for 5 minutes prior to the addition of the pre-diluted pan-specific biotinylated universal secondary antibody (Vector) and incubation for 15 minutes at room temperature. Sections were washed twice in PBS-Tween, a few drops of the streptavidin/peroxidase complex (Vector) added and incubated at room temperature for 5 minutes. Sections were washed twice in PBS-Tween and developed using the 3, 3'-diaminobenzidine (DAB) substrate kit (Vector), for 4 minutes or until strong staining was seen. Slides were rinsed in distilled H₂O to stop the DAB reaction. Nuclei were counter-stained using haematoxylin. The slides were then dehydrated in a series of ascending graded alcohols, cleared in xylene and mounted in DPX. Slides were allowed to air-dry and were subsequently imaged using a Leica Leitz DMRB light microscope (Leica, Germany).

2.2.9 Bromodeoxyuridine (BrdU) Assay.

Cells, in Basal medium, were seeded at 10⁴ cells per well in 12 well cell culture plates and incubated for 24 h at 37°C in a humidified atmosphere of 5% CO₂. Triplicate wells were established for each cell line. Medium was removed, replaced with basal medium containing 10 µM BrdU and cells incubated for 24 hrs. Cells were washed twice with PBS, fixed in ice-cold 70% (v/v) ethanol for 30 minutes at room temperature and washed again with PBS before storage at 4 °C for later analysis. Incorporated BrdU was detected using an anti BrdU monoclonal antibody (Table 2.1) using the peroxidase method described in section 2.8.2 with the modification that all antibody incubation steps were carried out at room temperature for 1 h. Cell layers were pre-treated with 1M HCl to denature the DNA. On completion of the protocol, plates were dried and glycerol added to each well as mounting medium and cells were viewed using a Nikon Eclipse TS100 light microscope. Images were taken from each

well (n=3) using a Nikon E4500 camera with x 20 objective. The total number of cells and the stained cells were counted. The percentage of stained cells was calculated by dividing positively stained cells by the total cell count using image J software.

2.2.10 Senescence associated β -galactosidase (SA β -Gal) staining.

Cells (in Basal medium) were seeded at 10^4 cells per well in 12 well cell culture plates and incubated for 24 h at 37°C in a humidified atmosphere of 5% CO₂. Triplicate wells were established for each cell line. Cells were washed twice in PBS-Tween prior to fixation in 2% formaldehyde and 0.2% glutaraldehyde in PBS for 5 minutes at room temperature. Following fixation, cells were washed in PBS, and then submerged in β -Gal solution (40 mM citric acid/phosphate, 1 mg/mL X-Gal, 150 mM NaCl, 2 mM MgCl₂, 5mM K₄(FeCN₆), 5mM K₃(FeCN₆), pH 6) and incubated for 16 hours at 37°C. Cells were washed twice with PBS (5 minutes) and twice with methanol before plates were air-dried. Plates were viewed using an inverted Nikon Eclipse TS100 light microscope and images were taken from each well (n=3) using a Nikon E4500 camera with x 20 objective magnification. There is a blue deposit of β -galactosidase at the cytoplasm of senesced cells (Debacq-Chainiaux *et al.*, 2009). The total number of cells and the stained cells were counted and the percentage of stained cells was calculated by dividing positively stained cells by the total cell count using image J software.

2.2.11 Flow cytometry.

Confluent cell layers were lifted using 5 ml of TryPLE solution (Life Technology, UK), washed in DMEM-PS and counted using a haemocytometer. Routinely 1×10^6 cells were re-suspended in 1 ml ice cold PBS containing 0.1% (w/v) bovine serum albumin (PBS/BSA). 10^5 cells (100 μ l) were transferred to 1.5 ml sterile microcentrifuge tubes

and cells were pelleted at 400 x g for 5 minutes. The supernatant was removed, the cell pellets re-suspended in 100 µl of PBS/BSA containing 10 µg/mL of the appropriate primary conjugated antibody (Table 2.2) and incubated in the dark at 4 °C for 30 minutes. An appropriate mouse IgG was used as a negative control. Cells were centrifuged, washed twice using 1 ml PBS/BSA to remove non-bound antibodies and then re-suspended in 500 µl of PBS/BSA. Each cell suspension was transferred to a 12mm FACS tubes (BD Biosciences, UK) for analysis using the FACS Canto flow-cytometer. Data were processed using the FACS Diva software (BD Biosciences).

Cells were analysed according to size and granularity to differentiate viable cells using forward and side scatter, respectively. Data were displayed in a series of density plots and IgG isotype data were displayed as a histogram overlay to show the overlap. The data were analysed using Flowing Software (v2.5, University of Turku, Finland). The level of antibody expression was calculated as the ratio between geometric mean fluorescence intensity (MFI) of positive stained cells against that of the isotype control.

Table 2. 2: Conjugated primary antibodies used for flow cytometry.

| Antibody name | Clone name | Conjugated type | Source | Species |
|-------------------|------------|-------------------|-------------|-----------------|
| Anti-CD90 (Thy-1) | 5E10 | PerCP-eFluor® 710 | ebioscience | Mouse (IgG1, κ) |
| Anti-CD105 | SN6 | APC | ebioscience | Mouse (IgG1, κ) |
| Anti-CD166 | 3A6 | PE | ebioscience | Mouse (IgG1, κ) |
| Anti-CD-34 | QBEND | FITC | Abcam | Mouse (IgG1) |
| Anti-CD144 | BV9 | APC | Biolegend | Mouse (IgG1, κ) |
| Anti-CD31 | M-20 | PE | Biolegend | Mouse (IgG1, κ) |
| Anti-VEGFR2 | 7D4-6 | PE | Biolegend | Mouse (IgG1, κ) |
| Anti-CD11b | ICRF44 | PE-Cyanine5 | ebioscience | Mouse (IgG1, κ) |
| Isotype Control | P3.6.2.8.1 | APC | ebioscience | Mouse IgG1 K |
| Isotype Control | P3.6.2.8.1 | PerCP-eFluor® 710 | ebioscience | Mouse IgG1 K |
| Isotype Control | P3.6.2.8.1 | PE | ebioscience | Mouse IgG1 K |
| Isotype Control | P3.6.2.8.1 | FITC | ebioscience | Mouse IgG1 K |

2.2.12 Molecular analysis:**2.2.12.1 RNA extraction from cells.**

Total RNA was isolated routinely from cell cultures using Trizol® (Invitrogen, UK) at 1 ml per $0.5-1 \times 10^6$ cells following the manufacturer's protocol. Trizol was added to cells which were lifted by repetitive pipetting and transferred to a 1.5 ml RNase-free microcentrifuge tube, after which 200 µl of molecular grade-chloroform was added and the samples mixed by inversion before allowing to stand for 15 minutes at room temperature. Samples were centrifuged for 15 minutes at 13,000 x g at 4°C. The top

aqueous-phase, containing the RNA was carefully removed without disturbing the DNA interface layer and transferred to a fresh 1.5 mL microcentrifuge tube. An equal volume of 70% ethanol was added to the aqueous phase and the sample carefully mixed by inversion.

RNA was isolated using the RNeasy mini-kit as per manufacturer's protocol. Briefly, the sample was transferred into an RNeasy spin column placed in a 2ml collection tube and centrifuged at 8000 x g for 30 sec. 350 µl of RW1 buffer was added to the spin column and centrifuged at 8000 x g for 30sec. To eliminate genomic DNA contamination, an on-column DNase digestion steps was carried out by adding 80 µl of DNase solution (10 µl of DNase I + 70 µl RDD buffer) onto the centre of the RNeasy spin column membrane and left for 15 minutes at room temperature. Subsequently, 350 µl of RW1 Buffer was added to the spin column and centrifuged at 8000 x g for 30 sec. RPE buffer (500 µl) was then placed onto the RNeasy column and centrifuged at 8000 x g for 30 sec. Another 500 µl of RPE buffer was added to the RNeasy column and centrifuged for a further 30 sec at 8000 x g. RNeasy spin column was then centrifuged at 8000 x g for 2 minutes to remove any left-over buffer. The spin column was transferred to a new 0.5 ml RNAase free microcentrifuge tube and the RNA eluted with 30 µl of RNase free water using a final spin of 8000 x g for 1 minute. RNA was quantified using a Nanodrop 2000c spectrophotometer using 260/280 nm and RNA was stored at -80°C until required.

2.2.12.2 Analysis of RNA using the Agilent 2100 Bioanalyzer.

The integrity of RNA (5 µl per sample) used in the Wnt-PCR array analysis of cell lines and custom-array (section 2.12.3) were subjected to detailed analysis using the

Agilent 2100 Bioanalyzer (Dr Claudia Consoli, Central Biotechnology Services, Cardiff University). The Agilent Bioanalyzer is an electrophoresis-based analysis system for the detection of RNA as well as proteins. It measures the integrity and presence of degraded material that might affect the purity of isolated total RNA. An accepted RIN value is >8 and representative figure of analysed material is shown in figure 2.1.

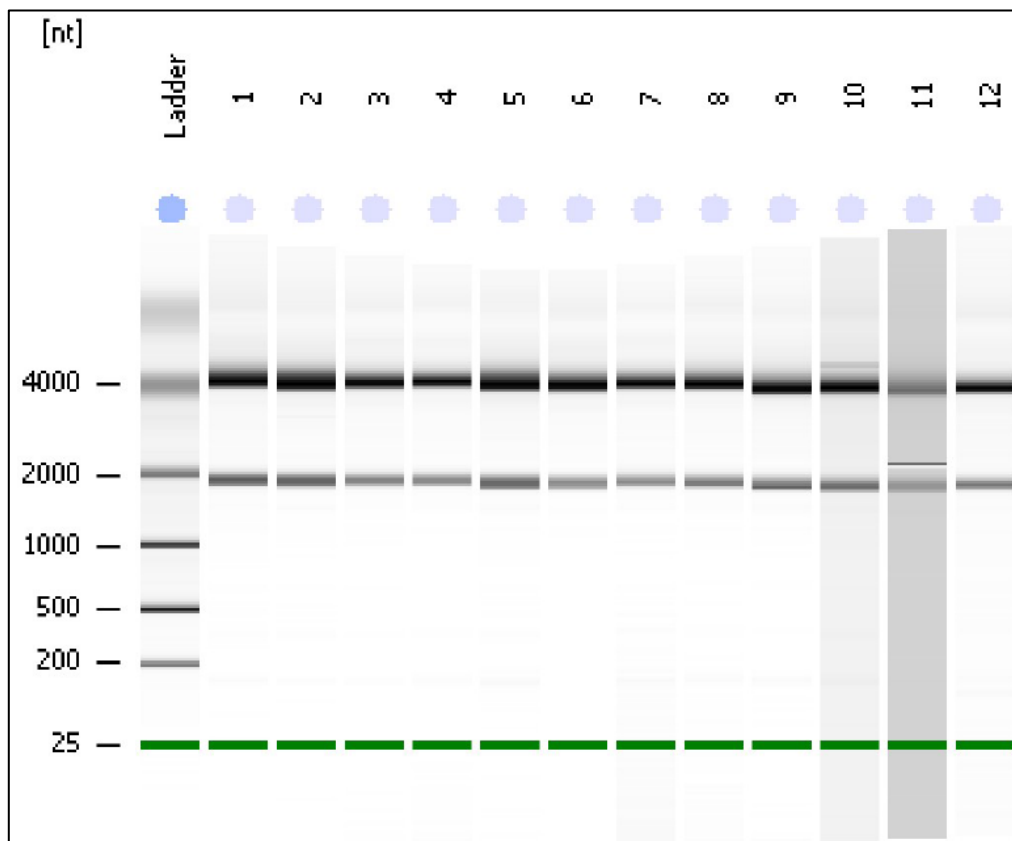


Figure 2. 2: Representative image of bioanalyzer® gel electrophoresis of total RNA.

Twelve samples were subjected to assessment of RNA integrity and RNA was visualised on a gel, with sharp bands depicting ribosomal 28S and 18S (top and bottom band are clearly demarcated respectively). There was no evidence of RNA degradation.

2.2.12.3 Gene expression analysis utilizing the RT² Profiler™ PCR Array.

Each 96-well plate contained primer assays for genes of interest (Table 2.3), housekeeping genes, a genomic DNA control, 3 reverse transcription controls and 3 positive PCR controls. cDNA was synthesised from 500 ng of RNA using the 'RT² First

Strand Kit' as per manufacturer's protocol. RNA was added to 2 μ l of the genomic DNA elimination buffer and RNase-free water was added to a volume of 10 μ l. The reaction mix was incubated at 42 °C for 5 minutes using the thermocycler. The samples were immediately removed and incubated on ice for 2 minutes. 10 μ l of RT cocktail buffer was added to the reaction mix and returned to the thermocycler programmed for 42 °C for 15 minutes, followed by 95 °C for 5 minutes (to stop the reaction). Finally, 91 μ l of H₂O was added to the cDNA reaction mix and stored at -20 °C until required. cDNA samples were thawed and 102 μ l was mixed with 1350 μ l of RT2 SybrGreenMastermix and 1248 μ l RNase-free water. Twenty five μ l of the reaction mix was added to each well of the RT² Profiler™ PCR plate. The plate was sealed with adhesive film and centrifuged for 2 minutes at 800 x g to remove air bubbles. The plate was placed in an Mx3000P q-PCR thermocycler (Stratagene, UK) and amplification was carried out using the following conditions: incubated for 10 minutes at 95°C to activate Hot Start DNA Taq polymerase; 95°C for 15 seconds, 60°C for 1minute (annealing), 72 °C, 30 sec for 40 cycles and then the machine stood at 4°C. To confirm the absence of non-specific amplification, a dissociation curve was generated. The CT values for all genes were exported to an Excel spreadsheet template and analysed using the Super Array Biosciences PCR Array analysis web-based software. Five housekeeping genes, ACTB, HPRT1, B2M, GAPDH and RPLP0, in all array experiments and the most stable housekeeping gene were identified using the in-built Qiagen software. Two housekeeping genes, β -2-microglobulin and GAPDH, were used as internal control for calculating Δ CT. Gene expression was calculated using the $2^{-\Delta\Delta CT}$ method. All genes that were ± 3 -fold different than the controls were considered for further target validation.

Table 2. 3: Wnt PCR-array plate layout.

| | | | | | | | | | | | |
|---------|-------|--------|--------|----------|-------|---------|--------|-------|---------|--------|----------|
| AES | APC | AXIN1 | BCL9 | BTRC | FZD5 | CCND1 | CCND2 | CCND3 | CSNK1A1 | CSNK1D | CSNK1G1 |
| CSNK2A1 | CTBP1 | CTBP2 | CTNNB1 | CTNNBIP1 | CXXC4 | DAAM1 | DIXDC1 | DKK1 | DVL1 | DVL2 | EP300 |
| FBXW11 | FBXW2 | FGF4 | FOSL1 | FOXN1 | FRAT1 | FRZB | FSHB | FZD1 | FZD2 | FZD3 | FZD4 |
| FZD6 | FZD7 | FZD8 | GSK3A | GSK3B | JUN | KREMEN1 | LEF1 | LRP5 | LRP6 | MYC | NKD1 |
| NLK | PITX2 | PORCN | PPP2CA | PPP2R1A | PYGO1 | RHOA | SENP2 | SFRP1 | SFRP4 | FBXW4 | SLC9A3R1 |
| SOX17 | T | TCF7 | TCF7L1 | TLE1 | TLE2 | WIF1 | WISP1 | WNT1 | WNT10A | WNT11 | WNT16 |
| WNT2 | WNT2B | WNT3 | WNT3A | WNT4 | WNT5A | WNT5B | WNT6 | WNT7A | WNT7B | WNT8A | WNT9A |
| B2M | HPRT1 | RPL13A | GAPDH | ACTB | HGDC | RTC | RTC | RTC | PPC | PPC | PPC |

2.12.4 Reverse Transcription of isolated RNA.

cDNA was synthesised by reverse transcription of total RNA (500 ng) using SuperScript™ III Reverse Transcriptase as per manufacturer protocol (Invitrogen, UK). RNA (500 ng) was added to 1µl random hexamers (250 ng final concentration), and 1µl of dNTP's (500 µM) and the final volume made up to 10 µl using molecular biology grade water. Samples were incubated at 65°C for 5 minutes in a thermocycler followed by incubation on ice for at least 1 minute, after which 0.5µl SuperScript III Reverse Transcriptase (100U final concentration), 4 µl 5X first strand buffer, 2 µl DTT (100 mM) and 1 µl of recombinant RNase inhibitor (125U) and 2.5 µl of molecular grade water were added. Samples were placed in a thermocycler programmed for 10 minutes at 25°C followed by 50 minutes at 42°C. Finally, the reaction was deactivated

by heating the sample to 70°C for 15 minutes. cDNA reaction sample (20 µl) was immediately used or stored at -20°C until required.

2.2.12.5 Quantitative Real-Time PCR (qPCR).

PCR primers for each gene of interest (Table 2.4) were designed using the NCBI software to span exon-exon boundaries selected primers were run through the NCBI BLAST database to ensure no homology to other genes. Primers were purchased (Sigma, UK) and were optimised prior to use in qPCR using the GoTaq Flexi DNA Polymerase (Promega, UK) kit as per manufacturers protocol and PCR reaction products were analysed on 1 % (w/v) agarose gels containing Safeview (10 µl per 40 ml) by electrophoresis in 0.5X TBE buffer at 75V for 40-50 minutes and visualise under UV. A molecular weight marker (100-1000 bp) was used to identify product sizes.

Quantification of mRNA levels for genes of interest were measured using qPCR with SYBR® Green kicqStart™ q-PCR ReadyMix™ (Sigma, UK). 20 µl reaction volumes were set up in a 96-well plate (Applied Biosystems), as follows: 7µl RNAase free H₂O; 1µl each of forward and reverse primers (0.3 µM); 10 µl kicqStart™ TaqReadyMix™ and 2 µl cDNA (from 500 ng RNA). qPCR reactions were carried out using an Mx3000P q-PCR system (Stratagene, UK) and amplified using the following conditions: 95 °C, 10 minutes for 1 cycle, 95 °C, 30 sec, 30 sec at the annealing temperature (see Table 2.4), 72 °C, 30 sec for 40 cycles a final extension cycle at 72°C 5 minutes and then 4°C. Relative quantification was analysed using the 2- $\Delta\Delta$ CT method (Livak and Schmittgen 2001). Briefly, normal and full depth chondrocytes and CPC were used as a control group to measure relative changes in the target gene of

osteoarthritic full depth chondrocytes and CPC samples. The relative change in gene expression was presented as a fold change normalised to GAPDH.

Table 2. 4: Polymerase chain reaction primer sequence. All primers are shown in the 5'-3' with annealing temperature and size.

| Gene ID | Sequence | Annealing temp & size | Accession Number |
|--|--|-----------------------|------------------|
| PPAR-γ F PPAR-γ-R | AAAGAAGCCAACACTAAACC TGGTCATTTTCGTTAAAGGC | 61 °C 78bp | NM_138711.3 |
| ACAN-F ACAN-R | TGAGTTTCCTGGTGTGAG AGACCTCACCCCTCCATC | 61 °C 100bp | NM_001135.3 |
| Runx-2 F Runx-2 R | AAGCTTGATGACTCTAAACC TCTGTAATCTGACTCTGTCC | 62 °C 164bp | NM_001278478.1 |
| LPL- F LPL- R | ACACAGAGGTAGATATTGGAG CTTTTTCTGAGTCTCTCCTG | 60 °C 105bp | NM_000237.2 |
| Osteonectin- F Osteonectin- R | AGTATGTGTAACAGGAGGAC AATGTTGCTAGTGTGATTGG | 60 °C 143bp | NM_003118.3 |
| CDH5- F CDH5- R | CGCAATAGACAAGGACATAAC TATCGTGATTATCCGTGAGG | 61 °C 51bp | NM_001795.3 |
| Hif1α- F Hif1α- R | AAAATCTCATCCAAGAAGCC AATGTTCCAATTCCTACTGC | 60 °C 181bp | NM_001243084.1 |
| VEGFA- F VEGFA- R | AATGTGAATGCAGACCAAAG GACTTATACCGGATTTCTTG | 60 °C 65bp | NM_001204385.1 |
| Col2α1- F Col2α1- R | GAAGAGTGGAGACTACTGG CAGATGTGTTTCTTCTCCTTG | 60 °C 165bp | NM_001844.4 |
| MMP-13 F MMP-13 R | AGGCTACAACCTGTTTCTTG AGGTGTAGATAGGAAACATGAG | 60 °C 101bp | NM_002427.3 |
| PECAM1- F PECAM1- R | AGATACTCTAGAACGGAAGG CAGAGGTCTTGAAATACAGG | 62 °C 120bp | NM_000442.4 |
| α-SMA-F α-SMA-R | AGATCAAGATCATTGCCCC TTCATCGTATTCTGTGTTTGC | 57 °C 116bp | NM_001613.2 |
| DKK1 -F | GAATAAGTACCAGACCATTGAC | 58 °C | NM_012242.2 |

| | | | |
|-----------------|----------------------|-------|----------------|
| DKK1-R | CCATTTTTGCAGTAATTCCC | 153bp | |
| GAPDH- F | ACAGTTGCCATGTAGACC | 60 °C | NM_001256799.2 |
| GAPDH- R | TTTTTGGTTGAGCACAGG | 95bp | |

2.2.13 Protein analysis:

2.2.13.1 Cell lysis.

Cells were washed twice with ice-cold PBS before the addition of ice-cold RIPA lysis buffer (150 mM sodium chloride, 1.0% v/v NP-40, 0.5% w/v sodium deoxycholate, 0.1% w/v SDS and 50 mM Tris, pH 8.0) solution (1 ml per $0.5-1 \times 10^6$ cells) containing a cocktail of protease and phosphatase inhibitors (Sigma, UK). The cell layer suspension was pipetted several times and transferred to a 1.5 ml microcentrifuge tube, centrifuged at 4°C for 15 minutes at 12000 x g. The supernatant was removed and stored at -20°C until required.

2.2.13.2 Protein assay (BCA).

The concentration of total soluble protein was determined using the Pierce BCA Protein Assay Kit as per manufacturer's protocol (Thermo Fisher Scientific, UK). Standard curves were constructed using increasing concentrations of BSA solution from 0 to 2000 µg/mL in dH₂O. 25 µl of standard and unknown samples were pipetted into 96-wells plates in duplicate and to each well, 200 µl of working reagent was added (containing cupric acid and BCA at 1:8 working ratio). Plates were left in the dark for 30 min at 37°C for full colour development and absorbance at 560 nm was measured using a plate reader (Fluostar Optima BMG labtech, Germany).

Concentration of unknown samples were calculated from the linear regression line generated from the BSA standards.

2.2.13.3 Western blotting.

Samples (typically 20 µg protein) were reconstituted in Laemmli sample buffer (62.5 mM tris HCl, pH 6.8 containing 4% (w/v) SDS, 20% (v/v) glycerol and 0.01% (w/v) bromophenol blue) containing 10% (v/v) β-mercaptoethanol and electrophoresed under reducing conditions on 10% slab gels poured using acrylagel and bisacrylagel from National Diagnostics (see Table 2.5). Samples were heated to 100°C for 5 minutes, to denature and reduce the proteins. 10 µl of Precision Plus Protein™ Molecular weight standards (Bio-Rad, UK) were carefully loaded into the wells of the stacking gel. Electrophoresis was then performed in running buffer (25mM trizma pH8.1-8.4 containing 192mM glycine and 0.1% (w/v) SDS) at 150V for 45-60 minutes. The gels were then transferred onto nitrocellulose membranes utilising the 7 minutes transfer protocol for the iBlot® Gel Transfer System (Life technologies, UK).

Table 2. 5: Reagents used to make up resolving and stacking gels.

| Resolving Gel | | Stacking Gel | |
|-------------------------------------|---------|-------------------------------------|----------|
| Reagents | Volume | Reagents | Volume |
| 40% Acrylamide bis acrylamide combo | 7.66ml | 40% Acrylamide bis acrylamide combo | 0.575 mL |
| 1 M Tris Buffer pH 8.8 | 7.26ml | 1 M Tris Buffer pH 6.8 | 1.3ml |
| 10% SDS | 200 µl | 10% SDS | 50 µl |
| dH2O | 14.1 ml | dH2O | 4.075 mL |
| 10% APS | 150 µl | 10% APS | 37.5µl |
| TEMED (added last) | 30 µl | TEMED (added last) | 7.5µl |

Following electrophoretic transfer the membranes were subjected to Western blot analysis. Membranes were blocked in 5% (w/v) non-fat milk solution (Marvel milk,

UK) in TBS-T for 30 minutes at room temperature with rocking. Membranes were rinsed in TBS-T and incubated with the appropriate primary antibody diluted in 1% (w/v) non-fat milk solution in TBS-T overnight at 4°C (Table 2.1). The membranes were washed with TBS-T (3 x 10 minutes) and incubated for 1 hour at room temperature with the appropriate secondary antibody conjugated to HRP (Goat anti-mouse or Goat anti-rabbit) diluted in 1% (w/v) non-fat milk solution in TBS-T. The membranes were washed in TBS-T (4 x 10 minutes.) and developed using the enhanced chemiluminescence (ECL) reagents as described in the manufacturer's protocol (GE Healthcare, UK). Membranes were exposed to X-ray film from 1 to 60 minutes, the film was developed manually and stopped by immersing in a fixative solution (Agfa, UK). X-ray film was then transferred to a container filled with tap water to remove any excess fixative solution before it was air-dried.

2.2.13.4 Proteome Profiler Human XL Oncology Array.

For the samples processed for this array, total protein concentration was determined using BCA assay (section 2.13.2). 50 µg protein from each sample was added to 1 ml of buffer 4 and the volume made to 2 ml using buffer 6. This was then added to an appropriate vessel containing the array membrane and incubated overnight at 4°C. The array membrane was washed several times in the supplied wash buffer after which the membrane was incubated with a biotinylated secondary antibody for 1 hr at room temperature on a rocking platform shaker. After several washes, the membrane was incubated in the streptavidin-HRP substrate. The membrane was extensively washed prior to incubation in the chemi-luminescent detection reagents and exposed to X-ray film (GE Healthcare, UK). The intensity of the capture spot reactions was quantified using Image J software (NIH) and dot density was measured using protein

array analyser plug-in software. Data are presented as mean of two wells per protein \pm standard deviation.

2.2.13.5 DKK-1 ELISA.

A kit based sandwich assay (human Dkk-1, R & D Systems DY 1906) was used to determine the concentration of Dkk-1 in culture media from a variety of cell lines following the manufacturer's protocol. Monoclonal mouse anti-human Dkk-1 capture antibody was diluted in PBS at a final concentration of 4.0 $\mu\text{g/ml}$ and used to coat 96-well microtiter plates (100 μl per well) which were then incubated overnight at room temperature. Plates were washed x 3 with PBS-Tween before blocking with 1% (w/v) BSA in PBS for 1 hr at room temperature. Plates were washed x 3 with PBS-Tween and standards added in triplicate (Dkk-1 recombinant protein in the range of 0 – 4000 pg/ml into designated wells along with unknown samples (in duplicate) at 100 μl /well and incubated at room temperature for 2hrs. The plate was washed x 3 in PBS-Tween and a secondary biotinylated detection Dkk-1 antibody (100 μl / well at a concentration of 50 ng/mL) was added to each well and incubated for 1hr at room temperature. The plate was washed x 3 in PBS-Tween, streptavidin-horseradish peroxidase solution added and then incubated for 20 minutes at room temperature. The plates were washed x 3 in PBS-Tween (5 minutes) after which substrate was added (100 μl per well) and the reaction stopped after 20 minutes by the addition of 2 N sulphuric acid. The optical density of each well was determined using a spectrophotometer at 450nm and 570nm. A standard curve was plotted using a four parameter logistic (4-PL) curve-fit and the concentration of unknown samples determined from this plot. Data were presented as mean and standard deviation after normalising the concentration total cell number.

2.2.14 T-Cell Factor (TCF) reporter assay.

The TCF assay as described by Ewan et al (2010) was used as a measure of activation of the canonical Wnt pathway through β -catenin. Briefly the assay utilizes a reporter plasmid (Figure 2.2) that has been stably transfected in HEK293 cells (7df-3 cell line) and can indirectly measure the activation of β -catenin. Briefly, 7df-3 cells were seeded into a 96 well plate (30,000 cell per well) and maintained for 24 hours in Basal medium (100 μ l per well) in an incubator at 37 °C and 5% CO₂. Following this period 80 μ l of the medium was removed from each well and replaced with 30 μ l of the Wnt inducing ligands (Wnt-3a and R-spo1 at a final concentration of 50 ng/mL and 24 ng/mL, respectively) combined with either 50 μ l of Basal medium (positive control); 50 μ l of doxycycline (final concentration of 50 μ g /mL) as a negative control, or 50 μ l of test medium and incubated for 24 h. After 24 h, 10 μ l of Water Soluble Tetrazolium salts (WST-1, Roche, UK) was added to each well and the plate was returned to the incubator for 1hr at 37 °C and 5% CO₂ after which absorbance was measured at 450 nm and 590 nm using the BMG Fluostar plate reader. These readings were used to calculate cell viability. Culture medium was then removed and 25 μ l of GloLysis buffer was added to each well following a 15 min incubation, 25 μ l of Bright Glo luciferase (Promgea, UK) and added to each well and luciferase activity was immediately measured using a FluoStar Optima plate reader (BMG Labtech). Data are presented as mean and \pm SD.

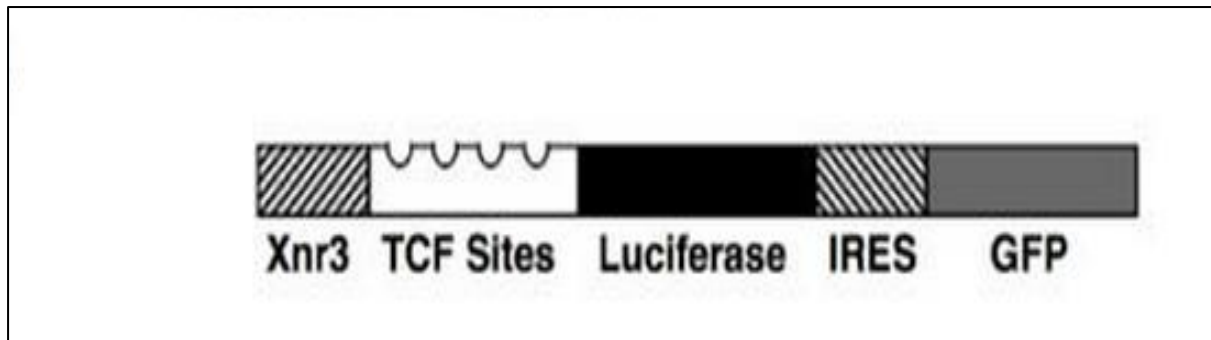


Figure 2. 3: Schematic description of the reporter construct stably transfected in epithelial HEK293-cell line (7df-3).

The TCF-luciferase-IRES-GFP reporter plasmid contained the Wnt response element under Xnr3 promoter and 4 multimerised TCF binding sites driving the transcription of luciferase and GFP reporter genes.

2.2.15 Statistical analysis.

All quantitative data are expressed as mean \pm SEM using the 'R' statistical software analysis programme (v2.15.0). The data were analysed by Student's t-test when comparing two groups. The distribution of the data was analysed using the Shapiro-Wilks test to confirm the normality of the data (occasionally after log-transformation) and homoskedasticity of variance using Flinger test (F test). After assuming homogeneity of data, to study differences in variances between groups, first we performed an ANOVA test followed by Tucky post-hoc test, and a P-value <0.05 was considered statistically significant. All experiments were repeated a minimum of three times unless otherwise stated. In addition, correlation analysis was carried out using the in-built Pearson's correlation plugged-in software to compare parametric variables.

CHAPTER 3: CHARACTERISATION OF CARTILAGE CHONDROPROGENITOR CELLS.

3.1 Introduction.

Articular Cartilage arises from mesenchymal stem cell differentiation that occurs during the process of chondrogenesis. It is a specialized tissue comprising of a single cell type, the chondrocyte, which is embedded in an extracellular matrix. Mesenchymal stem cells (MSCs) are multipotent cells that can undergo tri-lineage differentiation into bone, cartilage or adipose tissue. In addition, it has been recently proposed that MSCs possess higher plasticity than that was formerly known. It is believed that they are able to undergo a pluripotent lineage differentiation into myoblasts and several neural differentiations (Giordano *et al.*, 2006; Yang *et al.*, 2011). Pluripotent stem cells are crucial for giving rise to all cell types apart from germ cells. As these cells differentiate, a subset of their progeny lose some of their pluripotent characteristics. Thus in doing so they become adult stem cells that can retain self-renewal and multipotency.

Adult stem cells, unlike embryonic stem cells, have less self-renewal capacity and are not pluripotent. Recent studies have identified that adult stem cells, in many tissues, play a crucial regulatory role in tissue homeostasis. This process maintains a constant balance between undifferentiated (naïve) and specialised cells that are undergoing proliferation and differentiation (Huang *et al.*, 2014; Ware *et al.*, 2014).

According to the International Society for Cellular Therapy (ISCT), MSCs are characterised by their adhesion capacity in monolayer culture. And their differentiation potential into chondrocytes, osteocytes and adipocytes, in an *in vitro* settings

(Dominici *et al.*, 2006). The ISCT has also listed several cell surface markers that are common to MSCs but lack the expression markers of hematopoietic and leukocytes. Due of their inherent regenerative potential, MSCs are of a significant interest in the field of orthopaedic medicine mainly for cartilage regeneration. In addition, MSCs were noted to have an immune-modulatory response that enhances their regenerative potential (Petrie Aronin and Tuan, 2010).

Stem cells possess unique markers that differentiate them from other resident cells. This knowledge was utilised by Watts and colleagues to isolate epidermal stem cells found in skin tissues based on a tendency to have higher integrin receptor expression (Jones and Watt, 1993). Dowthwaite *et al.* (2004) following on from Jones and Watt's (1993) discovered a cohort of progenitor cells residing within articular cartilage exhibiting an increased expression of $\alpha 5\beta 1$ integrin in chondrocytes from the superficial zone of immature bovine cartilage. In addition, further studies deciphering these cells have also found the exclusive expression of the putative stem cell marker Notch-1. From this discovery, it was proposed that the spatial expression of $\alpha 5\beta 1$ integrin receptor expression and Notch-1 was down-regulated during terminal differentiation of the chondroprogenitor cells. This occurs as chondroprogenitor cells move from the un-differentiated state in the superficial zone to more differentiated chondrocytes in the middle and deep zones of articular cartilage (Hayes *et al.*, 2001; Hayes *et al.*, 2003; Archer *et al.*, 2003; Dowthwaite *et al.*, 2004).

From a developmental point of view, this finding, in part, suggests a possible hypothesis for the development of the synovial joint. It aids the notion that hyaline cartilage grows by apposition (Hayes *et al.*, 2001) and this has given rise to similar

observations noticed in tissues from adult normal cartilage and osteoarthritis (Alsalameh *et al.*, 2004; Williams *et al.*, 2010).

The objective of this section was firstly to characterise and compare polyclonal CPC populations isolated using the fibronectin adhesion assay from full-depth chondrocytes sourced from the articular cartilage of patients with osteoarthritis or from patients with normal joint tissue.

The second objective of this section was to establish the mesenchymal stem cell characteristics of polyclonal CPC from normal donors and patients with osteoarthritis and compare these with matched-bone marrow derived mesenchymal stem cells (BM-MSCs) from the OA patients. For the first objective polyclonal CPC lines from normal (herein termed N-CPC) and OA donors (herein termed OA-CPC) were characterised as follows:

- a) Initial adhesion
- b) Colony forming potential

For the second objective polyclonal N-CPC lines, polyclonal OA-CPC lines and matched BM-MSCs derived from the OA donors (herein termed OA-BM-MSCs) were characterised as stated below:

- c) Morphology on tissue culture plastic
- d) Cell proliferation
- e) Cell senescence
- f) Mesenchymal stem cell markers, CD105, CD166 and CD90. CD34 was selected as a negative marker

g) Differentiation to chondrocytes, osteoblasts and adipocytes

These characterised cell lines were then used in the studies described in this thesis.

3.2 Experimental Methods.

Articular cartilage was removed from the knee joint of normal donors (n=5) herein denoted as N-1 to N-5 and patients undergoing total knee arthroplasty (n=6) herein denoted as OA-1 to OA-2 etc. (see Appendix 1 for age and Mankin Score) as described in section 2.2.1 and subjected to enzymatic digestion in order to release chondrocytes and further subjected to the fibronectin adhesion assay (section 2.2.2) to isolate chondroprogenitor cells (CPC). For each donor full-depth chondrocytes were seeded onto one fibronectin coated 6 well tissue culture plate as described in section 2.2.2 and analysis for initial adhesion and subsequently colony forming efficiency was calculated from the data obtained from initial seeding of these 6 x 35 mm wells. After isolation of CPC from normal and OA donors, cell lines were either expanded as monoclonal or polyclonal cell lines (section 2.2.2) and each line was passaged as described in section 2.2.4. For analysis in this chapter only polyclonal cell lines were used.

Bone marrow mesenchymal stem cells were isolated from 6 OA donors as described in section 2.2.3 and passaged as described in section 2.2.4.

3.3. Results.

3.3.1. Analysis of the initial adhesion to fibronectin of isolated full-depth chondrocytes from OA and normal human articular cartilage.

Articular cartilage was dissected from the tibial plateau of five normal donors (mean age=43, range=29-55) and six OA patients (mean age 66 yrs.; range 53-80) (Figure 3.1). Chondrocytes were isolated from digested cartilage and the initial adhesion of cells isolated after seeding onto fibronectin coated tissue culture wells (n=6 wells per donor) were assessed by microscopy seven days after plating (Figure 3.3 A & B, respectively). The percentage of cells adhering to fibronectin from the five normal donors ranged from 7.2 -16% and those from the six OA donors ranged from 8 – 29%. Data from both donor groups fell into a normal distribution and 1-way ANOVA showed there was no statistical difference in the percentage of cells initially adhering to fibronectin from normal and OA cartilage (Figure 3.2 E, P>0.05). These adherent cells were defined as CPC.

3.3.2. Analysis of the Colony Forming Potential of CPC isolated from OA and normal human articular cartilage.

10 days post plating the normal (n=6 wells per donor) and OA (n=6 wells per donor) donor CPC were analysed using microscopy and Colony Forming efficiency was calculated as:

$$CFE = (\text{Number of colonies at day 10 } (> 32 \text{ cells}) \div \text{Number of the initial cells}) \\ * 100$$

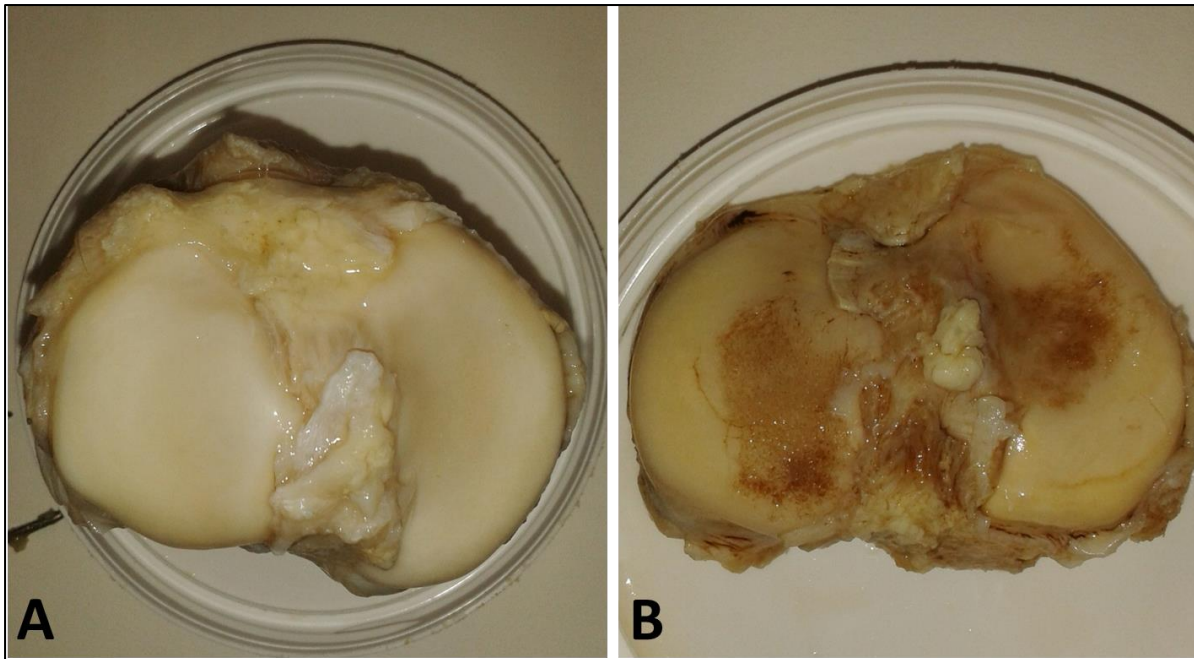


Figure 3. 1: Image of tibial plateaux isolated from normal (post-mortem) and osteoarthritic (arthroplasty) donors.

Tibial plateau from healthy donor has a smooth and intact articular cartilage surface with no evidence of abnormalities (A). However, in osteoarthritic plateau characteristics markers of osteoarthritis are evident marked by cartilage fibrillation and erosion and subchondral bone exposure (B).

CFE in CPC isolated from OA donor cartilage ranged from 0.1 to 0.73% whilst CFE from CPC isolated from normal donor cartilage ranged from 0.06 to 0.53% (Figure 3.2 C and D, respectively). Both group fell within a normal distribution and there was no statistically significant difference in the percentage CFE from normal versus OA CPC (Figure 3.2 F: $p= 0.34$). At 10 days of culture colonies of CPC in each of the 6 x 35mm wells were either isolated and expanded as monoclonal cell lines or further cultured as polyclonal cell lines. Table 8.1 summarises the number of monoclonal and polyclonal cell lines established for each of the normal and OA donors (Appendix 1).

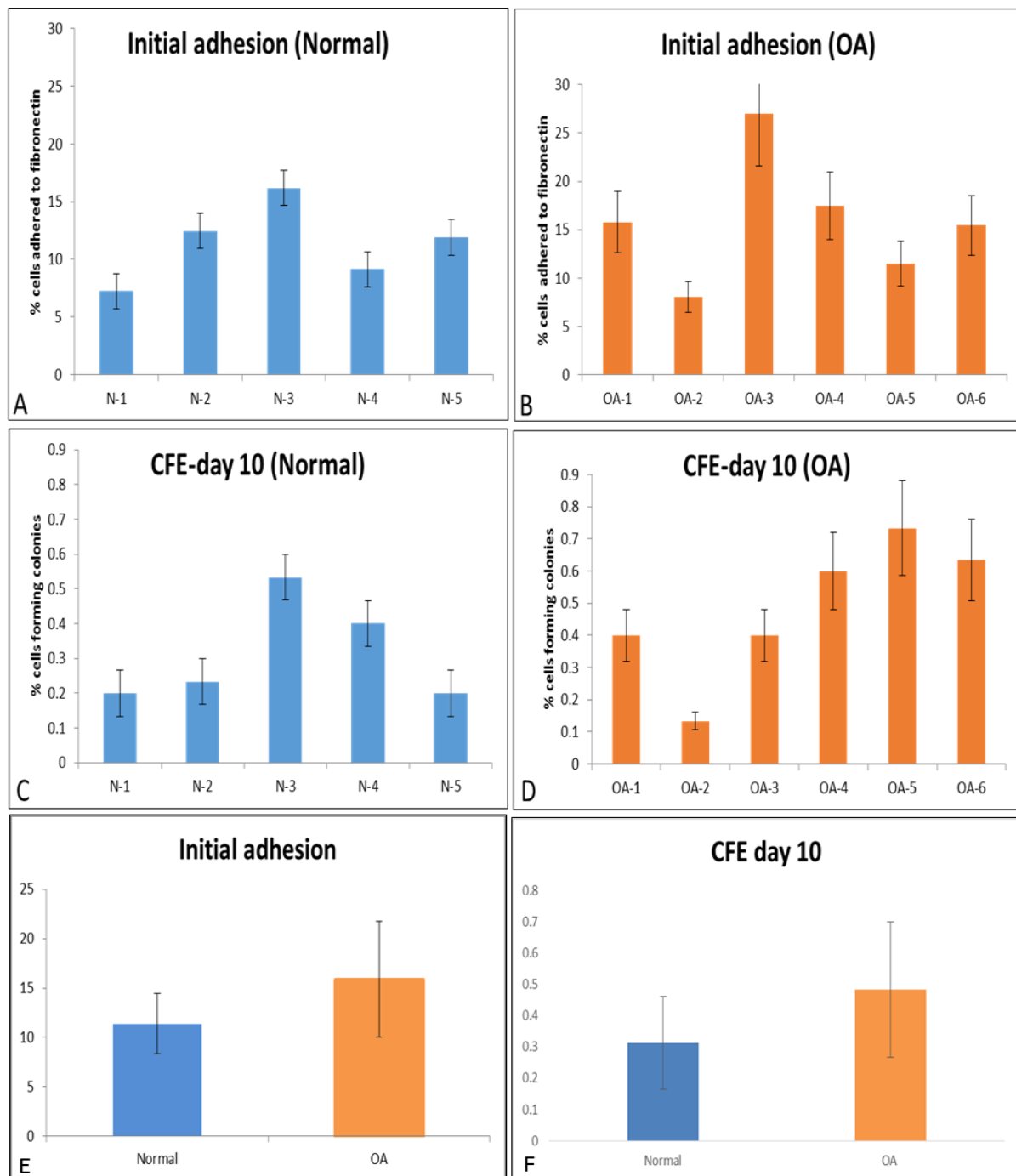


Figure 3.2: Initial adhesion to fibronectin and colony forming efficiency.

Panel A & B shows the initial percentage adhesion of chondrocytes to fibronectin 24hr after plating from normal (n=5) and OA donors (n=6), respectively. Panel C and D shows the colony forming efficiency (CFE) at day 10 (C-D) of isolated cartilage progenitor cells from normal (n=5) and osteoarthritic (OA) donors (n=6). Data was generated from seeding of 6 wells (1000 cells per 35mm well) of chondrocytes isolated from each donor onto fibronectin coated plates. Statistical analysis demonstrated a normal distribution for both normal and OA donors and 1-way ANOVA showed no statistically significance differences between initial cell adhesion ($p > 0.05$) and the percentage of CFE between normal versus OA CPC Panel E and F ($p = 0.34$).

3.3.3 Comparison of the cell morphology of polyclonal CPC lines (from cartilage of normal and OA donors) and matched-Bone-marrow derived MSCs (from OA donors).

Within four days post-plating, polyclonal CPC from normal or OA origin appeared as small colonies of a few cells and by day 10 several colonies consisting of more than 32 cells were evident. Ficoll® gradient isolated BM-MSCs of OA origin, attached to tissue culture plastic within 24 hours of plating and colonies appeared 4-10 days post seeding. On culture expansion both cell types showed a spindle-like morphology and no obvious morphological difference could be detected between polyclonal N-CPC (Fig 3.3D), OA-CPC (Fig 3.3E) and OA-BM-MSCs (Fig 3.3F). By three weeks, patient matched bone marrow mesenchymal stem cells and chondroprogenitor had similar population-doubling profiles (see Appendix 4).

3.3.4. Analysis of proliferating cells in CPC lines originating from cartilage of normal and OA donors and matched BM-MSCs from OA donors.

Proliferation of polyclonal OA-CPC lines, with matched OA-BM-MSCs and polyclonal N-CPC cell lines (n=1 per donor) were measured at a population doubling of 25 ± 2.5 using the BrdU assay as described in section 2.9 (Figure 3.4 & Figure 3.6). Three repeats were run for each cell line. There were variations in the percentage of positive BrdU cells from each donor (Figure 3.4) with the mean percentage BrdU positively labelled cells from each of the OA-CPC and matched OA-BM-MSCs donors calculated as $69.18 \pm 5.07\%$ and $65.69 \pm 4.23\%$, respectively, whilst $78.8\% \pm 1$ labelled positive for BrdU from N-CPC donors. All data sets showed a normal distribution and one-way

ANOVA showed no significant differences in cell proliferation between the selected cell lines ($p>0.05$).

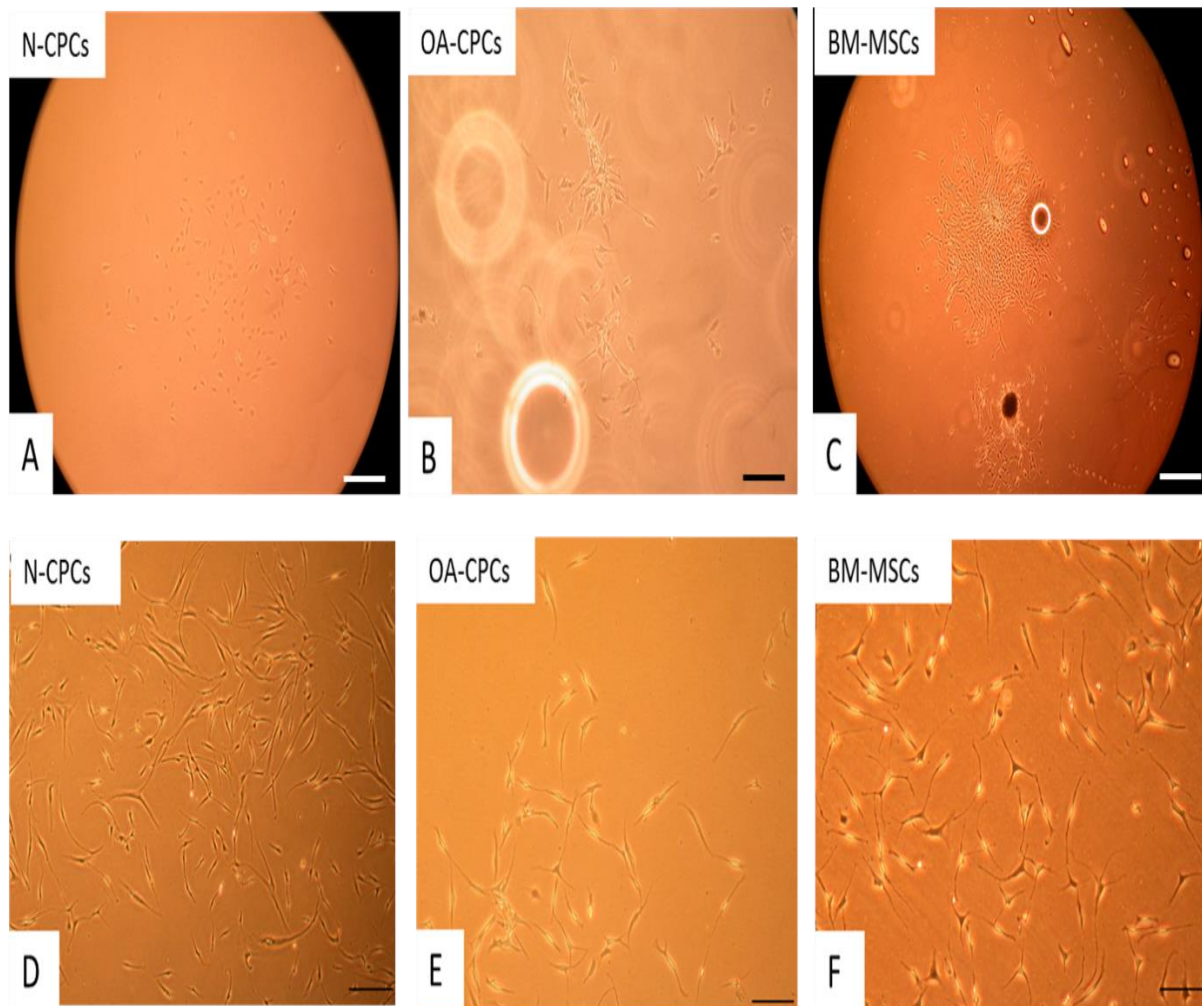


Figure 3. 3: Phase contrast images of cartilage progenitor cells and bone marrow MSC.

Image (A) colony formed chondroprogenitor cells from normal subject (N-CPC). Image (B) is from osteoarthritic cartilage progenitor cells (OA-CPC) while image C is from patient matched BM-MSCs. Image (D) is of isolated N-CPC after culture expansion and (E) from OA-CPC. Image (F) shows culture expanded bone marrow MSC. Scale bar: A-C = 100 μ m. Scale bar: D-F = 200 μ m.

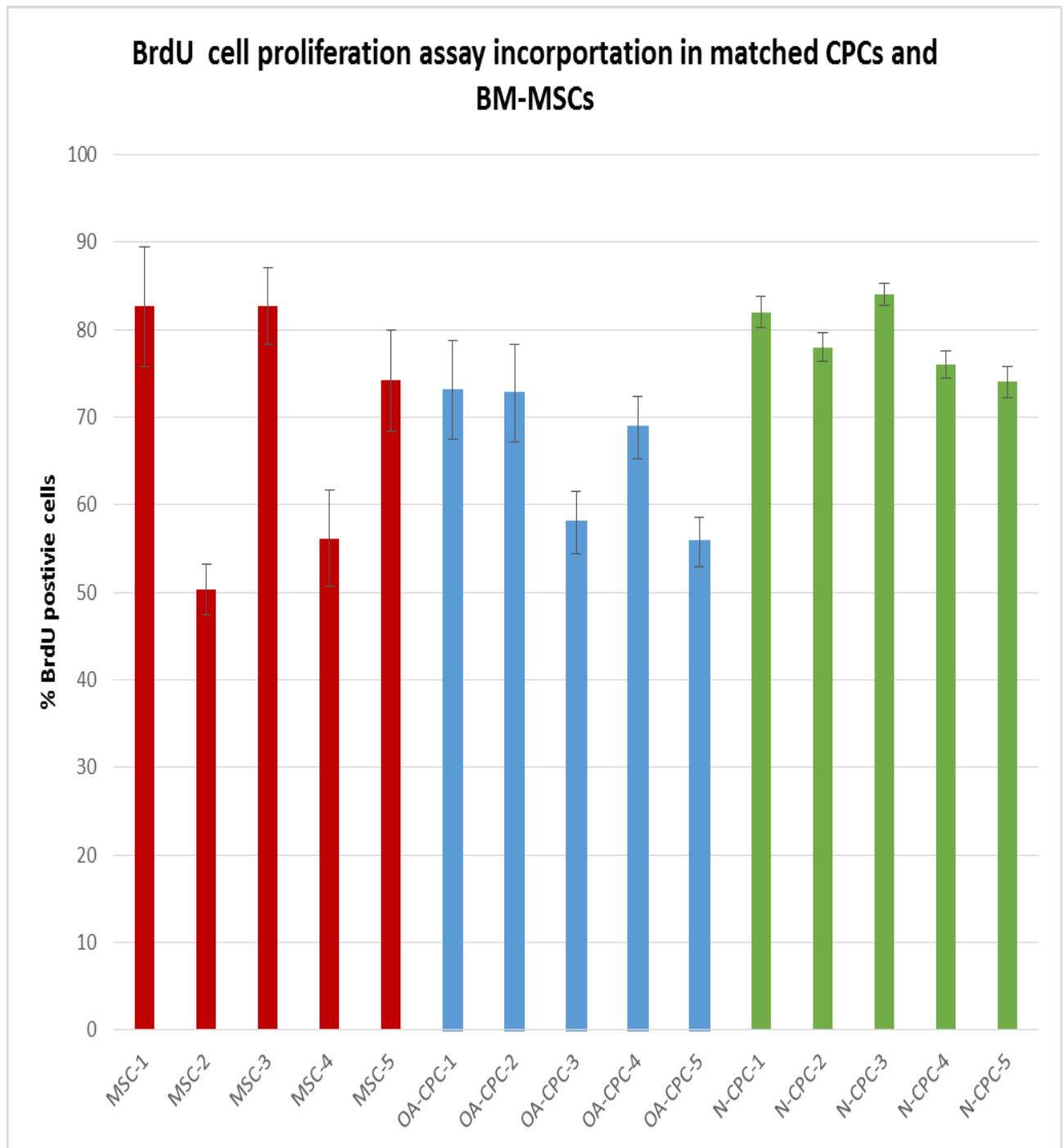


Figure 3. 4: Percentage incorporation of BrdU (5-bromo-2-deoxyuridine).

Cells were cultured in the presence of BrdU and incorporation was assessed by immunohistochemistry using an anti-BrdU antibody. The percentage of positive stained cells was calculated (n=3) for each cell line and data are presented as mean \pm SEM. Blue bars represent CPC lines from OA donors, Red bars represent cell lines from matched-MSC lines and Green bars represent CPC lines from normal donors.

3.3.5. Analysis of senescent cells in CPC lines originating from cartilage of normal and OA donors and matched BM-MSCs from OA donors.

The percentage of senescent cells in cultures of polyclonal OA-CPC lines with matched bone marrow derived OA-BM-MSCs and polyclonal N-CPC cell lines (n=1 per donor), were measured at a population doubling of 25 ± 2.5 using the senescence-associated β -galactosidase assay as described in section 2.10 (Figure 3.5 & Figure 3.6). Three repeats were run for each cell line. The percentage of senescent cells in cell line derived from OA-CPC and their matched-OA-BM-MSCs, were 0.59-6.7% and 0.7-9.8%, respectively, whilst a range of 0.8-2.4% was recorded for cell lines derived from N-CPC. All data sets showed a normal distribution and the mean values for senescent cells were $3.41 \pm 1.11\%$ OA-BM-MSCs, $2.58 \pm 1.05\%$, OA-CPC and 1.6 ± 0.58 N-CPC. One-way ANOVA showed no significant differences in cell senescence between the selected cell lines.

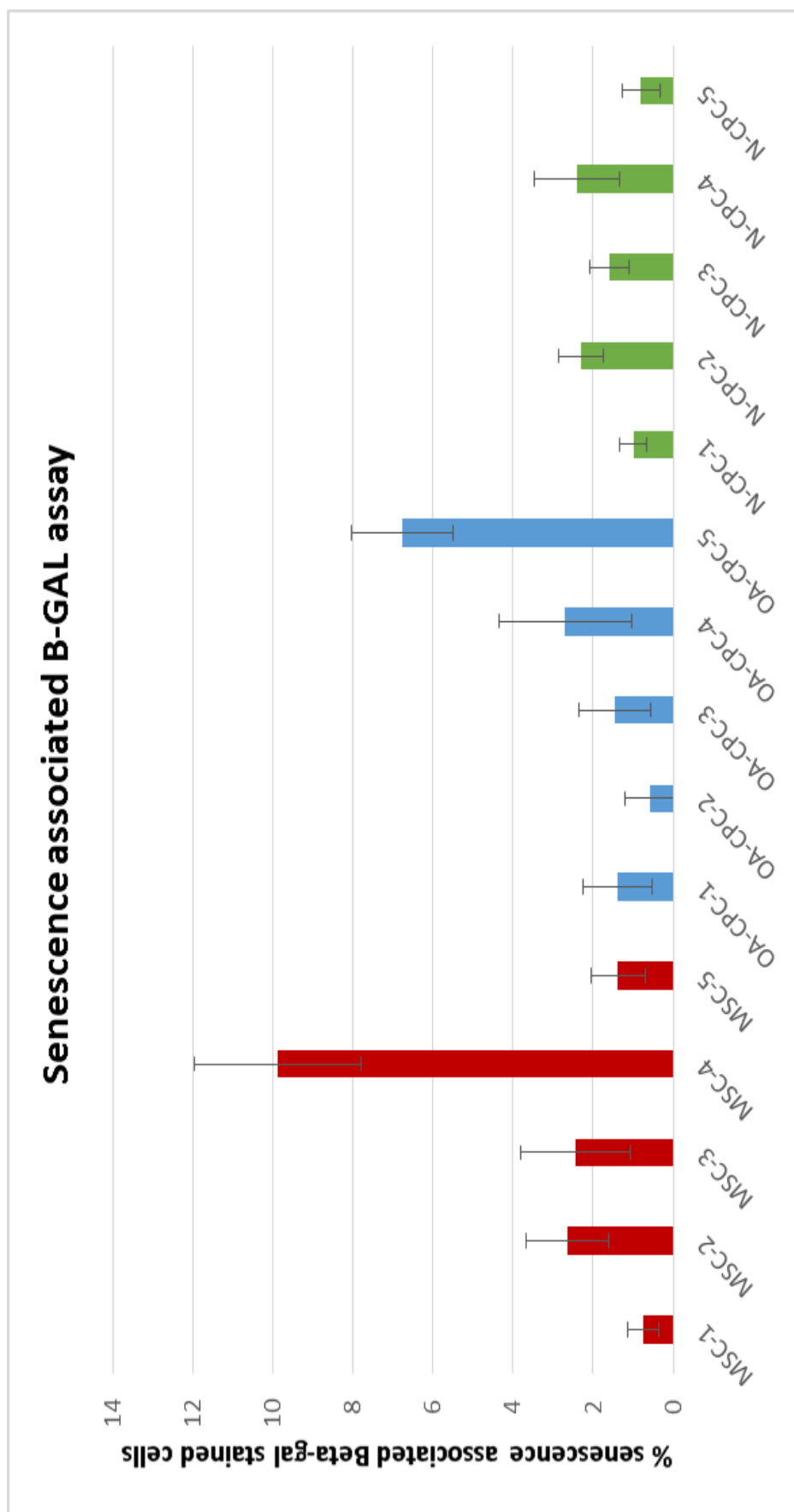


Figure 3. 5: Percentage of senescent cells from normal CPCs and OA-CPCs and BM-MSCs.

Cells were cultured and senescent cells were identified using the senescence-associated β -galactosidase assay. The percentage of positive stained cells were calculated ($n=3$) for each cell line and data are presented as mean \pm SEM. Blue bars represent CPC lines from OA donors, Red bars represent cell lines from matched-BM-MSCs lines and Green bars represent CPC lines from normal donors.

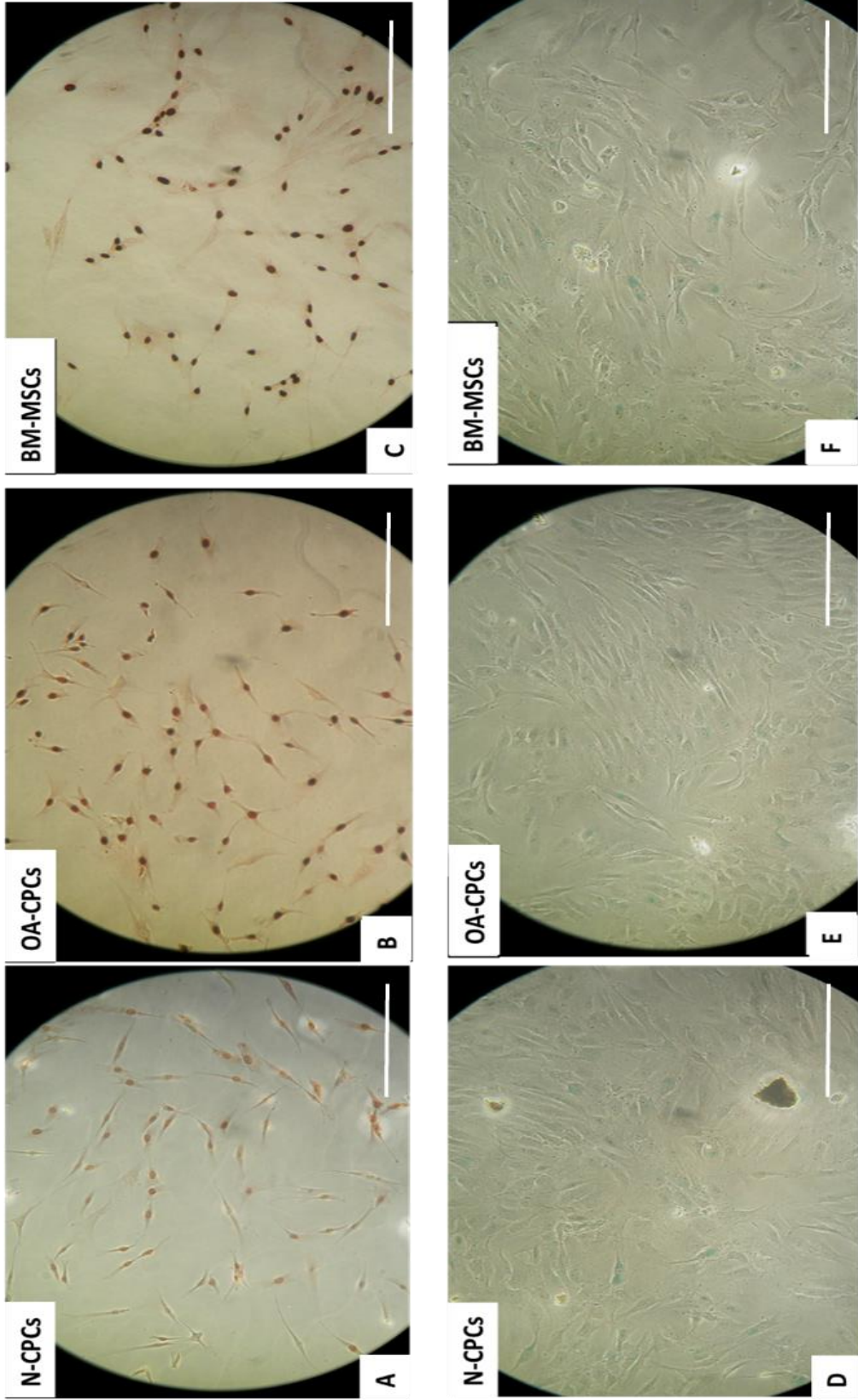


Figure 3. 6: BrdU labelling and senescence associated β -galactosidase assay of CPCs and BM-MSCs.

Representative images of polyclonal CPCs isolated from normal (A&D) OA cartilage (B & E) and their matched BM- MSC (C & F) stained for BrdU (A - C) and senescence associated β -galactosidase (D- F). Scale bar=200 μ m.

3.3.6. Interpatient variation of proliferation and senescence in CPC Vs

MSCs.

The proliferative potential of OA donor polyclonal CPC (n=5) and matched BM-MSCs (n=5) were measured at a population doubling of 25 ± 2.5 using a BrdU assay (Figure 3.7). By examining the interpatient BrdU incorporation, there were variations in the percentage of positive BrdU cells for each donor (Figure 3.7). Student t-test analysis examining the interpatient variation revealed that in patient 1 there were no statistically significant differences between the mean of the CPC and MSCs but in the remaining 4 patients there were statistical significant variation marked by p value < 0.05 . Interestingly, in the remaining four patients with statistical interpatient variations, in two patients MSCs had higher BrdU incorporation (Patient-3 and -5) while in two patients CPC had higher BrdU incorporation (Patient -2&-4).

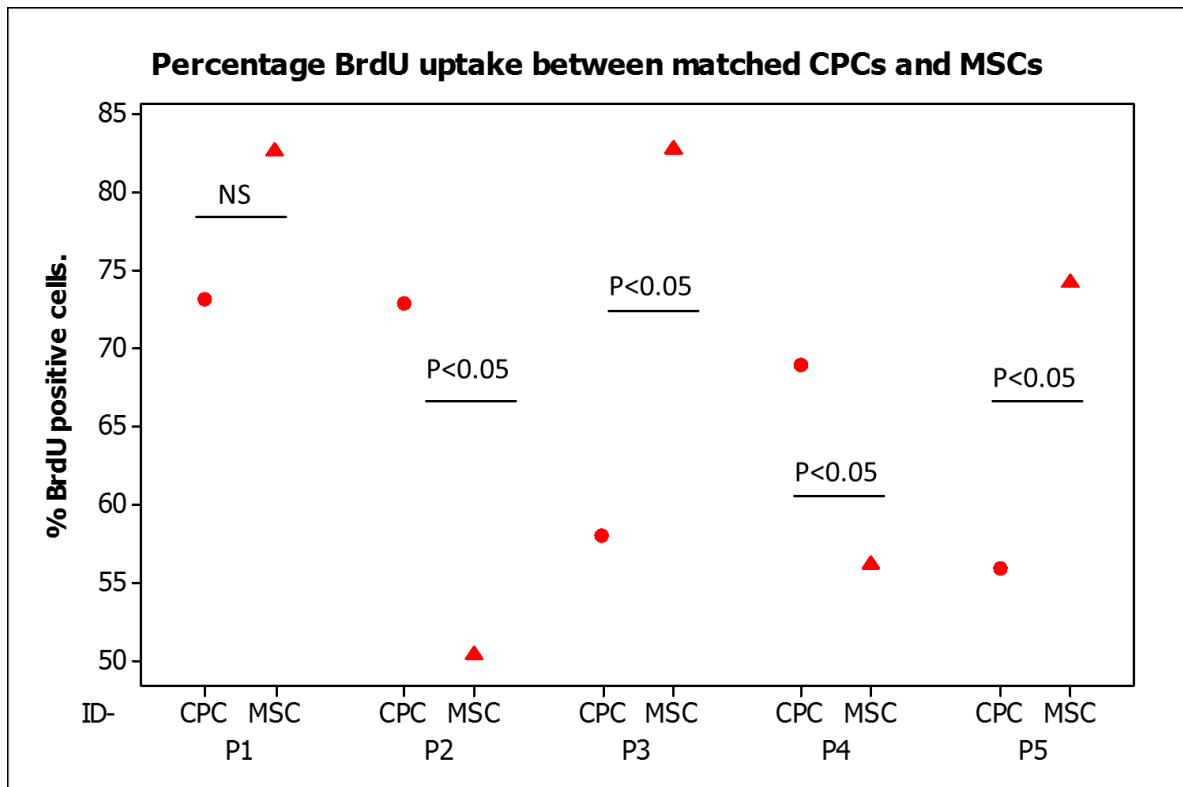


Figure 3. 7: Percentage BrdU uptake between matched CPC and MSCs. Percentage incorporation of BrdU (5-bromo-2-deoxyuridine) into matched CPC cell lines isolated from osteoarthritic cartilage (circle) and BM-MSCs (triangle) from five donor. Each cell line was analysed in triplicate. Data are presented as mean and analysed using a student t-test for statistical differences ($P < 0.05$, NS=not significant).

The senescence activity of polyclonal CPC with their matched BM-MSCs was analysed at a population doubling of 25 ± 2.5 using the associated β -galactosidase staining assay. By examining the interpatient β -galactosidase incorporation, there were variations in the percentage of positive senescent cells for each donor (Figure 3.8). Student t-test analysis examining the interpatient variation has revealed that three out of five patients were noted to have no statistical significant differences between the percentage β -galactosidase incorporation of CPC and MSCs respectively ($p > 0.05$). However, in the remaining two patients with statistical interpatient variations, patient-4 MSCs had higher BrdU incorporation ($p < 0.05$) while patient-5

had higher β -galactosidase incorporation in CPC cell line when compared to matched MSCs respectively ($p < 0.05$).

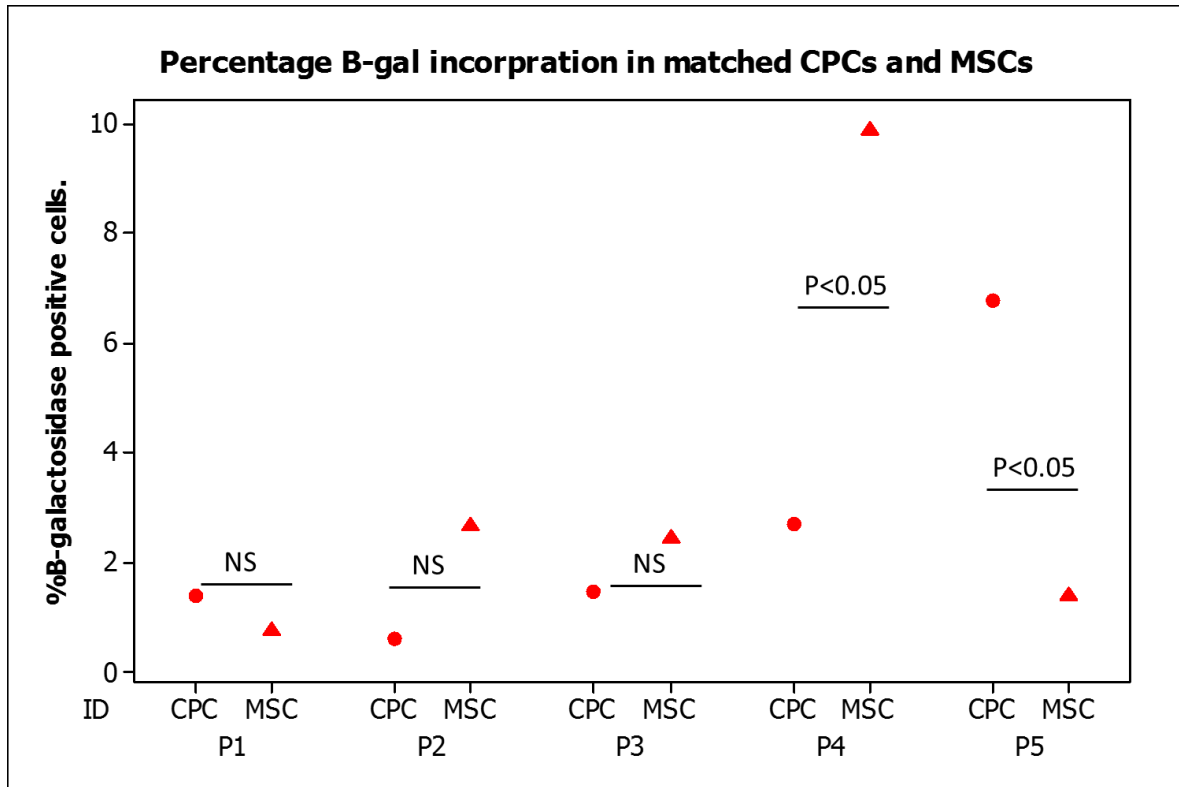


Figure 3. 8: Percentage B-galactosidase incorporation in matched CPC and MSCs.

Percentage incorporation of β -galactosidase into matched CPC cell lines isolated from osteoarthritic cartilage (circle) and BM-MSCs (triangle) from five donors. Each cell line was analysed in triplicate. Data are presented as mean and analysed using a student t-test for statistical differences ($P < 0.05$, NS=not significant).

3.3.7. Analysis of the expression of MSC cell surface markers in polyclonal CPC isolated from normal and OA donor cartilage with matched BM-MSCs from the OA donors.

Cell surface epitopes for the MSC cell surface biomarkers (CD-90, CD105, CD-166) were analysed in N-CPC, OA-CPC and matched OA-BM-MSCs cell lines using FACS (section 2.11). Analysis of the cell surface marker CD-34 was used as a negative

control for MSCs. CPC and OA-BM-MSCs cell lines were selected at a similar population doubling and analysis was carried out on one cell line per donor. Figure 3.9 shows a representative of the histograms generated from the analysis of OA-BM-MSCs, N-CPC and OA-CPC from one donor. Cell lines from all donors analysed showed positive expression of CD-90, CD-105 and CD-166 with a mean value of over 95% in the gated cells (i.e. live individual cells) with a unimodal expression indicative of a homogeneous cell population. There was however one exception as FACS analysis for polyclonal N-CPC with CD-166 showed a mean expression of 92.6% in gated cells that were positive for this stem cell marker. The mean expression of CD-34 (negative MSC marker) was 0.02% in N-CPC; 0.25% in OA-CPC and 0.53% in OA-BM-MSCs, ($P < 0.05$). Whilst the expression of CD-34 was somewhat higher in OA-BM-MSCs when compared to their matched OA-CPC and N-CPC lines, it was still within the accepted definition of a pure population of MSCs (Boxall and Jones, 2012, Kuhn and Tuan, 2010), [Table 3.1] as defined by the International Society for Cellular Therapy (ISCT). This data suggests that CPC have similar cell surface marker profiles to bone marrow MSCs.

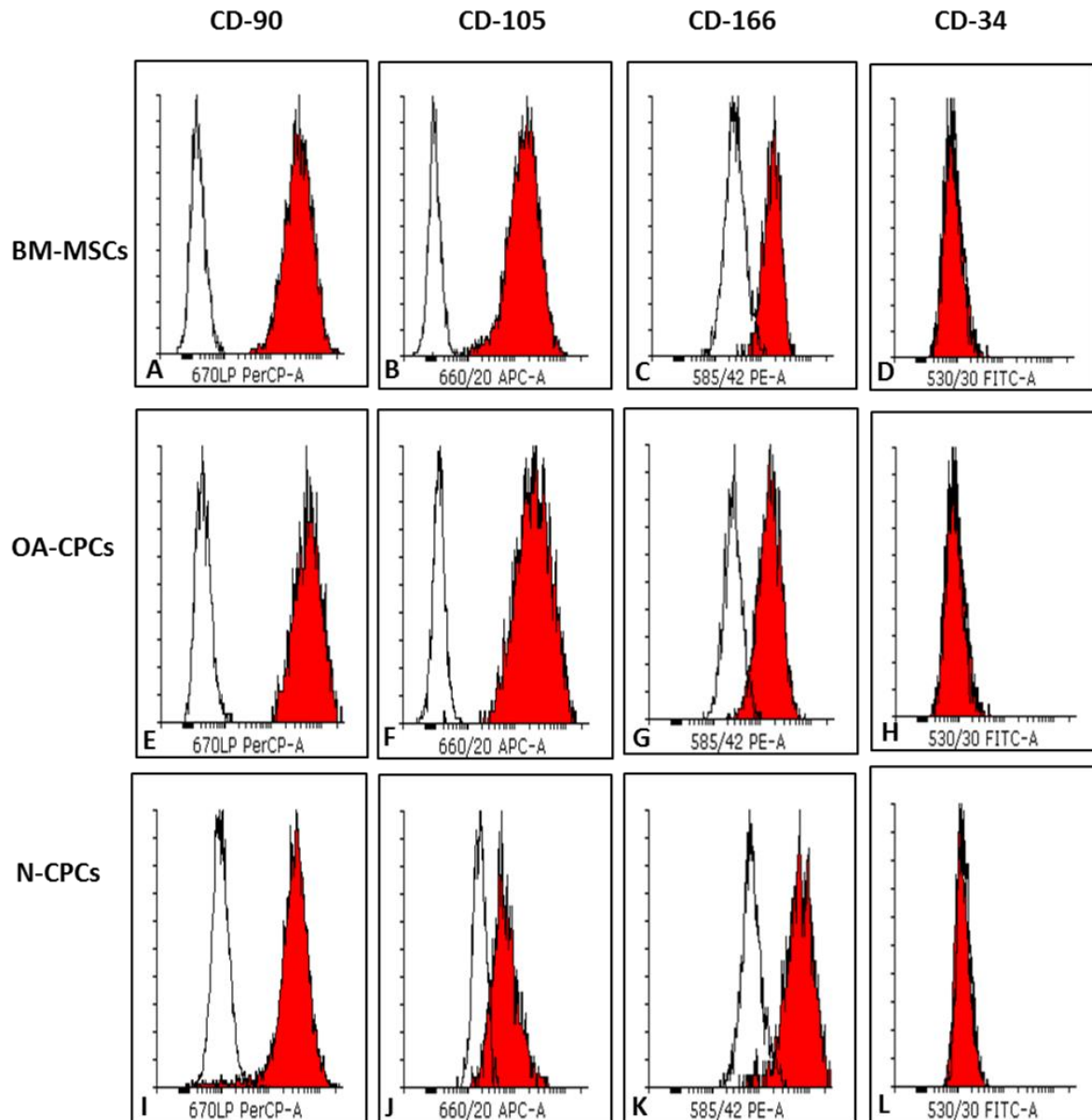


Figure 3. 9: Flow cytometry analysis of mesenchymal stem cells markers.

FACS analysis of the mesenchymal stem cell marker CD-90, CD-105 & CD-166 and the negative marker CD-34 was performed on CPC cell lines isolated from normal and osteoarthritic cartilage progenitor (CPC) and OA-matched bone marrow mesenchymal stem cell (OA-BM-MSCs). Representative histograms from an OA-BM-MSC cell line (Panel A-D), an OA-CPC cell line (E-H) and N-CPC cell line (I-L) are shown. The haematopoietic stem cells marker CD-34 was selected as a negative marker for MSCs and is shown in Panel D, H & L for each cell line. The Red filled histogram represents positively labelled cells and the un-filled histogram the matched isotype control.

Table 3. 1: Flow cytometry analysis of mesenchymal stem cells markers in isolated CPC and BM-MSCs.

| Cell line | CD-90 | CD-105 | CD-166 | CD-34 |
|------------------|--------------|---------------|---------------|--------------|
| N-1 | 96.33% | 94.65% | 91.95% | 0% |
| N-2 | 97.82% | 93.56% | 90.86% | 0.01% |
| N-3 | 99.46% | 91.37% | 94.89% | 0.04% |
| | | | | |
| OA-1 | 99.27% | 99.01% | 99.82% | 0.01% |
| OA-2 | 99.39% | 99.81% | 95.64% | 0.73% |
| OA-3 | 98.72% | 96.24% | 99.37% | 0.02% |
| | | | | |
| MSC-1 | 99.36% | 98.14% | 97.87% | 0.33% |
| MSC-2 | 99.65 | 97.77% | 99.72% | 1.18 5 % |
| MSC-3 | 99.14% | 99.50% | 94.92% | 0.72% |

3.3.8. Characterisation of multi-lineage differentiation of CPC and BM-MSCs.

Chondrogenic differentiation was initiated using 3D pellet cultures as described in section 2.2 using polyclonal N-CPC, polyclonal OA-CPC and matched OA-BM-MSCs from three donors, and cultures were terminated at 21 days. 3D pellet cultures were set up in 24 wells of a 96 well plate per donor per cell line and 12 wells were pooled for RNA analysis whilst 12 wells were processed for histochemistry.

Following 21 days in culture there was positive staining for Toluidine blue indicative of glycosaminoglycan synthesis during the culture period (Figure 3.10. A-C) in all cell lines tested. Visual analysis of N-CPC and OA-CPC pellets appeared to be slightly smaller and compact compared to OA-BM-MSCs. RT-PCR of isolated mRNA for expression of aggrecan (ACAN) and collagen II (col2a1) following chondrogenic differentiation showed all cell lines expressed message for these genes (Figure 3.10.D).

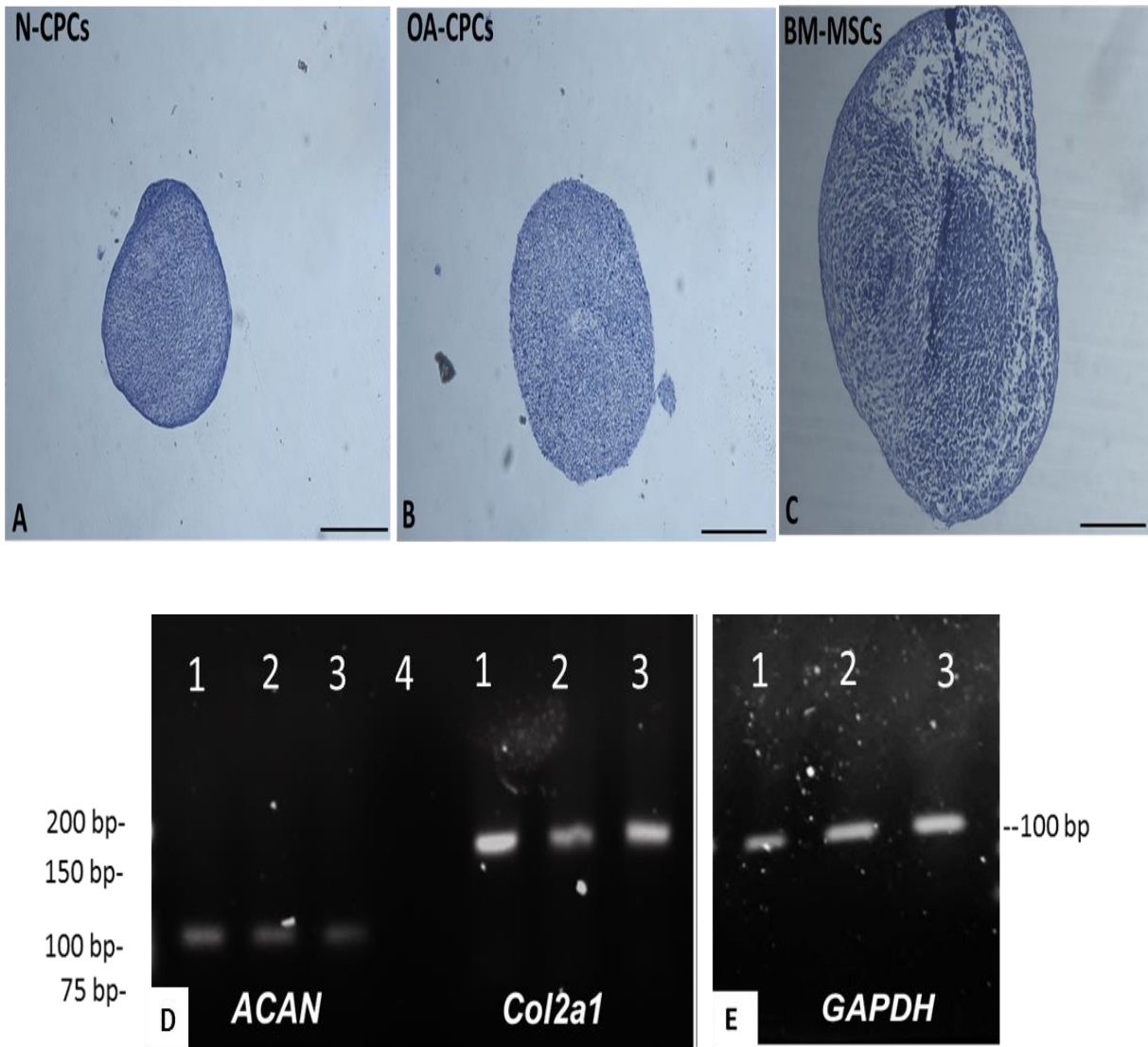


Figure 3. 10: Chondrogenic Differentiation of isolated CPC and MSCs.

Image A-C: Representative images of Toluidine blue stained pellets of N-CPC (A), OA-CPC (B) and matched OA-BM-MSC (C) lines after 21 days in culture. Image D-E: Representative images of PCR analysis for aggrecan (ACAN, 100bp), type II collagen (Col2a1, 165bp) and GAPDH (positive control, 95bp) mRNA expression. Cell lines stained positive with Toluidine blue indicating the synthesis of a glycosaminoglycan-rich matrix. Lane 1=N-CPC, Lane 2=OA-CPC, Lane 3= BM-MSCs and Lane 4=NTC. Scale bars = 50 μ m.

Osteogenic differentiation was initiated in monolayer cultures as described in section 2.2 using polyclonal N-CPC, polyclonal OA-CPC and matched OA-BM-MSCs from three donors, for 14 days and differentiation was assessed by staining for mineral deposition using Alizarin Red stain (Section 2.3.2) and isolation of mRNA for PCR analysis (Section 2.12.5) of the osteogenic markers, Runx-2 (Cbfa1) and Osteonectin (also known as SPARC). Staining with Alizarin Red showed a similar pattern of staining intensity in both N-CPC and OA-BM-MSC lines where both showed the presence of mineralized deposition. While in OA-CPC lines, despite the presence of calcium deposition, there were regions of no staining in the wells imaged (Figure 3.11).

RT-PCR analysis of the osteogenic differentiation markers Runx-2 and Osteonectin further supported the observed Alizarin Red staining as N-CPC, OA-CPC and OA-BM-MSC lines expressed mRNA for Osteonectin and Runx-2 (Figure 3.11.D).

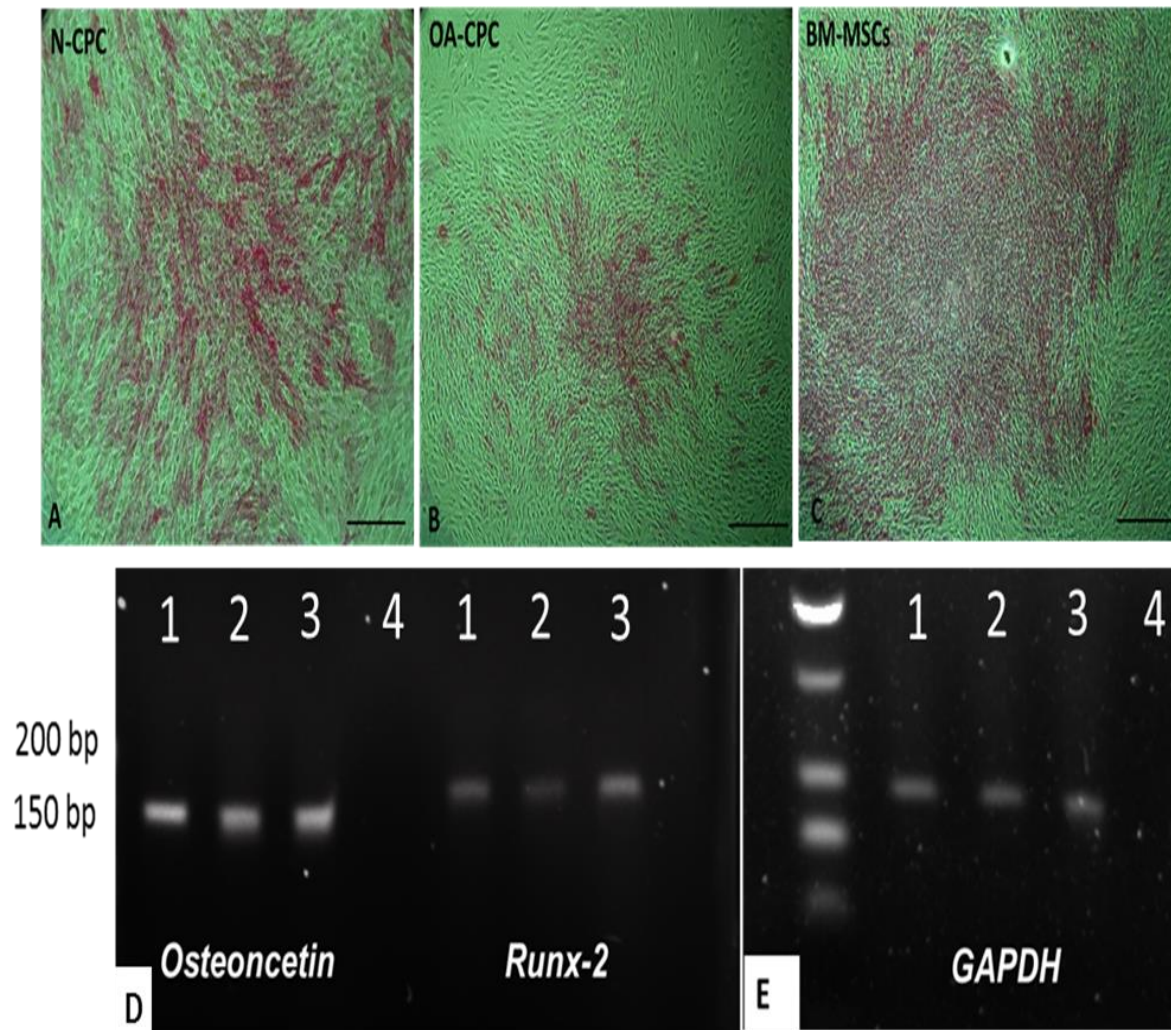


Figure 3. 11: Osteogenic differentiation of isolated CPC and MSCs.

Image A-C: Representative images of Alizarin Red staining in monolayer cultures of N-CPC, OA-CPC and OA-BM-MSC lines after 14 days of culture in osteogenic medium. Monolayers were stained using alizarin red to assess for calcium deposition a marker of osteogenic differentiation. Image D-E: Representative images from PCR analysis of mRNA expression of Runx-2 (164bp), Osteonectin (143bp) and GAPDH (control, 95bp) in N-CPC, OA-CPC and matched OA-BM-MSCs. Positive staining for Alizarin red was seen in all cell lines. Lane1=N-CPC, Lane 2=OA-CPC, Lane 3= BM-MSCs and Lane 4=NTC. Scale bars = 50 μ m.

Adipogenic differentiation was initiated in monolayer cultures as described in section 2.2 on N-CPC, OA-CPC and matched OA-BM-MSCs from three donors, for 1 week and differentiation was assessed by lipid deposition using Oil Red O stain as described in section 2.3.3 and isolation of mRNA for PCR analysis (Section 2.12.5) of the adipogenic markers, peroxisome proliferator-activated receptor gamma (PPAR- γ) (Figure 3.12.D) and lipoprotein lipase (LPL) (Figure 3.12.E). Staining for lipid was observed in CPC cell lines originating from cartilage obtained from normal donors and donors with OA and their matched BM-MSCs, confirming the adipogenic potential of these cell lines (Figure 3.12.A-C).

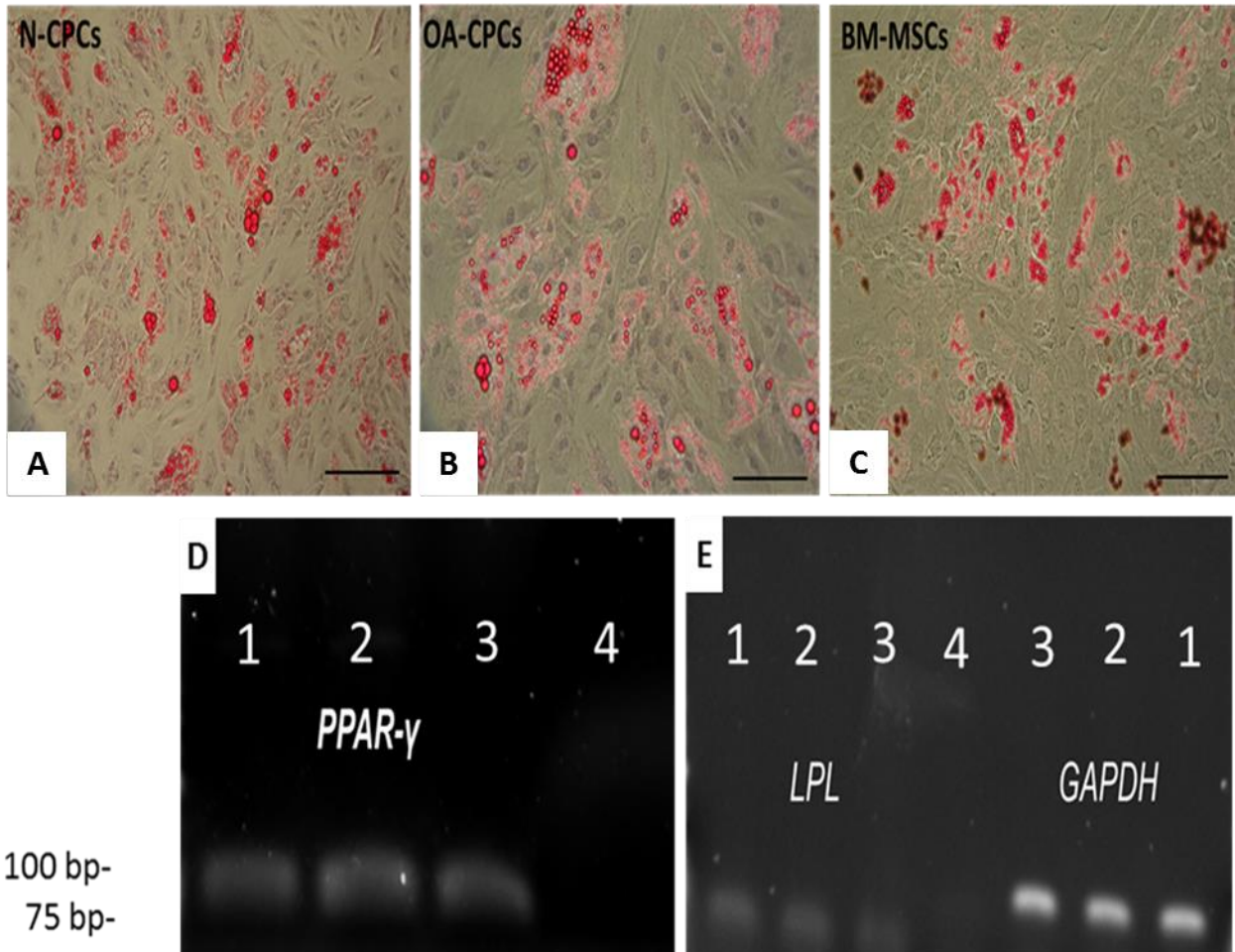


Figure 3. 12: Adipogenic Differentiation of isolated CPC and MSCs.

Images A-C: Representative images of Oil-red-O staining in monolayer cultures of N-CPC, OA-CPC and OA-BM-MSC lines after 1 week of culture in adipogenic medium. Deposition of lipid droplets can be seen in all cell lines as red staining with Oil-red O. Images D-E: Representative examples of RT-PCR adipogenic differentiation genes peroxisome proliferator-activated receptor- γ (D), PPAR- γ (78bp), and lipoprotein lipase (E), LPL (105bp), induction in monolayer cultures showing positive differentiation. GAPDH (95bp) was used as a housekeeping gene (E). Lane1=N-CPC, Lane 2=OA-CPC, Lane 3= BM-MSCs and Lane 4=NTC. Scale bars = 50 μ m.

3.4 Discussion.

The aim of this chapter was firstly to compare CPC lines isolated from normal and osteoarthritic cartilage and secondly to conduct a characterisation and comparative analysis of polyclonal CPC lines isolated from normal and osteoarthritic articular cartilage with isolated matched OA-BM-MSCs donors. BM-MSCs have been extensively studied as multipotent stem cells for use in a variety of tissue regenerative processes and most recently their use has been studied alongside autologous chondrocytes in the ASCOT trial for the repair of focal lesions in articular cartilage of young individuals (OsCell, 2013).

The isolation of CPC cells situated in mature human articular cartilage was accomplished by the use of the fibronectin adhesion assay, originally developed by Jones and Watt (1993) and later adopted by Dowthwaite *et al.* (2004). Based on the initial investigation of morphology, adherence to fibronectin and colony forming efficiency both normal and osteoarthritic CPC lines were shown to have similar morphological characteristics and statistically there were no difference in initial adhesion to fibronectin or colony forming efficiency between the two cell groups. Dowthwaite *et al.* (2004) showed that the mean percentage of CPC in a population of full-depth chondrocytes isolated from immature bovine articular cartilage following adhesion to fibronectin was 9%. Our findings from human articular cartilage were comparatively similar with an initial adhesion of 11.3% and 15.8% for normal and osteoarthritic CPC, respectively. In addition, Williams *et al.* (2010) and Nelson *et al.* (2014) reported an initial adhesion of OA-CPC ranging from 10.7-15.4%.

The colony forming efficiency of polyclonal N-CPC and polyclonal OA-CPC from the initially adhered cells was higher in OA-CPC (range from 6 donors; 0.1-0.73%) compared to N-CPC (range from 5 donors; 0.06-0.53%) but statistical analysis showed no significant difference ($p>0.05$). This data compare well with the published data from Nelson *et al.* (2014), Williams *et al.* (2010) and Dowthwaite *et al.* (2004) reporting CFE all at less than 1% isolated using the fibronectin adhesion assay. Interestingly, Grogan *et al.* (2009) reported a similar percentage of mesenchymal progenitor cells isolated from OA and healthy articular chondrocytes using FACS sorting of Hoechst 33342 labelled cells. Conversely, several other groups have reported a higher proportion of stem progenitor cells (10 -15%) isolated from articular cartilage chondrocytes by FACS sorting using a panel of MSC markers (Fickert *et al.*, 2004; Alsalameh *et al.*, 2004; Pretzel *et al.*, 2011). These percentages are similar to the initial adhesion to fibronectin and possibly reflect the combined population of stem progenitor cells and transient amplifying cell populations. Transit amplifying cells have a higher expression of $\alpha 5\beta 1$ integrin receptor compared to mature chondrocytes and so bind to fibronectin but subsequently these cells fail to proliferate upon clonal expansion (Dowthwaite *et al.*, 2004).

Isolation of OA-BM-MSCs were carried out using Ficoll™ density gradient centrifugation of the mononuclear cell fraction from the bone marrow aspirate from the tibial plateau of the knee joint of patients diagnosed with OA (Bajada *et al.*, 2009). Bone-marrow derived MSCs are generally a heterogeneous mixture of cells which are often difficult to isolate and separate based on clonal selection (Russell *et al.*, 2010; Papadimitropoulos *et al.*, 2014). Therefore these heterogeneous OA-BM-

MSCs were compared with polyclonal (i.e. heterogeneous) matched OA-CPC and N-CPC cell lines isolated from tibial plateau cartilage.

A characteristic feature of stem and progenitor cells is the ability to divide and renew for long periods in culture. Cumulative population doubling of all cell lines increased over a period of 80 days in culture (Appendix 2) and this was consistent with the published literature (Williams *et al.*, 2010; Nelson *et al.*, 2014). The proliferative capacity of all cell lines was further investigated using the BrdU assay. BrdU analysis of N- and OA-CPC and their matched OA-BM-MSCs revealed that all three cell types investigated showed strong proliferation potential with $78.8\% \pm 1$, $69.18 \pm 5.07\%$ and $65.69 \pm 4.23\%$, of cells recorded as positive for BrdU staining, respectively. This data suggests that OA-BM-MSC and their matched CPC, as well as N-CPC, have a similar proliferative capacity.

It has been reported that prolonged *in vitro* expansion of MSCs leads to an increase in cell senescence (Banfi *et al.*, 2000). In this study the cell senescence for each cell type was assessed using the senescence associated β -galactosidase assay first reported by Dimri *et al.*, (1995). The assay measures the activity of the alternative isoform of β -galactosides, known as senescence associated β -galactosidase, unlike the lysosomal β -galactosidase (Kurz *et al.*, 2000), this enzyme functions at neutral pH and was noted to be highly associate with cells found in permanent replicative arrest (Debacq-Chainiaux *et al.* 2009). Analysis showed that the percentage of senescent cells were $3.41 \pm 1.11\%$ OA-BM-MSCs, $2.58 \pm 1.05\%$, OA-CPC and 1.6 ± 0.58 N-CPC with no significant difference between the cell types analysed. Yu *et al.* (2011) have reported an increase in SA β -galactosidase activity with age,

however, in this study there was no statistical difference in cell senescence from mean age donors of 43yrs. from normal and 66 yrs. from OA derived cell lines. A lower percentage of cells were senescent in polyclonal N-CPC than in polyclonal OA-CPC and OA-BM-MSCs that could suggest that statistical significance was not reached due to the relatively low sample number. By examining the interpatient observation of matched OA derived CPC and MSCs, four donors showed variations in BrdU uptake between matched CPC and MSCs but only two out of 5 patient donors showed variation in percentage senescence rate. Interestingly, there were correlations in BrdU and β -galactosidase uptake in two donors only. For example, patient 4 showed higher proliferation marked by BrdU uptake in CPC when compared to matched MSCs while the MSC cell line had higher β -galactosidase expression. However, in patient 5 this pattern was reversed as there were more MSCs cell line with increased BrdU expression and less β -galactosidase expression when compared to the patient matched CPC cell line, respectively. Therefore, due to the limited 'n' number further work is needed before any conclusion can be made.

In 2006 the International Society for Cellular Therapy released guidelines for the minimal criteria for defining MSCs which included the expression of the cell surface markers CD105, CD73, CD90 and lack of expression of CD45, CD34, CD14 or CD11b or CD19 and HLA-DR surface molecules; plastic adherent when maintained in standard culture conditions and able to differentiate to osteoblasts, adipocytes and chondrocyte in an *in vitro* settings. Despite these criteria, there are notable differences in the cell surface marker expression profiles among MSCs isolated from

several tissues (Kern *et al.*, 2006; Miao *et al.*, 2006; Jin *et al.*, 2013) and also the ability to undergo tri-lineage differentiation (Grogan *et al.*, 2009).

All cell types investigated were able to adhere to tissue culture plastic and had the classical feature of spindle like morphology commonly seen in MSCs (Prokop, 1997). A novel finding in this study is the similar expression of putative mesenchymal stem cells markers found in CPC and BM-MSCs. Analysis of the mesenchymal stem cell markers, CD-90, CD-105 and CD-166 showed that both N-CPC as well as OA-CPC and matched OA-BM-MSCs cell lines (n=5, normal donors; OA=6 donors) had positive expression for all of the three cell surface markers. The expression profile of CD-90, also known as Thymocyte differentiation antigen 1(Thy-1), and that of CD-166, also known as Activated leukocyte cell adhesion molecule (ALCAM), was comparable between CPC and BM-MSCs providing further support of the similarities between these cell types and defining these cells as mesenchymal stromal cells. In contrast, there were differences in the expression of CD-105, also known as Endoglin, between N-CPC and OA derived cell lines, with 99% of OA derived cells positive for CD-105 but 95% of N-CPC positive for the mesenchymal stem cell marker. In addition, we found all cell types (i.e. CPC and BM-MSCs) to have almost no expression of the endothelial cell marker CD-34, hence confirming lack of contamination of cultures with other cell types.

Analysis of tri-lineage showed that all cell types were capable of differentiation to chondrocytes, osteoblasts and adipocytes. This data confirms that published by others investigating the tri-lineage potential of CPC cell lines (Williams *et al.*, 2010).

In summary, data collected in this study demonstrated that polyclonal N-CPC, polyclonal OA-CPC and patient derived matched OA-BM-MSCs show the classical defined characteristics that would define these cell types as multipotent mesenchymal stromal cells. This data further supports the notion that adult articular cartilage contains a cohort of stem/progenitor cells which could have a promising role in the regenerative process of articular cartilage.

CHAPTER 4: INVESTIGATING THE WNT SIGNALLING PATHWAY IN CLONAL PROGENITOR CELLS DERIVED FROM NORMAL AND OSTEOARTHRITIC DONORS.

4.1 Introduction.

Adult articular cartilage was, until recently, thought to have limited regenerative capacity. This was thought to be mainly due to a lack of blood supply that hinders stem cell migration to sites of injury. Dowthwaite *et al.* (2004) showed that a cohort of progenitor cells reside within the superficial zone of the articular cartilage and since this discovery, other groups have reported similar cohorts of progenitor cells in normal and osteoarthritic cartilage (Alsalameh *et al.*, 2004; Williams *et al.* 2010; Nelson *et al.*, 2014). The implication that these progenitor cells could have some inherent regenerative capacity to elicit self-repair has been proposed by several groups (Alsalameh *et al.*, 2004; Fickert *et al.*, 2004; Grogan *et al.*, 2009; Williams *et al.*, 2010; Pretzel *et al.*, 2011). The notion that this could provide a suitable cell-based source to the currently adopted approach of autologous chondrocytes implantation is pioneering (Hollander *et al.*, 2010).

A growing amount of evidence is emerging, which shows that the Wnt pathway plays a pivotal role in stem cell fate determination in many tissues including skeletal, skin, hematopoietic and gastrointestinal tissues (Hartmann, 2006; Sato *et al.*, 2009; Lander *et al.*, 2012; Staines *et al.*, 2012). Previous developmental work conducted on chicks and rodents have uncovered the important role the Wnt pathway plays in the process of chondrogenesis and chondrocyte homeostasis during postnatal development (Bafico *et al.*, 2001; Surmann-Schmitt *et al.*, 2009).

Genome Wide Association Studies (GWAS) have discovered several Wnt inhibitor genes with single nucleotide polymorphism mutations that may predispose individuals to OA (Loughlin *et al.*, 2004; Rodriguez-Lopez *et al.*, 2007; Blom *et al.*, 2009). Recently, several groups have observed that there is a reactivation of key skeletal developmental pathways (including the Wnt pathway) in models of OA (Zhu *et al.*, 2009a; Saito *et al.*, 2010; Yang *et al.*, 2010; Weng *et al.*, 2010; Zhen *et al.*, 2013). Current literature suggests that the Wnt pathway regulates the process of chondrogenesis and this pathway and its antagonists may also affect chondrocyte homeostasis leading to the development of OA (Staines *et al.*, 2012).

The aim of this study was to further our understanding of the Wnt pathway and the Dkk-1 antagonist of this pathway in CPC cells isolated from normal and osteoarthritic human articular cartilage to provide a more detailed characterisation of CPC with a view to optimising their use in tissue repair of cartilage defects.

The objective of this chapter was to examine the expression of Wnt pathway genes in CPC isolated from normal donors with healthy articular cartilage and from donors with evidence of osteoarthritis.

Identifying key regulators of CPC in the cartilage tissue would aid us in designing strategies for selecting CPC with optimum potential that could be used to produce large numbers of cells for clinical application.

4.2 Experimental Methods.

Monoclonal cell lines from N-CPC (n=3 donors) and OA-CPC (n=3 donors) were culture expanded as described in section 2.2.3 and total RNA was isolated (section 2.14). The expression pattern of the 84 Wnt pathway genes present in RNA isolated from these cell lines was assessed using the Wnt signalling pathway RT² Profiler PCR array (section 2.12.3).

Following analysis of the array data cultures of full-depth chondrocytes (OA n=6 donors; n=5 normal donors), monoclonal N-CPC (n=9 cell line) and monoclonal OA-CPC (n=20 cell lines), Table 4.2, were set up. Culture medium was collected and stored and cell layers were processed for RNA analysis. The expression levels of Dkk-1 from RNA isolated from the cell layers were analysed using qPCR and the culture media were analysed for Dkk-1 protein using the ELISA as described in section 2.12.5.

Following analysis of this data three clonal cell lines were selected per patient from osteoarthritic donors (n=5) and normal donors (n=4) and were plated into T75 flasks (1 x10⁶ cells) and cultured in basal medium consisting of DMEM+10% FBS+PS for 48hrs. Medium was collected and centrifuged to remove debris and dead cells and filtered using 0.2µm. Medium was then assessed for regulatory effects on the activity of the Wnt pathway, using the TCF-luciferase reporter assay as described in section 2.14.

From the results generated, CPC lines were characterised as Dkk-1^{high} or Dkk-1^{low} and selected to evaluate their chondrogenic differentiation potential.

Experiments were set up to evaluate the effect on chondrogenic differentiation of CPC cell lines secreting high concentrations of Dkk-1 (Dkk-1^{high}) with those secreting undetectable or low levels of Dkk-1 (Dkk-1^{low}). Three OA-CPC cell lines were selected that were shown to have high concentrations of Dkk-1 in the conditioned medium from three different donors and three N-CPC lines were selected that had undetectable levels of Dkk-1 from 3 different donors. RNA was extracted from 1 x10⁵ cells per cell line prior to initiating chondrogenic differentiation experiments and this served as the baseline for mRNA analysis. Cells were seeded to form 3D pellets as described in section 2.3.1. Hence, CPC were cultured under chondrogenic conditions as 12 replicates per CPC cell line/per patient/per time point in 96 well plates. For each time point (7, 14, 21 days) three wells were processed for histochemical/immunohistochemical analysis and the remaining 9 wells were processed for molecular analysis. For molecular analysis the RNA from three wells were pooled together (n=1) and the three triplicates generated were assayed using a custom-made RT² Profiler™ PCR Array to study expression levels of several genes implicated in chondrogenic differentiation (*ACAN*, *Sox-9*, *Col2a1*), hypertrophic chondrocyte differentiation (*Col1a1* and *MMP-13*), multi-potency morphology marker (*ALCAM*), degradation and inflammatory markers (*ADAMTS-4* and *IL-1β*) and the canonical Wnt target genes (*Dkk-1*, *Dkk-2*, *CTNNB1*). In addition, medium was harvested and pooled weekly and analysed for cell viability using the LDH assay (Section 2.4) and Dkk-1 concentration using ELISA (Section 2.13.5). Histochemical and immunohistochemical analysis was carried out on cell pellets harvested after 21 days of culture from 3 wells (section 2.8.1). Finally, topographical

immunolocalisation of Dkk-1 was studied in osteochondral tissues isolated from normal and OA donors.

4.3 Results:

4.3.1 Wnt signalling expression in human monoclonal CPC lines isolated from normal and osteoarthritic articular cartilage.

The differential expression pattern of Wnt pathway genes, using mRNA from monoclonal N- and OA-CPC were investigated using the Wnt signalling pathway RT² Profiler PCR array. Scatter plot analysis (Figure 4.1) of the processed data using the N-CPC as the control showed that of the 84 genes analysed 57 genes showed no significant difference in expression between the N-CPC lines and OA-CPC lines (Figure 4.1, black circles. $p \geq 0.05$). In addition, there was a down-regulation of MMP-7 and NKD-2 in OA-CPC cell lines (Table 4.1 and Figure 4.1 blue circles) and an up-regulation of 25 genes shown in Table 4.1 and Figure 4.1 (red circles; $p < 0.05$).

Interestingly, gene expression profiling showed that there was increased expression of genes involved in cell fate (Dkk-1 and Wnt3a); cell polarity (Axin2, Dvl2, MAPK8 & NKD1); growth and proliferation (CTBP1, DAB2, FOSL1, LRP5, PPARD, WISP1, WNT3 & MMP7) cell migration (Dkk-1 & LRP5) and cell cycle (CCND2, EP300, RHOU & TCF7L1). Several non-canonical Wnt pathway genes were also up-regulated in OA-CPC lines including (NFATC1, WNT2B, WNT4, WNT5A and WNT5B). However, a substantial number of Wnt inhibitors genes were also significantly up-regulated in the OA-CPC lines tested (AXIN2, CTBP1, DKK-1, DKK3, FBXW4, LRP5, TLE1 & NKD1) (Table 4.1).

Of the 25 up-regulated genes, Dkk-1 was over-expressed in OA-CPC lines with a fold-increase of 48.25 (Table 4.1). This gene was selected for further analysis by qPCR using cDNA isolated from full-depth chondrocytes (normal and OA), monoclonal N-CPC and monoclonal OA-CPC (see section 4.2). Using 2-way ANOVA comparing full-depth and CPC from normal and OA, q-PCR analysis of Dkk-1 showed that there was no significant difference in the expression of Dkk-1 between full-depth chondrocytes from normal and osteoarthritic donors and N-CPC isolated from macroscopically normal cartilage ($p > 0.05$). However, there was a significant increase in the expression of Dkk-1 in isolated monoclonal OA-CPC (Figure 4.2). Statistical analysis showed that there was a significant difference in the level of Dkk-1 between CPC isolated from normal articular cartilage versus CPC isolated from OA cartilage donors (Figure 4.2 N-CPC black triangle, OA-CPC red squares; $p < 0.05$).

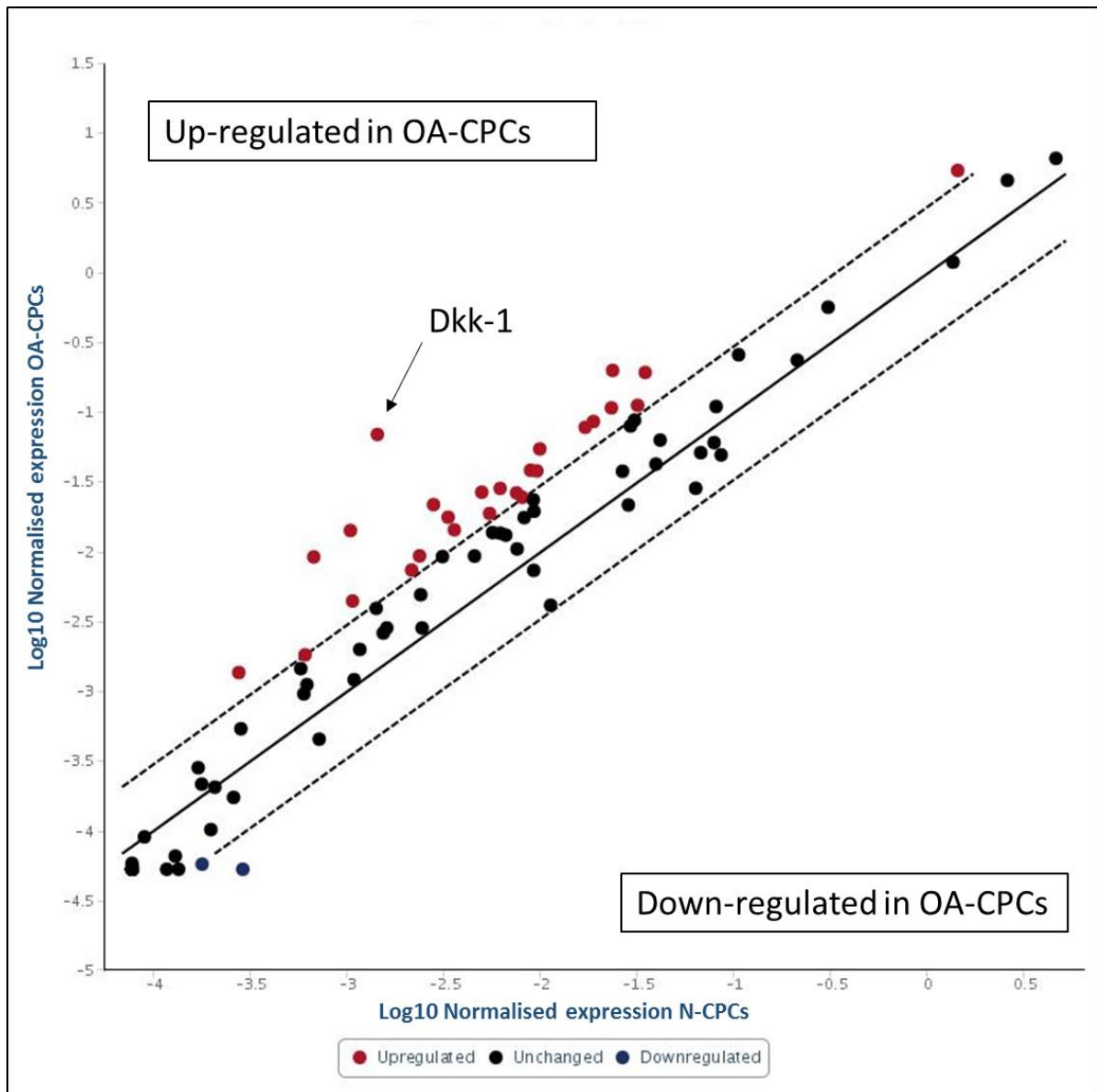


Figure 4. 1: Scatter plot of PCR array analysis of 84 genes involved in the Wnt signalling pathway.

PCR array analysis was performed using cDNA from RNA isolated from culture expanded monoclonal N-CPC and OA-CPC. N-CPC isolated from macroscopically normal articular cartilage served as the control. Scatter plots were generated using the SA Bioscience software package (version 5.2) to visualize up or down-regulated genes in OA-CPC. Red dots indicate genes up-regulated 3-fold or more from analysis using cDNA from RNA isolated from OA-CPC lines. The black arrows shows the location of Dkk-1 gene expression.

Table 4. 1: Table showing Wnt pathway genes up or down-regulated in OA-CPC cell lines.

The fold-change in Wnt gene expression was calculated for 3 OA-CPC cell lines taken from 3 donors relative to the gene expression in 3 N-CPC cell lines from 3 normal donors. To calculate the Δ Ct data for each gene, Ct values were normalised to the geometric mean of 2 housekeeping genes (ACTB, HPRT1, B2M, GAPDH and RPLP0). Genes up-regulated in OA CPC are depicted in red with fold change and genes down-regulated in OA-CPC lines are in blue.

| Genes differentially expressed between OA and Normal CPC | | | |
|---|--------------------|------------------------|---------------------|
| Position | Gene Symbol | Fold Regulation | 95% CI |
| A01 | AES | 4.5815 | (0.00001, 18.12) |
| A04 | AXIN2 | 3.9336 | (0.00001, 8.46) |
| A08 | CCND2 | 13.6028 | (0.00001, 67.74) |
| A11 | CTBP1 | 3.5206 | (0.00001, 9.08) |
| B04 | DAB2 | 8.4513 | (0.00001, 27.01) |
| B05 | DIXDC1 | 3.5206 | (0.00001, 10.11) |
| B06 | DKK-1 | 48.2514 | (0.00001, 123.99) |
| B07 | DKK3 | 4.3244 | (0.00001, 16.64) |
| B09 | DVL2 | 4.0069 | (0.00001, 14.53) |
| B10 | EP300 | 5.3858 | (0.00001, 17.79) |
| B12 | FBXW4 | 3.4323 | (0.00001, 10.25) |
| C02 | FOSL1 | 4.6241 | (0.00001, 16.78) |
| D08 | LRP5 | 5.3117 | (0.00001, 19.50) |
| D10 | MAPK8 | 3.0508 | (0.00001, 4.45) |
| E01 | NFATC1 | 4.5921 | (0.00001, 10.93) |
| E06 | PPARD | 3.9609 | (0.00001, 10.87) |
| E10 | RHOA | 13.6658 | (0.00001, 48.88) |
| F04 | TCF7L1 | 3.4482 | (0.00001, 9.24) |
| F05 | TLE1 | 7.7767 | (0.00001, 21.95) |

| | | | |
|-----|-------|---------|--------------------|
| F08 | WISP1 | 5.499 | (0.00001, 15.73) |
| G02 | WNT2B | 4.1482 | (0.00001, 12.39) |
| G03 | WNT3 | 3.0088 | (0.04, 5.98) |
| G05 | WNT4 | 4.9445 | (0.08, 9.81) |
| G06 | WNT5A | 5.55 | (0.00001, 15.82) |
| G07 | WNT5B | 4.571 | (0.00001, 10.66) |
| D11 | MMP7 | -3.0826 | (0.03, 0.62) |
| E02 | NKD1 | -5.4547 | (0.02, 0.35) |

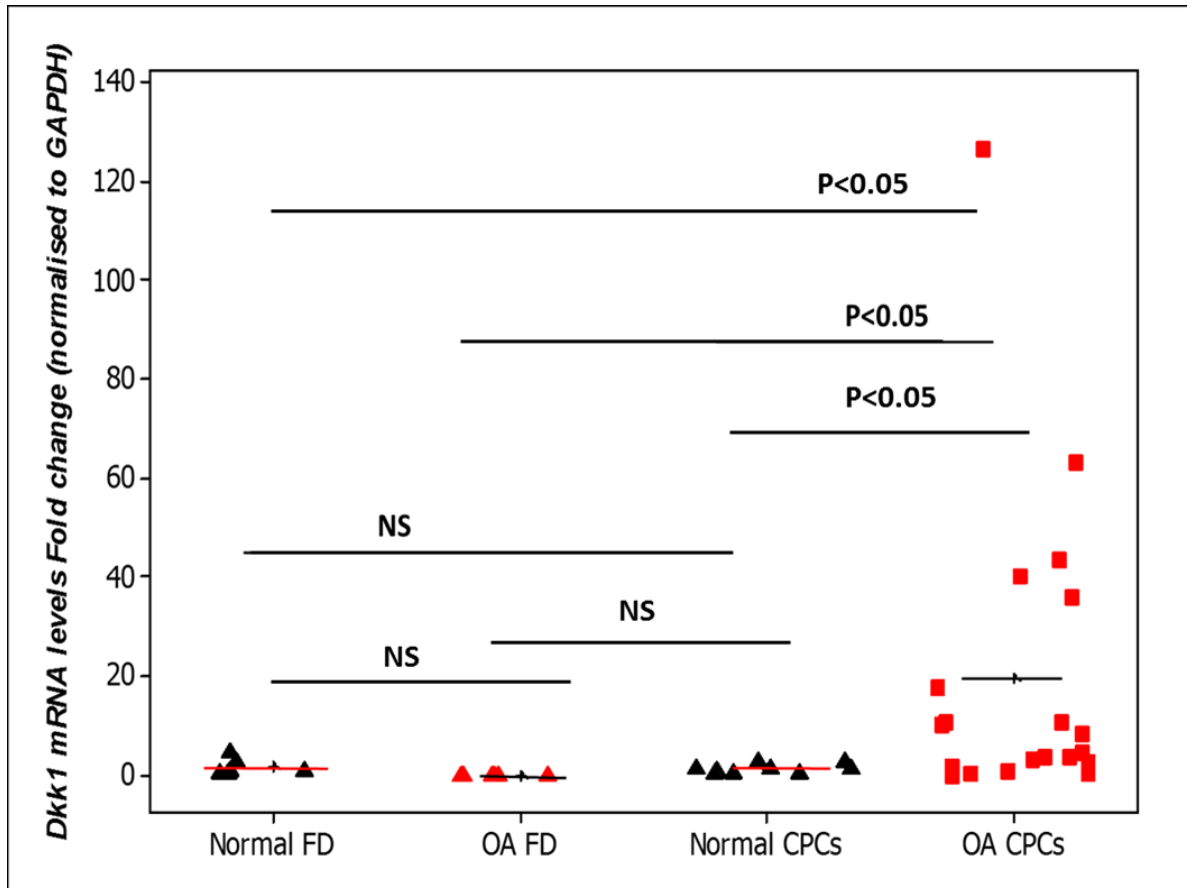


Figure 4. 2: Real-time quantitative PCR of DKK-1 mRNA expression in full-depth chondrocytes and CPC.

Dkk-1 mRNA expression in selected monoclonal CPC lines and full-depth (FD) chondrocytes from normal and OA donors were analysed by qPCR and the fold change calculated as described in section 2.12.5. (N-FD, n=5; OA-FD, n=6; N-CPC, n=9; OA-CPC, n=20). Horizontal lines in each sub-group show the mean value. Data are presented as mean and analysed using a 2-way ANOVA for statistical differences (* P < 0.05, NS=not significant).

4.3.2. Dkk-1 ELISA of conditioned media harvested from cultures of monoclonal N-CPC and OA-CPC lines.

Dkk-1 was measured using ELISA in a total of 10 OA-CPC cell lines across a selection of cell lines that had either a high or a low mRNA expression (Table 4.2) along with 11 N-CPC cell lines, the concentration of Dkk-1 in each cell line is presented in Table 4.2. The concentration of secreted Dkk-1 from the 10 OA-CPC lines (n=6 donors)

ranged from 1578.8 – 56605 pg/10⁶ cells and those from the 11 normal CPC (n=5 donors) ranged from undetected –1459.1 pg/10⁶ cells. Statistical analysis of this data (Figure 4.3) using one-way ANOVA showed a significant difference (p=0.01) between the concentrations of Dkk-1 in N-CPC lines to OA-CPC lines tested.

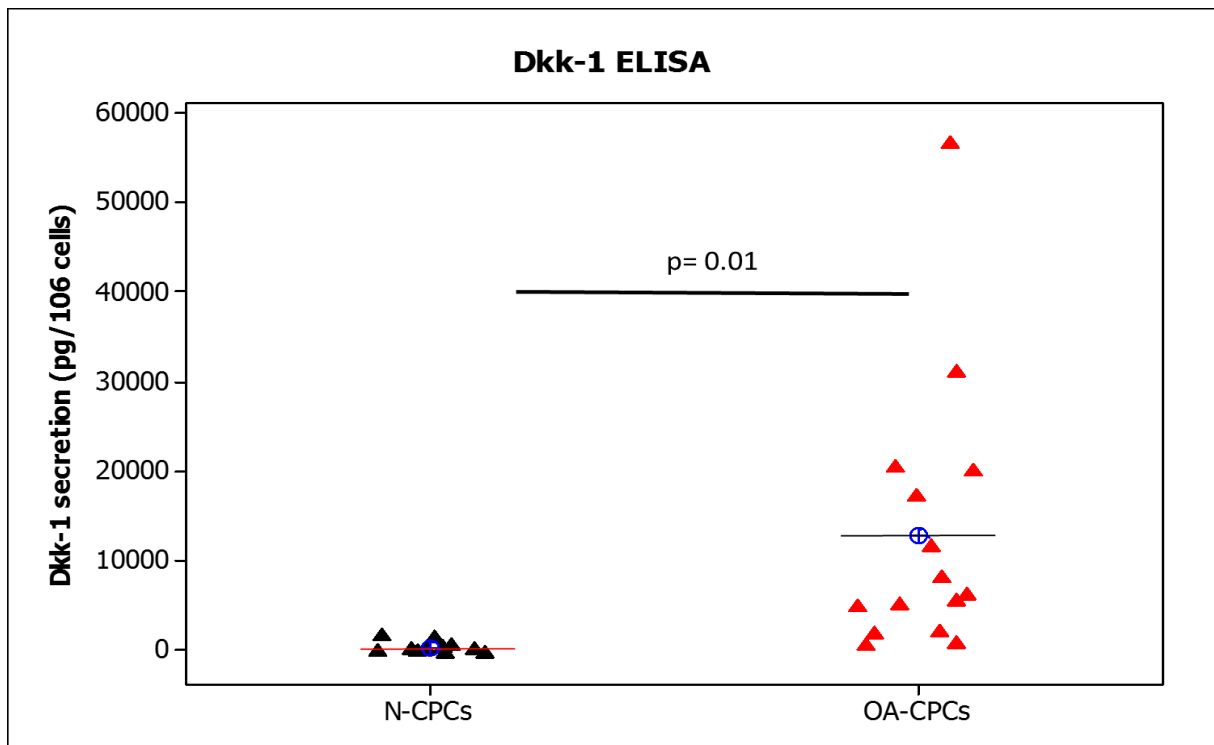


Figure 4. 3: Concentration of Dkk-1 in media from N-CPC and OA-CPC lines.

Concentration of Dkk-1 was measured in culture media using the Dkk-1 ELISA (R & D Systems). Concentration of Dkk-1 in N-CPC lines (n=11 from 5 donors) are seen as black triangles and in OA-CPC (n=10 from 6 donors) lines as red triangles. Concentrations were normalised to cell number. Horizontal lines in each sub-group show the mean value and analysed using a 1-way ANOVA for statistical differences (P < 0.01).

4.3.4 The effect of CPC conditioned media on the modulation of β -catenin using the TCF-luciferase reporter assay.

The TCF luciferase reporter assay (Ewan *et al.* 2010) utilizes a plasmid containing TCF that has been stably transfected into HEK293 cells. Addition of the Wnt ligand (Wnt3a) plus R-spo1 to culture media of the stably transfected HEK293 cells results

in the activation of β -catenin resulting in the downstream activation of TCF-luciferase and subsequently the activation of the LEF transcription factor. This activation results in the emission of light that can be measured and quantified as a measure of the activation of the canonical Wnt pathway. The activation of this pathway can be inhibited by a number of Wnt ligand antagonists and this results in a decreased light emission in this assay system. This assay was used to test the Wnt modulatory activity of conditioned media in the presence of Wnt 3a and R-spo1 from the culture of N-CPC or OA-CPC cell lines from a number of donors.

In the presence of Wnt3a and R-spo1 ligands there was an activation of the luciferase reporter plasmid in the HEK292-7df3 and this was taken as 100% activity and was used to calculate the percentage of Wnt activation in all experimental samples (Figure 4.4). In the presence of Dkk-1 at 50 ng there was a 40% reduction in Wnt activation and concentrations of Dkk-1 at 250 ng and 500 ng resulted in 85% and 90% reduction, respectively (Figure 4.4).

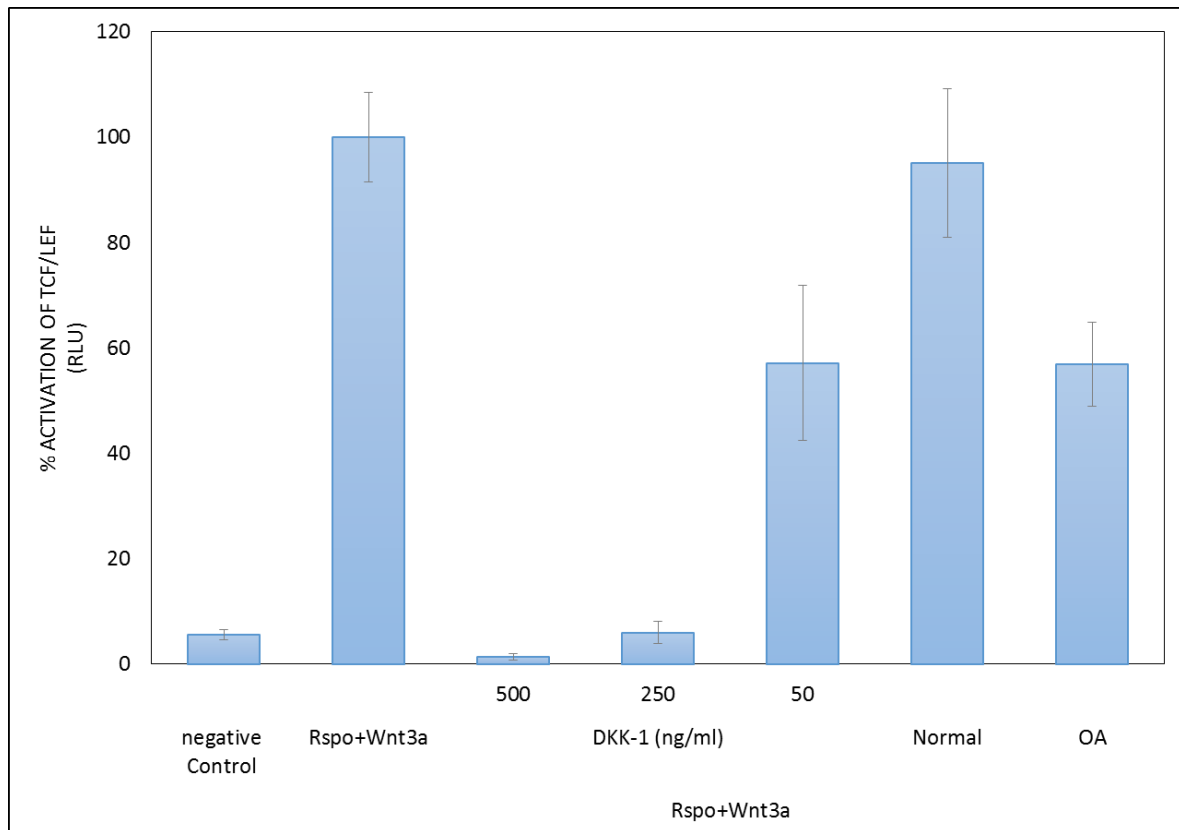


Figure 4. 4: Effects of CPC conditioned media on Wnt TCF-luciferase reporter assay.

The effect of recombinant Dkk-1 and secretome of CPC cell lines from normal and OA donors were examined using the 7df3 TCF-luciferase reporter cell assay. Forty eight hours prior to initiating the experiments, CPC of normal (n=4 donors) and osteoarthritic donors (n=5 donors) were cultured in basal media at 1×10^6 cells. Collected media were centrifuged and filtered before incubating with 7df3 TCF-luciferase reporter cells treated with a positive inducer of TCF activity (Wnt-3a (150 ng/mL) and R-Spo1 (24 ng/mL) and incubated for 24 hrs \pm exogenous Dkk-1 at (50, 250 and 500 ng/mL). In addition, a negative control of Doxycycline which inhibits β -catenin expression in reporter cells was included. After incubation period, cells were lysed using Glo lysis buffer and incubated with luciferase substrate (Promega Bright Glo) before measuring luciferase activity using a plate reader. Data are presented as percentage mean activation of TCF of 4 replicates per condition \pm SD. Data were analysed using 1-way ANOVA for statistical significance (* = $P < 0.05$, ** = $P < 0.01$).

Overall the TCF luciferase activity was not reduced by culturing reporter cells with the recombinant Wnt3a and R-spo1 proteins diluted in conditioned media derived from normal clonal CPC (Figure 4.5). However, osteoarthritic conditioned media showed greater variation in the presence of Wnt-3a/R-Spo-1 (Figure 4.5). The majority of clonal CPC from normal donors had a percentage activation of TCF ranging from 80-125% with the exception of 2 clonal cell lines that had 71.8 and 71.93% TCF activation (Figure 4.5). While clonal cell lines isolated from osteoarthritic donors showed a more heterogeneous inhibition on TCF reporter activity. The percentage activation of osteoarthritic clonal CPC ranged from TCF activation of 25.9- 86.4%. In addition, no adverse effect on reporter cell viability was observed when treated with conditioned media or recombinant Dkk-1 proteins (Figure 4.6).

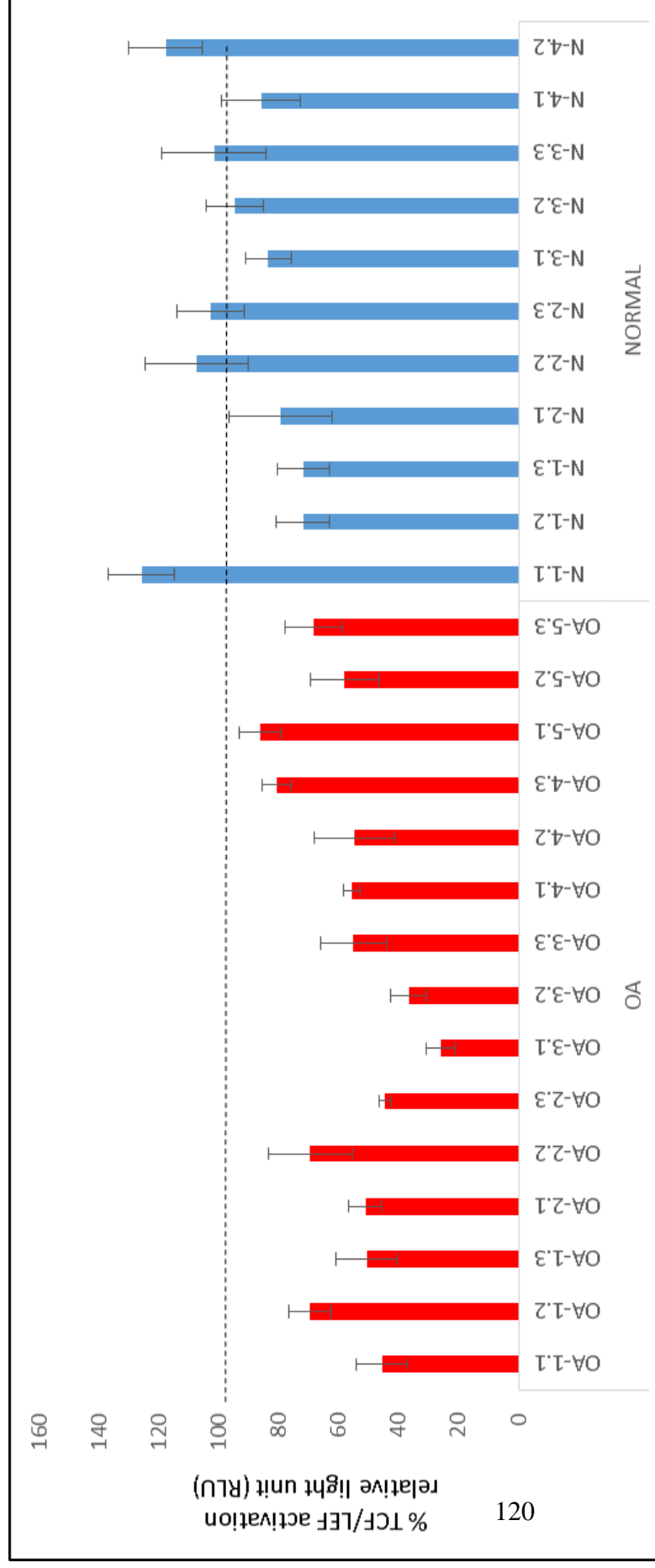


Figure 4. 5: Effects of CPCs conditioned media on Wnt TCF-luciferase reporter assay.

The modulatory effect of chondroprogenitor cells secreting different levels of Dkk-1 on the Wnt pathway was examined using the 7df3 TCF-luciferase reporter cell assay. 48hrs prior to initiating the experiments, CPCs of normal (n=4 donors, n=12 clonal cell lines) and osteoarthritic donors (n=5 donors, n=15 clonal cell lines) were cultured in basal media at 1 x 10⁶ cells. Collected media was centrifuged and filtered before incubating with 7df3 TCF- luciferase reporter cells treated with a positive inducer of TCF activity (Wnt-3a (150 ng/ml) and R-Spo1 (24 ng/ml) and incubated for 24hrs. 48 hours after incubation, cells were lysed using Glo lysis buffer and incubated with luciferase substrate (Promega Bright Glo) before measuring luciferase activity using a plate reader. Data are presented as percentage mean activation of TCF of 4 replicates per condition \pm SD. Data were analysed using 1-way ANOVA for statistical significance (* = $P < 0.05$, ** = $P < 0.01$). The horizontal line represents % activation of the positive control.

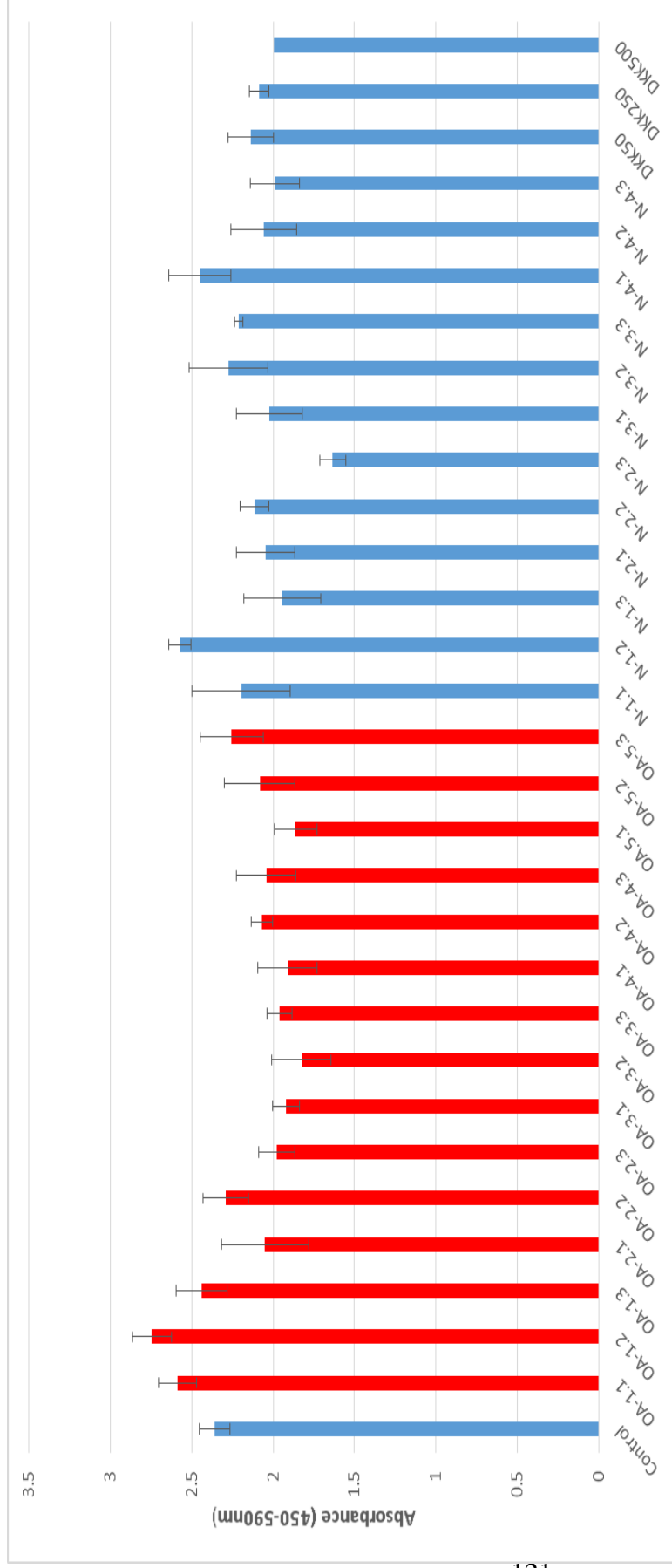


Figure 4. 6: Effects of CPCs conditioned media on cell viability.

7df3 TCF-luciferase reporter cells were treated with conditioned media from normal (n=4 donors, n=12 clonal cell lines) and osteoarthritic donors (n=5 donors, n=15 clonal cell lines) and recombinant Dkk-1 at 25, 250 and 500ng for 24hrs. Cell viability was measured using soluble Water Soluble Tetrazolium salts (WST-1) was added to each well and the plate was returned to the incubator for 1hr at 37 °C and 5% CO₂ after which absorbance was measured at 450 nm and 590 nm. Raw values of experimental group are compared to control (basal media only). CPCs of Data are presented as mean raw value of 4 replicates per condition ±SEM. 2-way ANOVA for statistical significance showed no significant difference between all groups.

A linear regression line was plotted in order to establish whether or not there was a relationship between Dkk-1 concentration, Dkk-1 mRNA fold-change and or % TCF-luciferase activation. Pearson's correlation test showed significant correlation between the Dkk-1 secretion and mRNA fold expression (Figure 4.7; $p < 0.05$), Dkk-1 secretion and % TCF-luciferase activation (Figure 4.8; $p < 0.05$) and between % TCF-luciferase activation and Dkk-1 mRNA fold change (Figure 4.9; $p < 0.05$). Interestingly, cell lines with higher expression of Dkk-1 at molecular and protein levels had lower percentage of TCF-activation and the R^2 regression ranged from of 0.6-0.65.

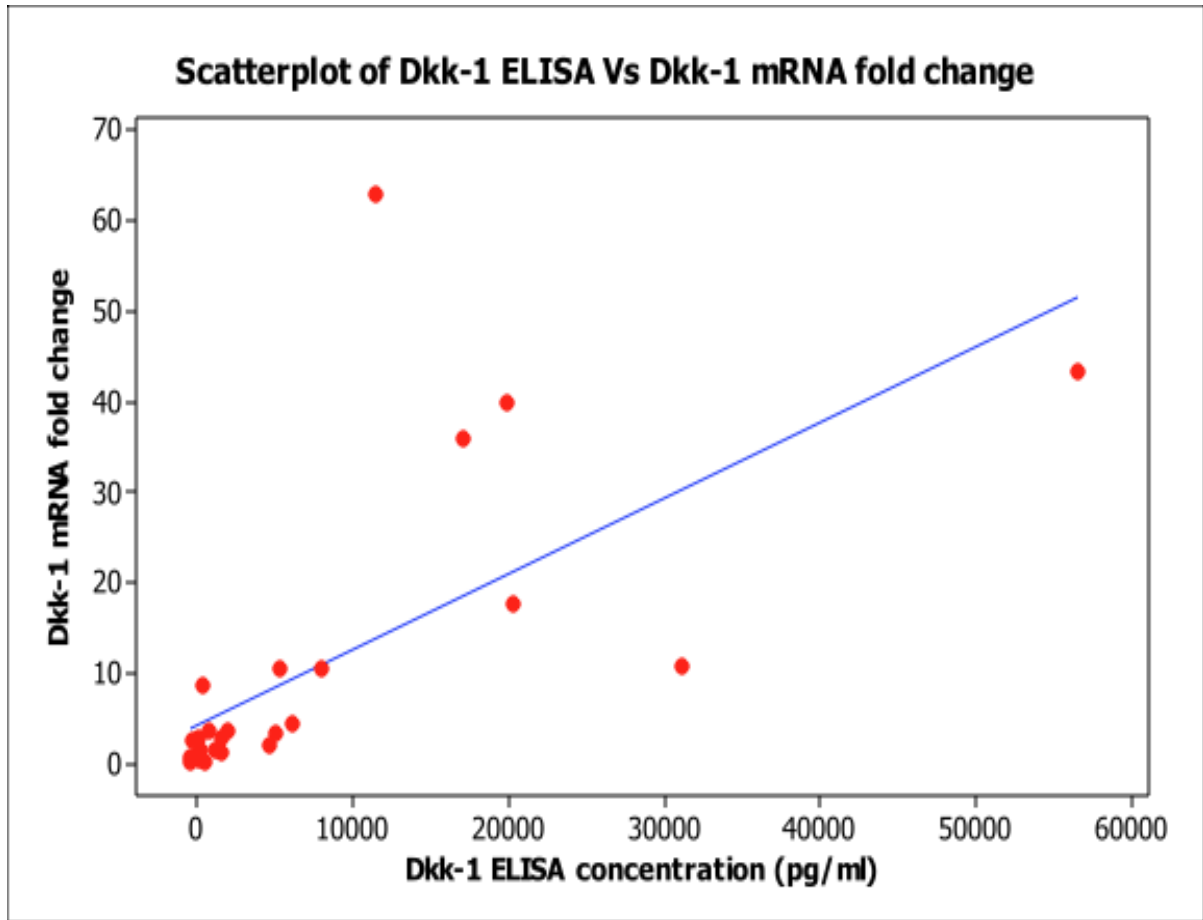


Figure 4.7: A scatter-plot figure of Dkk-1 concentration and mRNA fold-change.

A scatter-plot showing the correlation between the Dkk-1 secreted by CPC and the mRNA fold-change of Dkk-1 after normalisation to housekeeping gene (n=24 CPC cell lines). Blue line is indicative of the trend-line. Pearson's correlation coefficient test demonstrated a significant difference between the parameters ($p < 0.01$).

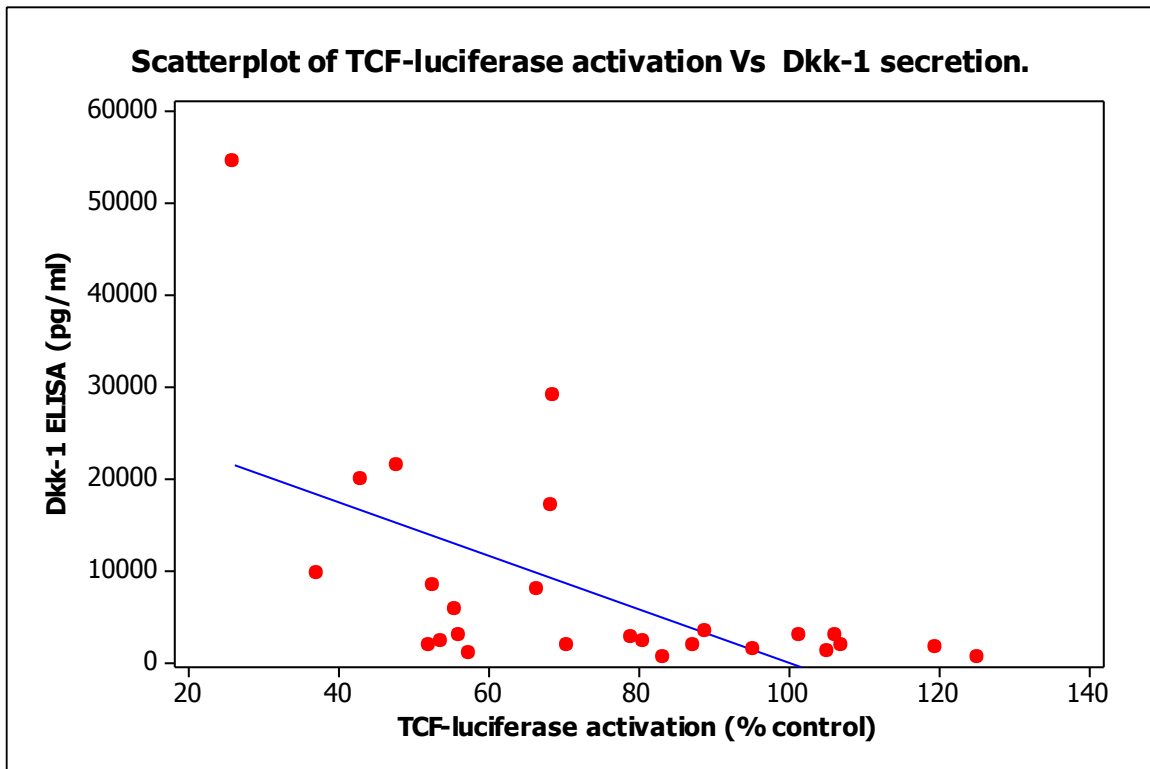


Figure 4.8: A scatter-plot figure of TCF-luciferase activation and Dkk-1 secretion.

A scatter-plot showing the correlation between the % TCF-luciferase activation and concentration of Dkk-1 secreted by CPC (n=27 CPC cell lines). Blue line is indicative of the trend-line. Pearson's correlation coefficient test demonstrates a significant difference between the parameters ($p= 0.002$).

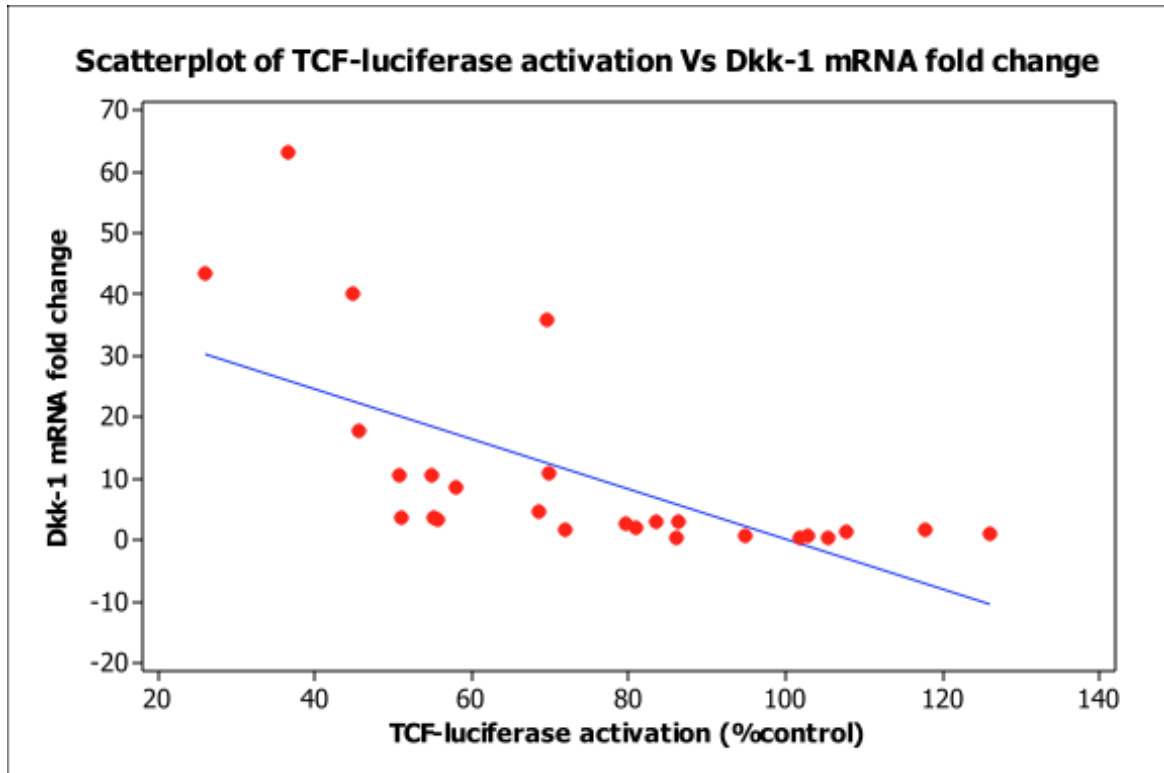


Figure 4.9: A scatter-plot figure of TCF-luciferase activation and Dkk-1 mRNA fold-change.

A scatter-plot showing the correlation between the % TCF-luciferase activation and the mRNA fold-change of Dkk-1 after normalisation to housekeeping gene (n=24 CPC cell lines). Blue line is indicative of the trend-line. Pearson's correlation coefficient test demonstrates a significant difference between the parameters ($p=0.001$).

Table 4. 2: Table showing Dkk-1 mRNA and protein expression and % activation of TCF-luciferase reporter assay of N-CPC and OA-CPC cell lines.

| Cell line | Dkk-1 ELISA concentration (pg/mL) | Dkk-1 mRNA fold change | TCF-luciferase activation (relative to % control) |
|------------------|--|-------------------------------|--|
| N1.1 | ND | NT | 125.91 |
| N1.2 | 1170.83 | 1.51 | 71.84 |
| N2.1 | ND | 2.58 | 79.51 |
| N2.2 | 1459.16 | 1.23 | 107.61 |
| N3.1 | ND | 0.60 | 102.92 |
| N3.2 | ND | 2.90 | 83.57 |
| N4.1 | ND | 0.71 | 94.74 |
| N4.2 | 410.16 | 0.27 | 101.74 |
| N4.3 | 40.16 | 0.41 | 85.93 |
| N5.1 | 211.33 | 1.48 | 117.87 |
| N5.2 | ND | NT | 105.27 |
| OA1.1 | 20326.25 | 17.67 | 45.59 |
| OA1.2 | 31075 | 10.84 | 69.71 |
| OA2.1 | 7938.75 | 10.43 | 50.76 |
| OA2.2 | 1885 | 3.52 | 51.08 |
| OA3.1 | 17107.5 | 35.97 | 69.56 |
| OA.3.2 | 19905 | 40.05 | 44.69 |
| OA4.1 | 56605 | 43.37 | 25.88 |
| OA4.2 | 5030 | 3.20 | 55.64 |
| OA4.3 | 667.5 | 3.55 | 55.16 |
| OA5.1 | 11408.75 | 63.07 | 36.66 |
| OA5.2 | 5317.5 | 10.58 | 54.95 |
| OA5.3 | 4625 | 1.88 | 80.78 |
| OA6.1 | 1578.75 | 2.77 | 86.42 |
| OA6.2 | 375 | 8.53 | 58.07 |
| OA6.3 | 6045 | 4.51 | 68.53 |

4.3.5 Chondrogenic differentiation of high and low expressing Dkk-1 CPC cell lines isolated and culture expanded from normal and osteoarthritic articular cartilage.

4.3.5.1. Analysis of cell viability using the LDH assay.

Assessment of cell viability during the differentiation process was measured by quantifying the amount of lactate dehydrogenase (LDH) released into the medium using the LDH based *in vitro* toxicology assay kit (Pierce, Thermo, UK). Absorbance values obtained for all cell cultures over the 21 days were below 0.3 OD units and were within the non-toxic range, confirming no adverse effect on cell viability in these culture conditions (Figure 4.9).

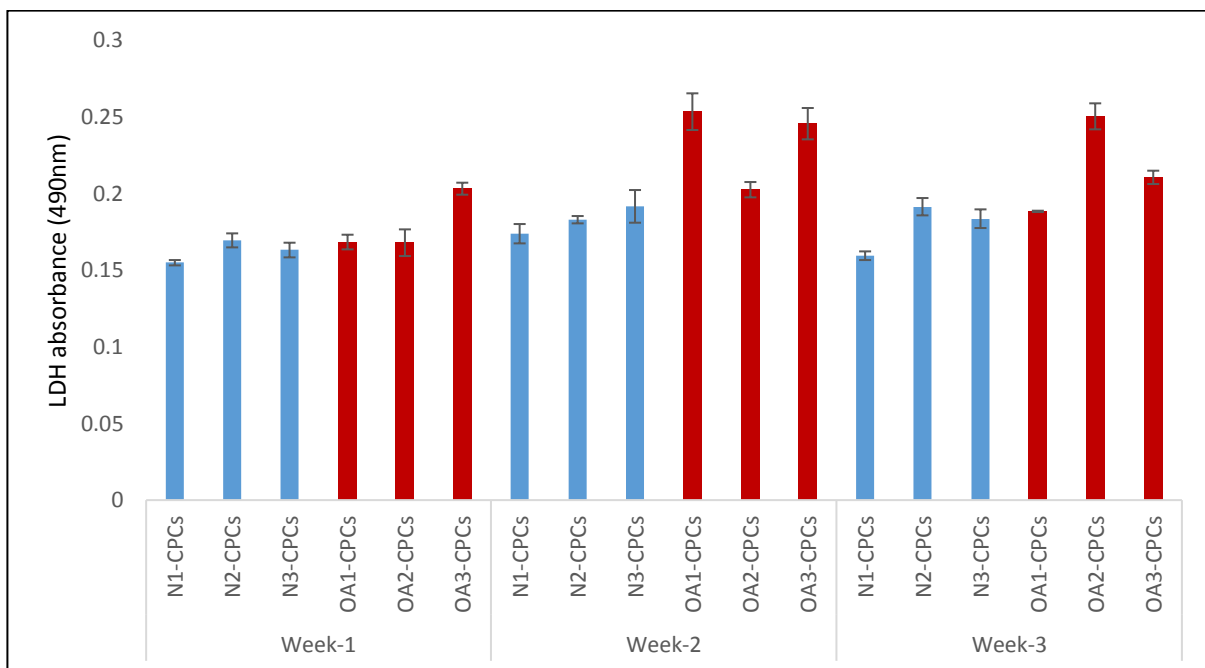


Figure 4.10: Assessment of secreted lactate dehydrogenase in the conditioned media of CPC.

Chondroprogenitor cells were cultured in chondrogenic differentiation media and LDH was measured in pooled media samples collected from day 0-7, 7-14 and 14-21). Blue bars represent N-CPC lines and red bars represent OA-CPC lines. Data are presented as the mean of the raw absorbance \pm SEM. Cell lines did not show a significant increase in LDH release during the duration of differentiation.

4.3.5.2. Analysis of Dkk-1 secretion post-differentiation.

Analysis of Dkk-1 from pooled culture media collected over day 0-7; 7-14 and 14-21 days is shown in Table 4.3 for all cell lines. Over the 21 day period of culture all of the Dkk-1^{high} OA-CPC lines maintained secretion of Dkk-1 protein. Interestingly, 2 of the 3 N-CPC lines had no detectable Dkk-1 over the 21 days in culture, however, in the N3-CPC line, Dkk-1 was detected in media collected from day 7-14 and day 14-21, 111 pg /mL to 218 pg/mL, respectively. To assess if the presence of Dkk-1 in the media had affected the chondrogenic differentiation of these CPC lines analysis was carried out to assess gene expression profiles of key markers of chondrogenic differentiation and the matrix deposition of pellets at 21 days of culture.

Table 4. 3: Quantitative levels of Dkk-1 secreted during chondrogenesis.

Clonal CPC from normal (n=3) and osteoarthritic donors (n=3) were cultured in chondrogenic differentiation settings at define time points (day 7, 14 and 21). At the selected time points, conditioned media were isolated and secreted levels of Dkk-1 protein was quantified using Dkk-1 ELISA kit. Data are presented as mean \pm SEM. Paired T-test was performed for each cell line and p value calculated. ND= not detected, NS= not significant.

| Chondrogenic differentiation duration period | Cell line ID | Dkk-1 Concentration (pg/mL)/10 ⁵ cells |
|--|--------------|---|
| Week-1 | N1-CPC | ND (p=NS) |
| | N2-CPC | ND (p=NS) |
| | N3-CPC | ND (p=NS) |
| | OA1-CPC | 1674.875 (\pm 209.8) |
| | OA2-CPC | 3958.625 (\pm 131) |
| | OA3-CPC | 310.125 (\pm 47.5) |
| Week-2 | N1-CPC | ND (p=NS) |

| | | |
|--------|---------|----------------------------------|
| | N2-CPC | ND (p=NS) |
| | N3-CPC | 111.875 (± 1.6) (p=0.03) |
| | OA1-CPC | 1526.875 (± 85.4) (p=0.17) |
| | OA2-CPC | 3057.5 (± 20.9) (p=0.02) |
| | OA3-CPC | 203.125 (± 6.5) (p=0.1) |
| Week-3 | N1-CPC | ND (p=NS) |
| | N2-CPC | ND (p=NS) |
| | N3-CPC | 218.5 (± 108.2) (p=0.11) |
| | OA1-CPC | 1008.875 (± 36.6) (p=0.08) |
| | OA2-CPC | 2794.5 (± 146) (p=0.002) |
| | OA3-CPC | 97.25 (± 9.5) (p=0.05) |

4.3.5.3 Analysis of mRNA expression of chondrogenic differentiated CPC.

4.3.5.3.1. Analysis at time point zero.

The molecular profile of all CPC lines used in the chondrogenic differentiation experiment were analysed at time point 0, day 7, day 14 and day 21 using the custom PCR array (Table 4.4) and the relative expression was normalised to the house-keeping genes as recommended by the manufacturer. Figure 4.10 shows the calculated relative gene expression for all 11 genes analysed at day 0, where the data from patients OA-1.1, OA-2.3 and OA-4.3 were combined and named Dkk-1^{high} CPC and from patients N-3.1, N-4.1, N-5.1 were combined and named Dkk-1^{low} CPC. There was no significant difference in the expression levels of Dkk-2, COL2A1, COL10A1, MMP-13, ADAMTS4 and IL-1 β in the two categories analysed (i.e. Dkk-

1^{high} and Dkk-1^{low}). Expression levels for Dkk-1 in the Dkk-1^{high} CPC were 11.5-fold greater than those of the Dkk-1^{low} CPC ($p < 0.001$) analysed, consistent with data shown in previous sections, for these cell lines. Interestingly, Dkk-1^{low} CPC had higher expression of β -catenin (CTNNB1; 2-fold change; $p = 0.01$) and Sox-9 (1.5-fold; $p = 0.01$) when compared to Dkk-1^{high} CPC. Although there was a difference in mRNA expression for ACAN ($p = 0.1$) and ALCAM ($p = 0.05$) this was not found to be statistically significant.

Table 4. 4: Custom- PCR-array plate layout.

| | 1 | 2 | 3 | 4 | 5 | 6 | 7 | 8 | 9 | 10 | 11 | 12 |
|---|---------|---------|---------|---------|---------|---------|---------|---------|---------|---------|---------|---------|
| A | DKK1 | ADAMTS4 |
| B | DKK2 | IL1B |
| C | CTNNB1 | ALCAM |
| D | COL2A1 | GAPDH |
| E | ACAN | B2M |
| F | SOX9 | HGDC |
| G | COL10A1 | RTC |
| H | MMP13 | PPC |

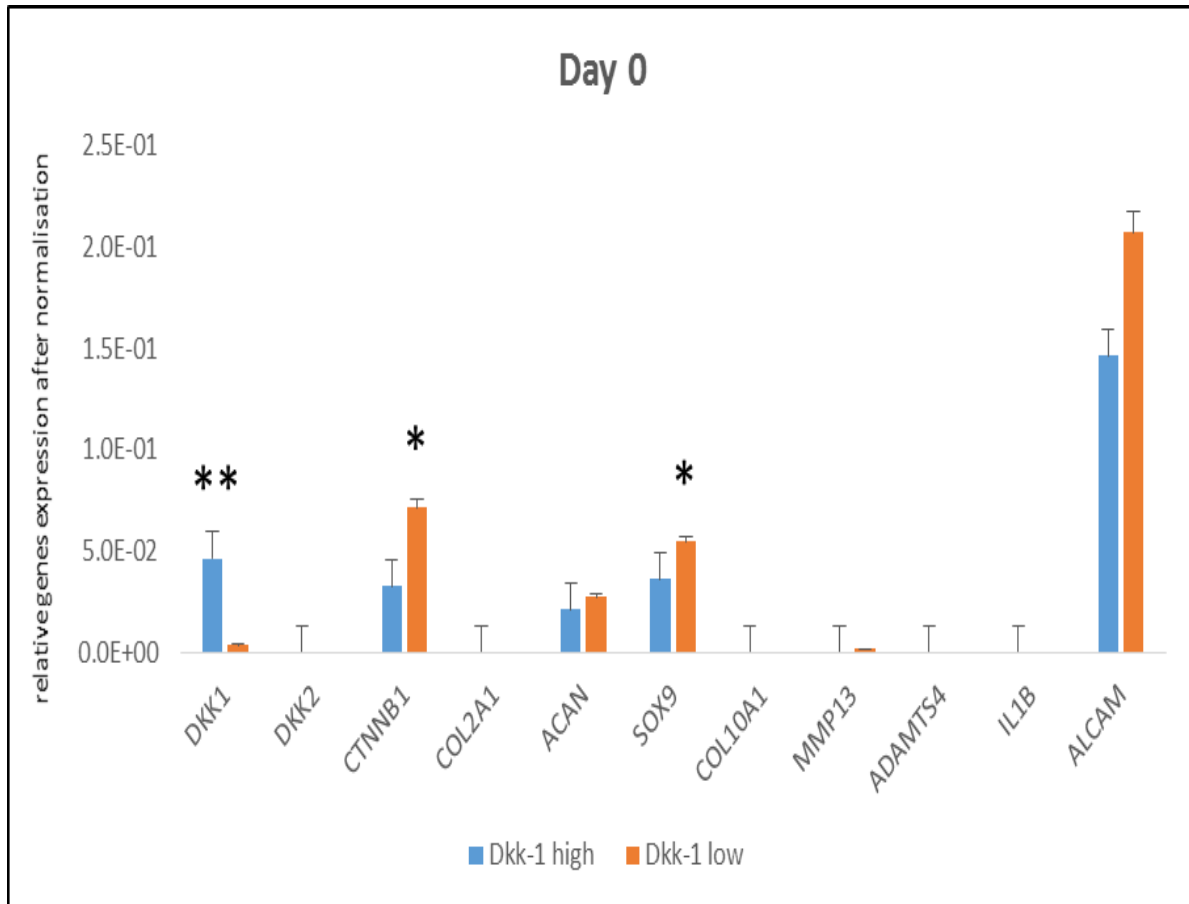


Figure 4.11: Effect of endogenous Dkk-1 levels on chondrogenic differentiation of CPC from healthy and osteoarthritic donors (Day 0).

Chondroprogenitor cells were cultured in chondrogenic differentiation medium and comparison of transcript levels of selected Wnt signalling pathway genes, multipotency marker genes, chondrogenic genes, hypertrophic chondrocyte genes and matrix degradation genes were analysed at defined time points (Day 0). Custom arrays were performed on mRNA from CPC prior to initiating the chondrogenic differentiation experiment and each cell line selected was assayed in triplicate (n=3 per donor). Data are expressed as mean \pm SEM after normalisation to GAPDH and B2M. Data were analysed using 1-way ANOVA (* = $P < 0.05$, ** = $P < 0.01$).

4.3.5.3.2. Analysis at 7 days post-differentiation.

Figure 4.11 shows the calculated relative gene expression for all 11 genes analysed at day 7, interestingly, there was expression of all genes analysed at this time point however, there was no significant difference in mRNA expression of ACAN (1.7-fold, $p=0.3$) between the two groups analysed. There was however, a significant increase in mRNA expression of Dkk-1 and a modest but significant increase in β -catenin mRNA and ALCAM mRNA in Dkk-1^{high} CPC compared with Dkk-1 low CPC (Figure 4.11, 24-fold, $p<0.001$, 1.7-fold, $p=0.01$, 3.41-fold, $p<0.001$, respectively). Interestingly, there was a dramatic up-regulation of MMP-13 at day 7 with a 40-fold difference in mRNA expression levels in Dkk-1^{high} CPC lines when compared to Dkk-1 low CPC lines (Figure 4.11, $p=0.001$). In contrast, Dkk-1^{low} CPC expressed higher levels of the chondrogenic marker genes Col2a1 and Sox-9 (Figure 4.11 nearly 75-fold, $p<0.0001$, 3.3-fold, $p<0.001$, respectively) than the Dkk-1^{high} CPC lines. Of interest, Dkk-2 was up-regulated in Dkk-1^{low} CPC by 2-fold (Figure 4.10, $p<0.001$).

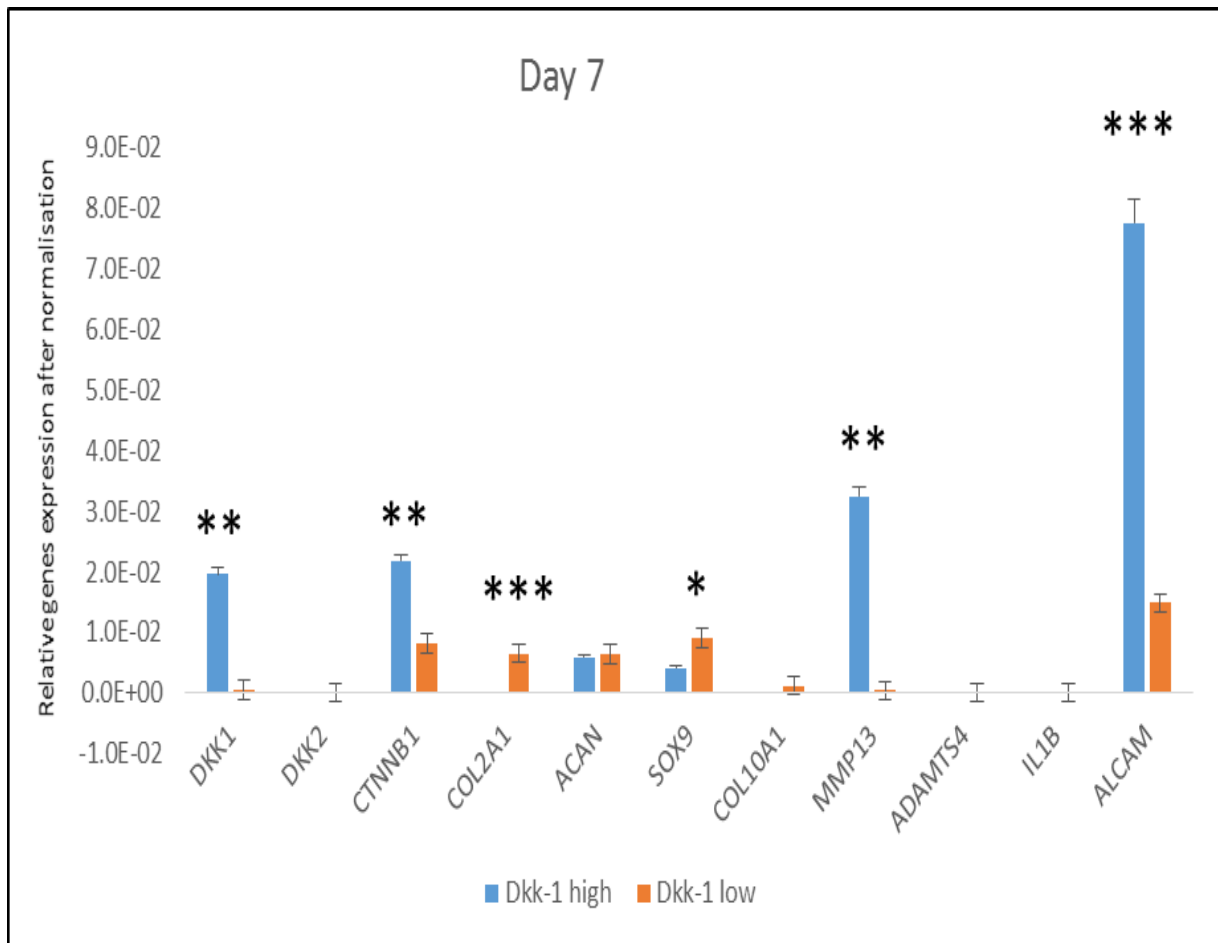


Figure 4. 12: Effect of endogenous Dkk-1 levels on chondrogenic differentiation of CPC from healthy and osteoarthritic donors (Day 7).

Chondroprogenitor cells were cultured in chondrogenic differentiation medium and comparison of transcript levels of selected Wnt signalling pathway genes, multipotency marker genes, chondrogenic genes, hypertrophic chondrocyte genes and matrix degradation genes were analysed at defined time points (Day 7). Custom arrays were performed on mRNA from differentiated pellets and each cell line selected was repeated in triplicate (n=3 per donor). Data are expressed as mean \pm SEM after normalisation to GAPDH and B2M. Data was analysed using 1-way ANOVA (* = $P < 0.05$, ** = $P < 0.01$).

4.3.5.3.3. Analysis at 14 days post-differentiation.

Furthermore, molecular analysis of Dkk-1^{high} and Dkk-1^{low} CPC at day 14 post-chondrogenic differentiation revealed that the molecular expression of Dkk-1^{high} CPC showed consistently maintained elevated levels of Dkk-1 (9.5-fold, $p < 0.001$). However, β -catenin between Dkk-1^{high} and Dkk-1^{low} CPC was down-regulated but not statistically significant (1.5-fold down-regulation, $p = 0.09$). Consistent with the reduction in Dkk-2 gene expression seen post-day 7 of differentiation, Dkk-2 was up-regulated in Dkk-1^{low} CPC by almost 14.5 folds ($p = 0.005$). But the interesting finding was the dramatic up-regulation of Col2a expression to over 400-folds ($p = 0.002$) while the expression of Col2a was hardly detectable in Dkk-1^{high} CPC (Figure 4.12). This increase in Col2a was consistent with an increase in Sox-9 expression in Dkk-1^{low} CPC by almost 5-fold ($p < 0.001$) as well as ACAN expression 2-fold ($p = 0.01$). Interestingly, Dkk-1^{low} CPC also appeared to show expression of COL10A1 and Interleukin-1 β although at low levels possibly suggesting some matrix remodelling (17-folds and 16-folds respectively, $p = 0.03$ and 0.007 respectively) while Dkk-1^{high} CPC showed hardly any expression of these genes (Figure 4.12). Similar to day 7 post-chondrogenic differentiation, Dkk-1^{high} CPC continued to express the MSCs marker ALCAM (2-fold, $p < 0.01$).

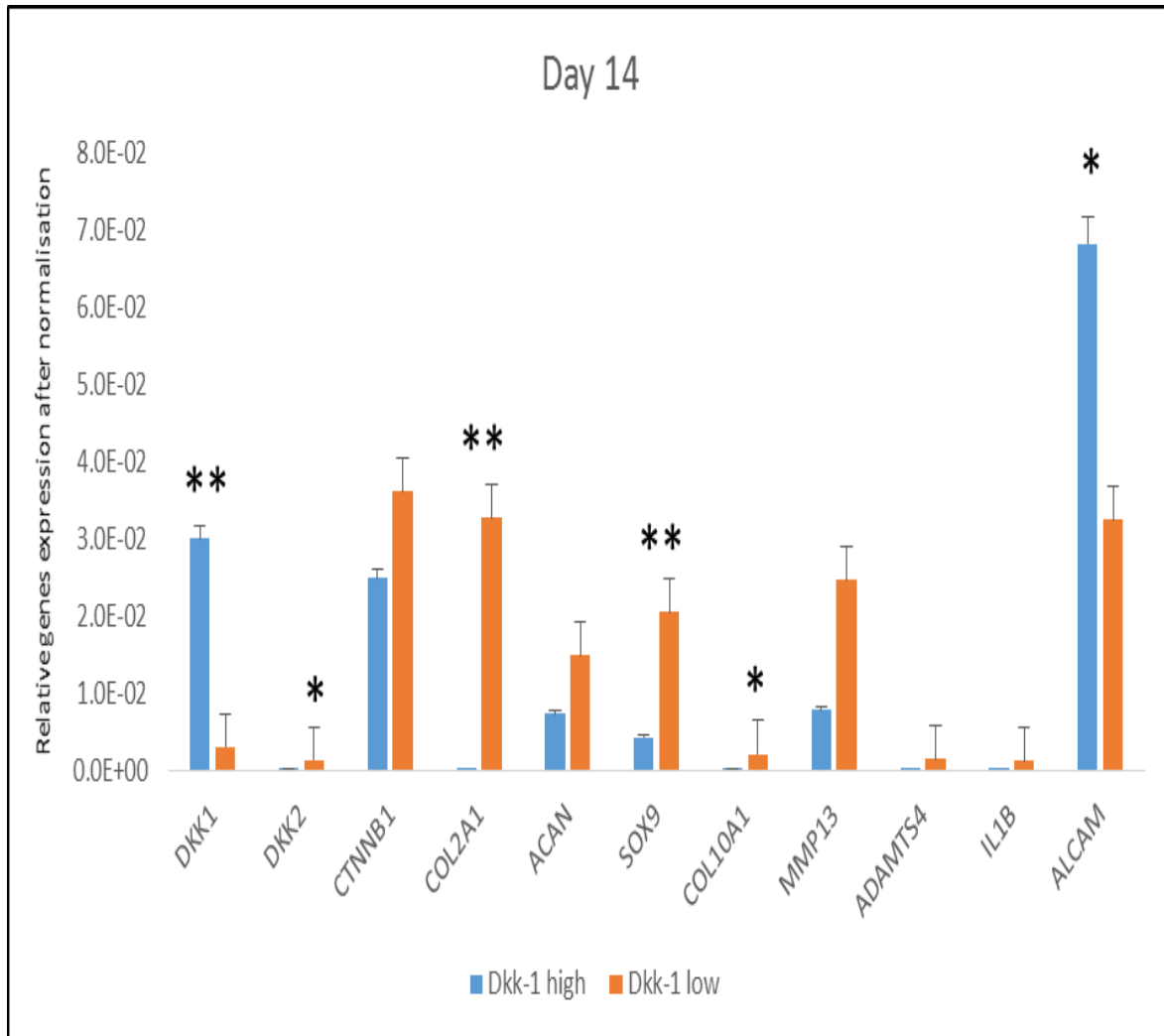


Figure 4. 13: Effect of endogenous Dkk-1 levels on chondrogenic differentiation of CPC from healthy and osteoarthritic donors (Day 14).

Chondroprogenitor cells were cultured in chondrogenic differentiation medium and comparison of transcript levels of selected Wnt signalling pathway genes, multipotency marker genes, chondrogenic genes, hypertrophic chondrocyte genes and matrix degradation genes were analysed at defined time points (Day 14). Custom arrays were performed on mRNA from differentiated pellets and each cell line selected was repeated in triplicate (n=3 per donor). Data are expressed as mean \pm SEM after normalisation to GAPDH and B2M. Data was analysed using 1-way ANOVA (* = $P < 0.05$, ** = $P < 0.01$).

4.3.5.3.4. Analysis at 21 days post-differentiation.

The analysis of the molecular profile of Dkk-1^{high} and Dkk-1^{low} CPC at day 21 post-chondrogenic differentiation is shown in Figure 4.12. The molecular expression of Dkk-1^{high} CPC showed consistently elevated although less fold change expression of Dkk-1 when compared to Dkk-1^{low} CPC (4-fold, $p=0.02$). Similarly, Dkk-2 expression in Dkk-1^{low} CPC show maintained up-regulation (41-fold, $p<0.01$ greater than Dkk-1^{high} CPC). Col2a expression continued to be expressed in Dkk-1^{low} CPC and was not detectable in Dkk-1^{high} CPC (81-fold, $p=0.0002$ greater than Dkk-1^{high} CPC). This increase in Col2a expression in Dkk-1^{low} CPC was consistent with an increase in Sox-9 expression by almost 4-fold ($p=0.008$) as well as ACAN expression 2.2-fold ($p=0.01$) relative to Dkk-1^{high} CPC. Interestingly, Dkk-1^{low} CPC also appeared to show expression of COL10A1 and MMP-13 at levels possibly suggesting some matrix remodelling or even hypertrophic differentiation (nearly 60-folds, $p<0.01$, and 31-fold, $p=0.02$ greater than Dkk-1^{high} CPC respectively). Furthermore, β -catenin and ALCAM were down-regulated in Dkk-1^{high} CPC but not statistically significant (Figure 4.13, 1.1-fold, $p=0.8$ and 1.4, $p=0.1$ greater than Dkk-1^{low} CPC respectively). Both cell groups showed no statistical differences in the expression of ADAMTS-4 and IL-1 β .

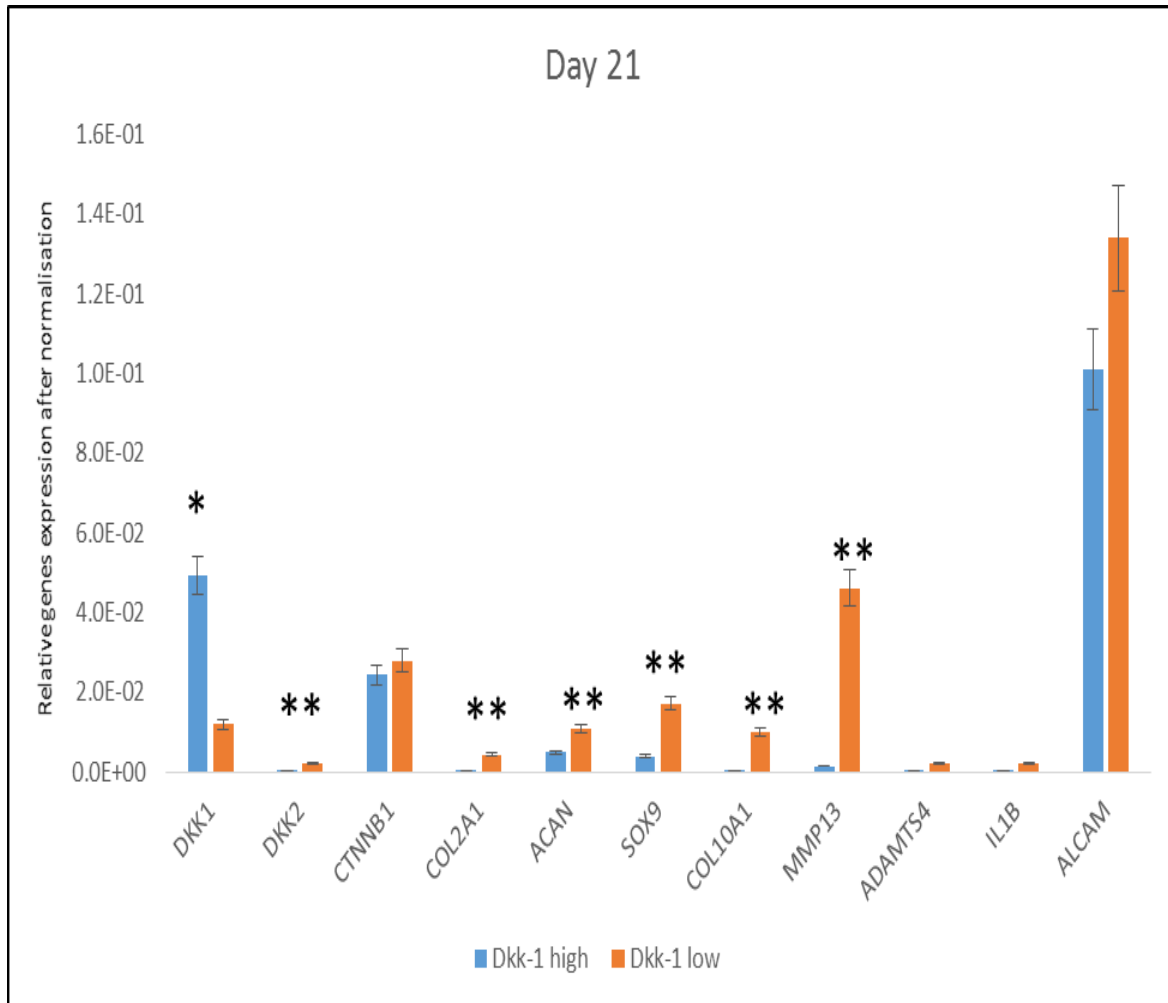


Figure 4. 14: Effect of endogenous Dkk-1 levels on chondrogenic differentiation of CPC from healthy and osteoarthritic donors (Day 21).

Chondroprogenitor cells were cultured in chondrogenic differentiation medium and comparison of transcript levels of selected Wnt signalling pathway genes, multipotency marker genes, chondrogenic genes, hypertrophic chondrocyte genes and matrix degradation genes were analysed at defined time points (Day 21). Custom arrays were performed on mRNA from differentiated pellets and each cell line selected was repeated in triplicate (n=3 per donor). Data are expressed as mean \pm SEM after normalisation to GAPDH and B2M. Data was analysed using 1-way ANOVA (* = $P < 0.05$, ** = $P < 0.01$).

4.3.5.3.5. Comparison of patient matched Dkk-1^{high} and Dkk-1^{low} CPC during chondrogenic differentiation.

Molecular analysis of patient derived clonal CPC showed marked variation in the expression of Dkk-1. This finding is interesting as it shows that not all clonal CPC are similar and that this might result in different outcomes if sub-optimal populations of clonal cells were selected for cartilage production. To investigate the effect of Dkk-1 variability at the patient level, CPC with endogenous Dkk-1^{high} and Dkk-1^{low} levels were taken from the same patient (n=2) and were induced to undergo chondrogenic differentiation. Dkk-1^{high} and Dkk-1^{low} CPC were able to form a pellet when cultured in chondrogenic differentiation medium.

After 21 days of culture in chondrogenic differentiation medium Dkk-1^{low} CPC and Dkk-1^{high} CPC lines showed evidence of successful differentiation marked by assessing expression of the chondrogenic lineage genes ACAN, Col2a1 and Sox-9 (Figure 4.14) (n=2 patients). By examining the molecular profile of osteoarthritic patient matched Dkk-1^{high} and Dkk-1^{low} CPC at day 21 post-chondrogenic differentiation, expression of Dkk-1^{high} CPC showed up-regulated expression of Dkk-1 when compared to Dkk-1^{low} CPC (1.5-fold, p=0.02). In addition, ALCAM, Sox-9 and ACAN were up-regulated in Dkk-1^{high} CPC but not statistically significant (Figure 4.14, 1.3-fold, p=0.21, 1.7-fold, p=0.2 and 1.6-fold, p=0.3 respectively). In contrast, Col2a1 expression in Dkk-1^{low} CPC was up-regulated when compared to Dkk-1^{high} CPC (92-fold, p=0.0006), while β -catenin was up-regulated in Dkk-1^{low} CPC however, not statistically significant (1.7-fold, p=0.8).

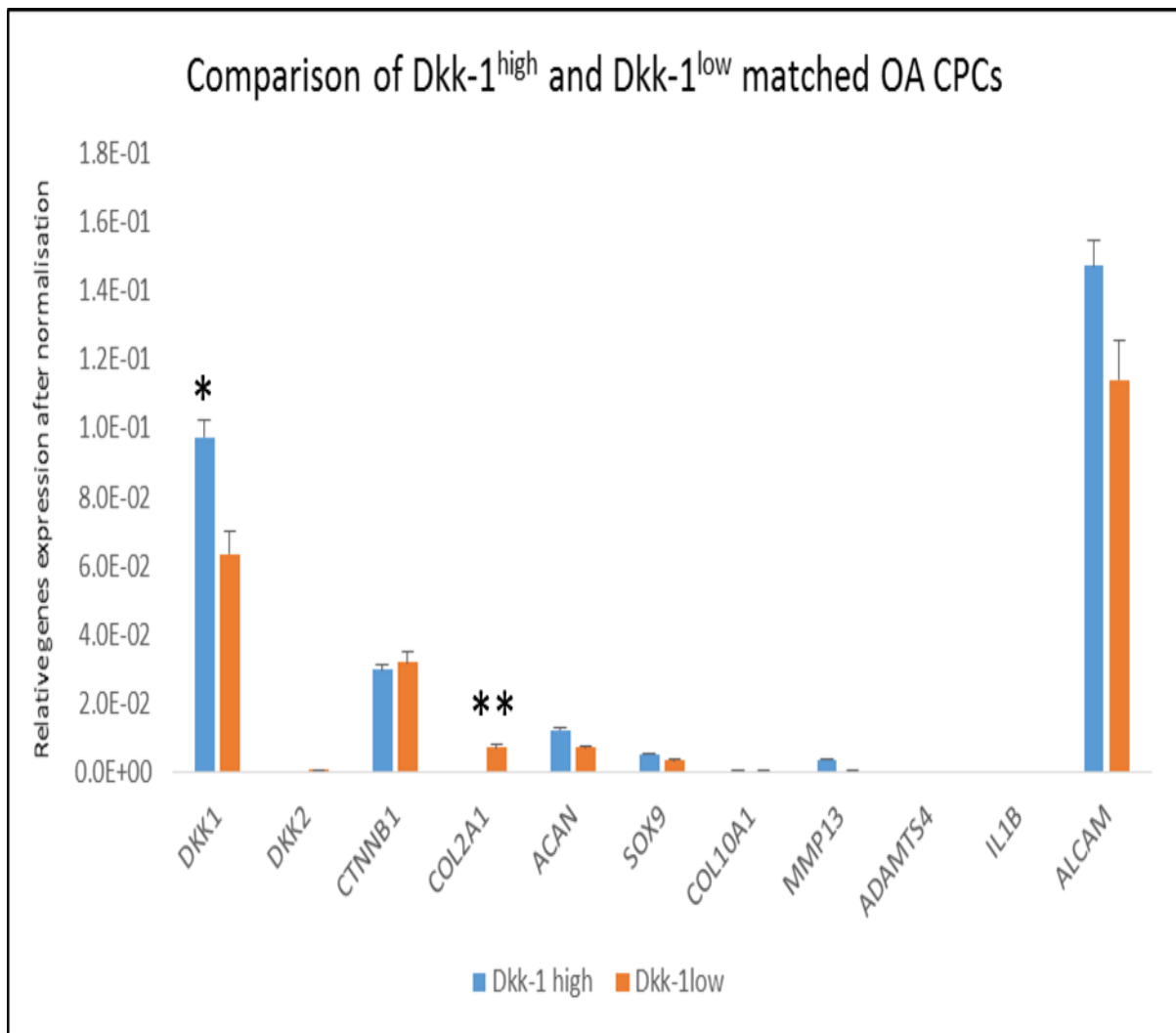


Figure 4. 15: Effect of differential expression levels of Dkk-1 on chondrogenic differentiation of CPC from the matched patients (Day 21).

Chondroprogenitor cells were cultured in chondrogenic differentiation medium and comparison of transcript levels of selected Wnt signalling pathway genes, multipotency marker genes, chondrogenic genes, hypertrophic chondrocyte genes and matrix degradation genes were analysed at defined time points (Day 21). Custom arrays were performed on mRNA from differentiated pellets and each cell line selected was repeated in triplicate (n=2 per donor). Data are expressed as mean \pm SEM after normalisation to GAPDH and B2M. Data was analysed using 1-way ANOVA (* = $P < 0.05$, ** = $P < 0.01$).

4.3.6 Protein analysis of differentiated pellets.

4.3.6.1. Histochemical analysis of chondrogenic differentiation of CPC.

The morphology of the spherical pellets cultured in chondrogenic differentiation media was similar at 21 days post-differentiation. All cell groups showed formation of 3D pellets (Figure 4.15 A-C). In addition, Dkk-1^{low} CPC from both normal and osteoarthritic CPC showed successful staining for Safranin-O as well as Toluidine blue staining (Figure 4.15 D-E and G-H respectively). Interestingly, it was observed that safranin-O of Dkk-1^{high} CPC was slightly weaker when compared to Dkk-1^{low} CPC groups. However, Toluidine blue staining in Dkk-1^{high} CPC was comparable to other groups.

Furthermore, by assessing the protein expression of aggrecan (6B4), Collagen type II and Sox9 using immunofluorescence microscopy, there was a clear pattern where Dkk-1^{high} CPC showed little protein labelling for the three selected markers (Figure 4.16, bottom panel). By comparison, their patient matched OA-Dkk-1^{low} CPC (Figure 4.16, middle panel) as well as healthy donor CPC N-Dkk-1^{low} CPC showed evidence of aggrecan, collagen II and Sox-9 further supporting the molecular data (Figure 4.16, upper panel).

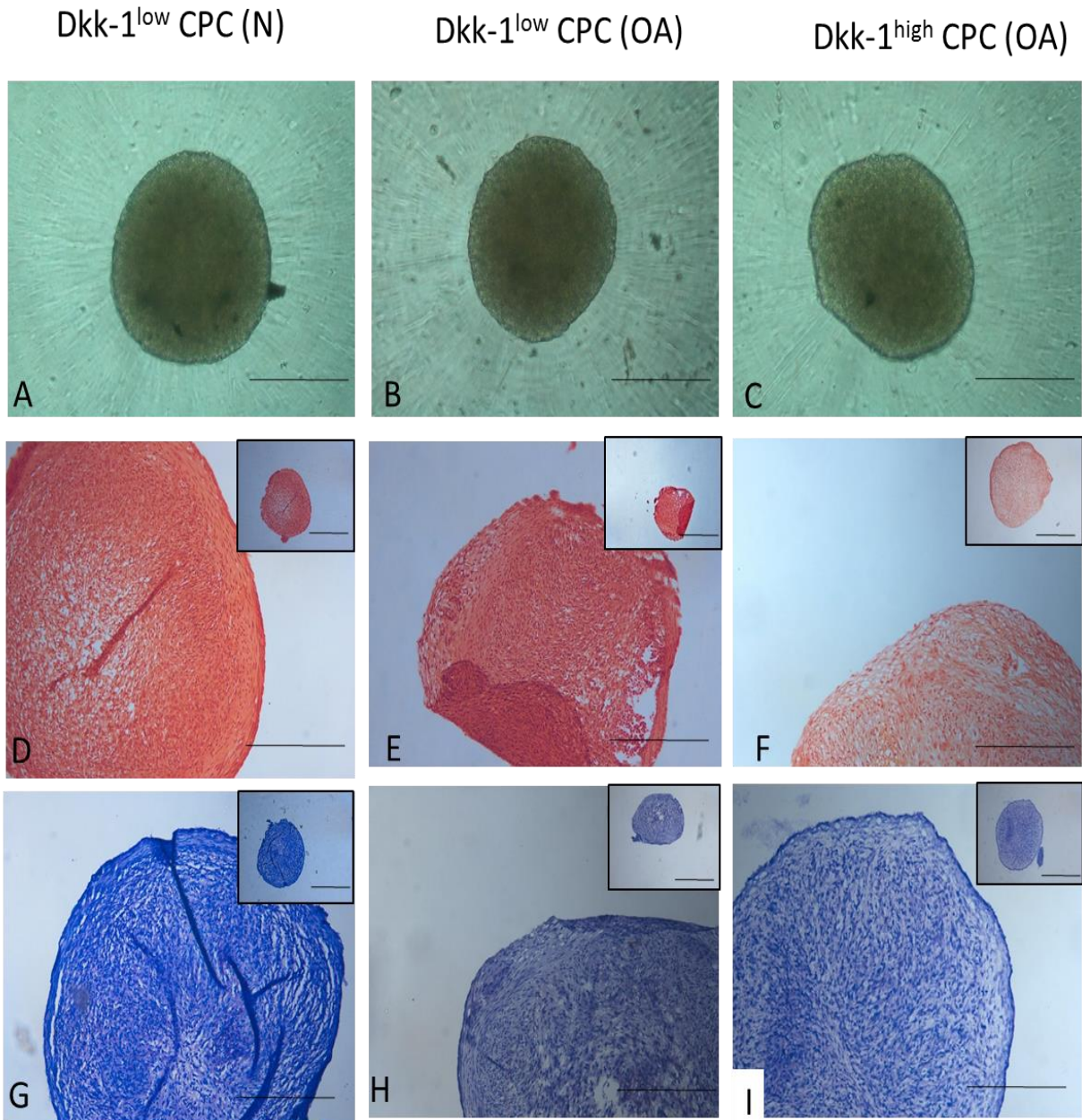


Figure 4. 16: Histochemical and phase-contrast images 3D cell pellets from Dkk-1^{low} CPC and Dkk-1^{high} CPC cell lines subjected to chondrogenic differentiation.

Phase contrast microscopic image of normal Dkk-1^{low} CPC (N) and osteoarthritic CPC Dkk-1^{low} CPC (OA) and Dkk-1^{high} CPC (A-C) and the corresponding Safranin-O (D-F) and Toluidine blue (G-I) stained sections after 21 days in chondrogenic culture conditions. Scale bar= 25 μ m, insert scale bar =50 μ m. Pellets that have undergone chondrogenic differentiation show successful matrix production in all of the three cell line investigated marked by Toluidine blue staining.

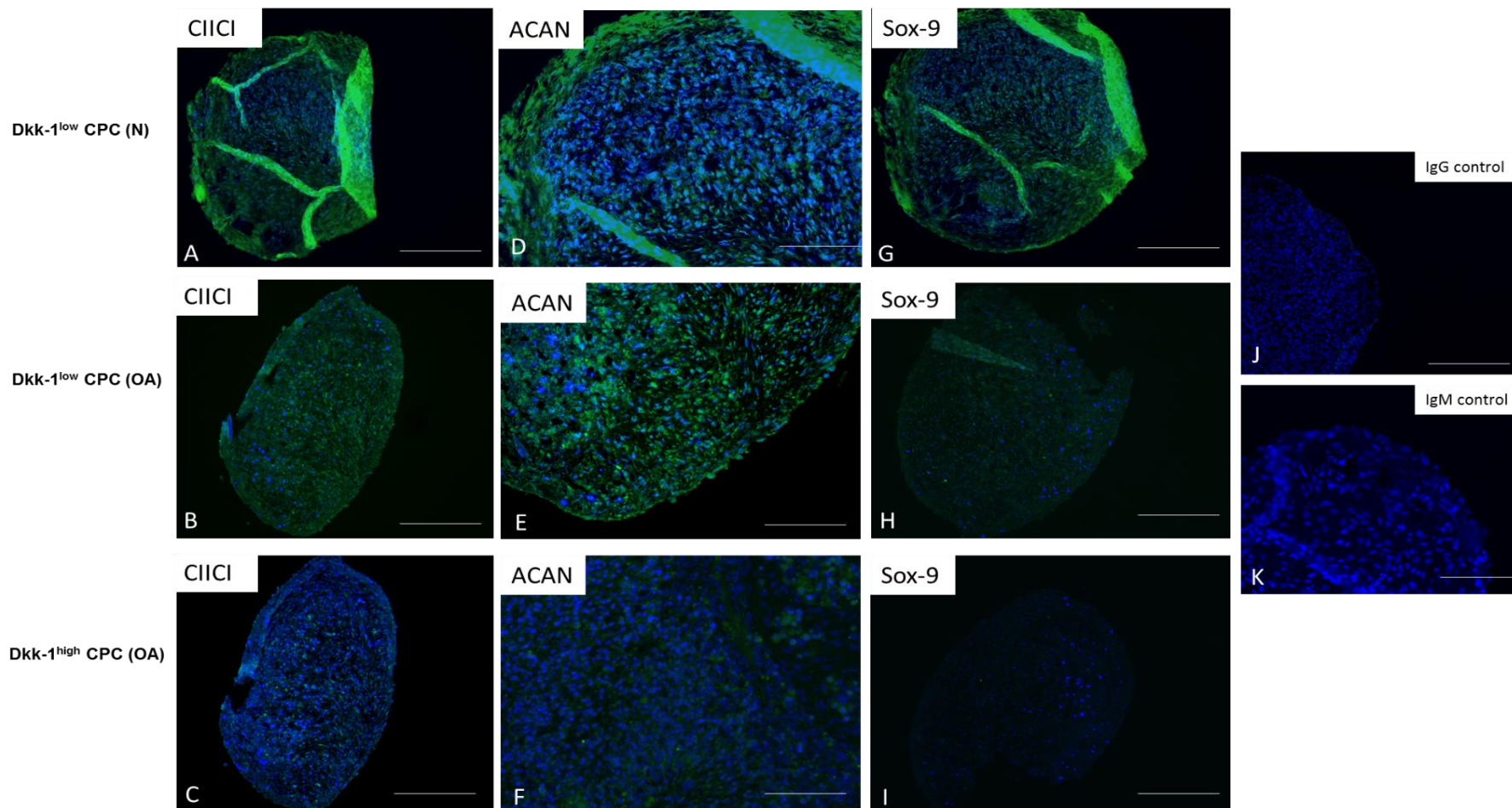


Figure 4. 17: Immunohistochemical analysis of 3D cell pellets from Dkk-1^{low} CPC and Dkk-1^{high} CPC cell lines subjected to chondrogenic differentiation.

Representative immunofluorescence images of Dkk-1^{high} CPC (OA donor) and Dkk-1^{low} CPCs (OA donor) and Dkk-1^{low} CPCs (Normal donor) lines were immuno-labelled for collagen type II/ CIIC (A-C), aggrecan/6B4 (D-F) and Sox-9 (G-I). Images J-K are representative of negative IgG controls (J) and IgM controls (K). Images A, B, C, G, H and I scale bar=50 μ m. Images D-F and J-K scale bar=25 μ m.

4.3.6.2. Immunohistochemical analysis of Dkk-1 in normal and osteoarthritic cartilage.

Subsequent to studying the Dkk-1 mRNA expression and protein secretion in isolated chondrocytes and chondroprogenitor cells, from normal and osteoarthritic donors, subjected to culture in basal medium and in chondrogenic differentiation medium we then investigated the topographical location of Dkk-1 in cartilage from normal and OA donors using immunohistochemistry. In sections taken from normal cartilage, Dkk-1 was present in the superficial zone and upper middle zone (Figure 4.17 A2-A3) of the tissue. This localisation of Dkk-1 appeared to be matrix associated. In addition, Dkk-1 was localised in a small number of chondrocytes within the deep zone of the tissue (Figure 4.17 A4). Similarly, in OA cartilage sections, Dkk-1 staining was present in the superficial zone (Figure 4.17 B1) but absent from the middle zone (Figure 4.17 B2). There was, however, intense localisation for this epitope within the pericellular matrix of deep zone chondrocyte clusters adjacent to the tidemark (Figure 4.17 B3). Immunohistochemical localisation of Dkk-1 in sections taken from the osteochondral plug of OA tissue was seen surrounding migratory cells from the subchondral bone region. These migratory subchondral bone cells had morphological features similar to mesenchymal stromal cells (Figure 4.17 B4). There was evidence of intense Dkk-1 staining around blood vessels (Figure 4.17 B3).

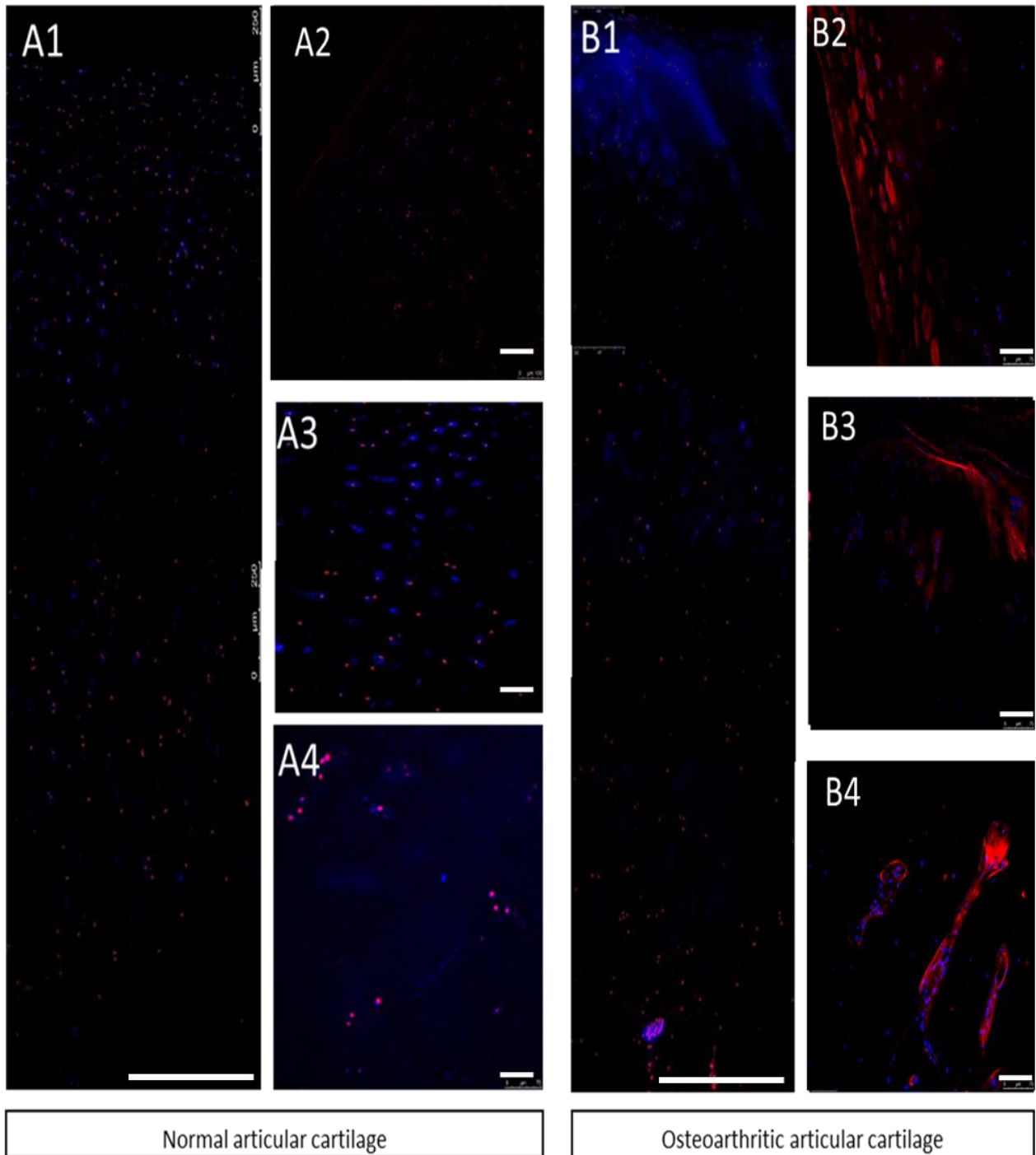


Figure 4. 18: Topographical expression of Dkk-1 in normal and osteoarthritic osteochondral tissue.

Dkk-1 expression in whole osteochondral sections of normal (A1) and osteoarthritic cartilage (B1) were studied using confocal immunohistochemistry. Confocal imaging showed immuno-labelling for the Dkk-1 in the superficial zone (A2, B2), mid zone (A3, B3) and deep zone of AC (A4, B4). Positive Dkk-1 labelling was found surrounding the cellular infiltrate from the underlying subchondral bone (B4). Dkk-1 protein was visualised using Goat anti-mouse Alexa Fluor 633 (red) and nuclei staining were attained using DAPI (blue). Image A1 & B1: scale bar =250µm. Image A2-A4 and B2-B4: scale bar =75µm.

4.4 Discussion.

The Wnt pathway is emerging as a crucial pathway involved in the regulation and homeostasis of the synovial joint (Bafico *et al.*, 2001; Diarra *et al.*, 2007; Surmann-Schmitt *et al.*, 2009; Blom *et al.*, 2009; Zhu *et al.*, 2009a; Saito *et al.*, 2010; Yang *et al.*, 2010; Zhen *et al.*, 2013). In this chapter, the differential expression pattern of 84 related-Wnt pathway genes were investigated in culture-expanded clonal CPC cell lines isolated from normal and osteoarthritic donors. For the Wnt-array, CPC cell lines were selected randomly and had similar cumulative population doubling to reduce variation that can arise from *in vitro* expansion process.

For the majority of selected Wnt genes, the transcriptional profile between normal and OA-derived CPC were comparable. However, several genes were up-regulated in OA-CPC including genes implicated in cell fate determination of cells such as Dkk-1, Wnt3a and genes involved in cell polarity including Axin2, Dvl2, MAPK-8 and NKD1. Wnt genes implicated in cell growth and proliferation including CTBP1, DAB2, FOSL1, LRP5, PPARD, WISP1 and WNT3 were also up-regulated in OA-CPC. In addition, Wnt genes involved in the regulation of cell migration such as Dkk-1 and its co-receptor LRP-5 and genes implicated in cell cycle regulation including CCND2, EP300, RHOU and TCF7L1 were over-expressed in OA-CPC when compared to normal CPC cell lines. Moreover, several non-canonical Wnt pathway genes were also up-regulated in OA-CPC lines when compared to normal CPC. But the interesting finding was the up-regulation of several Wnt inhibitors ligands including AXIN-2, CTBP-1, DKK-1, DKK3, FBXW4, LRP5, TLE1 and NKD1. This data are interesting as it indicates the differential expression of both canonical and non-canonical Wnt pathways in osteoarthritis. In particular, the Wnt pathway is known to regulate stem cell fate in

many tissues and its misregulation was found to be associated with several diseases (Nuuse, 2005, Clevers, 2006). In addition, this data are in agreement with recently published microarray data examining transcriptional profiles between normal and osteoarthritic hip cartilage OA (Xu *et al.*, 2012) and in MSCs isolated from Normal and OA patients (Churchman *et al.*, 2012) showing that Dkk-1 and Wnt antagonists were over expressed in OA chondrocytes and in OA- MSCs, respectively. Interestingly, the expression levels of Dkk-1 were nearly 50-fold higher in OA-CPC when compared to normal counterparts but no significant differences were found between OA and normal chondrocytes therefore suggesting that the CPC might be behind the higher expression levels of Dkk-1.

By examining mRNA expressional levels from larger set of donor cell lines (n=9 and 20 for normal and OA respectively) as well as full-depth cartilage chondrocytes (n=6 for normal and OA respectively), the expressional levels of Dkk-1 in culture expanded full-depth chondrocytes from normal and OA did not show any significant differences ($p \geq 0.05$). In addition, the expressional levels of Dkk-1 between normal CPC cell lines and both normal and osteoarthritic full-depth chondrocytes were not significantly different ($p \geq 0.05$). However, Dkk-1 expression was up-regulated in isolated osteoarthritic clonal CPC when compared to either full-depth chondrocytes or normal CPC ($p < 0.05$). This finding in this thesis is partially in agreement with other recently published work by Oh *et al.* (2012b), Weng *et al.* (2010) and Leijten *et al.* (2012), all showing an up-regulation of Dkk-1 in OA chondrocytes. However, a novel finding in this study is the discovery that only OA-CPC, a subset of chondrocytes selected based on their high fibronectin adhesion capacity (cartilage progenitor cells), show the elevated Dkk-1 expression. This finding suggest the

potential role of cartilage progenitor cells in the pathogenesis of osteoarthritis. In addition, Dkk-1 was also proposed as a potential biomarker for the progression of osteoarthritis (Lane *et al.*, 2007; Oh *et al.*, 2012a;). The function of Dkk proteins have been studied in inflammatory arthritis including rheumatoid arthritis and ankylosing spondylitis in both human and animal models (Diarra *et al.*, 2007; Daoussis *et al.*, 2010). But its role in osteoarthritis remains not fully understood and often published work show contradictory findings (Weng *et al.*, 2010; Oh *et al.*, 2012b; Leijten *et al.*, 2012). A recent study by Oh (2012a) reported an increase in mRNA expression for Dkk-1 in OA cartilage which was shown to be protective of cartilage degradation. On the contrary, Weng *et al.* (2010) found that Dkk-1 up-regulation in cartilage isolated from patients undergoing knee replacement and in rat models of OA were correlated with higher chondrocyte apoptosis. This highlights the complexity of the Wnt pathway and the need for more studies to understand the precise role of Wnt pathway in OA.

As mentioned in the chapter one, Dkk-1 is a secretory protein released by cells and act via an autocrine manner (see Appendix 4 for monensin-blocked Dkk-1 secretion), therefore, secreted Dkk-1 was measured using commercially available ELISA kit. Consistent with the OA-CPC molecular up-regulation of Dkk-1, the concentration of Dkk-1 was significantly higher in OA-CPC. However, both molecular and protein analysis of Dkk-1 in clonal CPC cell lines showed variation in Dkk-1 expression within OA group. Based on these data, OA-CPC were further subdivided into Dkk-1^{high} CPC and Dkk-1^{low} CPC. In contrast, normal CPC show more homogenous expression of Dkk-1 therefore were classed as Dkk-1^{low} CPC.

Having confirmed the differential expression of Dkk-1 in isolated CPC at the molecular and protein level, the next step was to examine if Dkk-1 up-regulation had a functional effect on the canonical Wnt pathway by modulating β -catenin. Therefore, 7df-3 cell line stably transfected with TCF-luciferase were used to assess the modulatory effect of conditioned media harvested from normal and OA-CPC (Dkk-1^{high} CPC and Dkk-1^{low} CPC) on the transcriptional role of β -catenin (Veeman *et al.*, 2003; Ewan *et al.*, 2010). This study, to our knowledge is the first to examine the effect of endogenous Dkk-1 secretion of CPC on β -catenin transcriptional TCF activation. Cell viability of 7df-3 cell line treated with conditioned media were not affected over 24 hrs period. In accordance with the differential expression of Dkk-1 in OA-CPC and normal CPC cell lines, it was shown that Dkk-1^{high} CPC overall resulted in reduction of TCF-luciferase expression by directly inhibiting Wnt-3a and R-Spo-1 activity. In contrast, normal CPC did not show any inhibitory effect on Wnt-3a and R-Spo-1 action. Interestingly, several normal CPC cell lines were shown to enhance the TCF-luciferase expressional levels more than the positive control hence suggesting the presence of β -catenin agonist factors released by the cell lines. Furthermore, addition of recombinant Dkk-1 at an increasing concentration showed the inhibitory role it exert on β -catenin transcriptional role. This data are in agreement with a study by Akiri *et al.* (2009) examining the effect of Dkk-1 on several β -catenin transcriptional role in non-small cells lung cancer. Moreover, there was an inverse correlation between the molecular and protein Dkk-1 expression and TCF-luciferase reporter activation.

Having confirmed the elevated levels of Dkk-1 in OA-CPC, it was hypothesised that the differences in Dkk-1 expression levels and soluble protein secretion might have a

functional effect on CPC fate. Therefore, clonal CPC cell lines with high and low Dkk-1 were induced to undergo chondrogenic differentiation. By comparing Dkk-1^{high} CPC and Dkk-1^{low} CPC prior to initiating chondrogenic differentiation, it was evident that Dkk-1^{high} CPC had higher levels of Dkk-1 mRNA expression. In contrast, Dkk-1^{low} CPC also had higher levels of β -catenin further supporting the inhibitory effect of high Dkk-1 on β -catenin message. Interestingly, Dkk-1^{low} CPC also showed higher expressional levels of the chondrogenic transcriptional factor Sox-9 when compared to Dkk-1^{high} CPC. This finding is in accordance with previously published work by Khan *et al.* (2009) which have shown that CPC were able to retain Sox-9 expression when expanded *in vitro* compared to full-depth chondrocytes.

Analysis of Dkk-1^{high} CPC and Dkk-1^{low} CPC from OA and normal clonal CPC cell lines at 7, 14 and 21 day interval have shown that CPC with initially higher levels of Dkk-1 consistently maintained a higher levels of Dkk-1 at both molecular and secretory levels throughout the three week chondrogenic differentiation period. Dkk-1^{high} CPC were unable to show evidence of chondrogenic differentiation both at molecular levels by examining mRNA levels of Sox-9, Col2a1 and aggrecan or at protein levels during the 3-week duration or by the immunofluorescence examination of these markers at the 21 day post-differentiation. In contrast, Dkk-1^{low} CPC from normal clonal CPC cell lines as well as OA-matched Dkk-1^{low} CPC both have shown evidence of successful chondrogenic differentiation.

Heterogeneity in Dkk-1 expression between clonal cell lines from matched donors was shown using several experimental methods. This heterogeneity was clearly found in the molecular expression as well as protein secretion of Dkk-1 and also by clonal cells conditioned media modulation of β -catenin activity using the TCF-

luciferase reporter assay. Whereas, most of the normal monoclonal CPC showed a homogenous expression of Dkk-1 and activation of the TCF-luciferase reporter assay, variation was seen in monoclonal osteoarthritic CPC where most of the cells lines conditioned media had pronounced inhibitory effect on TCF activation.

These findings also shed light on the role of Dkk-1 in chondrogenic differentiation of CPC and it suggests that high levels of endogenous Dkk-1 in OA CPC results in failed *in vitro* chondrogenic differentiation. As it is known that β -catenin is required for chondrogenic differentiation (Akiyama *et al.*, 2004; Kirton *et al.*, 2007). Dkk-1 could possibly result in failed chondrogenic differentiation of CPC by inhibition of β -catenin. Lyashenko *et al.* (2012) have recently studied the impact of β -catenin inhibition on mouse embryonic stem cell differentiation. In *in vitro* and *in vivo* mouse model studies, β -catenin knock out resulted in failure of embryonic differentiation down the mesodermal lineage. Despite the lack of cytoskeletal β -catenin was somehow compensated by plakoglobin (γ -catenin) but ESCs failed to undergo differentiation thus confirming the vital role of β -catenin in formation of mesoderm (Guo *et al.*, 2004; Lyashenko *et al.*, 2012).

Interestingly, expression of Dkk-1 and Dkk-2 were noted to be in a reciprocal manner to each other during chondrogenic differentiation of CPC. This opposing expression of Dkk-1 and its homolog Dkk-2 have been reported previously by Liu *et al.* (2010) and more recently by Reis *et al.*, (2012) and Oh *et al.* (2012). However, the reason behind this opposing expression remains to be investigated.

This data confirm the coexistence of Dkk-1^{high} and Dkk-1^{low} CPC in OA cartilage and that these endogenous levels of Dkk-1, in part, could play a role in determining the capacity of clonal CPC in undergoing chondrogenic differentiation. Taken together,

these data show that clonal lines do not share the same differentiation potential and confirm that individual clonal cell lines selected from the same donor in the same culture conditions are functionally heterogeneous. However, further work is required to ascertain the true nature of this heterogeneity.

In this study, we also demonstrated the immunolocalisation of Dkk-1 in the deep zone of normal and OA human cartilage. Expression of Dkk-1 in a small cohort of deep zone chondrocytes (potentially cartilage progenitor cells) might be in response to the local and systemic changes occurring in osteoarthritis. A recent study by Leijten *et al.* (2012) had shown that Dkk-1 over-expression in deeper part of foetal cartilage acts as a natural brake to prevent hypertrophic differentiation.

In summary, this study provides an insight into the molecular differences found in chondroprogenitor cells isolated from normal and osteoarthritic donors. By examining the expressional profile of the Wnt signalling pathway, it was found that the expression of the canonical Wnt antagonist Dkk-1 to be up-regulated in osteoarthritic CPC when compared to those isolated from healthy donors and full-depth chondrocytes. This difference, when interrogated further using TCF reporter assay and chondrogenic differentiation experiments, suggests that Dkk-1 has detrimental effects on chondrogenic differentiation of Dkk-1^{high} CPC by directly inhibiting the transcriptional role of β -catenin. Interestingly, this present study also demonstrate heterogeneity in clonal cells lines from the same donor and their expression of Dkk-1.

The Wnt pathway is emerging as a crucial pathway involved in the regulation and homeostasis of the synovial joint (Diarra *et al.*, 2007). There is also emerging

literature, which illustrates that the Dickkopf family of Wnt inhibitors plays a key role in the pathogenesis of osteoarthritis. In addition, Dkk-1 was also proposed as a potential biomarker for the progression of osteoarthritis (Lane *et al.*, 2007; Oh *et al.*, 2012a). As discussed in the introduction many signalling pathways have confirmed or proposed roles in the regulation and pathogenesis of osteoarthritis. Here we investigated the role of the Wnt pathway in detail with a particular emphasis on the role of the Wnt canonical inhibitor Dkk-1 using CPC as a model system. The overall purpose was to characterise CPC isolated from normal and OA donors and assess their chondrogenic differentiation potential.

CHAPTER 5: OSTEOCHONDRAL INTERFACE CHARACTERISATION OF CELLULAR INFILTRATION AND THE WNT ANTAGONIST DKK-1

5.1 Introduction.

As previously outlined, osteoarthritis (OA) is a chronic degenerative disease affecting synovial joints leading to articular cartilage destruction, accompanied by underlying bone remodelling. Cartilage is as an avascular tissue and therefore nutritional and oxygen exchange is provided by diffusion from the synovial joint to the upper parts of articular cartilage. For the deeper part of the articular cartilage, oxygen and nutrients supply is provided via the underlying subchondral bone (Buckwalter, 1999; Hunziker, 2002). Subchondral bone is at the interface between non-calcified cartilage and the trabecular bone of the skeletal system. It is separated from the articular cartilage by a thin basophilic acellular region known as the tidemark. The subchondral microenvironment is composed of a variety of cell types that influence the angiogenic response of endothelial cells in osteoarthritis. Subchondral bone hosts several cell types including bone cells (osteoblasts, osteoclasts and osteocytes), endothelial and mesenchymal progenitor cells. Features indicative of subchondral bone pathology in osteoarthritis include; tidemark duplication and cellular and vascular infiltration leading to cartilage angiogenesis (Suri and Walsh, 2012; Yuan *et al.*, 2014).

Involvement of angiogenesis in tumour metastasis is a widely accepted concept in the field of cancer research. The role of angiogenesis in the pathogenesis of many diseases, including that of degenerative arthritis, has recently attracted the interest

of many researchers, as it is thought that the subchondral bone plays a key role in the development of osteoarthritis (Hillen and Griffioen, 2007).

Angiogenesis is defined as the generation of new blood vessels from pre-existing ones. It is a vital process for organ formation during embryonic and postnatal development and depends on a complex network of activators and inhibitors (growth factors and morphogens) that are regulated in a temporal and spatial manner in order to facilitate vasculogenesis (Weis and Cheresh, 2011). In addition, development of new blood vessels continues during adult life to accommodate for physiological demands. This area of research has attracted significant attention in cancer studies as tumour metastasis is significantly influenced by blood vessel development (Bergers and Benjamin, 2003; Streit and Detmar, 2003).

Of the observed changes that affect articular cartilage in osteoarthritis, it is thought that changes affecting the extracellular matrix structure of cartilage might be attributed to overall tissue weakness to invading cells from the underlying subchondral bone. Normal mature articular cartilage contain factors that are shown to be anti-angiogenic (thrombospondin-1) (Hsieh *et al.*, 2010). Furthermore, the balance of cartilage matrix formation and breakdown in normal cartilage tissue is carefully regulated by the activity of metalloproteases (MMPs and ADAMTs) and their inhibitors (TIMPS) (Kim *et al.*, 2011). During osteoarthritis, this balance is tilted towards cartilage degradation therefore, indirectly might encourage tissue angiogenesis. This process is poorly understood and several regulatory pathways, thought to be implicated, such as Notch and the Wnt pathway, have been shown to play a role in activating in synovial joint tissues proliferation and angiogenesis. This alteration in tissue metabolism might, in part, be triggering angiogenesis as the

demand for higher oxygen and nutrient levels increase (Pfander *et al.*, 2001; Walsh *et al.*, 2007; Weng *et al.*, 2012).

Little is known about the factors promoting cellular infiltration and angiogenesis during late-stage osteoarthritis and in particular whether the Wnt signalling pathway is involved in such processes (Reis *et al.*, 2012; Saito *et al.*, 2012; Weng *et al.*, 2012). *In vivo* studies using transgenic mice have been conducted to further elucidate the role of Dkk-1 in growth-plate cartilage angiogenesis. Conditional over-expression of Dkk-1 in endothelial cells of developing synovial joints in mice showed defects in endochondral ossification and growth plate size (Oh *et al.*, 2013). This finding was due to failure of endothelial cell to maintain their phenotype, which has resulted in ultimate aberrant endochondral process. Another study by Reis and colleagues have shown that aspects of the Wnt/ β -catenin pathway were implicated in glioma tumour metastasis (Reis *et al.*, 2012). In their study, Dkk-1 over-expression in brain-derived endothelial cells had a detrimental effect on the integrity of the blood brain barrier leading to glioma cell metastatic behaviour by activating platelet derived growth factor (PDGF). Dkk-1 was noted to have a pro-angiogenic effect on tumour progression whereas β -catenin activation, by Wnt-1, showed a rescuing role leading to blood vessel regression.

In the previous chapter, Dkk-1 staining was observed to be along the cellular infiltrate from the underlying subchondral bone. Therefore, the aim of this chapter is to initially characterise the phenotype of invading cells by examining osteochondral tissues isolated from normal and osteoarthritic donors. In addition, the role Dkk-1 plays in subchondral cellular infiltrate would be further studied using a well-known *in*

vitro endothelial cell model system to decipher if Dkk-1 exhibit pro-angiogenic and migratory effects on endothelial cells.

5.2 Experimental methods.

Osteochondral tissues were isolated from normal donors (n=6) and osteoarthritic donors (n=10) and were graded using the modified Mankin score system (Appendix 1). To assess the phenotype of invading cellular structures at the osteochondral interface, sequential sections were examined. Sections were examined for the presence of endothelial cells using CD-34 immunostaining (section 2.8.2). In addition, the presence of migratory mesenchymal stem cells were examining using immunofluorescence confocal microscopy using the putative stem cells markers CD-105 (Endoglin) and CD-166 (ALCAM). Furthermore, mature-osteoclasts are known to stain positive for TRAP. Therefore, for the characterisation of osteoclast infiltrate into the articular cartilage, was assessed using the Acid Phosphatase, Leukocyte (TRAP) Kit purchased from Sigma and used as per manufacturers' protocol (section 2.7.3). Moreover, the number of CD-34 positive blood vessels invading the tidemark were manually quantified and the percentage of microvessel density measurement were recorded. Finally, the associative expression of Dkk-1 and endothelial cells markers were further examined using immunohistochemical labelled consecutive sections of osteoarthritic osteochondral tissues. To study the functional role of several canonical Wnt pathway modulators on endothelial cells, a well characterised and robust human endothelial cell line (HECV) was utilised to perform a series of assays assessing the effect of the canonical Wnt factors on endothelial cells the canonical Wnt pathway response marked by assessing β -catenin and plakoglobin (γ -catenin) levels. In

addition, endothelial cell proliferation, migration and invasion and angiogenesis were also examined in cells exposed to canonical Wnt factors.

5.3 Results:

5.3.1. Histological staining of osteochondral plugs.

Osteochondral plugs were dissected from normal and osteoarthritic donors and sectioned as described in Chapter 2. Histological staining was carried out to study morphological and topographical features associated with OA osteochondral tissue from a range of patients. Figure 5.1 shows the Safranin O staining of tissue sections taken from one normal and five OA patients. Changes affecting the articular cartilage were observed including loss of cartilage proteoglycan. Patients coded OA-1 and OA-6 showed proteoglycan loss indicative of the early stages of OA with a loss of Safranin O from the superficial zone of cartilage along with roughening and slight irregularity at the surface of the cartilage (Figure 5.1.B and C, respectively). In addition, patient coded OA-8 (Figure 5.1 D) showed a marked reduction of Safranin-O staining in the superficial and mid zone of the cartilage and, damage to the superficial zone was found to increase from surface irregularity to mild fibrillation (Figure 5.1.D) indicating a more advanced stage of disease. Furthermore, as OA disease progression was seen in, subchondral changes with bone cysts (arrow) and cellular infiltration from the subchondral bone clearly noted in figure 5.1.D.

Patients coded OA-10 and OA-2 (Figure 5.1F and E, respectively) showed advanced stages of OA, the cartilage superficial zone was completely lost and large fissures extending to the middle zone became frequent histological observations (Figure 5.1.E and F). Chondrocyte morphology was also altered resulting in increased

cellular proliferation and chondrocytes clustering. Chondrocytes clusters extended from the deep regions of the cartilage and cellular infiltration was clearly apparent (Figure 5.1.E and F). The cellular composition of the articular cartilage included hyper-proliferated cells that did not have the classical chondrocyte morphology (Figure 5.1.F). Moreover, bone and vascular tissues were found to have invaded the cartilage and were in close proximity to deep zone chondrocytes (Figure 5.2.E-F). In addition, significant proteoglycan loss was observed in the mid zone and extended into the deep zone of the tissue.

An interesting phenomenon observed was the presence of numerous atypical cellular infiltrations into the articular cartilage from underlying subchondral bone. These cells were distinct from native chondrocytes. Infiltrated cells appeared to be heterogeneous in nature, consisting of bone-marrow stromal cells, bone cells and endothelial cells. Figure 5.1.E-F shows an example of many groups of large, clear, stromal cells in small clusters and are visible by histological staining. In addition, tidemark duplication was clearly evident in some regions.

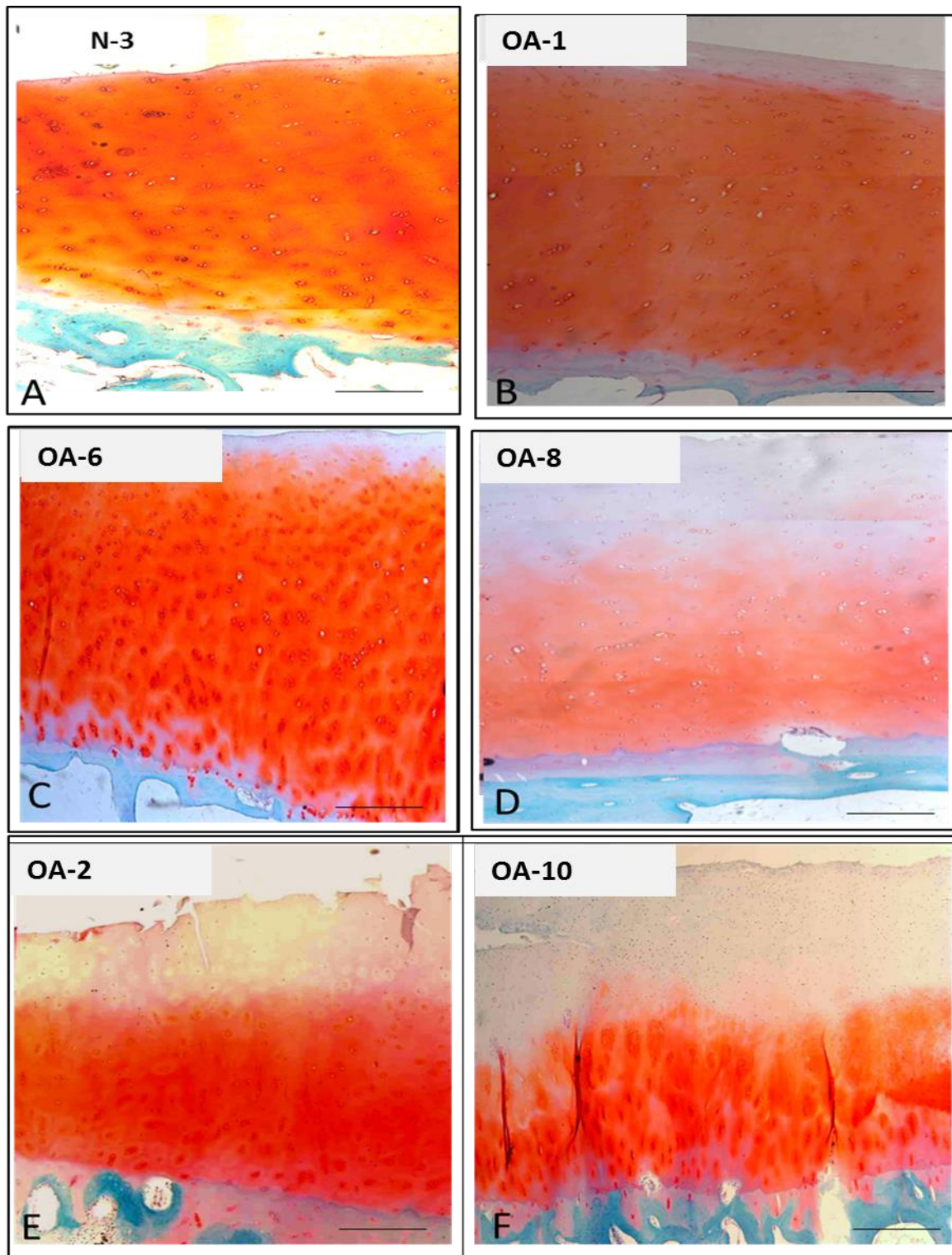


Figure 5.1: Histochemical staining of normal and osteoarthritic osteochondral tissues.

Representative images of Safranin-O and Fast Green stained osteochondral sections from normal (A) and osteoarthritic donors (B-F). Scale bar= 500 μ m.

5.3.2. Immunohistochemical labelling of Mesenchymal stem cell makers.

Figure 5.2 shows representative confocal images of sections taken from osteochondral plugs stained for the MSC marker CD-105 (Endoglin) from normal and late-stage OA patient donors. Staining for CD-105 was not observed to be present in the superficial zone (Figure 5.2.A1) of normal donors but comparatively the middle zone of the tissue demonstrated positive immunolocalisation of CD-105 at the cell surface of chondrocytes with occasional labelling seen in cluster of chondrocytes arranged in columns in the deep zone of the tissue (Figure 5.2.A2). The staining patterns seen in the deep zone was found to be similar to the middle zone mainly at the cell surface of the chondrocytes with additional cytoplasmic staining (Figure 5.2.A3).

However sections stained from patients with late-stage osteoarthritis showed altered immunolocalisation patterns of the CD-105 marker which was found throughout the tissue (Figure 5.2 B1). In the superficial zone, some immunolabelling was noted especially around the first three layers of superficial zone chondrocytes (Figure 5.2.B1 and higher magnification in Figure 5.2.B2). However, expression of CD-105 in the middle zone was absent (Figure 5.2.B2). CD-105 expression in the deep zone chondrocytes was present in two patterns. Chondrocytes in deep zones were positive for CD-105 (Figure 5.2.B) and in addition, an intense region of CD-105 labelling was evident particularly around the subchondral cellular infiltrate (Figure 5.2.B4).

Figure 5.2 shows representative confocal images of sections taken from osteochondral plugs stained for the MSC marker CD-166 from normal and late-stage OA patient donors. Unlike the immunolabelling pattern of CD-105, the expression

patterns of the mesenchymal stem cell marker CD-166 in normal cartilage, was more wide-spread and found predominantly in the middle zone with less staining in the superficial and deep zones of the articular cartilage (Figure 5.3 A1). The expression pattern of CD-166 was observed to be mainly at the cell surface. However, in osteoarthritic tissue, this pattern changed with a generalised reduction in CD-166 immunolabelling throughout the articular cartilage (Figure 5.3 B1). One exception was seen in superficial zone where CD-166 immunostaining, was intense in superficial zone regions where evidence of fibrillation was noted (Figure 5.3 B2). Similar to CD-105 immunolabelling in OA tissues, middle zone chondrocytes appeared to have reduced labelling of CD-166 (Figure 5.3. B3). However, CD-166 was intensely expression around cellular infiltrates from the subchondral bone (Figure 5.3 B4).

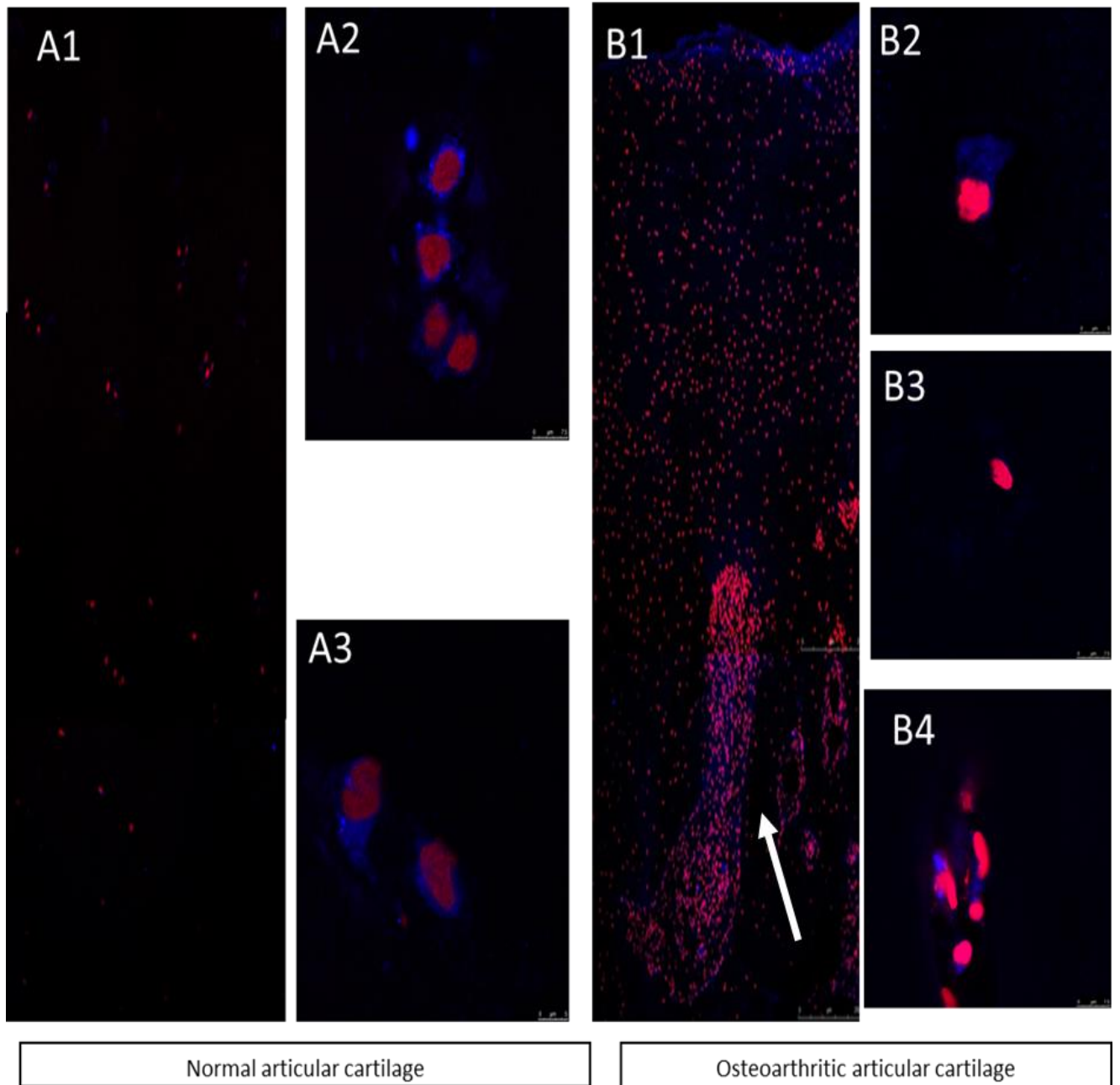


Figure 5.2: Confocal images of immunohistochemical analysis of the CD-105 protein in osteochondral tissues.

Confocal images of CD-105 protein in normal (A) and osteoarthritic osteochondral tissues (B) from the full-depth of articular cartilage (A1, B1), superficial zone (B2), mid zone (A2, B3) and deep zone of articular cartilage (A3, B4). In addition, cellular infiltration from the underlying subchondral bone positively labelled for CD-105 protein (blue) are evident in (B1) image (white arrow). CD-105 was visualised using Goat anti-mouse Alexa Fluor 633(blue) and nuclei staining were attained using propidium iodide (red). Scale bar=75µm.

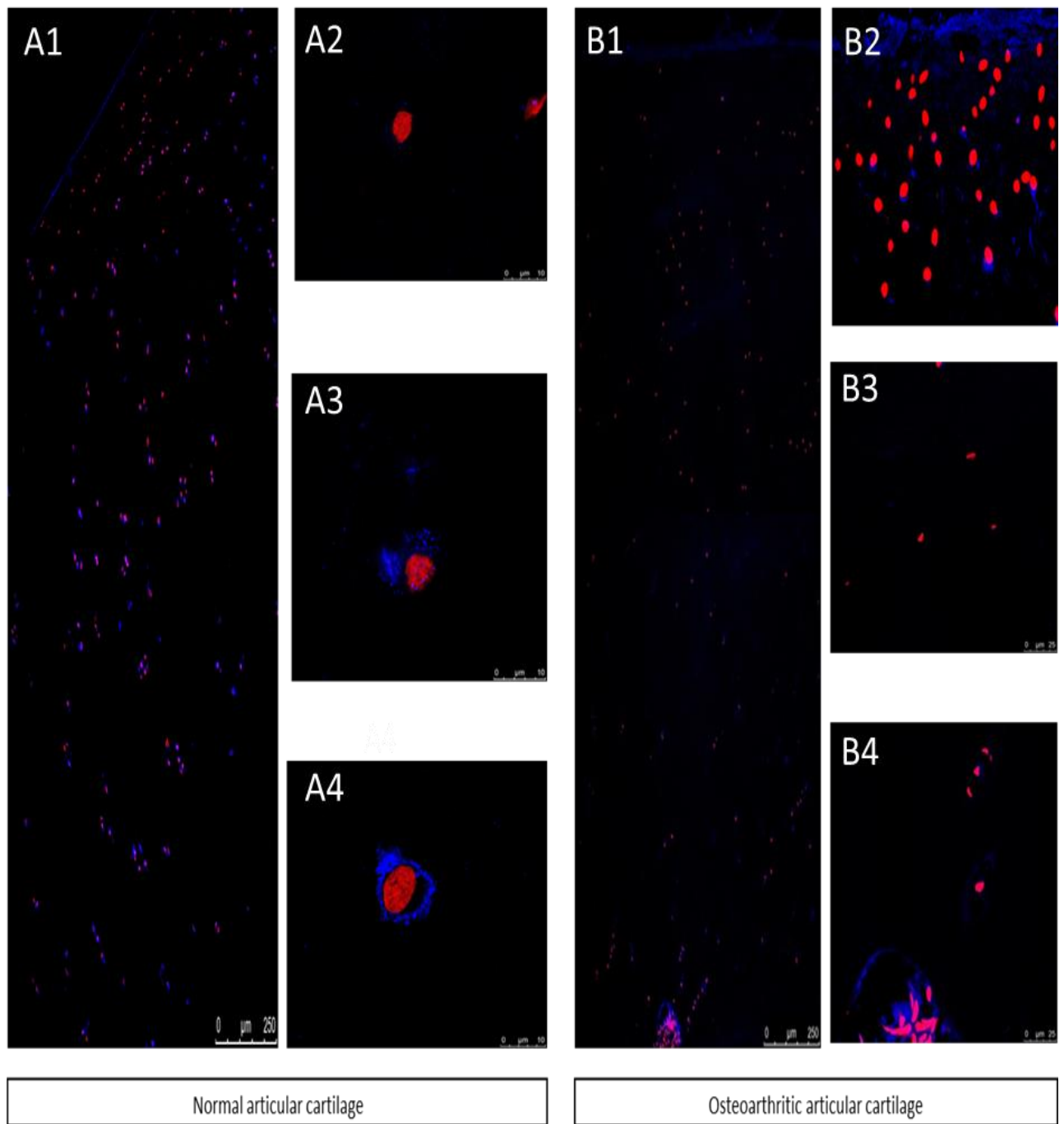


Figure 5.3: Confocal images of immunohistochemical analysis of the CD-166 protein in osteochondral tissues.

Immuno-labelling of CD-166 in normal (A) and osteoarthritic osteochondral tissues (B) from the superficial zone of articular cartilage (A2, B2), mid zone (A3, B3) and deep zone of articular cartilage (A4, B4). (B4) image shows positive staining in cellular infiltrates from the underlying subchondral bone for CD-166 protein (blue). CD-166 was visualised using Goat anti-mouse Alexa Fluor 633 (blue) and nuclei staining were attained using propidium iodide shown as red. Scale bar=75μm.

5.3.3. TRAP staining of osteochondral plugs: Involvement of osteoclast cells in cartilage invasion.

Figure 5.4 shows representational TRAP staining of sections taken from normal and OA donors which was carried out in order to examine if the cellular infiltrate from the underlying subchondral bone were associated with the recruitment of osteoclast cells. The distribution of tartrate resistant acid phosphatase (TRAP) positive cells in osteochondral tissues from normal (n=6) and osteoarthritic (n=10) osteochondral tissues were investigated using the Acid Phosphatase, Leukocyte (TRAP) Kit as per manufacturer's protocol. In osteochondral tissues isolated from normal donors (Figure 5.4. A-B, representative section), there was no evidence of osteoclast invasion to the articular cartilage show by a lack of cells staining positive for TRAP. However, in the osteoarthritic samples, a clear trend was observed showing an apparent increase in the number of TRAP positive multinucleated osteoclasts found in the calcified regions of the subchondral bone (Figure 5.4.C&D, representative sections). In some regions, a tip and stalk dynamic was noted where in some samples the osteoclasts were positioned at the tip (Figure 5.4.E). At other locations, the endothelial cells were leading the invasion and the osteoclast were located at the stalk (Figure 5.4.F). However, in certain regions of the osteochondral interface, there was no evidence of osteoclast association with vascular and stromal cell invasion (Figure 5.4.G-I).

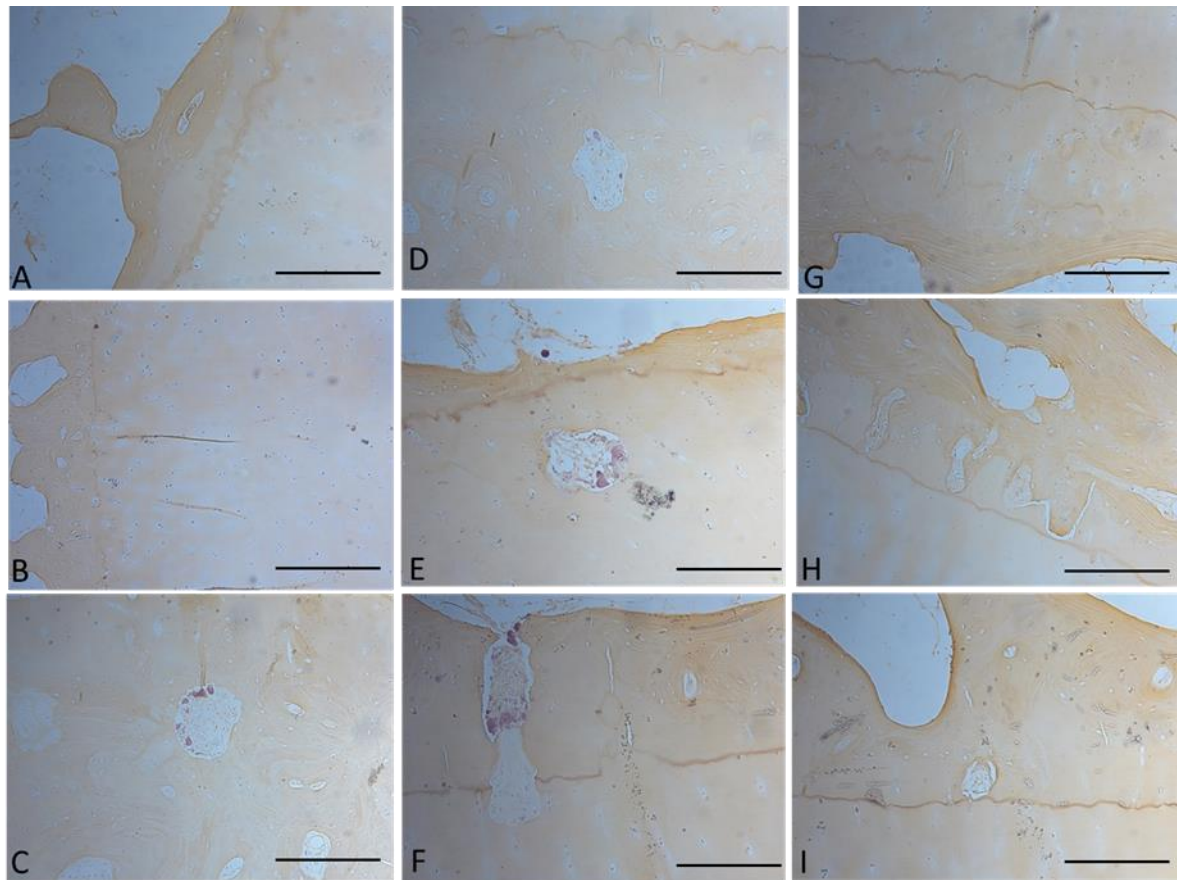


Figure 5.4: TRAP staining assay of osteochondral tissues.

Tartrate-resistant acid phosphatase (TRAP) staining of sections taken from normal and osteoarthritic osteochondral plugs. (A-B) Show absence of TRAP positive cells in normal tissues while (C-E) show evidence of TRAP positive (arrow; purple) in either the subchondral bone (C-D) or breaching the tidemark into non-calcified articular cartilage (E-F). Also, evidence are TRAP negative cellular infiltrates seen in several tissues (G-I). Scale bar=200µm and inset is 100µm.

5.3.4. Microvessel density measurements.

Immunohistochemical labelling of osteochondral plugs taken from OA patient donors with CD-34 antibody, an endothelial cell marker, showed positive staining around vessel-shaped infiltrating cells (Figure 5.5.G-I). From immunohistochemical studies, a positive trend in CD-34 labelled blood vessels and osteoarthritic disease severity was observed. This is marked by clear loss of articular cartilage and increased bone

sclerosis (Figure 5.5.A-C). The number of blood vessels increased with increasing severity of cartilage loss (Figure 5.5.A-C).

In tissue with increased blood vessel invasion, Dkk-1 staining appeared to be surrounding the infiltrated blood vessels (Figure 5.5.D, F). In addition, immunolocalisation of Dkk-1 was also found in chondrocyte clusters present in the fibrillated superficial zone of articular cartilage (Figure 5.5.E). Microvessel density measurement of CD-34 positive cells in normal and OA osteochondral tissues showed that the mean CD-34 cell number positive in OA and normal were (12.82 ± 1.7 and 4.3 ± 0.7 , $p < 0.05$ respectively, Figure 5.6.A-C)

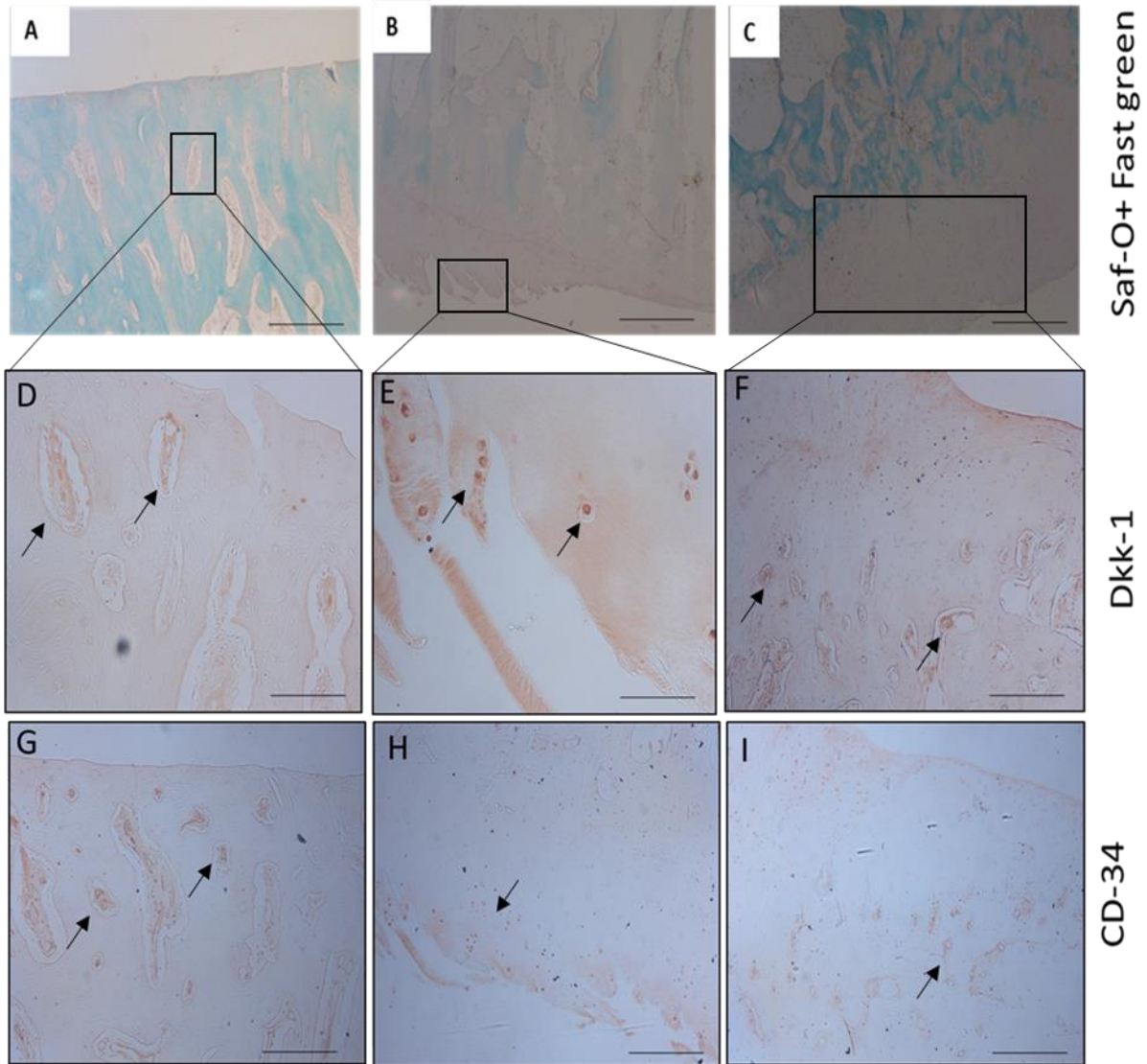


Figure 5.5: Representative immunohistochemical images of sections taken from osteochondral plugs from different stages of OA.

Safranin-O and Fast green staining (A-C), Dkk-1 (D-F), CD-34 (G-I) in osteoarthritic osteochondral tissues. Chondrocytes in OA cartilages displayed intense expressions of Dkk-1 around blood vessels infiltrating from the subchondral bone (dark arrows; D&F) and also in the superficial zone chondrocytes (dark arrows; E). The pattern of Dkk-1 staining around blood vessels appeared to be similar to CD-34 staining in consecutive sections (D-G and F-I). Scale bar=200 μ m.

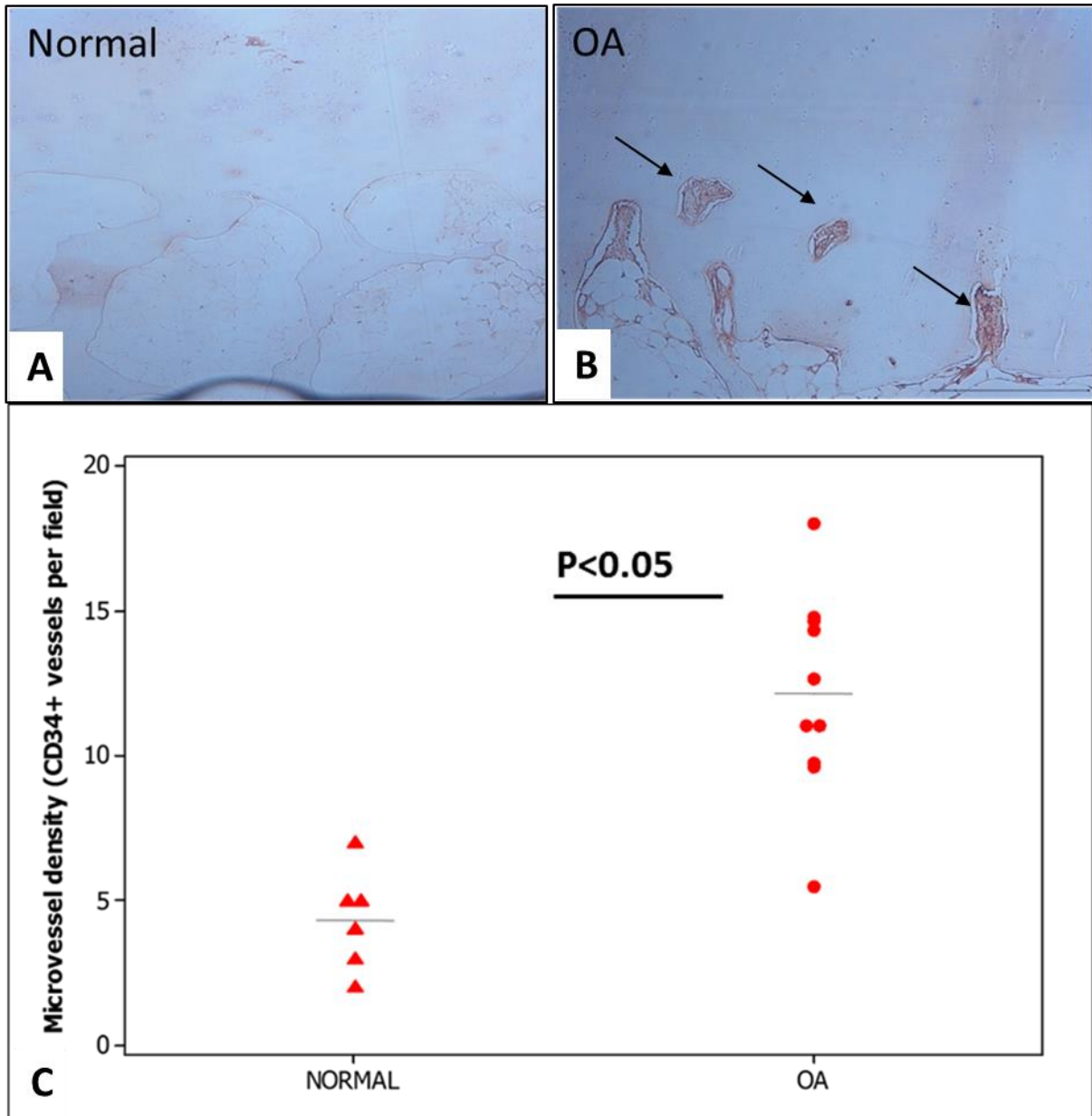


Figure 5.6: Representative CD-34 immunohistochemical staining of sections taken from normal and OA osteochondral tissues.

Images A&B show CD-34 immunostaining of vascular infiltrates at the osteochondral interface from normal (A) where there are no vascular breaching of the non-calcified articular cartilage and OA (arrow; B) donors showing CD-34 positive endothelial cells breaching non-calcified cartilage. Number of blood vessels were quantified (C) (n=6 normal, n=10 OA, $p < 0.05$). Data are presented as the mean of three slides per patient stained for CD-34.

5.3.4 Characterisation of endothelial cells.

To further understand the role that Dkk-1 plays in endothelial cell angiogenesis and invasion of articular cartilage in late-stage osteoarthritis (Figure 5.7. A-B), we used a well-known human endothelial cell line (HECV) that is known to retain their primary cell characteristics while being able to be cultured *in vitro* for up to 15 passages.

Flow cytometry was used to characterise the expression profile of CD-31 (Figure 5.7.C), CD-34 (Figure 5.7.D) and CD-144 (Figure 5.7.E) as endothelial cell markers while CD-11b was used as a negative marker (Figure 5.7.F). Endothelial cells showed positive expression of CD-31 and CD-144 in over 95% of the gated cells using FACS, with a unimodal expression and 89% for CD-34 expression. In addition, expression of CD-11b, a negative marker for endothelial cells, was around 2%.

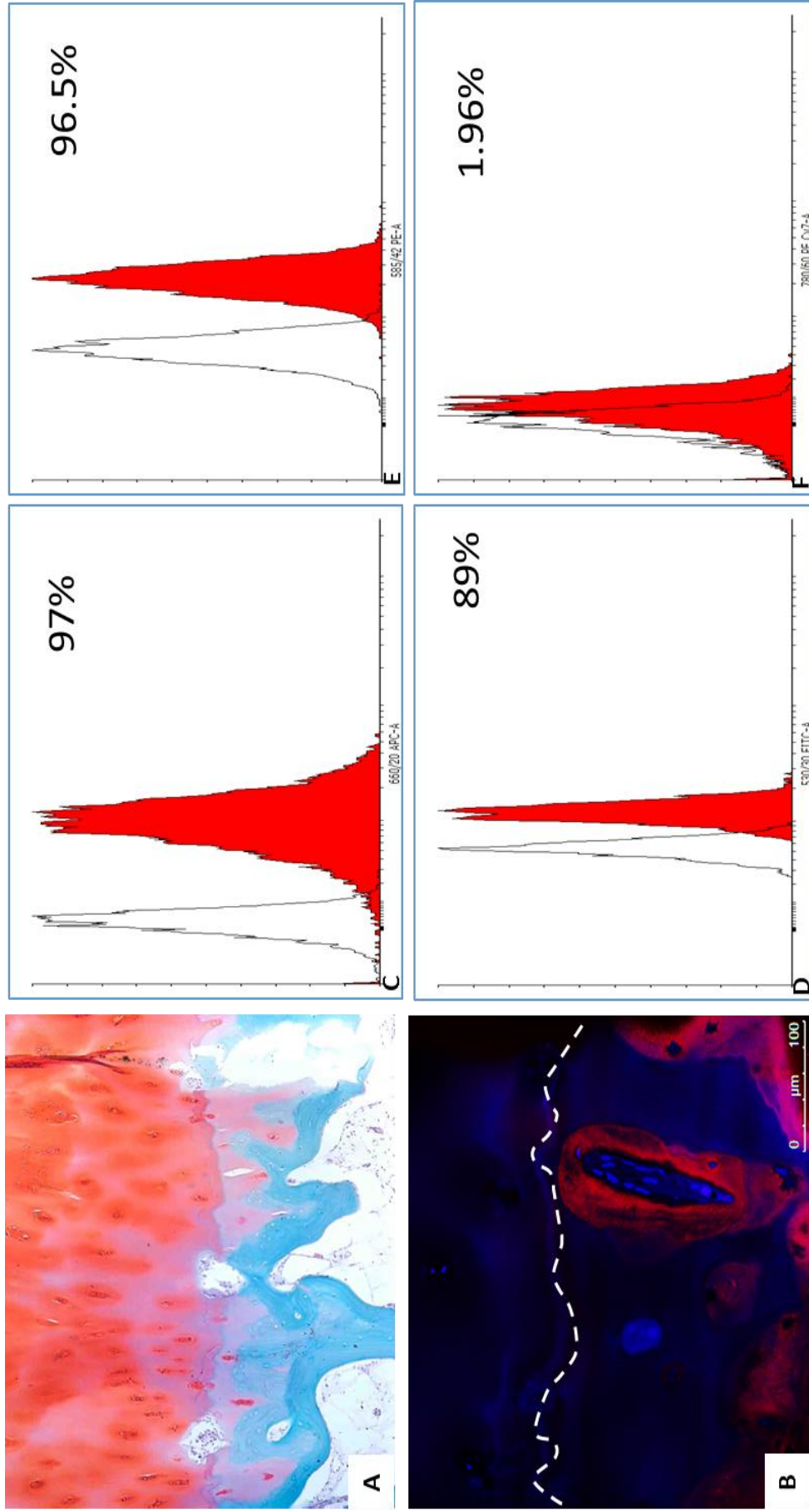


Figure 5. 7: Flow cytometry characterisation of endothelial cell lines (HECV).

Safranin-O and Fast-green staining of OA-osteocondral tissue showing blood vessel invasion of articular cartilage (A). Figure B show immunolocalisation of osteochondral plugs with Dkk-1 antibody where Dkk-1 positive-labelling is seen around blood vessel and breaching tidemark (dotted line). Figure C-F Flow cytometry characterisation and percentage of positive endothelial cells using a panel of endothelial cell surface markers CD-31(C), CD-34 (D), CD-144 (E) and the negative marker of endothelial cells CD-11b (F).

5.3.4.1. Dkk-1 inhibits the nuclear translocation of β -catenin in cultured endothelial cells.

The addition of several canonical Wnt pathway modulators on endothelial cells in culture was examined to see if they had an effect on the cellular localisation of β -catenin (Figure 5.8). Addition of recombinant Dkk-1 (100ng) resulted in reduced β -catenin nuclear expression when compared to control (Figure 5.8). However, addition of Dkk-2 at 100 ng/mL showed no obvious reduction in β -catenin nuclear expression (Figure 5.8). Similarly, addition of Wnt-3a (100 ng/mL) or lithium chloride, an inhibitor of GSK-3 β , at 10 mM showed increased positive staining of β -catenin (Figure 5.8). Moreover, addition of a small molecule inhibitor of Dkk-1, WAY-262611 (1 μ M) in addition to Dkk-1 (100 ng/mL), also increased the nuclear β -catenin translocation in comparison to Dkk-1 treated cells (Figure 5.8).

Having established that endothelial cells respond to modulators of the canonical Wnt pathway, as characterised by β -catenin cellular localisation, next western blot analysis was used to quantify the protein. Consistent with confocal results, western blot analysis showed a significant down regulation of total β -catenin levels in response to exogenous Dkk-1 treatment (Figure 5.9), while Dkk-2, had no obvious effects on total β -catenin levels when compared to untreated (control) cells (Figure 5.9). Interestingly, addition of exogenous Wnt-3a, a positive canonical Wnt activator, resulted in increased total β -catenin levels (Figure 5.9). In addition, both lithium chloride (10 mM) and the addition of, a small molecule inhibitor of Dkk-1, WAY-262611 (1 μ M), also increased the total β -catenin levels (Figure 5.9).

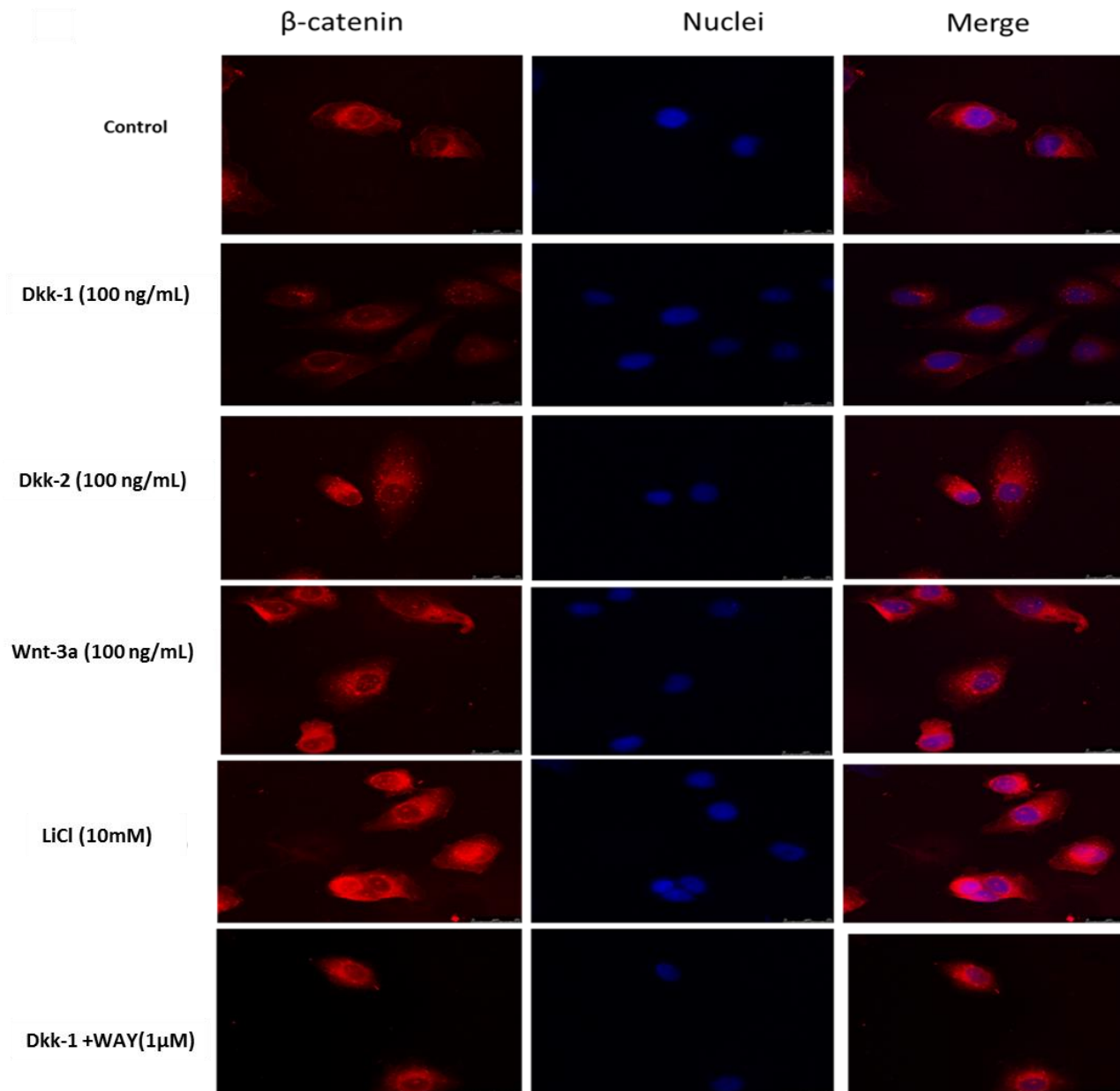


Figure 5. 8: Assessment of β -catenin nuclear localisation in response to exogenous treatment of several canonical Wnt pathway modulators.

β -catenin immunofluorescence confocal imaging of endothelial cells with different treatments of exogenous Wnt proteins modulators. Nuclear localisation of β -catenin was examined in EC treated with basal media \pm Dkk-1, Dkk-2, Wnt-3a treated, and LiCl (10mM), WAY inhibitor (1 μ M) treatment.

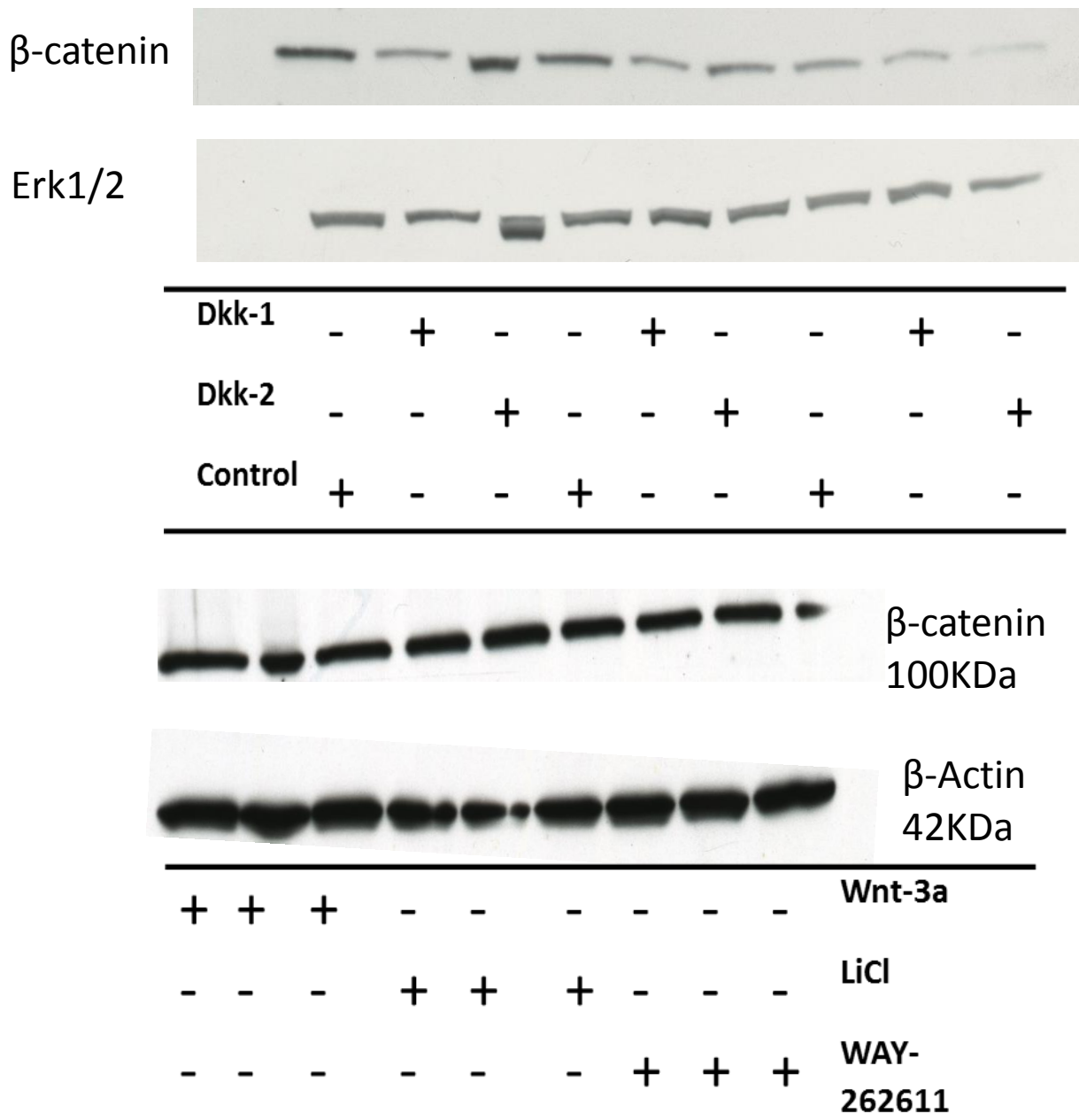


Figure 5.9: β-catenin protein analysis in response to exogenous treatment of several canonical Wnt pathway modulators. Endothelial cells treated with basal media +/- recombinant Dkk-1, Dkk-2 and Wnt-3a proteins all at (100 ng/mL) or LiCl (10 mM) and WAY-262611 (1μM) for 96hrs before total protein (20 μg/lane) was extracted and analysing using SDS-PAGE. Total Erk and β-actin were used as loading control. Experiments were conducted in triplicates per group.

5.3.4.2. Dkk-1 has an inhibitory effect on canonical β -catenin but does not alter its other catenin members.

As mentioned in chapter one, β -catenin has a dual role in the cell, acting as a transcriptional factor when involved in the canonical Wnt pathway. In addition, β -catenin is also involved in the cell cytoskeleton as it is a component of the adherence junctions linking isoforms of cadherin to the actin molecules. This role is also mediated in relation to other members of the catenin family including γ -catenin (Plakoglobin). This is important as alteration in a cells cytoskeleton can affect cell motility. Western blots were used to assess if Dkk-1 exerts any effect on the cytoskeletal role of catenin family members using γ -catenin. Plakoglobin (γ -catenin) only directly binds to β -catenin, therefore any alteration in β -catenin cytoskeletal levels would ultimately alter Plakoglobin (γ -catenin) levels. Western blot analysis showed that exogenous Dkk-1 treatment did not any effect the total levels of cytoskeletal Plakoglobin (γ -catenin) (Figure 5.10).

5.3.5 Dkk proteins stimulate endothelial tubule formation.

One of the most specific tests for angiogenesis is the ability of endothelial cells to form three-dimensional tubules. The effects of several canonical Wnt proteins on endothelial tubule formation (Figure 5.11) was examined. VEGF-C recombinant protein was used as a positive pro-angiogenic factor where tubule formation was assessed by culturing endothelial cells on Matrigel™ gel before adding recombinant Dkk-1 and Dkk-2 at 100 ng/mL or control medium alone (DMEM+PS+0.1% BSA). Dkk-1 and Dkk-2 showed positive tubule formation similar to VEGF treatment (Figure

5.11A). There was no significant difference at 24 hours between Dkk-1, Dkk-2 or VEGF, suggesting that Dickkopf proteins (Dkk-1 and Dkk-2) have positive angiogenic properties on endothelial cells in an *in vitro* setting while control did not exhibit any noticeable angiogenic response (Figure 5.11D). Examining the total branching points, number of rings and total tubes formed showed a statistically significant increase in all of Dkk-1, Dkk-2 and VEGF treated endothelial cells when compared to control ($p < 0.05$)

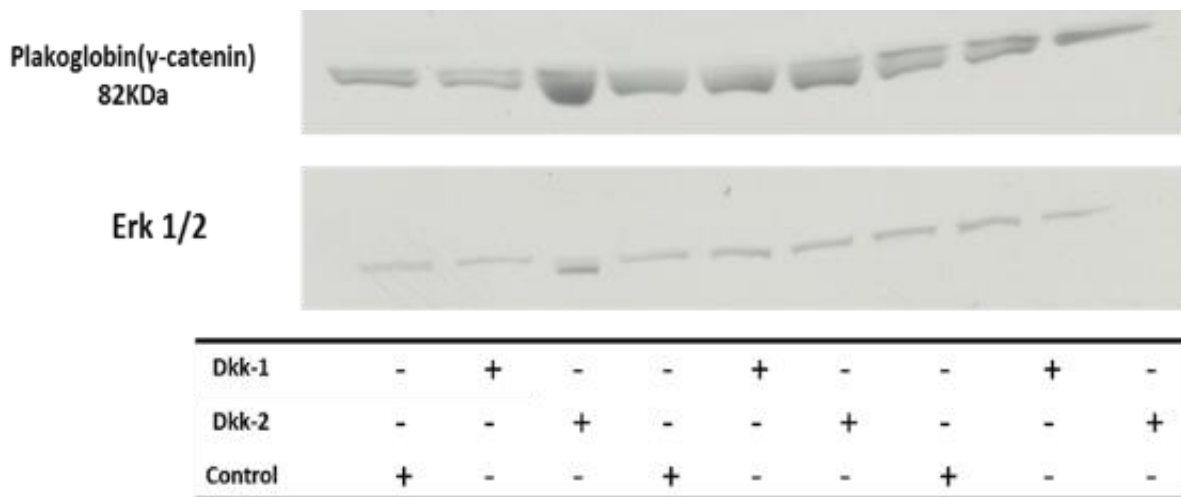
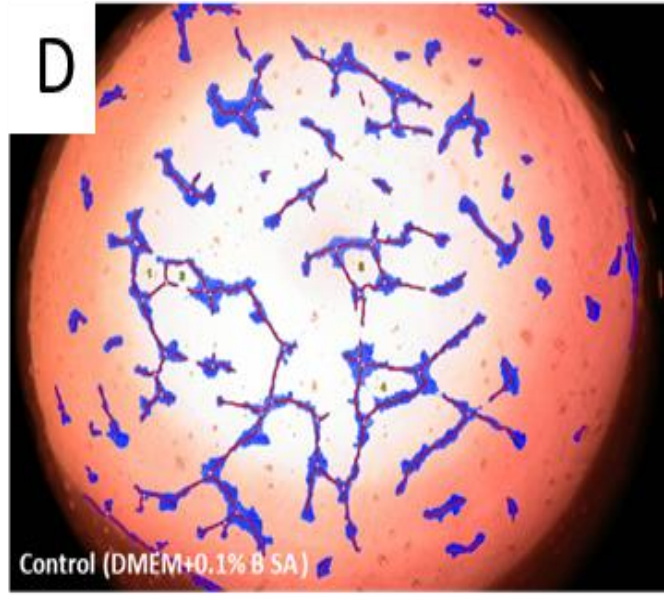
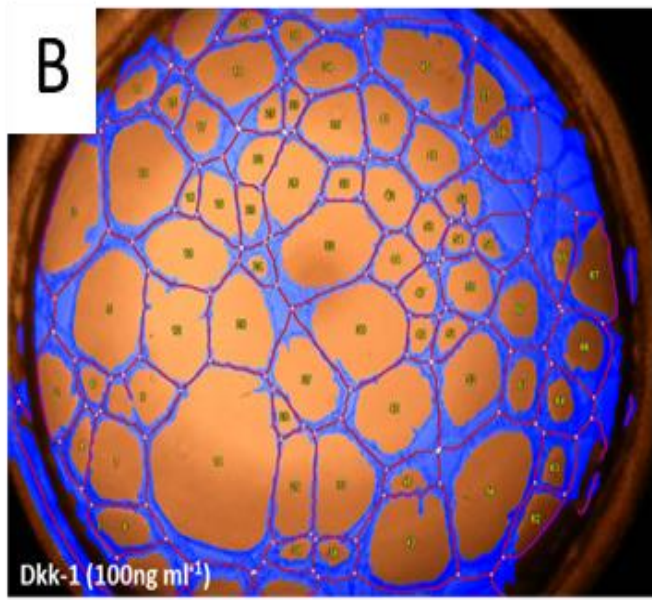
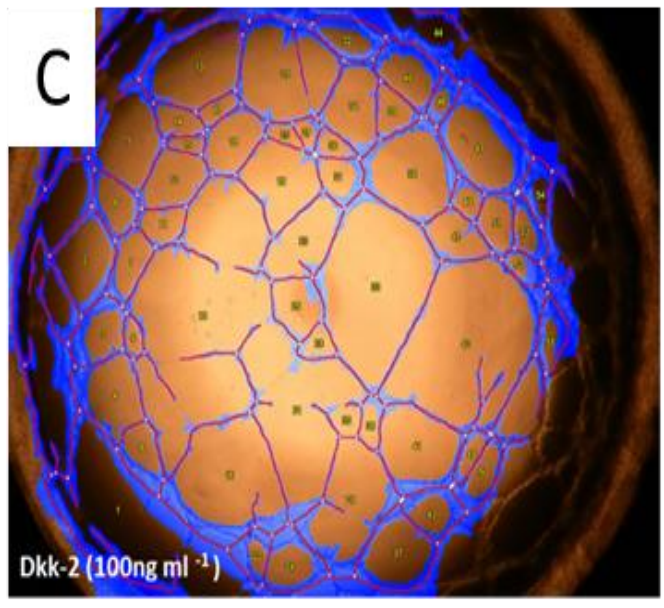
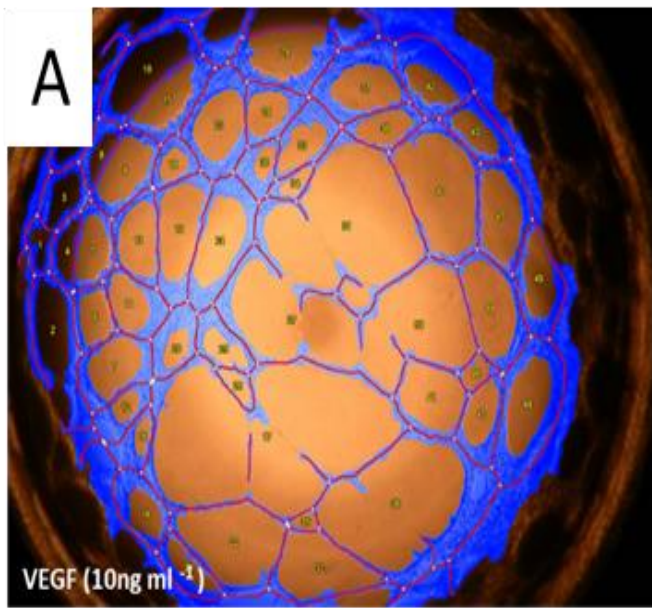


Figure 5.10: Plakoglobin (γ -catenin) protein analysis in response to exogenous treatment of several canonical Wnt pathway modulators.

Endothelial cells treated with basal media +/- recombinant Dkk-1 and Dkk-2 proteins all at (100 ng/mL) for 96hrs before total protein (20 μ g/lane) was extracted and analysing using SDS-PAGE. Total Erk was used as loading control. Experiments were conducted in triplicates per group.



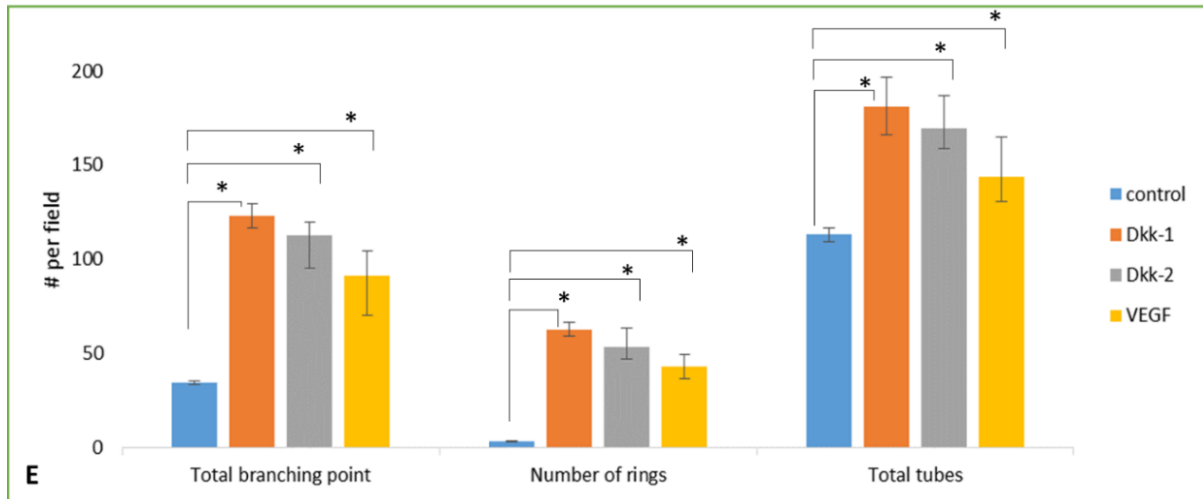


Figure 5.11: Tubule formation assay of endothelial control cells and cells treated with VEGF, Dkk-1 and Dkk-2 recombinant protein.

Representative images of tubule formation assay are shown (A-D). The ability of human endothelial cells to form capillary-like structures was assessed using 24-well plates coated with Matrigel™ treated with media alone- Control (DMEM+0.1% BSA; D) and media with Dkk-1(100 ng/mL; B), Dkk-2(100 ng/mL; C) or VEGF (10 ng/mL) as positive angiogenic control (A). Cells were plated in Matrigel™ and were incubated for 24 hrs and images were taken using an inverted light microscope (n=6 per group). E) Histogram showing mean total branching point, number of rings and total tubes per group. Data are presented as mean ± SEM (n=6 per group. 1-Way ANOVA, *p<0.05).

5.3.6 Dkk-1 encourages endothelial cell migration and wound closure.

Endothelial cell migration has an important role in the process of angiogenesis and neovascularisation. The effect of modulators of the canonical Wnt pathway was assessed in the wound closure assay. Figure 5.12 shows that Dkk-1 treated endothelial cells completely resulted in wound closure after 24 hrs while control cells were unable to close the generated wound in the same setting and this finding was statistically significant (Figure 5.12). Other factors including Dkk-2, Wnt-3a and LiCl all showed evidence of wound closure although statistically, this was not significantly different from control (Figure 5.12.B, p<0.05) This finding was further analysed using ANOVA which has shown that Dkk-1 treated cells had a higher migration rate

which was statistical significant ($P < 0.05$) but among other treatment groups, there were no statistical significant difference with control ($P > 0.05$).

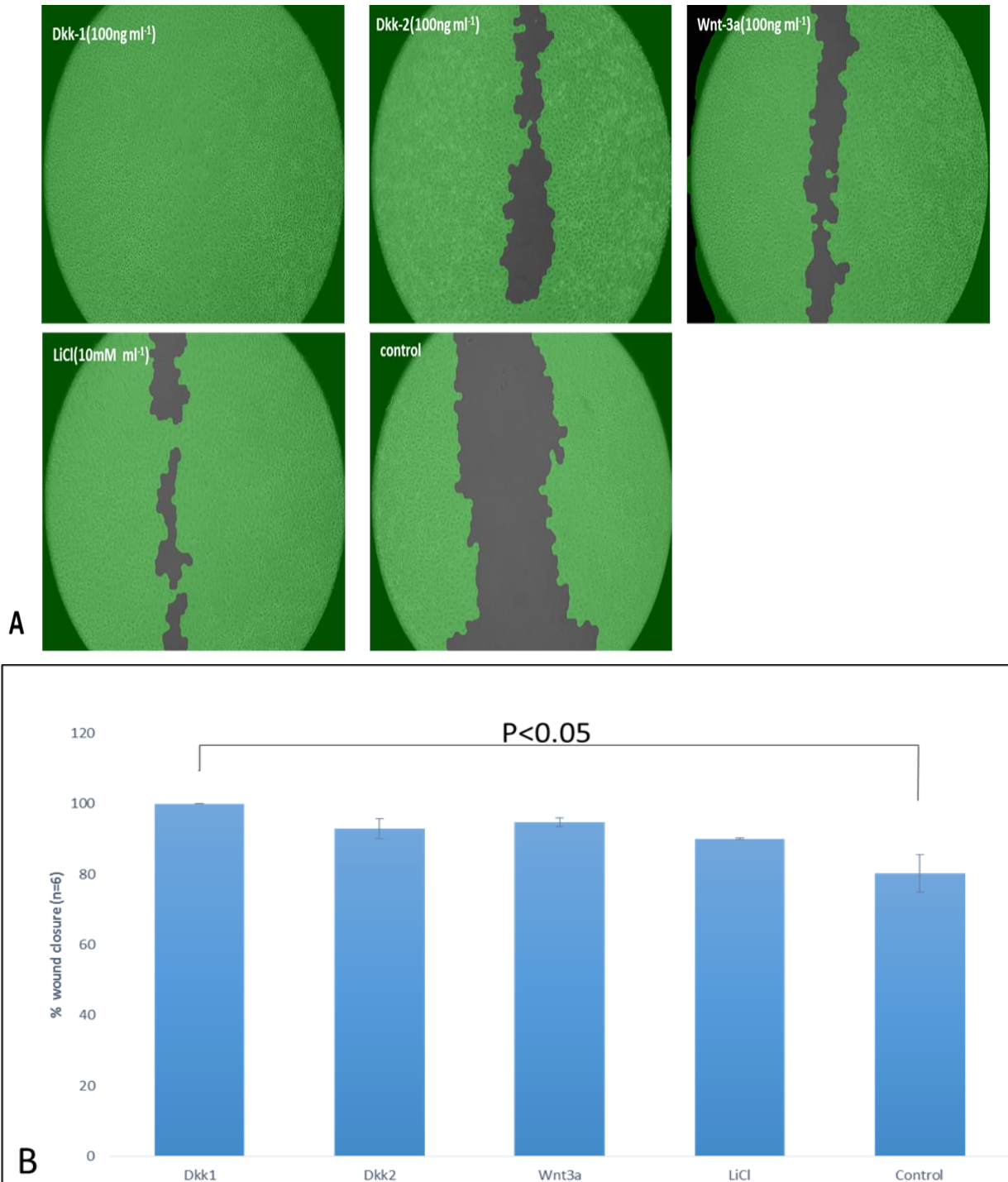


Figure 5.12: Migratory capacities of endothelial cells after stimulation with several canonical Wnt modulators as measured by the scratch wound closure assay.

Representative photographs of endothelial wound closure after 24 hrs incubation with control media (DMEM+PS+0.1% BSA) \pm Dkk-1, Dkk-2 and Wnt-3a all at (100 ng/mL) and LiCl (10 mM). B) Histogram showing percentage wound closure of different treatment groups where Dkk-1 treatment showed strong wound closure compared to control. Data are presented as % Control \pm SEM (n=6 per group. 2-Way ANOVA, *p<0.05).

The positive cell motility role of Dkk-1 was further analysed using a Transwell-migration assay. The Transwell migration assay examines the migratory capacity of cells under the chemotactic influence of test sample or paracrine factor in a directional setting. Transwell migration assays identified that endothelial cell migration in Dkk-1 treated groups was greater than that of the control group (Figure 5.13.A). A 1.8-fold increase was observed in the number of migrating cells in the experimental group compared with the control group (P<0.05; figure 5.11B). Inhibiting Dkk-1 using the small molecule compound (WAY-262611) at 1 μ M resulted in reduction of endothelial cell migration to levels found similar to that of control groups (Figure 5.13.A-B). In addition statistical analysis using two-way ANOVA of the number of migrated cells in the three groups have shown that there was a significant difference between Dkk-1 treated and control (P<0.05) and between Dkk-1 and WAY-262611 inhibited cells (P<0.05) while there were no significant differences between control and Dkk-1 inhibition (WAY-262611)(P>0.05).

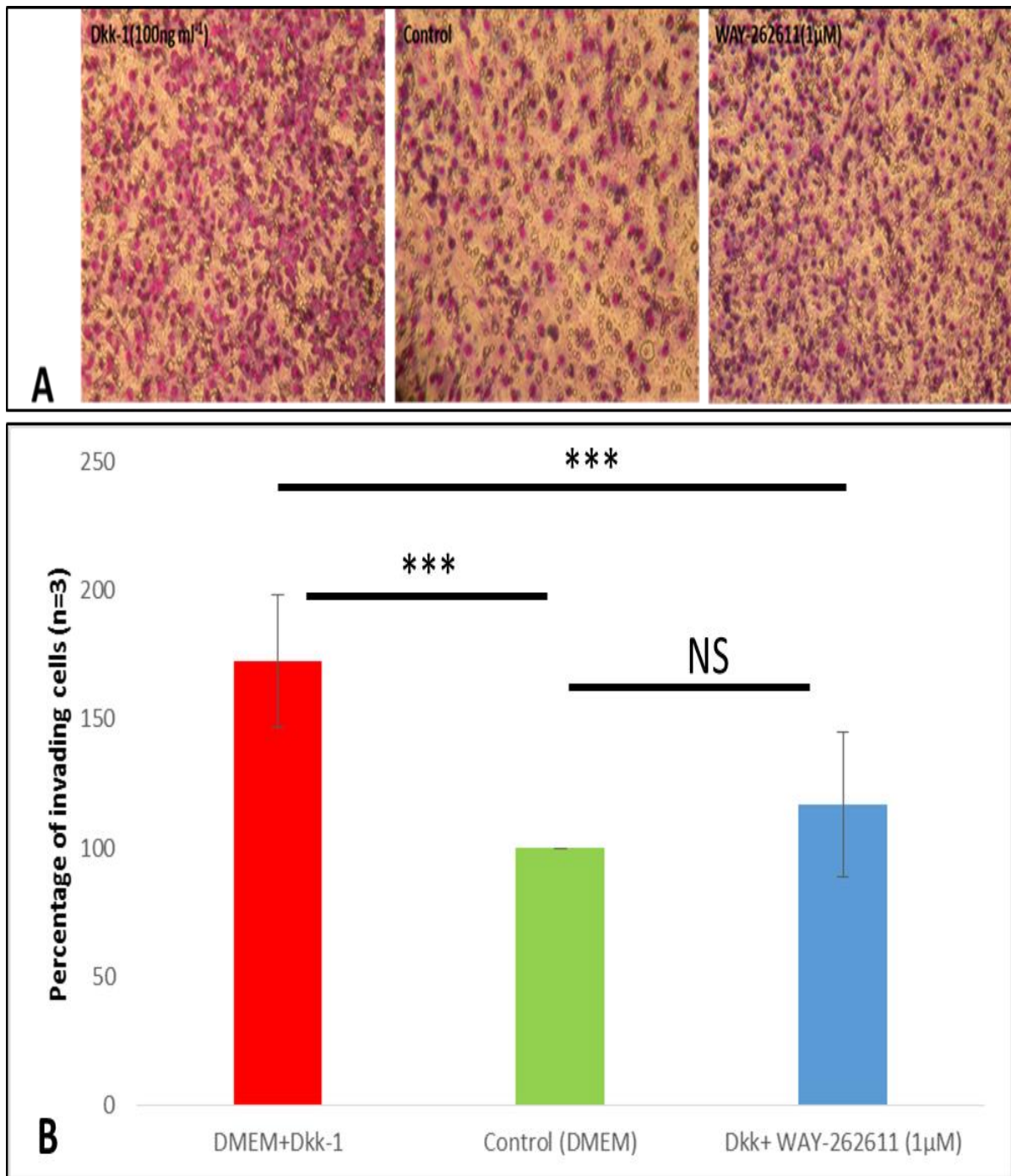


Figure 5.13: Transwell migration assay.

Figure A) Representative images of endothelial cells treated with Dkk-1 (100 ng/mL), WAY-262611, small molecule inhibitor of Dkk-1, at 1 μM and control (DMEM+PS+0.1% BSA). Transwell cell migration assay was performed for 24 hrs followed by fixing migrated cells and staining with Gimesa staining. B) Number of migrated cells as per treatment groups were counted using an inverted microscope (n=3 per group, data are presented as mean ± SEM, NS= not significant, ***P<0.01; 2-way ANOVA).

5.3.7 Cell cycle analysis of endothelial cells treated with Wnt proteins.

The cellular proliferation effect of canonical Wnt pathway modulators on endothelial cells was studied and determined by measuring the DNA content using the propidium iodide flow cytometry assay. Dkk-1 and Dkk-2 treated cells exhibited a shifting pattern of cells from a pre-mitotic phase (G0/G1) into more cells present in mitosis stage (G2/M) (Figure 5.14 and Table 5.1). Exposure of human endothelial cell lines to exogenous Dkk-1 and Dkk-2 (100 ng/mL) resulted in a significant decrease of cells in G0/G1 phase (73 ± 0.5 and 70.35 ± 0.22 respectively), and no alteration of cells in S phase, but doubling of cells in G2/M (9.9 ± 0.06 and 11.15 ± 0.58 respectively) compared with control (Table 5.1).

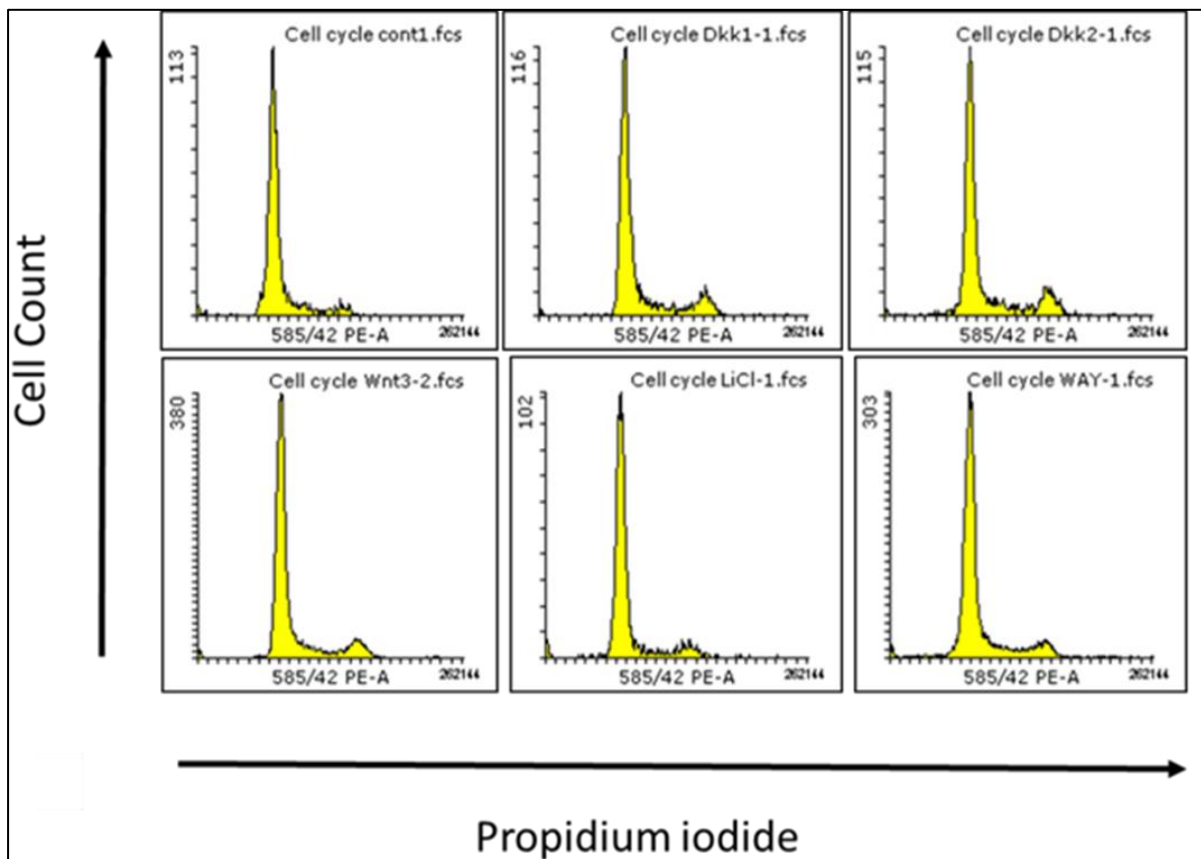


Figure 5. 14: Effect of different modulators of the canonical Wnt pathway on cell cycle profile of an endothelial cell line.

Endothelial cells were serum starved overnight before treating with basal media (control) +/- different Wnt modulators (Dkk-1, Dkk-2 and Wnt-3a, LiCl & WAY-262611) for 48hrs. Cell cycle profiles were determined by labelling cells with propidium iodide and data were attained using flow cytometry (n=3 per group).

Table 5. 1: Distribution of endothelial cells between cell cycle phases in control and treated groups.

Endothelial cells were incubated with basal media (control) +/- different Wnt modulators (Dkk-1, Dkk-2 and Wnt-3a, LiCl & WAY-262611) for 48hrs. Analysis of cell cycle distribution was performed using ethanol-fixed, RNase-treated and PI-stained cells by flow cytometry. The percentage of cells in G0/G1, S and G2/M cell cycle phases were analysed with the FACS Canto flow-cytometer. Data are presented as mean \pm SEM. (n=3 per group). ANOVA between endothelial cells of control and treated for each cell cycle phase are marked with *p<0.05. The experiment was repeated 3 times.

| Treatment | G0/G1 phase (%) | S phase (%) | G2/M phase (%) |
|------------------|------------------------|--------------------|-----------------------|
| control | 80.51 \pm 0.36 | 11.42 \pm 0.11 | 5.3 \pm 0.24 |
| Dkk-1 | 73.76 \pm 0.58* | 12.03 \pm 0.64 | 10.01 \pm 0.07* |
| Dkk2 | 70.35 \pm 0.22* | 13.94 \pm 0.27 | 11.1 \pm 0.58* |
| Wnt3a | 75.63 \pm 0.46* | 12.51 \pm 0.02 | 8.90 \pm 0.35* |
| LiCl | 80.70 \pm 0.32 | 8.86 \pm 0.19* | 7.13 \pm 0.19 |
| WAY | 74.68 \pm 0.43* | 12.7 \pm 0.09 | 8.02 \pm 0.13* |

5.4 Discussion.

The purpose of this study was to examine cellular changes occurring in the deeper zones of articular cartilage and particularly at the osteochondral interface. With this in mind, we used osteochondral plugs isolated from healthy tissues donated post-mortem and osteoarthritic tissues from patients undergoing total knee replacement. The first part of this study characterised infiltrating cellular phenotypes using markers for endothelial and mesenchymal stromal cells. In addition, the involvement of bone cells in particular osteoclast was also investigated using the TRAP assay.

This work suggests that changes affecting the subchondral bone marked by alteration in proteoglycan composition, loss of tidemark integrity and invasion of blood vessels from the subchondral bone is apparent even in early stages of the disease where there is little damage affecting the superficial zone of the articular cartilage. This observation needs to be further supported by increasing the sample number at each osteoarthritic histological stage before a definitive hypothesis can be deduced. However, this finding is interesting as it is increasingly becoming more evident than in osteoarthritis, changes in the underlying bone including microfracture which are thought to occur due to abnormal joint loading, might supersede that of articular cartilage (Radin *et al.* 1970; Radin and Rose 1986; Quasnichka *et al.* 2006; Zamli *et al.* 2014).

Vascularisation of articular cartilage is thought to be through a series of blood vessel migration and channel extension from subchondral bone into the non-calcified layers of articular cartilage. Under a normal situation articular cartilage is hostile to vascular invasion, in part due to its matrix composition (Walsh *et al.*, 2007; Hsieh *et al.*,

2010). Beyond the contributions of specific cell type to blood vessels angiogenesis, loss of cartilage matrix in particular loss of cartilage proteoglycans during osteoarthritis is thought to be implicated in cartilage's increased susceptibility to attack from the subchondral bone (Hsieh *et al.*, 2010; Bara *et al.*, 2012). It can also influence vascular recruitment at early stages of OA and to drive disease progression at later stages. Indeed, in this report there was a positive association of the loss of proteoglycan content in articular cartilage investigated by Safranin-O staining seen in tissue sections and the number of cellular infiltrates from the subchondral bone (Bara *et al.*, 2012).

Migratory subchondral cells are thought to exploit their environment by releasing cytokines and growth factors to activate normal, quiescent cells around them and initiate a cascade of events that quickly becomes dysregulated.

Immunohistochemical studies of osteochondral tissue from OA donors suggest the multicellular origin of these migratory subchondral cells marked by CD-34 positive invading endothelial cell and CD-105 and CD-166 positive mesenchymal stem cell infiltration. The precise steps involved in the angiogenesis of articular cartilage is not clearly understood, however, results in this study also suggest that the expression of putative MSCs markers, CD-105 and CD-166 recognised is altered in osteoarthritis as there was noted to be loss of expression in mature human articular cartilage of advanced stage of OA and it's re-expression around invading mesenchymal stem cells from underlying bone (Alsalameh *et al.*; 2004, Koelling *et al.*, 2009; Pretzel *et al.*, 2011). It has been postulated that the association of vascular endothelial cells with bone-marrow MSCs supports blood vessel migration by secreting pro-

angiogenic and pro-migratory proteins all enhancing further vascular invasion of articular cartilage (Walsh *et al.*, 2007).

The concept of bone-marrow mesenchymal stem cell migration into articular cartilage in late-stage osteoarthritic has been described by Koelling *et al.* (2009). It was postulated that MSCs migration into articular cartilage might be in response to stimulatory factors by articular cartilage encouraging cellular infiltration from underlying subchondral bone. This suggests that the joint might be attempting to undergo some form of reparative process (Koelling *et al.*, 2009). Interestingly, a differential expression of CD-166 was found between normal and osteoarthritic osteochondral tissues. There was an increase in CD-105 and CD-166 around fibrillated superficial zone chondrocytes and at the osteochondral interface. However, the success of migratory MSCs in replacing damaged chondrocytes is unclear.

By examining the association of bone cells particularly osteoclast with endothelial cells at the osteochondral interface, the results showed that osteoclasts play a role in altering articular cartilage integrity. In normal osteochondral tissues, there was no evidence of TRAP positive cells approaching the tidemark of the osteochondral interface. TRAP positive cells appeared to be mainly found in osteoarthritic tissues. Furthermore, there seemed to be a strong association between endothelial cells, bone marrow mesenchymal stem cells and osteoclast cells in an interesting manner where endothelial cells act like a 'Trojan horse' by invading articular cartilage eventually leading to cartilage loss (Bruni-Cardoso *et al.*, 2010). These findings helps one to understand the complex and intricate relationship between different cell types

found in the subchondral bone in osteoarthritis (Cackowski *et al.*, 2010; Stacker *et al.*, 2014)

Findings in OA osteochondral tissue for Dkk-1 and CD-34 immuno-labelling have suggested an increased expression around blood vessels of late-stage osteoarthritis. Unlike normal angiogenesis of skeletal tissues where blood vessel formation ceases to occur once pro-angiogenic stimuli is discontinued, in osteoarthritis it is thought that driving forces that stimulate angiogenesis seem not to stop as newly formed blood vessels are thought to be constantly exposed to stimulatory pro-angiogenic signals ultimately leading to cartilage disruption (Bonnet and Walsh, 2005; Walsh *et al.*, 2007; Ashraf *et al.*, 2011).

The mechanisms by which endothelial cells are activated in osteoarthritis is poorly understood and was an aim of this chapter. In this study, the focus was on the role of the canonical Wnt signalling pathway, and in particular, the role Dkk-1 plays in angiogenesis and migration of endothelial cells. *In vitro* angiogenesis assay studying the biological role of Dkk-1 as well as the role Dkk-2 have shown that both Dickkopf proteins to be pro-angiogenic. This finding is in agreement with recently published work by Smajda *et al.* (2010) and Weng *et al.* (2012) both showing that Dkk-1 had a pro-angiogenic role in both endothelial progenitor cells and umbilical cord endothelial cells.

In addition, the pro-angiogenic role of Dkk-2 seen in this study is also supported by a study by Min *et al.* (2011) using both *in vitro* Matrigel plug assay as well as *in vivo* corneal angiogenesis assay. Interestingly, both this study and another study (Oh *et al.*, 2010b) reported conflicting findings to ours and others (Weng *et al.*, 2012,

Smadja *et al.*, 2010; Reis *et al.*, 2012) where it was shown that Dkk-1 had an opposite effect of being anti-angiogenic.

The dichotomous role of Dkk-1 in modulating angiogenesis is intriguing. By looking at the study of Min *et al.* (2010), addition of Dkk-1 recombinant proteins was noted to be higher than that of ours and indeed Weng *et al.* (2012) and Smajda *et al.* (2010). One possible explanation to this discrepancy in the angiogenic role of Dkk-1 could be attributed to whether the levels of Dkk-1 are high enough to inhibit total β -catenin that is crucial for cell viability. Whereas some studies show that Dkk-1 expression is elevated in osteoarthritis has led to tissue destruction (Diarra *et al.*, 2007; Weng *et al.*, 2010), others show that it has a protective role against advancement of osteoarthritis (Lane *et al.*, 2007, Oh *et al.*, 2012a). In addition, its angiogenic role is also debated in recent studies whereas some studies document Dkk-1 is an anti-angiogenic factor (Oh *et al.*, 2012b; Min *et al.*, 2011) others show that Dkk-1 plays a crucial pro-angiogenic role. This demonstrate that the role of Dkk-1 might be highly contextual and more studies are required before the definitive role of Dkk-1 can be decided. However, this PhD study has shown that Dkk-1 might play a detrimental role in osteoarthritis by modulating angiogenesis in articular cartilage. In addition, Dkk-1 in part, also plays a key role in endothelial cells migration. However, the process at which Dkk-1 promotes endothelial cell migration is not fully understood and would be the aim of the next chapter.

In addition, Dkk-1 also resulted in promoting endothelial cells to undergo proliferation by increasing cells entry into mitosis and G2 phase of cell cycle. Endothelial cell proliferation and migration is essential for successful angiogenesis and inhibition of Dkk-1 using the small molecule (WAY-262611) resulted in the

reduction of cell migration. Cell migration is principally governed by a chemo-attractant encouraging a cells movement in a defined gradient (Raggatt *et al.*, 2006). However, despite this modest shifting in cell cycle state of endothelial cells exposed to exogenous Dkk-1, there were no discernible differences in the proliferative state of Dkk-1 on endothelial cells when compared to control which suggest that cell proliferation is not the main cause of the enhanced angiogenesis and migration of Dkk-1 treated endothelial cells.

In summary, this chapter suggest that the expression of Dkk-1 protein is enhanced around subchondral blood vessels invading articular cartilage of osteoarthritic osteochondral tissues. In addition, vascular channels extending from the subchondral bone were often associated with multicellular infiltrates of MSCs and bone osteoclast cells. By studying the role Dkk-1 plays in endothelial cells using a series of *in vitro* assays, it was clear that Dkk-1 had a pro-angiogenic and pro-migratory role in endothelial cells. Whether this conclusion can be considered to be the case in osteoarthritis is to be seen. However, this finding could provide an initial understanding of possible mechanisms involving the Wnt pathway in osteoarthritic angiogenesis. Understanding these alterations at the osteochondral junction and regulating pathways implicated in their initial occurrence will lead to a greater knowledge of the pathophysiology of osteoarthritis.

CHAPTER 6: AN *IN VITRO* MODEL TO STUDY THE INTERACTION OF CHONDROCYTES AND ENDOTHELIAL CELLS.

6.1 Introduction.

The synovial joint is composed of a variety of cell types and tissues. Some have direct contact with each other, such as the calcified cartilage and subchondral bone and other areas have indirect contact such as the articular cartilage and synovial membrane. Due to this alignment, changes which affect one location would inevitably have an influence on the synovial joint as a whole.

Classical features of OA are the presence of foreign cells in the articular cartilage that include blood vessels and stromal cells. This results in the disruption of the homogenous cellular structure found mainly in articular cartilage. Little is known about what drives subchondral cellular and specifically endothelial cells to migrate towards articular cartilage. It is postulated that pathological changes that occur at the superficial zone might encourage these cellular infiltrations by exposing the underlying subchondral cells to migratory factors found in the synovial joint space.

During osteoarthritis, the superficial region of articular cartilage is thought to be exposed to excessive biomechanical factors leading to surface zone fibrillation. In addition, alteration to biomechanical properties of injured tissue results in the development of longitudinal fissures. These fissures extend from the surface zone to the underlying subchondral bone. Its development leads to the exposure of the subchondral bone to cytokines and growth factors that are normally found in the synovial space. This might encourage cellular proliferation and migration from subchondral bone. It is therefore reasonable to hypothesise that alterations in the

synovial joint micro environment stimulates subchondral cellular migration including vascular and endothelial progenitor cells.

A major difficulty in understanding the pathological changes at the synovial joint is the lack of earlier warning signs from the articular cartilage due to its avascular properties. Therefore, for the vast majority of cases diagnosed with osteoarthritis, diagnosis is usually at the late-stage where the underlying subchondral bone is affected.

It is not clear what stimulates endothelial cells to migrate towards articular cartilage. Under normal physiological circumstances, endothelial cells appear to be quiescent (Deanfield *et al.* 2007). With the exception of repairing lost or damaged vessels, endothelial cells resume a state of dormancy for the most part of adult life (Bergers and Benjamin 2003). Therefore, the mechanisms responsible for the abnormal endothelial activity leading to their propagation and invasion remains elusive and needs to be investigated. It is therefore crucial to understand what activates endothelial cells in osteoarthritis and ultimately encourages vessel invasion of articular cartilage.

There is an absence of well-established models system to study the dynamic interactions between articular cartilage chondrocytes and endothelial cells. We therefore designed an indirect Transwell co-culture system that allowed the study of the impact of chondrocytes on endothelial cells. This study also would address if co-culturing endothelial cells with chondrocytes leads to an endothelial to mesenchymal transformation (EnMT) phenotype formation in the latter cell type.

6.2 Experimental Methods.

Due to lack of a defined model to study the dynamic interaction that occur at the osteochondral interface between chondrocytes and endothelial cells, this study utilised the Transwell co-culture model system. This system assessed the paracrine effect of chondrocytes on primary endothelial cells from umbilical vein (EC) for a seven day duration. In addition, the transformative effect of co-culturing endothelial cells with normal as well as osteoarthritic chondrocytes were examined using confocal immunofluorescence for a series of proteins implicated in EnMT and further validated using Western blot.

To further investigate the transformative effect that co-culturing chondrocytes had on endothelial cells, by promoting mesenchymal transition, total protein was isolated from control and both, normal and osteoarthritic, chondrocytes. Subsequently, this was subjected to a proteome profiler array that analysed the expressional patterns of 84 different proteins implicated in EnMT from those isolated proteins (See section 2.6).

In addition, conditioned media from normal and osteoarthritic chondrocytes (n=3 donors per group) were collected and centrifuged for 5minutes at 400 x g to remove debris and dead cells before filtering the collected media using 0.2µm filter. Endothelial cells were grown in chamber slides overnight to allow adherence before culturing cells in chondrocyte conditioned media or basal media for seven days. The media was changed three times a week and replaced with a conditioned media and fresh basal media at 1:1 ratio. In order to examine the role of Dkk-1 on EnMT, endothelial cells were treated with recombinant Dkk-1 (100 ng/mL) for seven days

and mRNA levels of a list of genes implicated in EnMT were examined using q-PCR (see section 2.12.5).

Finally, normal and osteoarthritic derived osteochondral tissues were examined to assess the expression of EnMT using immunohistochemical staining (see section 2.8.1 and 2.8.2). In addition, co-localisation experiments for MMP-13, CD-34 were carried out using osteoarthritic osteochondral tissue to assess for cellular and vascular infiltration at the osteochondral interface (see section 2.8.1).

6.3 Results:

6.3.1. Characterisation of chondrocytes and endothelial cells.

The primary articular cartilage chondrocytes formed a spindle-fibroblast-like morphology, when cultured in *in vitro* setting (Figure 6.1.F). Endothelial cells, on the other hand, assumed a cobblestone morphology when examined using a phase-contrast microscope (Figure 6.1.I). Prior to initiating the experiment, we characterised chondrocytes and endothelial cells using markers known to be expressed in the two cell groups. Immunofluorescence analysis showed that chondrocytes stained positively for integrin (CD-29), hyaluronan (CD-44), Stro-1, Notch-1 and CD-166 (Figure 6.1. A-E). Whilst the endothelial cells, showed positive expression for VE-cadherin (Figure 6.1. G) and Pecam-1 (Figure 6.1. H).

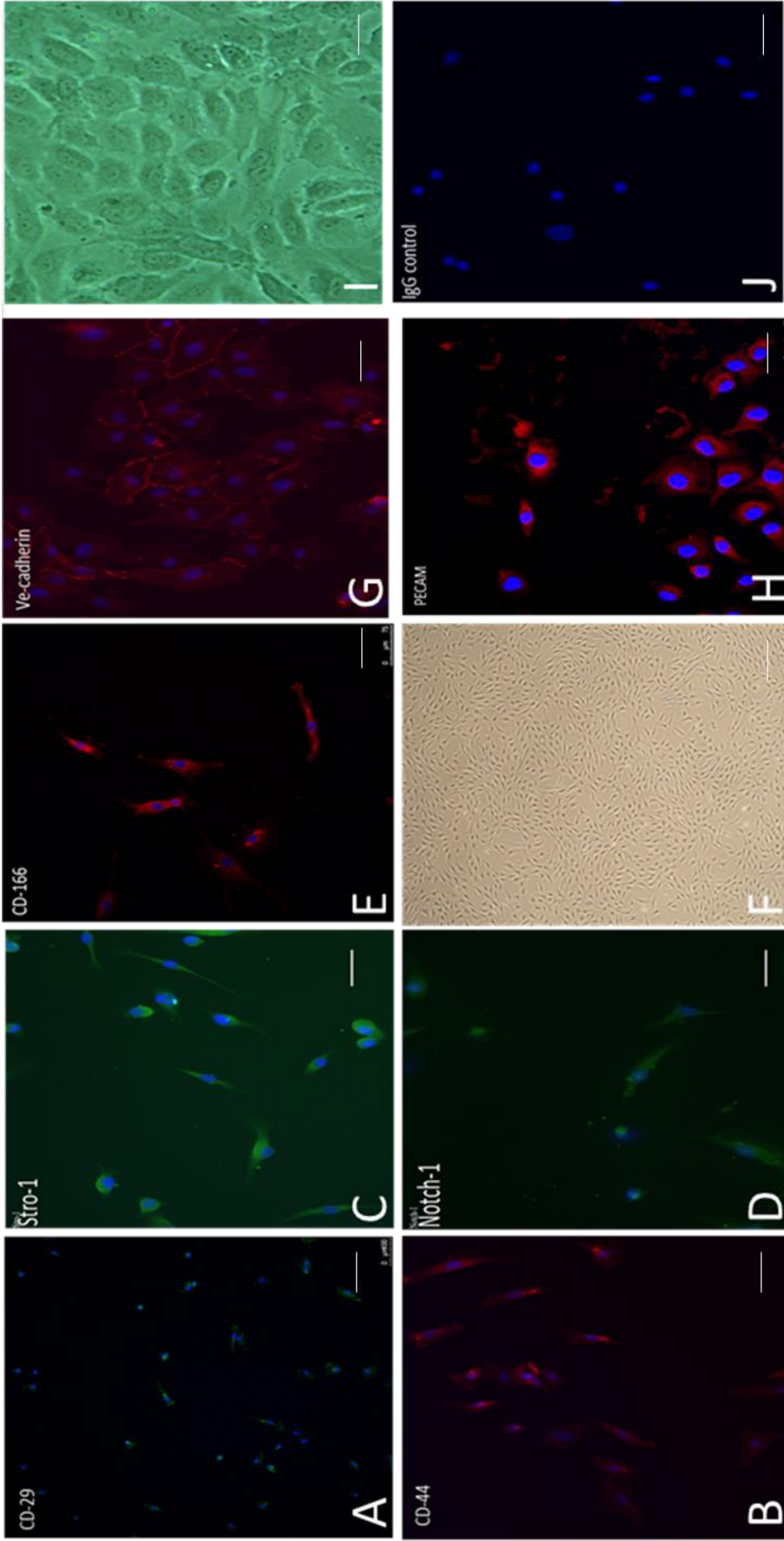


Figure 6. 1: Morphological characterization of primary human umbilical vein-derived endothelial cells (EC) and primary chondrocytes isolated from knee joint of normal donors.

Phase contrast image of chondrocytes (F) and endothelial cells (I) at passage 3. Characterization of primary endothelial cells (HUVEC) and primary chondrocytes including immunofluorescence microscopy of chondrocyte markers (CD-29, CD-44, Stro-1, Notch1 and CD-166, image A-E respectively) and endothelial markers (Pecam-1/CD-31, VE-cadherin, image G&H respectively). Nuclei are counterstained with DAPI. Scale bar=100µm.

6.3.2. Primary endothelial and chondrocytes co-culture promotes EnMT.

Chondrocytes from normal and osteoarthritic donors were seeded on the top compartment in the experimental group while at the bottom compartment of the Transwell insert endothelial cells were seeded (Figure 6.2.A). In the control group, endothelial cells were seeded in both compartments. By day five, normal co-cultured chondrocytes, isolated from the knee joint, with endothelial cells, resulted in the endothelial cells losing their closely backed cell-cell junctions and resulted in the formation of spindle shaped cells embedded in the rest of the endothelial cells. This had no effect on their viability (see Appendix 3 for Annexin-V/7-AAD viability assay). By day seven, the majority of endothelial cells lost their cobblestone morphology, marked by a complete loss of cell-cell contacts, and the adoption of a spindle-shaped morphology similar to that observed for mesenchymal cells (Figure 6.2. B II, IV).

In order to explore if endothelial cells had undergone EnMT phenotype, the protein expression of key endothelial and mesenchymal markers were examined using immunoblotting and immunofluorescence microscopy. The control group was found to express VE-cadherin at the junction between adjacent endothelial cells (white arrows; Figure 6.3.C). Interestingly, endothelial cells co-cultured with normal as well as osteoarthritic chondrocytes clearly started to lose expression of the endothelial marker VE-cadherin (Figure 6.3. A, E, I). Reduction of VE-cadherin was more pronounced in endothelial cells co-cultured with osteoarthritic chondrocytes (Figure 6.3.I). In endothelial cells co-cultured with normal chondrocytes there was a significant shift in VE-cadherin expression from the cell membrane into a nuclear location (white arrows; Figure 6.3.E).

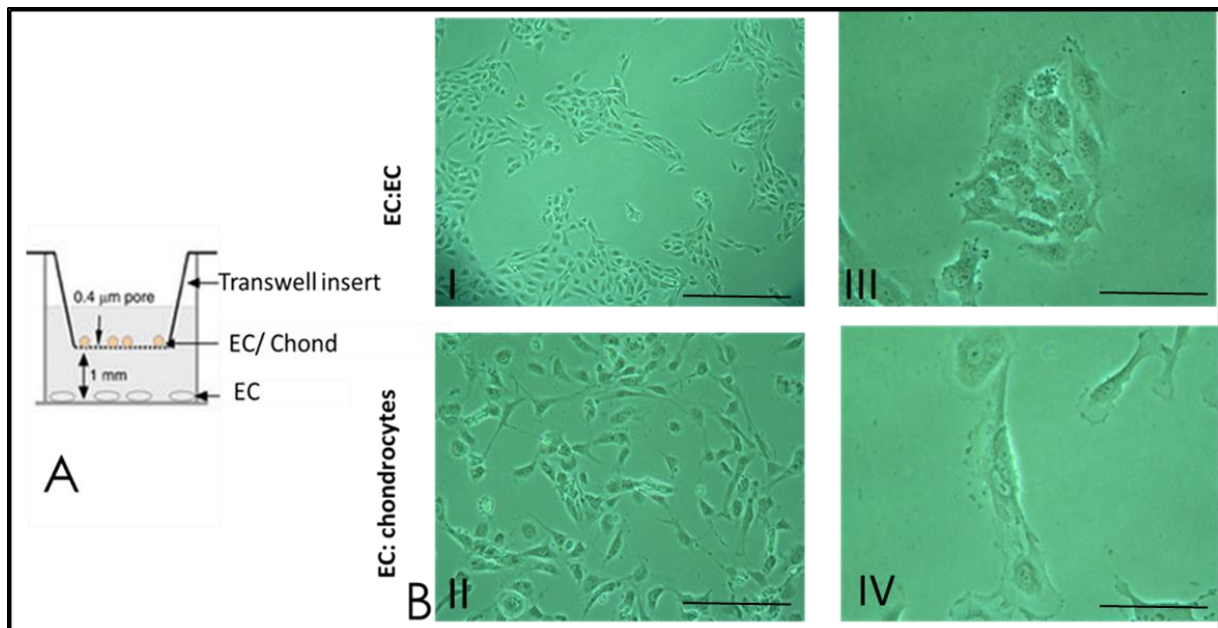


Figure 6. 2: Morphological changes in endothelial cells following co-culture with chondrocytes.

Primary endothelial cells (EC) were either mono-cultured with EC serving as control or with primary normal and osteoarthritic chondrocytes cells (Chon) using Transwell co-culture assay for 7days (Panel A). Panel B shows the morphological changes in control (I and III) or co-culture group were evaluated using an inverted microscope 96hrs after incubation under 100x magnification (II, IV). In Transwell co-culture setting, EC: Chon induced spindle-like morphological changes while EC: EC mono-culture showed classical endothelial cobblestone morphology. Scale bar for panel B images I and II=100μm and images III and IV =500μm.

Subsequently, the expression of β -catenin, which forms a cell-cell junction protein complex with VE-cadherin, was examined. The control group was found to express β -catenin at the cell surface as well as in the cytoplasm hence showing two locations of β -catenin accumulation in the cell (Figure 6.3.C). Interestingly, as the cell-cell junction was disrupted and the cells lost their apical-basal polarity. β -catenin was found only in the nuclei of the endothelial cells that had been co-cultured with normal chondrocytes. More nuclear presence of β -catenin were observed in cells that adopted a front-rear polarity similar to that seen in mesenchymal stem cells in endothelial cells co-cultured with normal chondrocytes (white arrows ; Figure 6.3. G).This shifting patterns seen here with VE-cadherin and β -catenin from the cell-

junction to the cytoplasm and nuclear suggest that these factors play a transcriptional activity.

Examination of markers of mesenchymal morphology alpha-smooth muscle actin (α -SMA) showed that there was no expression of α -SMA in the control group (Figure 6.3. B). As endothelial cells lost their phenotype in the presence of chondrocytes, expression of α -SMA was evident in endothelial cells co-cultured with both normal chondrocytes (white arrows; Figure 6.3.F) as well as osteoarthritic chondrocytes (white arrows; Figure 6.3. J).

The process of EMT and EnMT is thought to result in the alteration of actin filaments as cells change their polarity. In this study, F-actin was investigated by staining the control group and the co-cultured endothelial cells with Phalloidin-conjugated-488. The control endothelial cells were found to lack any evidence of actin stress fibre formation.

In contrast the endothelial cells co-cultured with normal and osteoarthritic chondrocytes resulted in the induction of stress fibre formation (Figure 6.3. D, H, L). The presence of actin stress fibres were more prominent in endothelial cells co-cultured with osteoarthritic chondrocytes compared to normal chondrocytes (Figure 6.3. L).

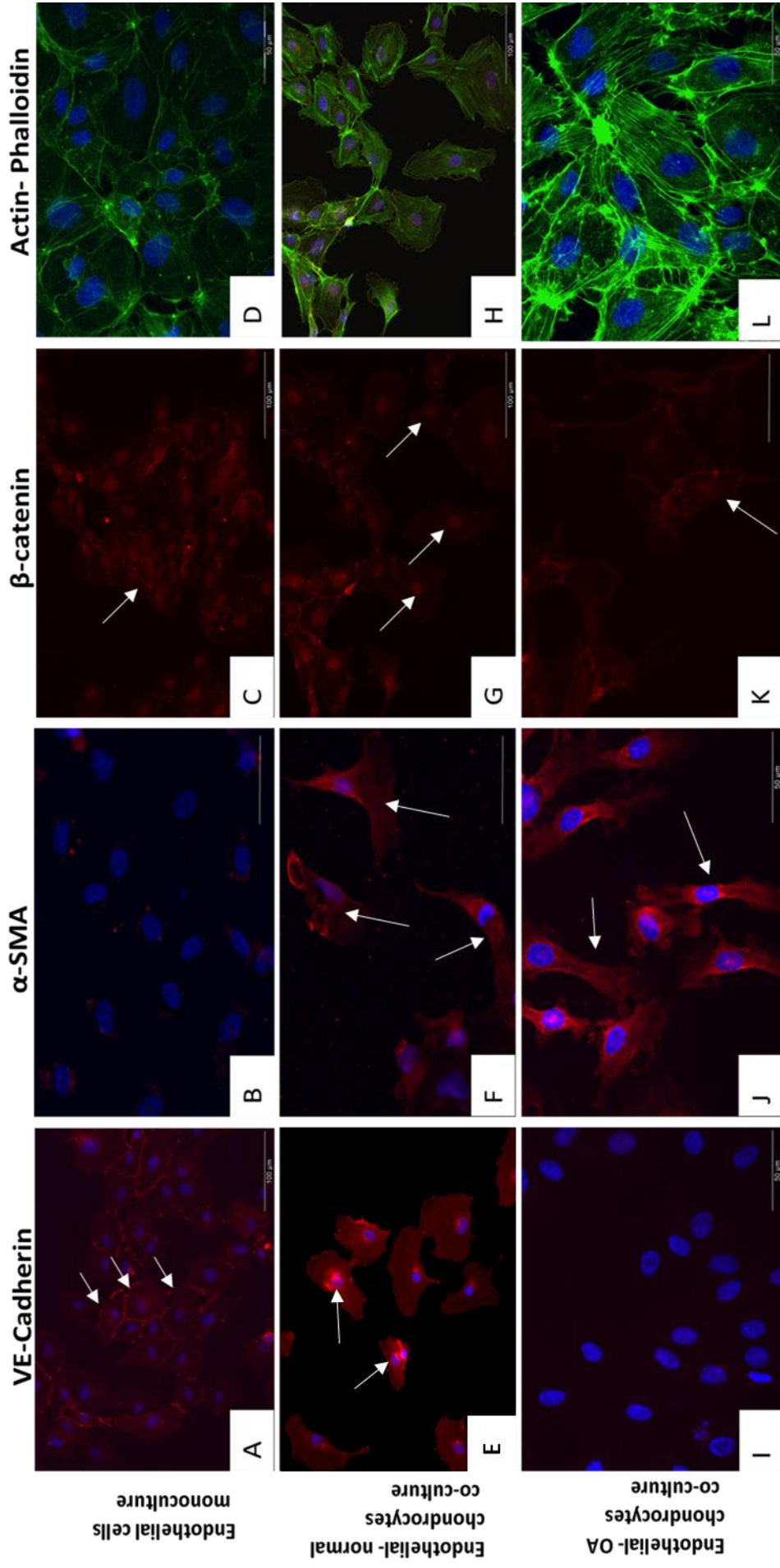


Figure 6. 3: Endothelial and chondrocytes co-culture induced EnMT in co-culture.

Expression of EnMT-related proteins was detected by immunofluorescence staining of the endothelial cells control (A-D) or co-cultured with normal chondrocytes (E-H) and osteoarthritic chondrocytes (I-L). VE-cadherin (A,E,I), α -SMA(B,F,J), β -catenin (C,G,J) and actin-Phalloidin (D,H,L). Nuclei are counterstained in blue using 4', 6-diamidino-2-phenylindole (DAPI). Scale bar=100 μ m.

Analysis of protein lysate from control group and endothelial co-cultured group confirmed a clear reduction of VE-cadherin in the co-culture group (Figure 6.4). In addition, control and experimental groups showed differences in the total β -catenin levels, where the expression showed some reduction in experimental groups more evident in endothelial cells co-cultured with normal chondrocytes. Furthermore, there was an associated increase in vimentin protein expression in endothelial cells co-cultured with osteoarthritic chondrocytes but the levels of vimentin in endothelial cells co-cultured with normal chondrocytes were comparable (Figure 6.4).

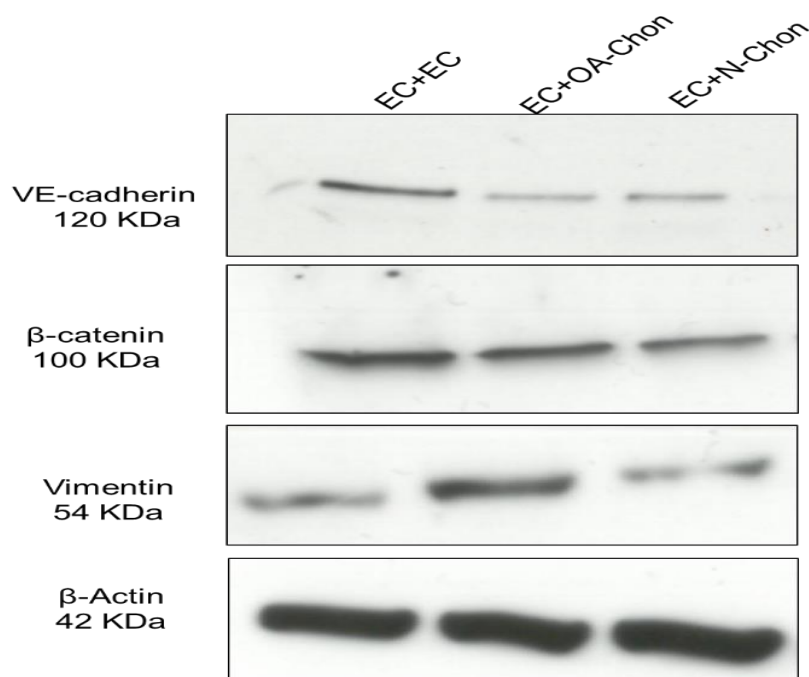


Figure 6. 4: Western blot analysis of EnMT markers in co-culture experiments.

Protein lysates from endothelial cells monoculture (EC+EC) serving as control and endothelial cells co-cultured with osteoarthritic derived chondrocytes (EC+OA-Chon) or normal chondrocytes (EC+N-Chon) were harvested using RIPA buffer and the protein expression of EnMT markers including VE-cadherin, β -catenin, vimentin were examined by Western blot analysis. B-actin protein expression served as loading control.

6.3.3. Chondrocytes conditioned media resulted in endothelial cell alteration.

Data from the previous section suggests that chondrocytes from normal and osteoarthritic subjects stimulated endothelial cells to undergo mesenchymal transformation under a co-culture setting. Hence one can speculate that chondrocytes had a transformative effect on endothelial cells in a paracrine manner. Cultivation of endothelial cells with conditioned media from normal chondrocytes as well as osteoarthritic chondrocytes, resulted in the endothelial cells displaying changes in morphology as marked by loss of apical-basal cell polarity and adoption of spindle-like morphology (Figure 6.5). In both endothelial cells, treated with normal and osteoarthritic conditioned media not all endothelial cells, when immunolabelled for the mesenchymal transformation marker, α -SMA, showed complete mesenchymal transformation (Figure 6.5).

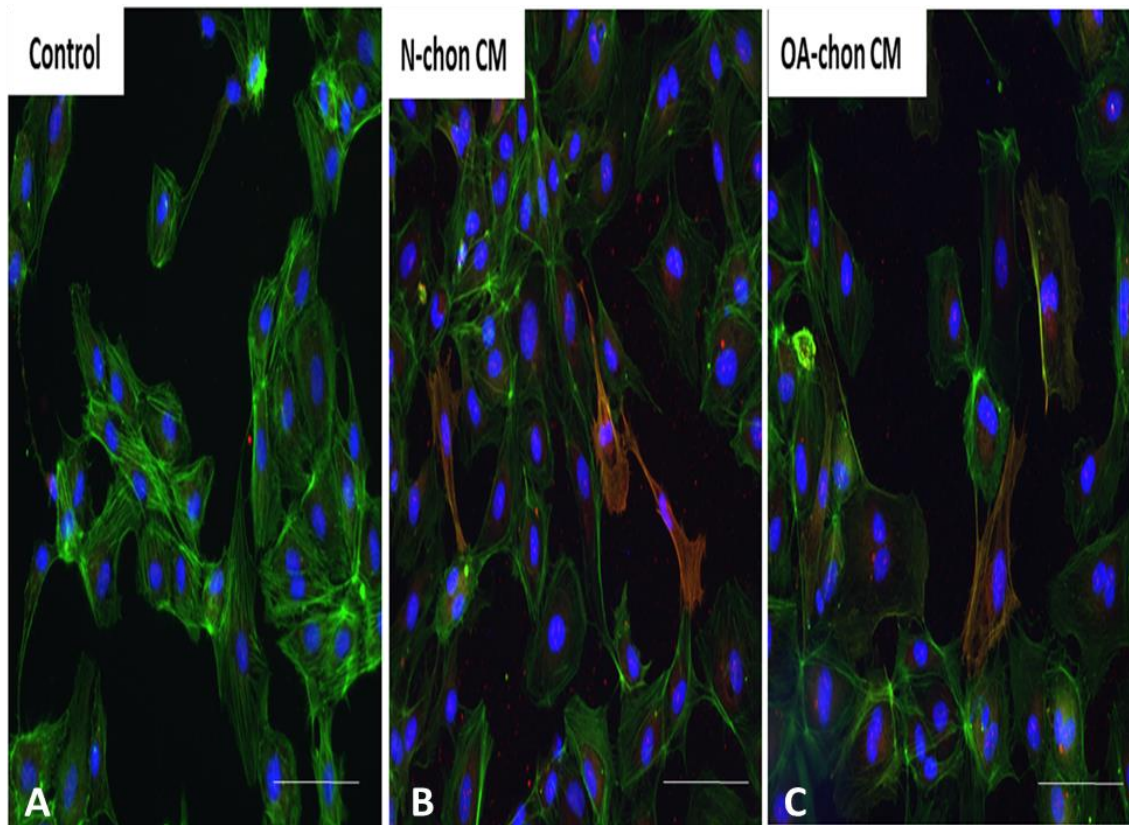


Figure 6. 5: Chondrocytes induced EnMT through secretory factors.

Endothelial cells were seeded in chamber slides and cultured with basal media (Control; A) or conditioned media from normal (N-Chon CM; B) and osteoarthritic chondrocytes conditioned media (OA-Chon CM; C) for 7 days. Fixed cells were immuno-labelled with α -SMA (red) and F-actin (green). Nuclei are counterstained with DAPI. Scale bar=100 μ m.

6.3.4. Proteomic profiling of EnMT.

Proteomic array study of endothelial cells co-cultured with normal chondrocytes showed significant down-regulation in several endothelial marker proteins including VE-cadherin (1.7 fold, $p=0.03$), Endoglin (3.5 fold, $p=0.04$), eNOS (2.6 fold, $p=0.05$), PDGF-AA (3.9 fold, $p=0.01$), Pecam-1 (4 fold, $p=0.001$) and Tie-2 (3.6 fold, $p=0.01$). Additional proteins that were observed to be down-regulated included CA-9 (1.17 fold, $p=0.03$) and Cathepsin B (2.0 fold, $p=0.03$). In contrast, proteins that were observed to be up-regulated in endothelial cells co-cultured with normal chondrocytes included Dkk-1 (1.5 fold, $p=0.3$), Lumican (2.1 fold, $p=0.03$), CCL-

2/MCP-1 (3.8 fold, $p=0.02$), MMP-9 (2.0 fold, $p=0.03$) and Snail (1.2 fold, $p=0.8$) (Figure 6.6).

On the Other hand, the protein profile of the endothelial cells co-cultured with osteoarthritic chondrocytes showed the down regulation of several endothelial marker proteins compared to the control. These proteins included VE-cadherin (4.3 fold, $p=0.03$), Endoglin (4.2 fold, $p=0.01$), eNOS (2.4 fold, $p=0.08$), PDGF-AA (2.8 fold, $p=0.003$), PECAM (4.9 fold, $p=0.001$) and Tie-2 (6.2 fold, $p=0.007$). Furthermore, proteins that were observed to be down-regulated included CA-9 (1.6 fold, $p=0.02$), Cathepsin B (1.5 fold, $p=0.01$). Meanwhile, proteins that were up-regulated in endothelial cells co-cultured with normal chondrocytes included Dkk-1 (4 fold, $p=0.01$), Lumican (5.5 fold, $p=0.03$), CCL-2/MCP-1 (4.6 fold, $p=0.01$), MMP-9 (1.9 fold, $p=0.01$), Snail (1.3 fold, $p=0.7$) and vimentin (6 fold, $p=0.002$).

The proteomic array study of endothelial cells co-cultured with chondrocytes showed that Dkk-1 was up-regulated in endothelial cells that had been co-cultured with osteoarthritic chondrocytes (Figure 6.6). This increase in Dkk-1 levels in co-culture group coincided with reduction of several endothelial markers (VE-cadherin, pecam-1, PDGFR and Tie-1). Furthermore, there was an increase in vimentin protein by 4 fold. These data indicate that chondrocytes had a transformative effect on endothelial cells by demoting several markers of endothelial cells and promoting markers of mesenchymal stem cells.

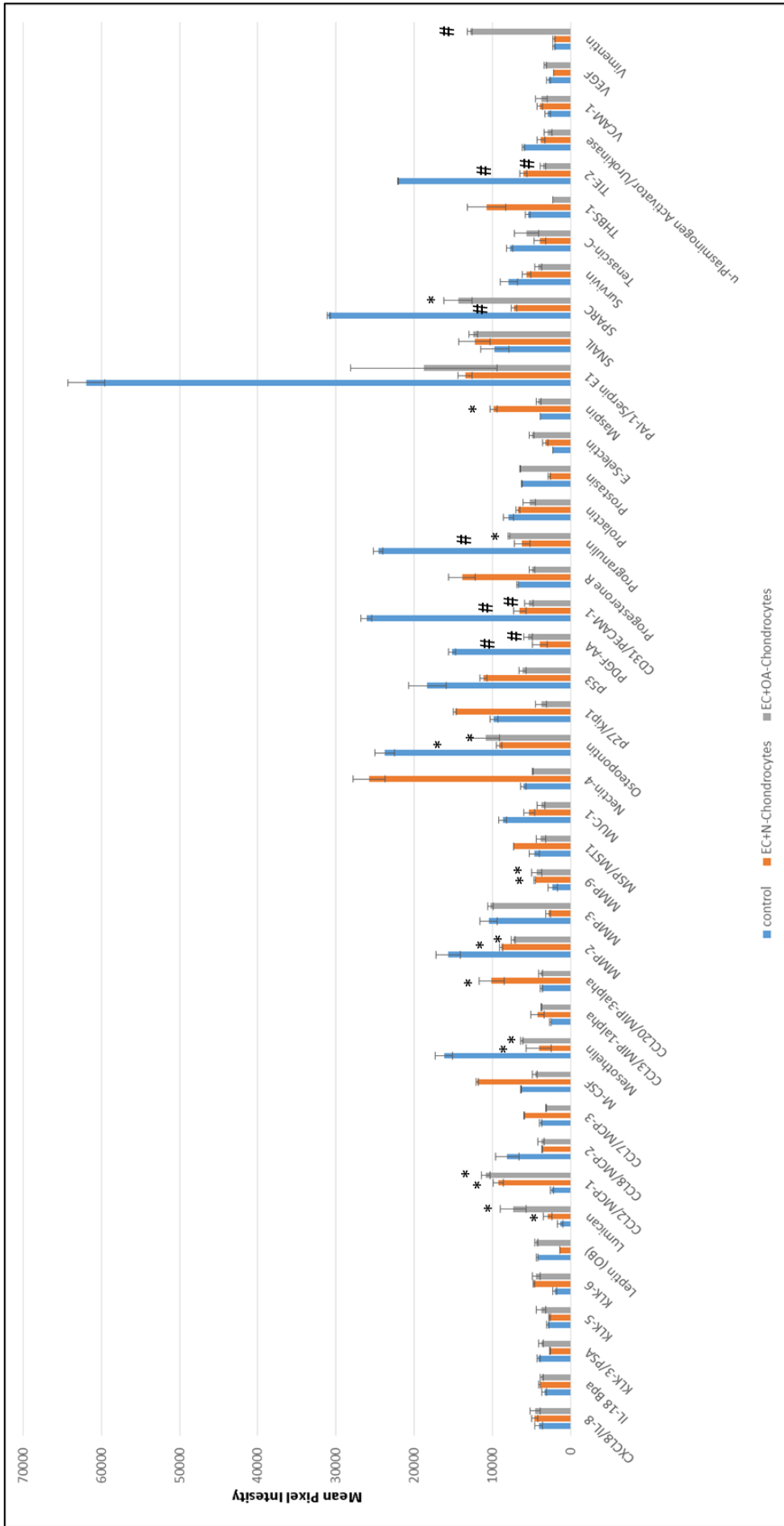


Figure 6. 6: Protein array profiler of endothelial to mesenchymal transition markers.

Relative expression of 84 different cancer related proteins including EnMT proteins were studied using Proteome Profiler Human XL Oncology Array (Bio-technique). Primary endothelial cells (EC) was either co-cultured with EC serving as control or with primary chondrocytes from normal (EC+N-Chon) and osteoarthritic donors (EC+OA-Chon) using Transwell co-culture assay for 7days. Protein lysates from the two experimental groups were collected and subjected to proteome Profiler Array as per manufacturer's protocol. Equal concentration of proteins were used in all experiments (50µg). All proteins were determined in duplicate and based on optical densitometry dot plot analysis using Image J protein Array profiler plugin. Fold change was expressed relative to control and data were analysed using paired t-test. #, $p < .001$, * $p < .005$.

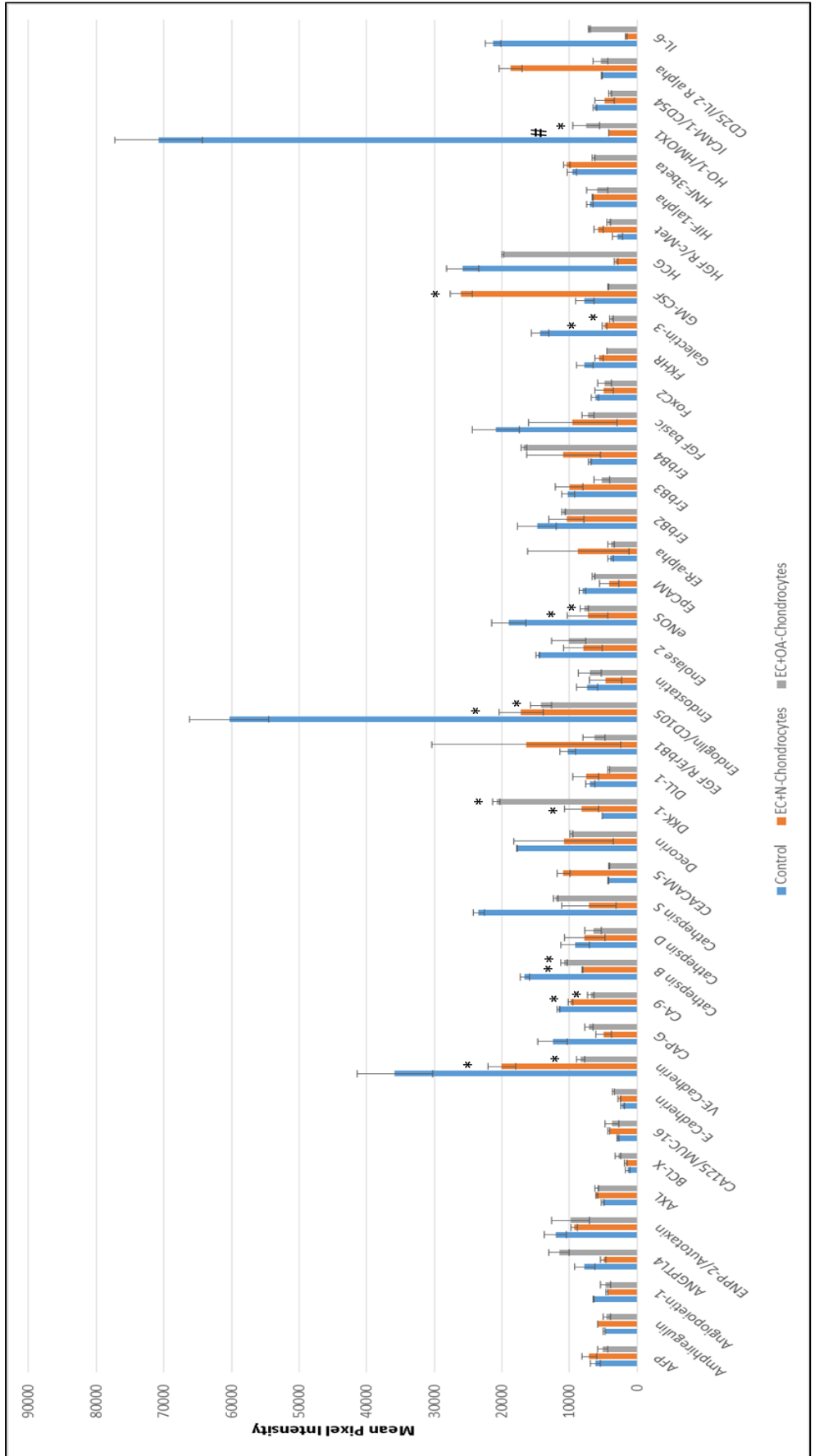


Figure 6. 6: Protein array profiler of endothelial to mesenchymal transition markers.

Relative expression of 84 different cancer related proteins including EnMT proteins were studied using Proteome Profiler Human XL Oncology Array (Bio-technie). Primary endothelial cells (EC) was either co-cultured with EC serving as control or with primary chondrocytes from normal (EC+N-Chon) and osteoarthritic donors (EC+OA-Chon) using Transwell co-culture assay for 7days. Protein lysates from the two experimental groups were collected and subjected to proteome Profiler Array as per manufacturer's protocol. Equal concentration of proteins were used in all experiments (50µg). All proteins were determined in duplicate and based on optical densitometry dot plot analysis using Image J protein Array profiler plugin. Fold change was expressed relative to control and data were analysed using paired t-test. #, p < .001, * p < .005.

6.3.5. Dkk-1 influence MMP-13 expression and other markers of the EnMT-like transition in endothelial cells.

Endothelial cells treated with Dkk-1 showed morphological alterations, changing from cobblestone to spindle like structures. Moreover, molecular analysis of endothelial and mesenchymal markers genes using RT-PCR showed that Dkk-1 treated endothelial cells, when compared to control, showed a marked reduction in the mRNA levels of VE-cadherin, PECAM-1 and VEGF-A and up-regulation of α -SMA and MMP-13. Interestingly, no effect on the mRNA levels of Hif-1 α (Figure 6.7) was observed.

In previous chapters, Dkk-1 expression was generally localised around vascular and stromal tissues invading articular cartilage. Therefore, the expression of MMP-13 around vascular invasions from the subchondral bone was investigated using immunohistochemical staining. Interestingly, expression of MMP-13 and Dkk-1 and CD-34 were co-immunostained in the deep zone of osteoarthritic cartilage and subchondral bone. The expression of CD-34 was mainly localised to the cell surface of endothelial cells invading articular cartilage (Figure 6.8. H&K) while MMP-13 was confined to the periphery especially at the leading edge (Figure 6.8. A, D, G & J). The expression of Dkk-1 on the other hand was predominantly extracellular and intensely expressed around cellular and invading vascular tissues and some locations were superimposed in some locations with that of MMP-13 and in other invading vasculature adjacent to it (Figure 6.8. A&D).

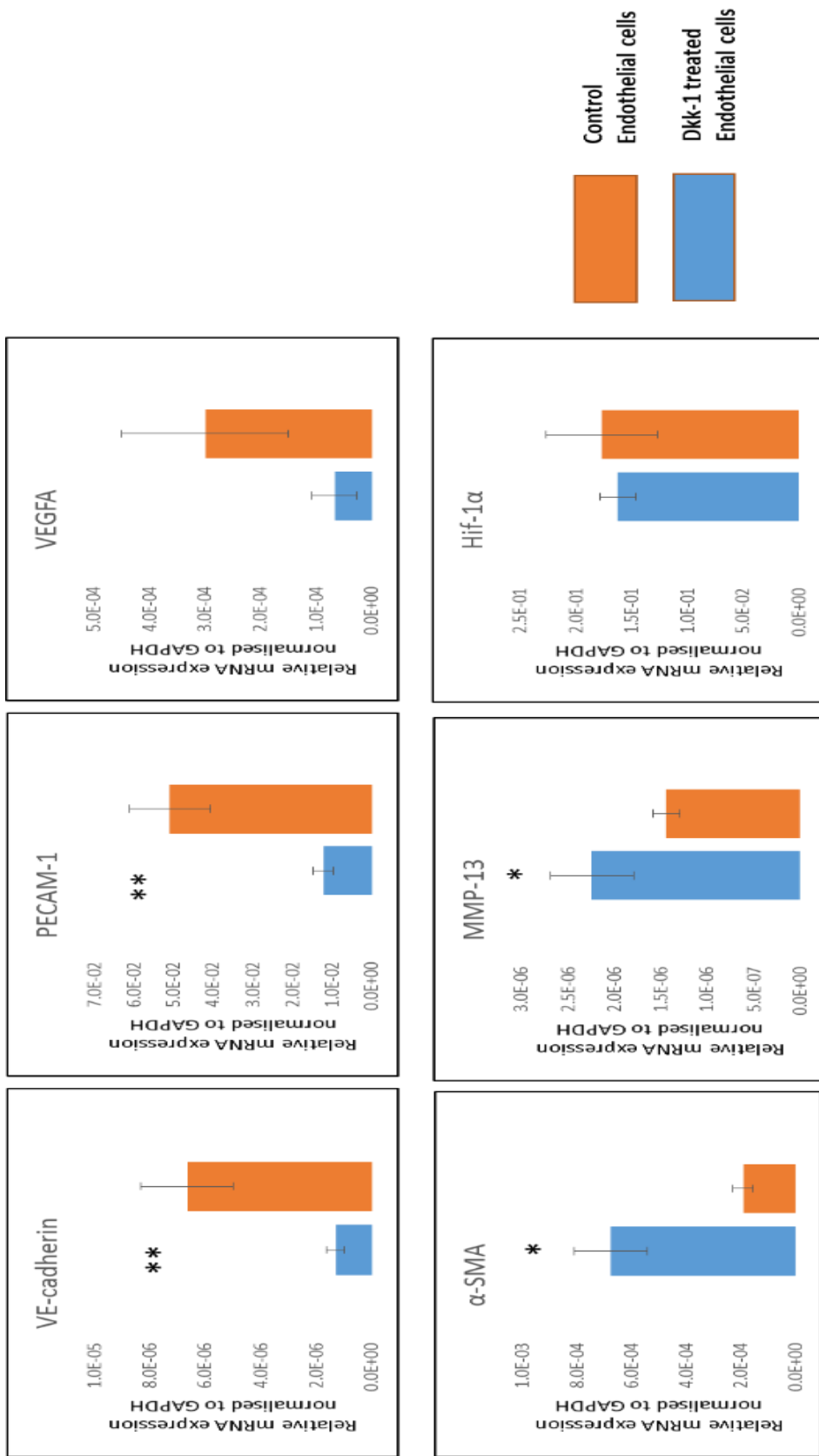


Figure 6. 7: Effects of Dkk-1 on endothelial cell phenotype.

Human endothelial cells (HUVEC) were starved for 8hrs, followed by incubation in basal media (control) or with Dkk-1 (100ng ml⁻¹) for 7 days. mRNA expression of VE-cadherin, Pecam-1 and VEGFA were studied using RT-PCR. (n = 3 per group, data was normalised to GAPDH, *P<0.05, **P<0.01).

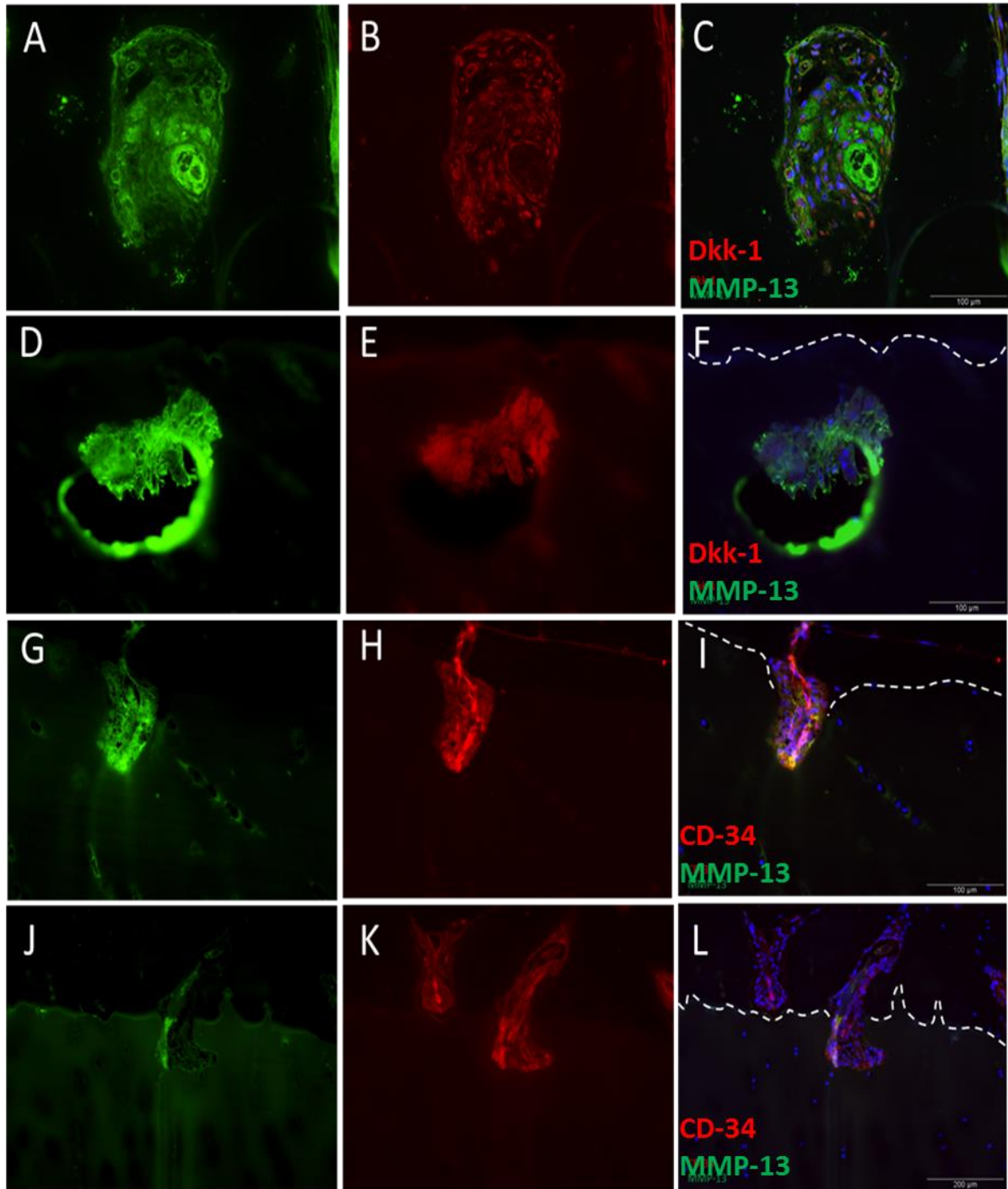


Figure 6.8: MMP-13, Dkk-1 and CD-34 co-localisation in invading OA-osteochondral interface tissues.

Double immuno-labelling of Dkk-1 and MMP-13 (panel A-F) and CD-34 and MMP-13 (panel G-L) in invading vascular tissues found at the interface of the osteochondral region. Expression of CD-34 reveals highly vascularized area at the osteochondral interface of osteoarthritic tissues. Double-immunofluorescence-labelling of Dkk-1 (red) and MMP-13 (green) and CD-34 (red) in the same area shows strong co-localisation expression of these proteins close to the tidemark and often breaching it (dashed line). Nuclei are counterstained with DAPI. Scale bar embedded in the image.

6.3.6 Endothelial to mesenchymal transitions in human osteochondral tissues.

6.3.6.1. Expression of Aggrecan.

Aggrecan is a proteoglycan found in abundance in articular cartilage. It is usually associated with providing anchorage of the cell to the surrounding pericellular matrix. In healthy articular cartilage, aggrecan immunostaining was found throughout the cartilage tissue surrounding the pericellular regions of the ECM (Figure 6.9. A-D). Furthermore, there were occasional aggrecan expression in the extracellular region of superficial zone articular cartilage. However in osteoarthritic osteochondral tissues, aggrecan showed a different pattern of expression compared to healthy cartilage. In osteoarthritis, osteochondral tissue labelled for aggrecan showed a marked reduction in the overall proteoglycan staining with a noted reduction in extracellular aggrecan in all regions of articular cartilage (Figure 6.9. E). In addition, with this generalised reduction in aggrecan, a shift of intense cytoplasmic staining was observed in severe osteoarthritis in chondrocytes of the surface and middle zone (Figure 6.9. F). Furthermore, the subchondral region and deep zone of articular cartilage showed vascular and stromal invasion highly expressing aggrecan especially around the peripheries of the invading stromal and vascular tissues (Figure 6.9. G-I).

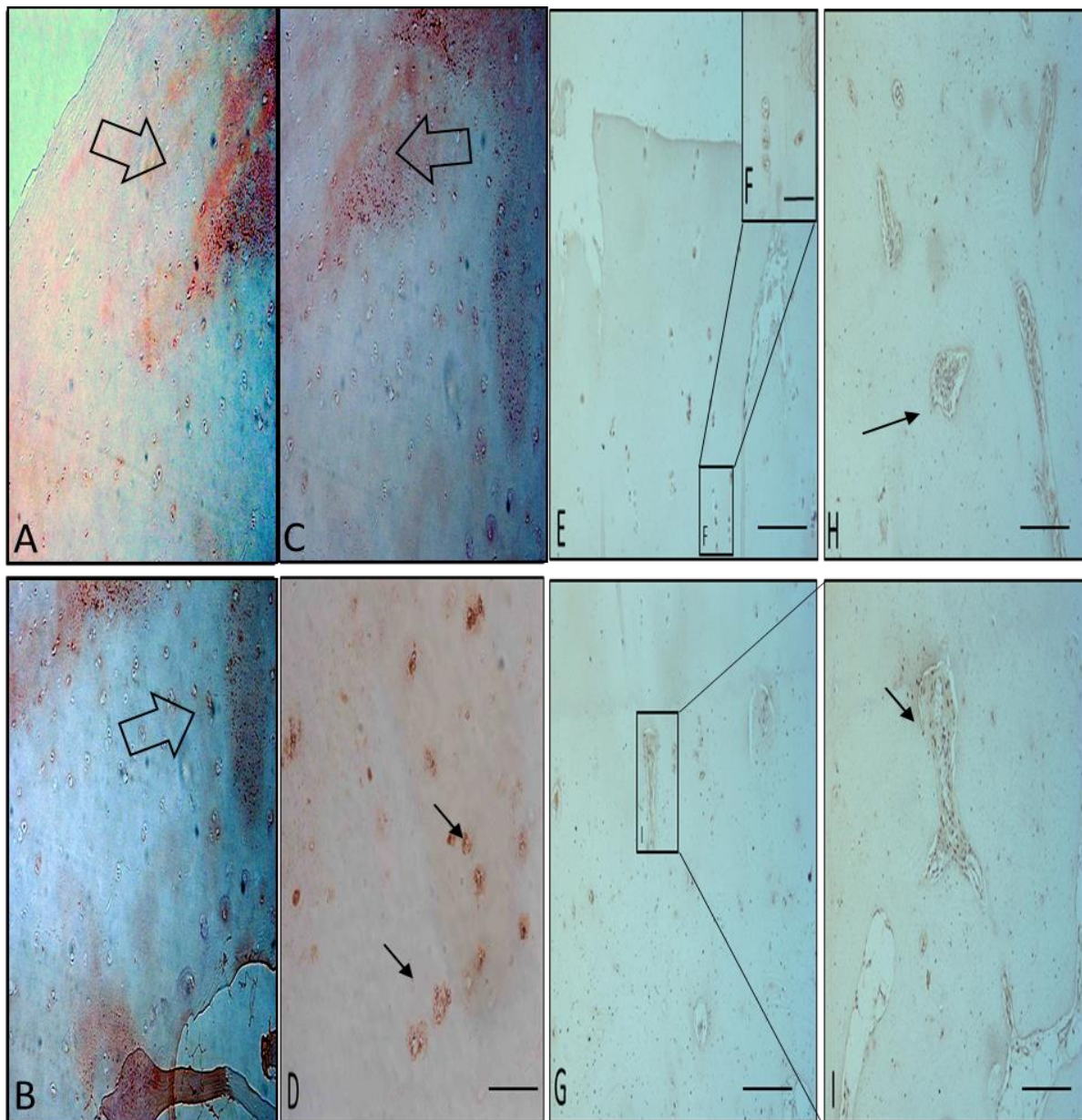


Figure 6.9: Aggrecan immunolabelling in normal and OA osteochondral tissues.

Representative Immunohistochemical figures of normal and OA osteochondral tissue showing aggrecan labelling. Aggrecan labelling in normal tissue in superficial zone chondrocytes is found in the extracellular matrix of superficial zone (empty arrow; A) as well as middle zone (empty arrow; C) and in the pericellular region of most chondrocytes (A-D). Extracellular expression of aggrecan is also seen in the deep zone and subchondral bone (empty arrow; B). High power image of deep zone chondrocytes showing labelling in the pericellular region (D). Aggrecan labelling in OA superficial tissue (E) and a high power of chondrocytes in superficial zone (F). Subchondral OA tissues displayed generalised loss of aggrecan from extracellular regions and occasionally intense expressions of aggrecan around blood vessels infiltrating from subchondral bone (G-I). Scale bar= 100 μ m. High magnification images scale bar=200 μ m.

6.3.6.2. Expression of Alpha smooth muscle actin.

In normal osteochondral tissue, α -SMA immunostaining was absent in any regions of articular cartilage (Figure 6.10. A and B). In addition, subchondral bone blood vessels and stromal tissues also lacked any expression of α -SMA at protein level (Figure 6.10. B). In osteoarthritic tissue investigated, the pattern of α -SMA immunostaining was associated with the severity of the tissue as α -SMA expression and was observed in chondrocytes along a severely damaged region (Figure 6.10. C and D). Furthermore, there was a large increase of α -SMA immunostaining in subchondral bone blood vessels (Figure 6.10. C, E, F and G). Endothelial cells in subchondral bone of osteoarthritic patients appeared to be enlarged when compared to healthy group and intensely labelled for α -SMA (G).

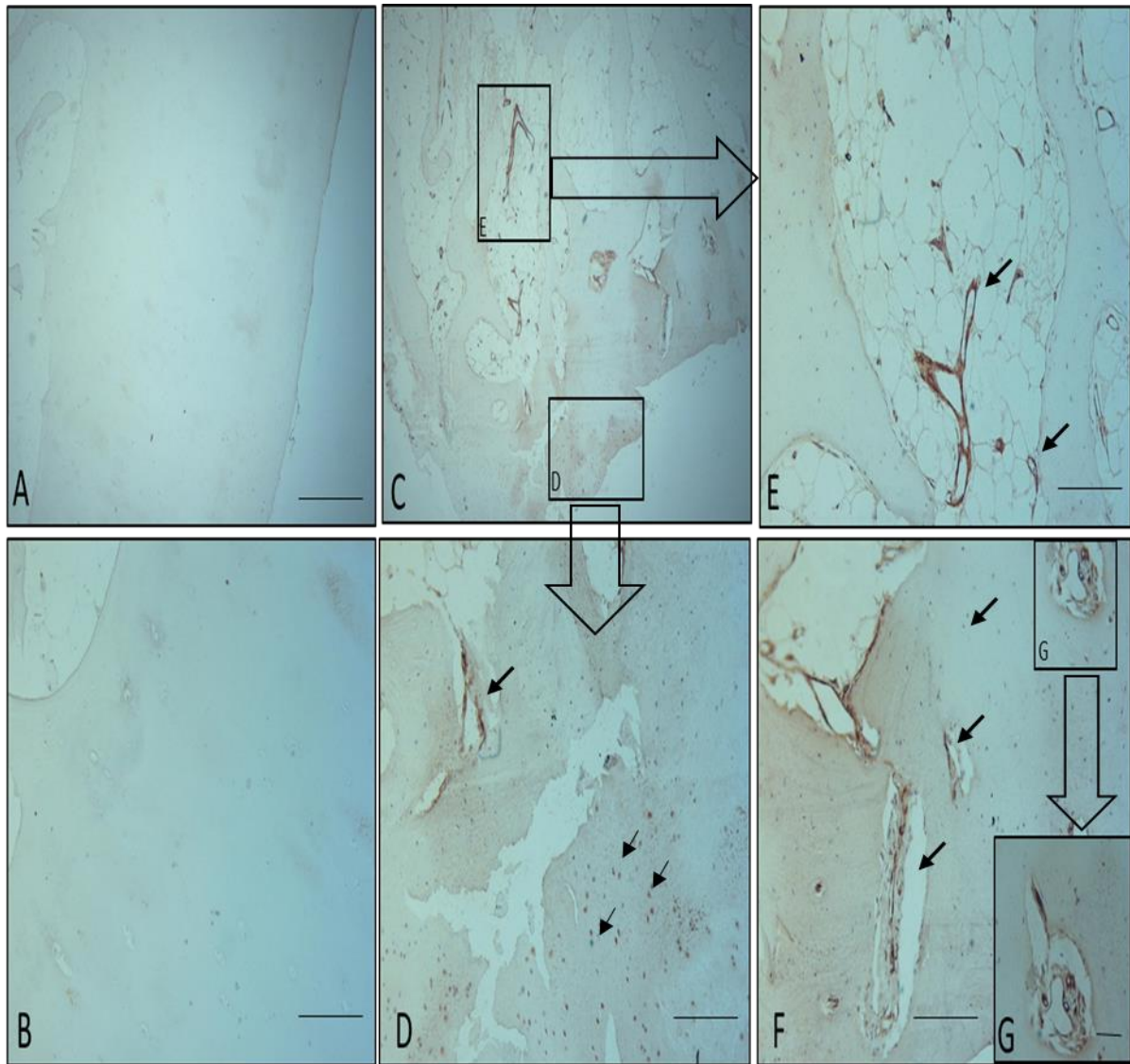


Figure 6.10: α -SMA Immunolabelling in normal and OA osteochondral tissues.

Representative Immunohistochemical figures of normal and OA osteochondral tissue showing α -SMA labelling. α -SMA labelling in normal tissue in superficial zone chondrocytes is absent in all regions of chondrocytes (A) and also in the subchondral tissue (B). In OA osteochondral tissues, α -SMA labelling was observed in regions where there was high damage (C). High power image of chondrocytes located in the fibrillated superficial zone intensely express α -SMA in the cytoplasm (D and F). In addition, subchondral regions displayed intense expressions of α -SMA around blood vessels infiltrating from subchondral bone (E, F and G). Scale bar for A-B= 50 μ m. Scale bar for C and F = 100 μ m and high magnification images (D, E, F). Scale bar=200 μ m.

6.3.6.3. Expression of vimentin staining.

In normal osteochondral tissue, the expression of vimentin was cytoplasmic in nature and restricted to regions of the superficial zone of articular cartilage (Figure 6.11.D). Occasionally, there was vimentin immunostaining observed in deep zone chondrocytes (Figure 6.11. A). In the zone of calcified cartilage, however, vimentin staining was weak around blood vessels and there was no evidence of vascular or mesenchymal stem cell infiltration to the non-calcified cartilage (Figure 6.11. B).

In moderate to severe osteochondral tissue studied, fibrillated surface zone articular cartilage showed an intense vimentin immunostaining (Figure 6.11. H). Furthermore, intense vimentin expression was evident in the deep zone chondrocytes (Figure 6.11.E). Remarkably, areas of intense vimentin immunolabelling was arising from invading vascular and stromal tissues in deep zone and throughout the subchondral region of osteochondral tissue (Figure 6.11. E, F, I and J). This was particularly enhanced in blood vessels stromal tissue infiltrating the tidemark (Figure 6.11.C, F and J).

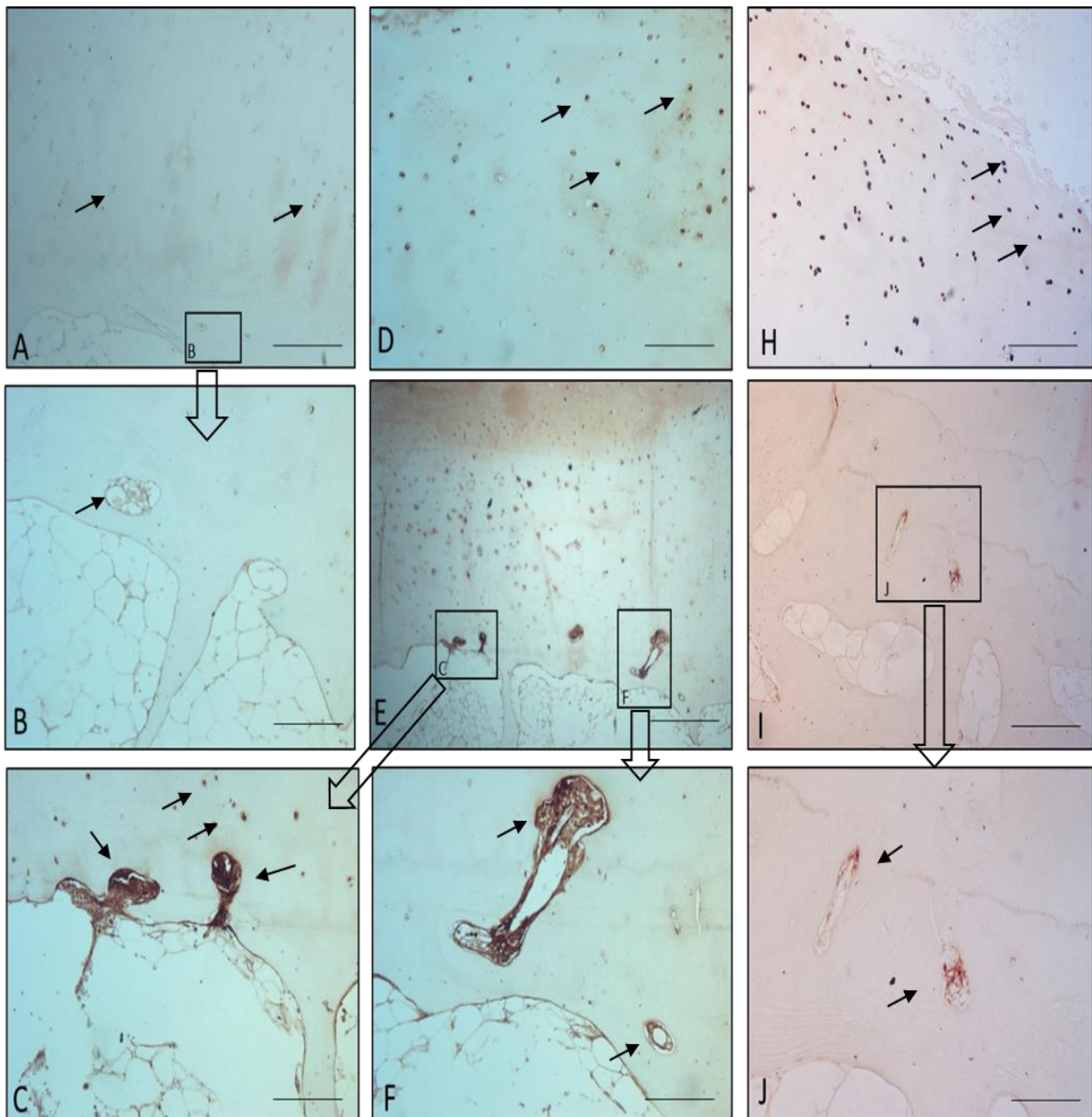


Figure 6.11: Vimentin immunolabelling in normal and OA osteochondral tissues.

Representative immunohistochemical figures of normal and OA osteochondral tissue showing vimentin labelling. Vimentin labelling in normal tissue in upper regions was expressed in the superficial and mid zone chondrocytes (D) and mildly expressed in deep zone chondrocytes (A). Vimentin labelling in the subchondral tissue was absent (B). In OA osteochondral tissues, vimentin labelling was observed in regions where there was high damage (C, E, F, H, J and I). Chondrocytes located in the fibrillated superficial zone intensely express vimentin in the cytoplasm (H). In addition, deep zone chondrocytes also showed intense expression of vimentin (E). But the highest expression was seen in subchondral regions displaying intense labelling for vimentin around blood vessels infiltrating from subchondral bone (C, F and G). Scale bar = 100 μ m. Scale bar for high magnification C, F and J = 200 μ m.

6.3.6.4 Expression of Snail.

Snail is a zinc finger related transcriptional factor that was found to play a central role in the EMT process (Cano *et al.* 2000). In osteoarthritis tissues, a moderate nuclear localisation of snail was observed particularly around migratory blood vessels approaching articular cartilage (Figure 6.12.A-D). This expression was noted to be located at the periphery of blood vessels (Figure 6.12. B and D).

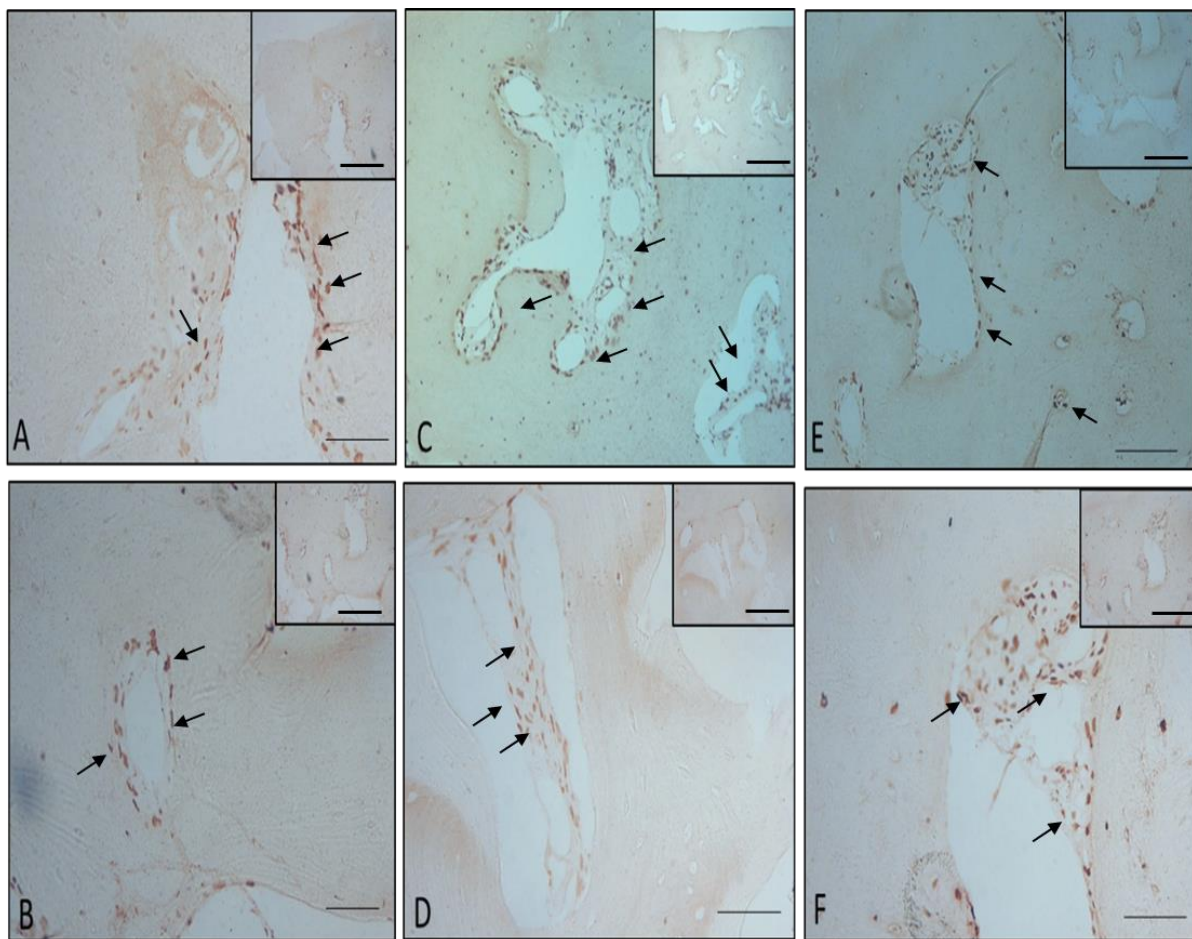


Figure 6.12: Snail immunolabelling in OA osteochondral tissues.

Representative immunohistochemical figures of OA osteochondral tissue showing snail transcriptional factor labelling. In OA osteochondral tissues, Snail labelling was observed in regions where there was activity particularly around invading vasculature (A-D). High power image of subchondral bone show intense expression of snail at the periphery of blood vessels approaching articular cartilage (D). Scale bar = 100 μ m. Scale bar for high magnification inset B & D = 200 μ m. Arrows highlight the expression of Snail in the nuclei of infiltrating blood vessels.

6.4 Discussion.

In the previous chapter, we examined cellular infiltrations at the osteochondral interface of pathological osteoarthritic tissues. This endeavour sought to design a co-culture model system to understand the crucial interaction between articular cartilage and the underlying subchondral bone. In particular, whether chondrocytes influence endothelial cell phenotype by enhancing its migration towards articular cartilage.

A novel, and somewhat unexpected, finding in this study was that by co-culturing endothelial cells with both normal as well as osteoarthritic chondrocytes, we observed a phenotypic switch in endothelial cells when indirectly co-cultured using Transwell co-culture inserts. Traditionally, endothelial cells assume a classical cobble-stone arrangement when grown *in vitro*. This statement was true in control groups. However, in endothelial cells co-cultured with normal and osteoarthritic chondrocytes, spindle-like morphology often associated with MSCs and fibroblast was observed. This phenotypic switch in endothelial cells is often associated with a developmental process known as EnMT. Therefore, it was decided to investigate if by co-culturing chondrocytes and endothelial cells, chondrocytes lead endothelial cells to transform into more MSCs-like cells.

A hallmark of EnMT is the down-regulation of endothelial markers and up-regulation of mesenchymal markers. By examining a series of endothelial markers and mesenchymal markers, we observed that the endothelial cells co-cultured with normal chondrocytes and osteoarthritic chondrocytes expressed the down-regulation of the VE-cadherin protein. The reduction of VE-cadherin was more pronounced in

endothelial cells co-cultured with osteoarthritic chondrocytes. In addition, with this reduction, there was evidence of disruption of cell-cell junctions which ultimately affected the cytoskeletal role of β -catenin. Furthermore, there was a reciprocal increase in the expression of mesenchymal markers α -SMA in both normal and osteoarthritic co-cultured group when compared to control. α -SMA immunofluorescence labelling clearly showed that endothelial cells had adopted a MSCs-like feature of having front-rear polarity. Moreover, with EnMT and to similar extent epithelial to mesenchymal transition, there was an increase of actin cytoskeleton remodelling marked by presence of stress fibres. By examining endothelial cells co-cultured with normal and osteoarthritic chondrocytes, there was clear evidence of actin re-organisation and stress fibres formation that was more pronounced in the osteoarthritic co-cultured group.

These observations were further supported by examining the total protein using Western blot. Both endothelial cells co-cultured with normal and osteoarthritic chondrocytes showed marked reduction in total VE-cadherin when compared to control. In addition, endothelial cells co-cultured with osteoarthritic chondrocytes showed a marked increase in the mesenchymal marker vimentin using Western blot. However, there were no obvious differences between endothelial cells (control) and those co-cultured with normal chondrocytes on the protein expression levels of vimentin. The total β -catenin levels between all three experimental groups were not markedly different. Although these particular findings have never been reported in literature, a recent paper by (Sigurdsson *et al.* 2011) studied the transformative effect of endothelial and breast cancer cell lines co-culturing using a similar approach to this study. More recently, (Nie *et al.* 2014) using a similar Transwell co-

culture system to study the interaction of endothelial cells with oesophageal adenocarcinoma cells have shown that cancer cells enhanced endothelial to mesenchymal transition. EnMT is a key developmental and physiological phenomena vital for several organogenesis including heart and vessel formation. Moreover, this also extends to blood vessels repair in adulthood. EnMT and EMT are activated pathologically during tissue fibrosis and wound healing. They were found to be highly implicated in tumour metastasis (Lamouille *et al.* 2014). In addition, seminal work carried out by Medici and colleagues have shown endothelial cells were permissive to undergo mesenchymal transformation and ultimately were able to possess multi-lineage differentiation into chondrocytes, osteoblasts and adipocyte (Medici *et al.* 2010; Medici 2015)

This study also suggested that the mediated effect of chondrocytes on endothelial cells is probably via a paracrine mechanism (Sigurdsson *et al.*, 2011). Exposing endothelial cells to conditioned media secreted by both normal and osteoarthritic chondrocytes showed some evidence of cellular transformation. It was observed that transformation of endothelial cells cultured in OA-chondrocyte conditioned media showed greater loss of apical-basal polarity and presence of more spindle-features when compared to endothelial cells cultured in conditioned media from normal-chondrocytes. In addition, α -SMA immunolabelling appeared to be located at both the cytoskeleton of the cells but also there is evidence of punctate expression of α -SMA in the nuclei of normal and OA conditioned media exposed endothelial cells. However, as the paracrine factors secreted by chondrocytes are largely unknown. Future studies would to be conducted to unveil these factors. Moreover, there was some interesting differences noted between endothelial cells treated with normal

and osteoarthritic chondrocytes. In endothelial cells co-cultured with osteoarthritic chondrocytes vimentin expression at protein level, was significantly up-regulated. However, there was no noteworthy difference observed in vimentin protein expression in normal chondrocytes group. This finding highlights that the rate of EnMT is possibly accelerated in OA more so than normal chondrocytes.

Protein array studies of endothelial cells co-cultured with chondrocytes have revealed a list of proteins that are implicated in EMT that could be potential candidates for EnMT induction in our model system. Based on the protein array data, endothelial phenotype markers were all down-regulated significantly in co-culture settings when compared to control. In addition, there was reciprocal activation of mesenchymal phenotype marker proteins. In addition, this study also highlighted the differential regulation of other proteins whose roles in transcriptional regulation of EnMT is yet to be studied. For example, expression of carbonic anhydrases (CA-9), a member of a family of zinc metalloenzymes that are activated in response to hypoxia, were found to be a strong promoter of tumour metastasis by inducing epithelial to mesenchymal transition (Shin *et al.*, 2011; McDonald *et al.*, 2012).

By examining factors implicated in EnMT in normal and patient derived adult human osteochondral tissues, a significant up-regulation of several of these factors around invading cellular tissues at the osteochondral interface, were noted. Reduction in ECM is a prognostic marker of osteoarthritis (Attur *et al.*, 2013). Aggrecan is a highly abundant proteoglycan in articular cartilage. In normal osteochondral tissue, aggrecan expression was predominantly found throughout the matrix of chondrocytes throughout the tissue. In addition, there was occasional expression of aggrecan in the pericellular matrix of the superficial zone. However in osteoarthritis,

a generalised reduction in aggrecan immunostaining was observed throughout the tissue. Strikingly, in late-stage osteoarthritis, evidence of intense aggrecan expression was observed in regions of vascular and stromal tissue invasion. This suggested that the ECM was undergoing an intense remodelling process around blood vessels and stromal infiltrates (Puisieux *et al.* 2014). Interestingly, aggrecan over-expression in superficial zone chondrocytes was predominately cytoplasmic in nature. Aggrecan is strongly negatively implicated in neovascularisation and the angiogenesis in many diseases are somewhat associated with reduction of aggrecan (Iozzo and Sanderson, 2011). Furthermore, it has been postulated that aggrecan is an anti angiogenic proteoglycan (Bara *et al.*, 2012; Johnson *et al.*, 2005; Fenwick *et al.*, 1997). Therefore reduction in aggrecan at the articular cartilage region might enhance neovascularisation and endothelial invasion in osteoarthritis.

Vimentin is an intermediate protein found in many musculoskeletal tissues. Its role in the cell is to form the cytoskeleton of cells in combination with other cytoskeletal proteins. In articular cartilage, vimentin forms the main component of intermediate filaments. In this study, by focusing on vimentin immunolabelling, in normal cartilage there was mild cytoplasmic vimentin expression in normal chondrocytes. However, for vimentin immunostaining in osteoarthritic tissue, there were areas of intense labelling at the superficial zone chondrocyte with occasional presence of pockets of positive vimentin expression around deep zone chondrocytes. Interestingly, the highest level of vimentin immunostaining was found in regions of vascular and stromal invasion along the osteochondral interface. But this finding was absent in normal tissue. In cancer studies, vimentin expression is generally the hallmark of mesenchymal transformation. Epithelial acquisition of the mesenchymal phenotype

enhances tumour migration and invasion capacity to local surrounding and distant regions. It is also indicative of aggressive behaviour of tumour cells and usually patients presented with relapse of cancer, frequently have an elevated levels of vimentin expression, indicating tumour metastasis (Mendez *et al.*, 2010; Vuoriluoto *et al.*, 2011).

Alpha smooth muscle actin (α -SMA) is an isoform of actin filament. It is found in smooth muscle cells, myofibroblast and, occasionally, epithelial cells and fibroblast. However, endothelial cells do not appear to express α -SMA. Therefore, the expression of α -SMA is a classical marker for EnMT (Willis *et al.*, 2005). Pattern of α -SMA was similar to the expression of vimentin, where endothelial cells invading the non-calcified cartilage expressed high level of alpha smooth muscle actin protein. While in normal tissue, there was hardly any α -SMA expression. This finding was further supported by *in vitro* EnMT assay of normal endothelial cells co-cultured with chondrocytes.

Finally, we examined the immunohistochemical expression of the down-stream Snail protein. Snail and Slug are zinc finger binding transcriptional factor believed to be master repressors of e-cadherin (Vincent *et al.*, 2009). We demonstrated that, in osteoarthritic osteochondral tissues, snail nuclear expression was observed around the peripheries of blood vessels. This finding was in agreement with a recent study by (Maddaluno *et al.*, 2013). Their study revealed that in cavernous malformation, there was a significant correlation between slug expression, another close relative to snail, and EnMT. In addition, snail expression was positively associated with the expression of vimentin. The expression of activated snail in endothelial cells found in osteochondral tissue, suggested that the tissue was possibly undergoing EnMT.

Based on the proteome array data, there was a four-fold up-regulation of Dkk-1 protein expression in endothelial cells co-cultured with osteoarthritic chondrocytes, which was statistically significant. However, in endothelial cells co-cultured with normal chondrocytes, despite Dkk-1 levels being up-regulated by 1.5 fold, this finding was not statistically significant. These findings were interesting as we routinely observed the expression of Dkk-1 around blood vessels invading articular cartilage. Studies by Frei *et al.* (2013) investigating the role of Dkk-1 in inflammatory bowel disease, showed that Dkk-1 promote epithelial to mesenchymal transition in inflammatory bowel disease therefore promoting large fistula formation. Concurrent with this, Cheng *et al.* (2013) investigating the role of Dkk-1 in cardiovascular disease, has found that to be a strong inducer for EnMT in mouse models of Dkk-1 over-expression led to aortic vascular calcification.

Exposure of endothelial cells to exogenous Dkk-1, to see if Dkk-1 had a transformative effect on endothelial cell phenotype, resulted in the downgrading of several endothelial phenotypes genes. This occurs whilst enhancing the expression of genes implicated in remodelling. We report here that the addition of Dkk-1 over seven day period had significantly resulted in the reduction of mRNA expression of VE-cadherin and pcam-1 and to a lesser extent VEGF-A with additional increase in mRNA levels of α -SMA. In addition, the mRNA expression of MMP-13 was significantly up-regulated in Dkk-1 treated group when compared to control. These findings suggest that the aberrant expression of the Wnt antagonist protein Dkk-1 may be a marker for angiogenesis and vascular invasion in osteoarthritis. Examining the expression of MMP-13 in invading endothelial cells at the osteochondral interface using dual immunostaining of MMP-13 study have shown a direct co-localisation of

MMP-13 with Dkk-1 or CD-34. The expression of MMP-13 was found to be predominantly surrounding the tip of these invading blood vessels. This finding suggests that MMP-13 locally degrades basement membrane of blood vessels and the ECM. Therefore, enhancing endothelial cells to migrate towards the articular cartilage. This occurs presumably via a chemotactic mechanism yet to be identified (Zigrino *et al.*, 2009).

In summary, trends in the expression of EnMT markers; such as VE-cadherin, extracellular matrix markers proteins, Wnt pathway and snail transcriptional factors, showed that EnMT was likely implicated in the pathogenesis of osteoarthritis. This is, to our knowledge, the first study suggesting that endothelial-mesenchymal transition occurs in osteoarthritis. This thesis proposes that in OA, cellular changes occurring in the AC, marked by surface zone fibrillation and reduced proteoglycan synthesis, support an increase in an endothelial cell invasion from the subchondral bone. Subsequently, it encourages vascular and stromal cellular invasion from the subchondral bone by which these cells undergo EnMT, possibly as a final reparative attempt.

CHAPTER 7: GENERAL DISCUSSION.

7.1 General Discussion.

Osteoarthritis (OA) is generally regarded as a chronic degenerative disease and cartilage degradation a hallmark feature of this disease. OA is the most common form of polyarthritis disease. The aetiology of the condition is believed to be multi-factorial (Noth *et al.*, 2008). In the UK, there are over 2.6 million cases of symptomatic OA affecting knee joints in male population and over 3.1 million cases in female population. The majority of these cases affect more than one joint and the prevalence is on the rise (ARUK key facts, 2013).

The core of the OA disease process is a breakdown of the articular cartilage which could ultimately lead to the need for joint replacement surgery (arthroplasty). Arthroplasty surgery has revolutionised the treatment of osteoarthritis by restoring mobility to many affected individuals. However, arthroplasty is not suitable for individuals with limited or focal defects. The commonest predisposing factor to the development of OA in relatively young individuals is trauma to articular cartilage and or subchondral bone. In addition, in patient diagnosed with end-stage OA, there are several exclusion criteria including age and presence of other co-morbidities. Therefore, the use of biological therapies such as cell-based regenerative surgery is becoming a new promising treatment modality for osteoarthritis. The current "gold standard" method of cell base therapies is autologous chondrocyte implantation (ACI) where some success has been well documented (Viste *et al.*, 2012; Corpus *et al.*, 2012). However, this procedure is costly and the resurfaced cartilage is not necessarily the same native form of cartilage found in the synovial joint. Also

expansion of chondrocytes *in vitro* is limited therefore this approach is restricted to the treatment of small focal defects.

Articular cartilage and subchondral bone arise from mesenchymal stem cell differentiation during chondrogenesis. It is a specialized tissue comprising a single cell type, the chondrocyte that is embedded in extracellular matrix composed of collagens and proteoglycans. Histological evaluation of mature articular cartilage reveals it is composed of anisotropic structure of whose prime functions are allowing frictionless articulation between bones and transmitting load across diarthroidal joints. Being avascular and aneural in composition, its limited in reparative potential in comparison to vascularised tissues (Freyria *et al.*, 2011).

Chapter three of this PhD thesis discussed the successful isolation of chondroprogenitor cells (CPC) using the well reported fibronectin adhesion assay method developed by Jones and Watt (1993) and adopted by Dowthwaite *et al.* (2004). CPC were isolated from normal and osteoarthritic articular cartilage. Initial studies were carried out on isolated CPC from normal and osteoarthritic articular cartilage. Results for both normal and osteoarthritic CPC were shown to have a comparable cell morphology, initial adherence to fibronectin and colony forming ability. Statistically, no-apparent differences were noted between the two cell groups. The percentage of colony forming cells in this study was comparable to previously published data (Alsalameh *et al.* 2004; Dowthwaite *et al.* 2004; Williams *et al.* 2010). In addition, using Ficoll™ density gradient centrifugation, matched-bone marrow derived MSCs were isolated from patients diagnosed with OA. Bone marrow mesenchymal stem cells (BM-MSCs) were also successfully isolated from the tibial plateau of the knee joints. The isolation and characterisation of osteoarthritic derived

CPC is very important as they could provide an allogeneic cell source for tissue repair.

This research study (chapter three), to our knowledge, is the first to conduct comparative analysis of adult human chondroprogenitor cells (CPC) and BM-MSCs from matched patient-derived samples and comparing with CPC isolated from macroscopically normal cartilage from donors. Proliferation studies were carried out in patient matched CPC and OA-BM-MSCs as well as normal CPC. Based on these studies, all three cell types reached 20 population doublings in 30 days or less. Despite both OA-CPC and OA-BM-MSCs slowing in their proliferation rate post 30 days, incidences of cell senescence were found to be relatively low. Moreover, analysis of cell proliferation using BrdU incorporation assay showed that all cell types were in a proliferative state when examined at cumulative population doubling of 25 ± 2.5 . By examining cell MSCs surface marker expression of OA-CPC, OA-BM-MSCs and N-CPC, all three cell types showed positive MSC stem cell marker expression for CD-90, CD-105 & CD-166 while lacking the cellular expression for CD-34 thus confirming both cell types were of mesenchymal lineage.

Further functional characterisation of adipogenic, chondrogenic and osteogenic differentiation of isolated CPC and BM-MSCs by were studied. Based on histochemical studies of differentiated CPC and BM-MSCs as well as molecular analysis using RT-PCR, CPC as well as BM-MSCs were able to undergo successful tri-lineage differentiation. This initial studies further encouraged us to conduct a detailed study comparing normal and osteoarthritic CPC. The notion that articular cartilage holds a population of stem/progenitor cells is becoming widely accepted. The potential that CPC could hold a regenerative capacity have been proposed by

several groups and where it can provide suitable cell-based source for cartilage regeneration (Alsalameh *et al.*, 2004; Williams *et al.*, 2010; Fickert *et al.*, 2004; Pretzel *et al.*, 2011; Grogan *et al.*, 2009). However, further studies are needed to assess if patient derived CPC are comparable to cell lines derived from healthy individuals. In particular, detailed molecular and functional studies are needed to assess the true potential of these unique cell source which served the aim for chapter 4.

Regulatory pathways including the FGF, TGF- β and the Wnt signalling pathways are known to be important in the development of the musculoskeletal system in the processes of chondrogenesis and osteogenesis (Hartmann 2006; Hidaka and Goldring 2008). The Wnt proteins have a wide range of role ranging of action from the several developmental and homeostasis process including patterning of anterior-posterior axis to cell and calcium ion movement, cell proliferation, differentiation and morphogenesis (Clevers and Nusse 2012; Niehrs 2012; Nusse 2012). In addition, the Wnt pathway is emerging as a crucial pathway involved in the regulation and homeostasis of the synovial joint (Diarra *et al.* 2007).

A growing amount of evidence is emerging, which shows that the Wnt pathway plays a pivotal role in stem cell fate determination in many tissues including skeletal, skin, hematopoietic and gastrointestinal tissues (Hartmann 2006; Sato *et al.* 2009; Lander *et al.* 2012). Previous developmental work conducted on chicks and rodents have uncovered the important role the Wnt pathway plays in the process of chondrogenesis and chondrocyte homeostasis during postnatal development. There is also emerging literature showing the Dickkopf family of Wnt inhibitors to play a

role in the pathogenesis of osteoarthritis and to have the potential to be useful biomarkers for the progression of osteoarthritis (Lane *et al.* 2007; Oh *et al.* 2012).

In chapter four, the expression levels of Wnt signalling pathway genes were studied using targeted Wnt pathway array. Examination of the differential expression levels of Wnt pathway genes in both normal and osteoarthritic CPC, revealed the up regulation of several Wnt antagonist genes in OA-CPC. This finding was in good agreement with previously published studies investigating mutations of several Wnt inhibitors and increased predisposition to OA development (Loughlin *et al.* 2004; Rodriguez-Lopez *et al.* 2007; Blom *et al.* 2009). Of the several Wnt antagonist genes up-regulated in osteoarthritis, Dkk-1 was shown to be highly up-regulated in OA-CPC with nearly 50-fold up-regulation when compared to normal CPC. Because of this discovery the molecular expression of Dkk-1 was further investigated in full-depth chondrocytes, isolated from macroscopically normal cartilage and osteoarthritic patients and monoclonal CPC cell lines isolated from either macroscopically normal cartilage or osteoarthritic cartilage. Congruent with this Wnt-array data, the expression of Dkk-1 at the mRNA level was found to increase in CPC isolated from OA donors, relative to CPC isolated from macroscopically normal cartilage and full-depth chondrocytes. A recent study (Oh *et al.* 2012) also reported increases in mRNA expression for Dkk-1 in OA chondrocytes. Uniquely, however, this research study (chapter four) showed that when OA-chondrocytes were further separated into full-depth and CPC, only CPC had displayed the elevated expressional levels of Dkk-1. This results suggests that the expression of Dkk-1 is highly up-regulated in the stem cells compartment of articular cartilage in osteoarthritis.

The role of elevated Dkk-1 in osteoarthritis has recently attracted a lot of attention. The Wnt pathway is emerging as a crucial pathway involved in the regulation and homeostasis of the synovial joint (Diarra et al. 2007). Oh *et al.* (2012) showed that elevated levels of Dkk-1 in the DMM surgically induced mouse model of OA ameliorated cartilage degradation by inhibiting matrix metalloproteinase through ubiquitination of β -catenin. Contrary to these findings, (Thorfve *et al.* 2012) and (Weng *et al.* 2010) found that Dkk-1 up-regulation in cartilage isolated from patients undergoing knee replacement and in rat models of OA were correlated with higher chondrocyte apoptosis. These contradictory results highlights the complex nature of the Wnt pathway and was discussed in a recent review (Funck-Brentano and Cohen-Solal 2011). This inconsistency in published literature was thought to be attributed the differences to be due to the differences in the experimental models used in these studies as well as the potential of Dkk-1 having canonical as well as non-canonical roles. Adding to these remarks, Dkk-1 might have a Wnt independent role by directly activating inflammatory cascades (Gunn *et al.*, 2006). A more detailed study by Weng *et al.* (2009, 2010 and 2012) tried to ascertain the role of Dkk-1 in human and animal models of osteoarthritis and showed that inhibition of Dkk-1 significantly reduced cartilage degradation and bone remodelling. Chapter four highlighted that by relating the molecular expression of Dkk-1 with the severity of cartilage damage found that higher Dkk-1 levels was positively correlated with an increase in Mankin score.

Articular cartilage is a highly organised and a homogenous tissue that functions to provide a frictionless surface for load-bearing synovial joints, hence enabling smooth gliding movements. Scientific literature, from several research groups, have

previously demonstrated that isolated cartilage progenitor cells, upon culture expansion, show marked variation in both their colony formation efficiency as well as their proliferation rate (Williams, 2010; Nelson *et al.*, 2014).

In this study (chapter four), targeted Wnt array molecular characterisation as well as reporter assay and protein analysis of normal and osteoarthritic clonal CPC cell lines, demonstrated that osteoarthritic CPC have an inherent variation in their initial adherence to fibronectin, colony forming ability and proliferation capacity. Heterogeneity was also observed in Dkk-1 expression between clonal cell lines from matched donors using molecular and protein approaches. Furthermore, this variation was also documented in the ability of osteoarthritic CPC conditioned media to modulate β -catenin activity using the TCF-luciferase reporter assay. Therefore, based on the endogenous expression of Dkk-1, CPC were sub-divided into Dkk-1^{high} CPC of osteoarthritic origin and Dkk-1^{low} CPC of normal and low Dkk-1 expressing OA-CPC cell lines. Heterogeneous expression embryonic stem cells based on their Wnt expression was recently investigated by Nusse and colleagues (Blauwkamp *et al.* 2012). In addition, stem cell heterogeneity has been previously described in embryonic stem cells (MacArthur *et al.* 2012; Kumar *et al.* 2014) and in adult stem cells found in several tissues including intestine (Barker *et al.* 2007; Yan *et al.* 2012), epidermis (Janich *et al.* 2011), hematopoietic bone-marrow (Ratajczak 2015) among some tissues, (reviewed in more detail by (Goodell *et al.* 2015)). The concept of stem cell heterogeneity has been widely studied in cancer, in order, to understand the hierarchal nature of cancer which is thought to be governed by cancer stem cells (Al-Hajj *et al.* 2003; Ricci-Vitiani *et al.* 2007; Singh *et al.* 2007). Using custom-based PCR array, a detailed transcriptional profile of Dkk-1^{high} CPC from osteoarthritic

donors and Dkk-1^{low} CPC from normal donors were generated. Based on transcriptional profiling of chondrogenic differentiated pellets, distinctive differences between Dkk-1^{high} CPC, Dkk-1^{low} CPC were found. In addition, to gain further insight into the distinct subset of OA-CPC based on their Dkk-1 expressional levels, patient matched osteoarthritic Dkk-1^{high} CPC and Dkk-1^{low} CPC cell lines were examined. Interestingly, Dkk-1^{high} CPC were unable to undergo chondrogenic differentiation. In contrast, both normal and osteoarthritic CPC cell lines with low endogenous levels of Dkk-1 protein were able to show evidence of chondrogenic differentiation at a molecular as well as protein levels. Inability of Dkk-1^{high} CPC to undergo successful chondrogenic differentiation could be partly explained by the inhibitory role Dkk-1 on the canonical Wnt pathway which is required for chondrogenesis (Akiyama *et al.* 2004; Kirton *et al.* 2007). This PhD data is in accordance with Lyashenko *et al.* (2012) which recently studied the impact of β -catenin inhibition on mouse embryonic stem cells differentiation. In *in vitro* and *in vivo* mouse model studies, knock out of β -catenin resulted in failure of embryonic differentiation. Lack of cytoskeletal β -catenin was somehow compensated by plakoglobin (γ -catenin) but ESCs failed to undergo differentiation thus confirming the vital role of β -catenin in formation of three-germ layers (Guo *et al.*, 2004; Lyashenko *et al.*, 2012). An interesting observation of our study, at day 7 and 14 of differentiation, was the slight increase in β -catenin levels in Dkk-1^{high} CPC. This finding might be postulated by an up-regulation of β -catenin via a negative feedback mechanism and is probably insufficient to counteract the constantly high levels of Dkk-1 during the three weeks period. One aspect of the chondrogenic differentiation assay that was not investigated due to time limitations, but should be done in the future, is to perform

the assay in the presence of the Dkk-1 inhibitor, WAY-262611, in order to investigate if inhibiting Dkk-1 in Dkk-1^{high} CPC can rescue chondrogenic differentiation.

For a long time, emphasis on OA research was mainly on studying the role of hyaline cartilage (primary diseased tissue) during OA progression. However in the last two decades or so, it is becoming more evident that whole joint is affected and in particular the underlying subchondral bone where the majority of force transmission into the articular cartilage arises from. In addition, it is debated that during osteoarthritis, changes of the underlying bone including microfracture, tidemark duplication and changes in calcified cartilage, which normally thought to constitute as a barrier to cartilage vascularization are disrupted, are thought to supersede that of cartilage loss (Quasnicka et al. 2006; Zamli et al. 2014). Therefore, there is a shift among scientist studying osteoarthritis by looking at changes affecting the joint as an “organ” and not exclusively focusing on changes at a “tissue” level (Lajeunesse *et al.* 1999; Lajeunesse et al. 2003; Hollander *et al.*, 2010; Luyten *et al.*, 2009). Chapter four’s examination of the topographical expression of Dkk-1 in osteochondral tissues, isolated from normal and osteoarthritic donors, resulted in positive immunolabelling in chondrocytes located at the superficial zone and deep zone regions of articular cartilage. In addition, in late-stage osteoarthritis, there were regions of intense Dkk-1 immunolabelling mainly around the peripheries of invading blood and stromal tissues.

In osteoarthritic tissues investigated in this report, a strong ECM remodelling process was observed around blood vessels and stromal infiltrates from underlying subchondral bone. Proteoglycans are strongly implicated in neovascularisation and

the angiogenesis in many diseases (Iozzo and Sanderson, 2011). In addition, it has been postulated that aggrecan is an anti angiogenic proteoglycan (Fenwick *et al.*, 1997; Johnson *et al.*, 2005; Bara *et al.*, 2012). Beyond the contributions of specific cell type to blood vessels angiogenesis, loss of cartilage matrix in particular loss of cartilage proteoglycans during osteoarthritis is thought to be implicated in cartilage's increased susceptibility to attack from the subchondral bone (Hsieh *et al.* 2010; Bara *et al.* 2012). It can also influence vascular recruitment. Indeed, the composition of the extracellular matrix is altered measured by reduction in Safranin-O and aggrecan staining seen in osteoarthritic tissues in this report. Therefore reduction in aggrecan at the articular cartilage region might enhances neovascularisation and endothelial invasion in osteoarthritis.

Angiogenesis play a vital role in endochondral ossification during embryonic and postnatal development and is a crucial step for normal skeletal tissue formation. However, reactivation of angiogenesis in osteoarthritis is a process that is not fully understood. Possible hypothesis include the reactivation of pathways implicated in synovial joint development as an attempt to undergo reparative attempt (Cornelis *et al.*,2011). Nonetheless, this process ultimately alters the homogenous cellularity of articular cartilage due to cellular infiltration from the underlying subchondral bone.

The precise steps involved in the angiogenesis of articular cartilage is not clearly understood. However, results in this study suggested that the expression putative MSCs markers, CD-105 and CD-166 around MSCs infiltrating breaching the tidemark (Alsalameh et al. 2004; Koelling *et al.* 2009; Pretzel *et al.* 2011). In cancer studies, it was suggested that mesenchymal stromal cells exploit alterations in local microenvironment by releasing cytokines and growth factors to activate quiescent

endothelial cells around them and initiate a cascade of events that quickly becomes dysregulated.

The aim of chapter five was to elucidate the role canonical Wnt pathway play in angiogenesis of articular cartilage, endothelial cells were exposed to a range of putative canonical Wnt modulators. Based on *in vitro* assay of angiogenesis, migration and invasion studies, Dkk-1 was found to be highly pro-angiogenic and stimulate endothelial migration and invasion. This finding was reassuring as the pro-angiogenic role of Dkk-1 was previously observed by (Smajda *et al.*, 2010; and Weng *et al.*, 2012). In addition, the pro-migratory and invasive role of Dkk-1 in endothelial cells although novel, is supported by several studies using cancer cell line as model system and where Dkk-1 inhibition was found to abrogate the invasive properties of cancer cells (Chen *et al.*, 2013; Shi *et al.*, 2013).

In Chapter 6, the aim was to design a co-culture system consisting of endothelial cells and chondrocytes with the purpose of evaluating how endothelial cell and chondrocyte interactions within the osteochondral interface contribute to the progression of osteoarthritis. Both cells types (chondrocyte and endothelial cells) are generally considered to be quiescent for the majority of normal adult life (Bergers and Benjamin, 2003). The mechanisms responsible for the aberrant endothelial activity leading to their propagation and invasion of articular cartilage was investigated in direct co-culture studies using normal and osteoarthritic chondrocytes and endothelial cells. The results of chapter six indicated that the chondrocytes had a transformative effect on endothelial cells. In EnMT, endothelial cells lose cell-cell junction marked by a reduction in membrane-associated vascular endothelial VE-cadherin protein expression. This, in turn, results in VE-cadherin translocation from

the cell membrane to the cytoplasm with further down-stream target activation of key transcriptional factors implicated in EnMT including c-Myc, Twist, Zinc-finger E-box-binding 1 (Zeb-1) and snail (Lamouille *et al.*, 2014). Concurrent with changes occurring at the cell surface, chapter six highlighted the down regulation of genes crucial for endothelial programming including VE-cadherin, PECAM (CD31) and Tie-2. Simultaneously, genes involved in mesenchymal phenotype transformation were switched on including N-cadherin, vimentin and alpha-smooth muscle actin (α -SMA). Furthermore, transcriptional factors Snail-1 and Snail-2, also known as Slug, were triggered and resulted in potent repression of cadherin genes. This further enhanced cell reprogramming to mesenchymal morphology by activating factors involved in remodelling of the ECM, including MMPs (Kovacic *et al.*, 2012). Based on chapter six's protein analysis (using immunofluorescence microscopy, immunoblotting, immunohistochemical staining of several EnMT marker proteins in normal and osteoarthritic osteochondral tissue) and its proteomic array data it is evident that endothelial cells co-cultured with chondrocytes showed EnMT transformation characteristics and that EnMT is possibly activated in osteoarthritis.

Previous studies attempting to understand angiogenesis, in relation to tumour invasion and metastasis, have unveiled an important clue to how tumour cells overcome their microenvironment and start to invade local and distant sites. It was shown that tumour cells undergo a process of mesenchymal transition by which tumour cells adopt a highly motile configuration ultimately allow for tumour propagation and metastasis (Quail and Joyce 2013).

Endothelial to mesenchymal transition (EnMT) is a key cellular process vital during the development of embryo. More recently, it was noted that EnMT is reactivated in

several pathological processes including tumour invasion and kidney and cardiac diseases (Lamouille *et al.*, 2014).

A seminal study by Medici *et al.* (2010) have shown that endothelial cells showed a remarkable plasticity by being able transform into mesenchymal stem cells and therefore give rise to chondrocyte and osteoblast in a rare an debilitating condition known as fibrodysplasia ossificans progressiva. It was then discovered that a mutation in the ALK5 gene was causing blood vessels to undergo a constant state of endothelial to mesenchymal transition (EnMT). Moreover, a review by Shoshani and Zipori (2011) commenting on the study by the Olsen group have raised the question whether endothelial to mesenchymal transition occurs in osteoarthritis. As it is evident in osteoarthritis, that endothelial cells are motile and invade articular cartilage, it possible to postulate that EnMT might be partially implicated in endothelial cells migration.

Chapter six used proteomic array data to confirm that endothelial markers proteins were all down-regulated in endothelial cells co-cultured with chondrocytes when compared to control. Based on the proteome array data, several proteins were differentially expressed between control and experimental group. These proteins were not known to play a role in EnMT and further investigation is therefore required to determine their role. Furthermore, Dkk-1 protein was up-regulated in endothelial cells co-cultured with chondrocytes. Therefore, to determine the role Dkk-1 plays, endothelial cells were treated with exogenous Dkk-1. Molecular analysis results suggested that Dkk-1 down-regulated mRNA levels of endothelial phenotype genes (VE-cadherin and PECAM-1 and to a lesser extent VEGF-A) while promoting mesenchymal marker α -SMA. A recent study investigating the role of Dkk-1 in

cardiovascular disease has found that Dkk-1 was a strong inducer for endothelial-mesenchymal transition in mouse models leading to aortic vascular fibrosis and calcification (Cheng *et al.*, 2013). Moreover, Dkk-1 was shown to enhance the expression of MMP-13 and this is in agreement with work by Weng *et al.* (2010) and Nalesso *et al.* (2011) both showing a positive effect of Dkk-1 on MMP-13 expression on chondrocytes. By examining the protein localisation of Dkk-1, MMP-13 in endothelial cells, it was shown that the two protein co-localise around invading blood vessels of osteoarthritic tissues. The expression of MMP-13 was found to be predominantly surrounding the tip of these invading blood vessels. This finding suggests that MMP-13 locally degrades basement membrane of blood vessels and the ECM. Therefore, this enhanced endothelial cells to migrate towards the articular cartilage (Zigrino *et al.*, 2009).

In conclusion, this study shows that the canonical Wnt pathway is differentially expressed in osteoarthritic chondroprogenitor cells. This study shows that the expression of Dkk-1 proteins is enhanced around subchondral blood vessels invading articular cartilage at the early and late stages of osteoarthritis.

There are clear differences in the expression of Dkk-1 between normal and osteoarthritis cartilage progenitor cell lines. The data from this thesis suggests that these differences may indicate a role for the Wnt pathway in osteoarthritis progression. Studying the role Dkk-1 played, using *in vitro* assays, it is clear that Dkk-1 has a pro-angiogenic and pro-migratory role on endothelial cells. Whether this conclusion can be considered to be the case in osteoarthritis is to be seen. However, findings in this report and others provide an initial understanding of possible mechanism involving Wnt pathway in osteoarthritic angiogenesis. Understanding

these alterations at the osteochondral junction and regulating pathways implicated in their initial occurrence will lead to a greater knowledge of the pathophysiology of osteoarthritis with development of pharmacological therapies. Figure 7.1 is proposed role of Dkk-1 at the osteochondral interface.

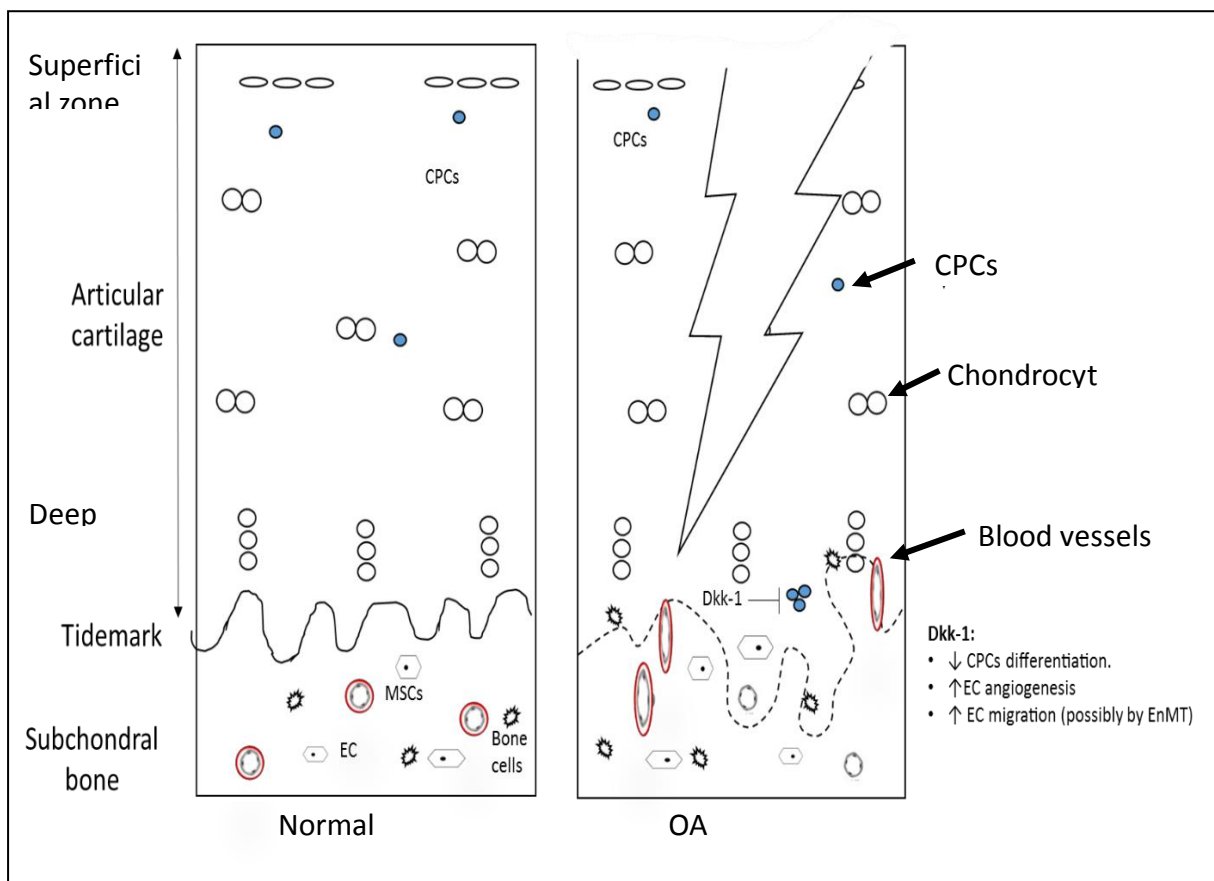


Figure 7. 1: Proposed model of the role of Dkk-1 in the osteochondral tissues.

In normal synovial joint, articular cartilage and subchondral bone are nicely separated by tidemark. Endothelial cell are inactive and MSCs a bone cells show no evidence of cartilage invasion. In the articular cartilage, CPC are located at the

superficial zone and upper-middle zone and there are plenty of ECM produced marked by strong Safranin-O staining. However, in osteoarthritis, articular cartilage degradation and loss of tidemark integrity exposes the underlying subchondral bone to stimulatory factors secreted by chondrocytes. This in turn promote vascular and cellular migration which is in part regulated by Dkk-1. At the cartilage region, Dkk-1 is proposed to have an inhibitory role on CPC differentiation. In addition, endothelial cells migratory capacity is enhanced as these cells possibly undergo transformation into motile mesenchymal cells hence further promoting their invasive capacity.

7.2 Limitation and future work

As it was difficult to study patient derived endothelial cells in this PhD thesis due to lack of ethical approval, we used primary and endothelial cell lines. Despite the wealth of information that endothelial cells provide, an important limitation is the nature of endothelial cells used in this study (macro-vascular endothelial cells). The advantage of using normal macro-vessel endothelial cells is the ease of isolation from umbilical cord vessels and commercial availability of a homogenous cells. Future studies should be carried out to investigate patient-derived endothelial cells from human peripheral blood and or marrow aspirate (microvascular endothelial cells) provide similar outcome and in particular if Dkk-1 expression can be examined directly.

Whilst chondroprogenitor cells were successfully isolated using fibronectin adhesion assay, it is becoming evident that there are marked variability of CPC proliferation and differentiation. This heterogeneity is found between individuals and also among cell clones obtained from the same individual. Suitability of CPC application in tissue

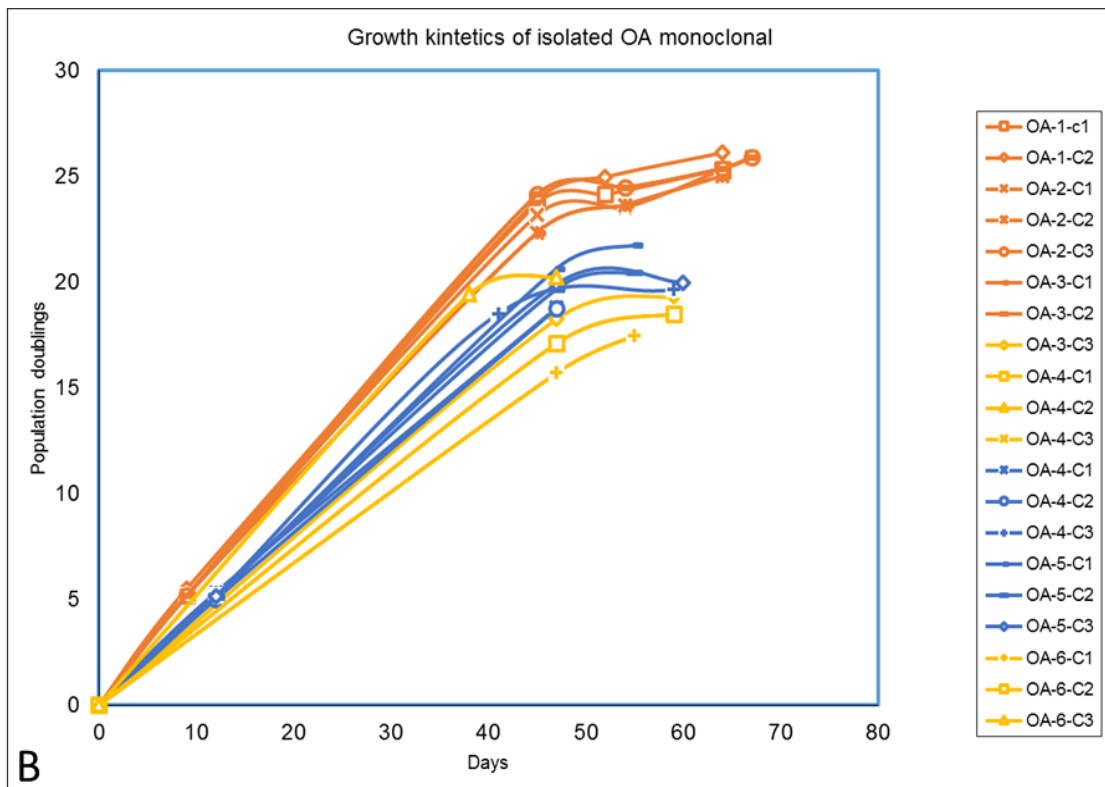
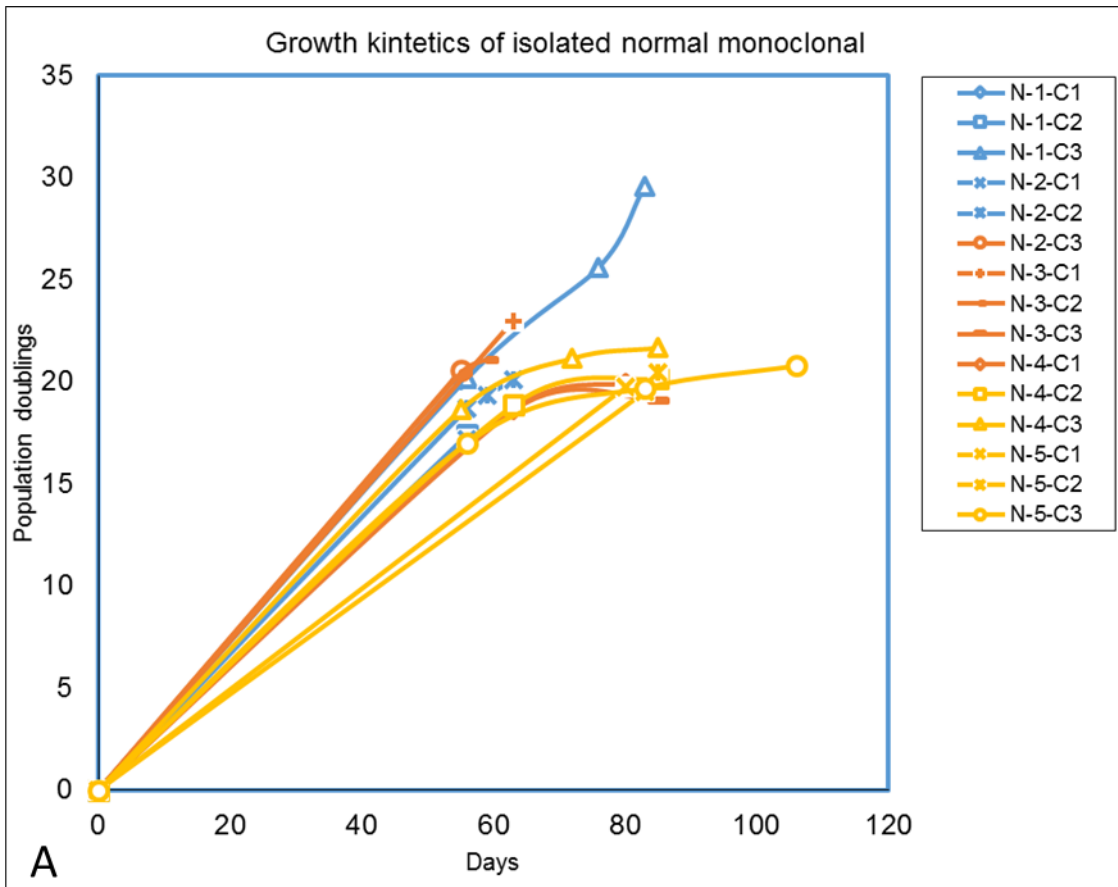
engineering is dependent on identifying cells with the optimum “stemness” potential and development of an efficient and time-saving method of isolating CPC. In addition, full characterisation of isolated CPC are required with regards to their differentiation potential. Little is known about key regulators of CPC self-renewal and multipotent state “stemness” (Hayes *et al.*, 2007; Fuchs and Horsley, 2012; Lander *et al.*, 2012; Churchman *et al.*, 2012). Therefore, based on data generated using targeted Wnt-array, it would interesting to investigate the role of other Wnt antagonist transcripts that were up-regulated in OA-CPC.

In addition, although this study confirmed the heterogeneous nature of patient derived CPC in relation to their chondrogenic differentiation capabilities, due to time limitation, we were unable to examine osteogenic and adipogenic differentiation of Dkk-1^{high} and Dkk-1^{low} CPC. However, recent work by Bajada *et al.* (2009) examining osteogenic differentiation of MSCs and Gustafson *et al.* (2012) examining adipocyte differentiation both concluded that Dkk-1 had inhibitory effect of osteogenesis while promoting adipogenesis. It would be interesting to examine if Dkk-1^{high} CPC were lineage biased towards adipogenesis.

Appendix 1:

| Sample | Age | Sex | Mankin Score | Connective Tissue Type | | | |
|--------------|-----|--------|--------------|------------------------|-------------------------|----------------|---------------------------------|
| ID# | | | | BM-MSCs | Full depth chondrocytes | polyclonal CPC | monoclonal CPC |
| OA-1 | 63 | Male | 4 | - | OA-1-FD | OA-1 (P) | OA-1(3 monoclonal cell lines) |
| OA-2 | 70 | Female | 7 | - | OA-2-FD | OA-2 (P) | OA-2 (3 monoclonal cell lines) |
| OA-3 | 53 | Female | 8 | OA-3-MSCs | OA-3-FD | OA-3 (P) | OA-3 (3 monoclonal cell lines) |
| OA-4 | 58 | Male | 10 | OA-4-MSCs | OA-4-FD | OA-4 (P) | OA-4 (3 monoclonal cell lines) |
| OA-5 | 79 | Male | 8 | OA-5-MSCs | OA-5-FD | OA-5 (P) | OA-5 (3 monoclonal cell lines) |
| OA-6 | 62 | Female | 3 | OA-6-MSCs | OA-6-FD | OA-6 (P) | OA-6 (3 monoclonal cell lines) |
| OA-7 | 60 | Female | 4 | OA-7-MSCs | OA-7-FD | OA-7 (P) | OA-7 (3 monoclonal cell lines) |
| OA-8 | 75 | MALE | 6 | OA-8-MSCs | OA-8-FD | OA-8 (P) | OA-8 (3 monoclonal cell lines) |
| OA-9 | 70 | male | 13 | OA-9-MSCs | OA-9-FD | OA-9 (P) | OA-9 (3 monoclonal cell lines) |
| OA-10 | 69 | Female | 9 | - | OA-10-FD | OA-10 (P) | OA-10 (3 monoclonal cell lines) |

Appendix 2:



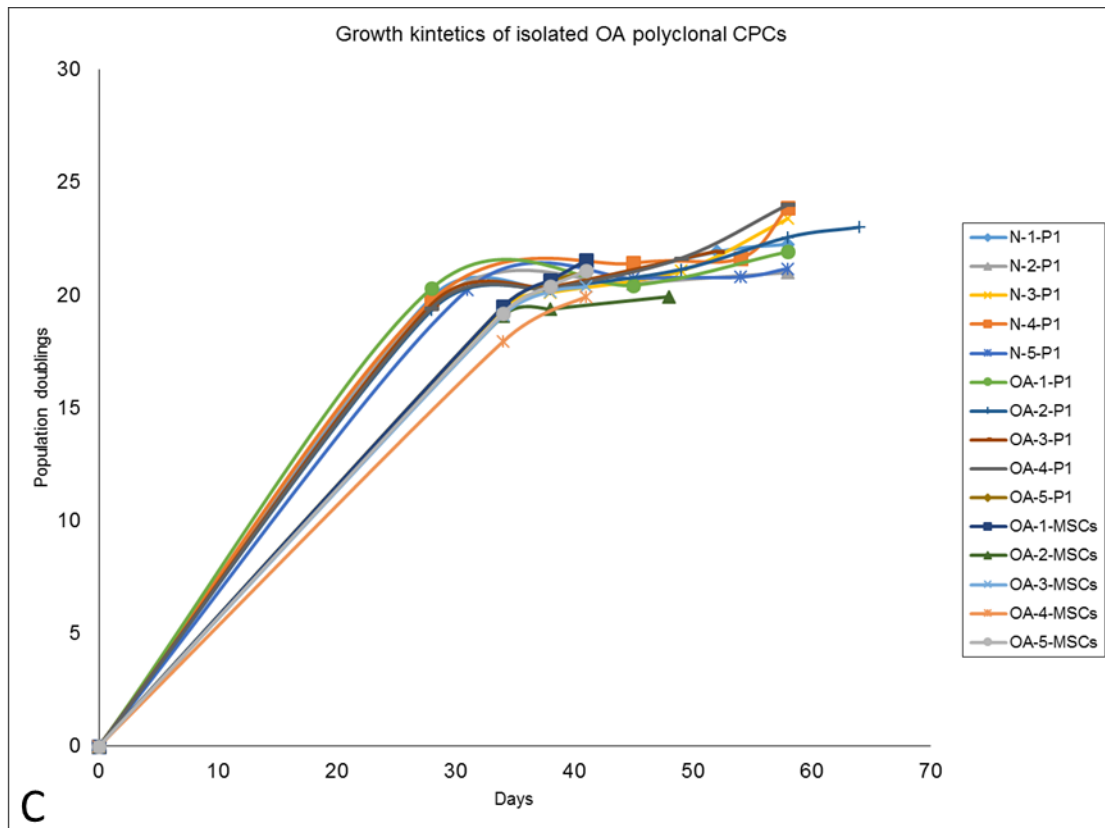


Figure 8. 1: Cumulative population doublings of isolated CPCs and MSCs. Cumulative population doublings of isolated monoclonal CPCs from normal donor (A) and OA donor (B) as well as normal and OA polyclonal CPCs and OA BM-MSCs (C).

Appendix 3:

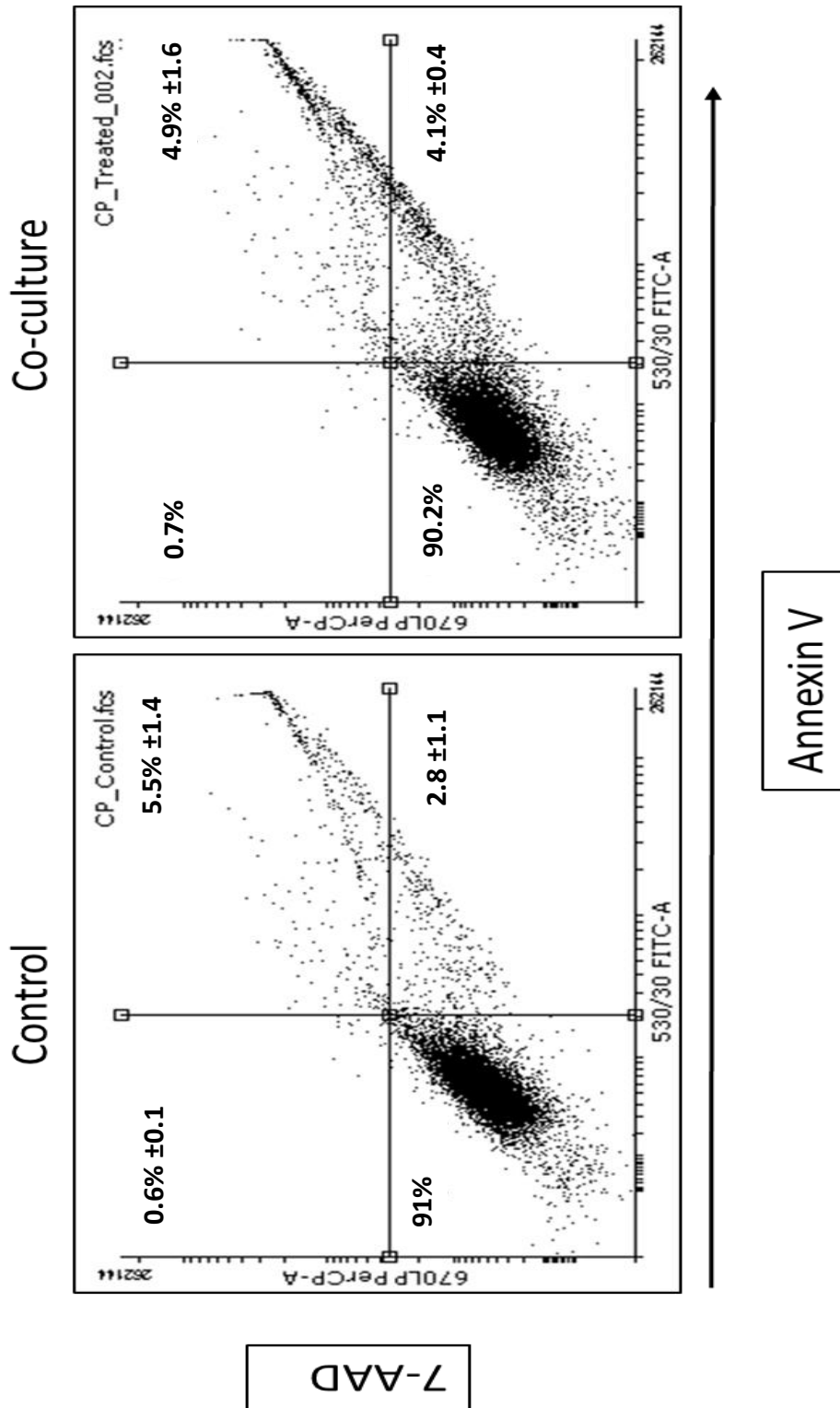


Figure 8. 2: Effect of chondrocytes and endothelial cells co-culture on cell viability with membranous FITC-Annexin V/7-AAD staining and the statistics between control (endothelial cells) and co-culture group.

Appendix 4:

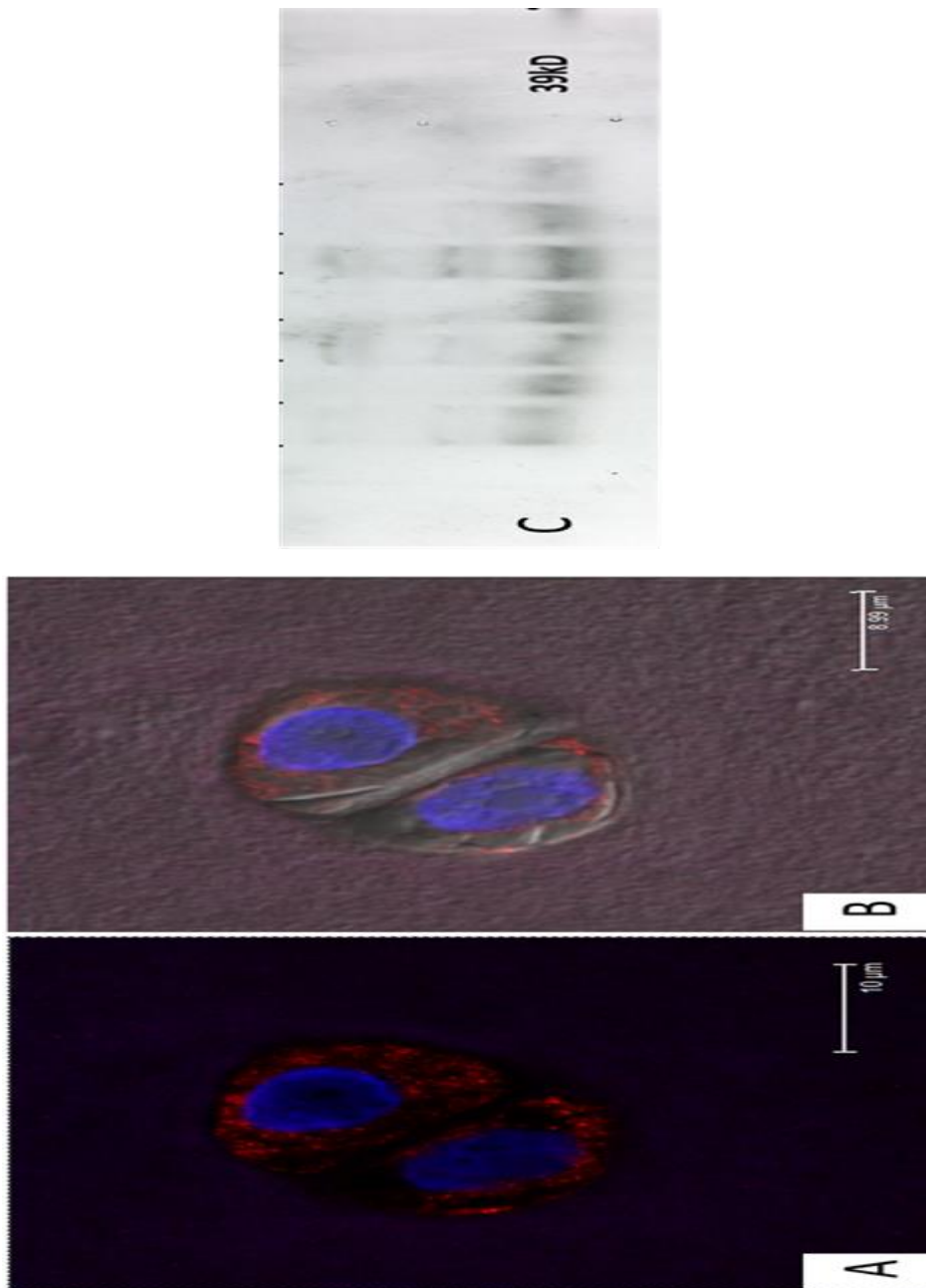


Figure 8. 3: Figure 8.3: Confocal scanning images of Dkk-1 protein in monensin blocked full-depth osteoarthritic cartilage.

Positive intracellular labelling of vesicles containing Dkk-1 proteins (red). X63 Magnification with cellular localisation of Dkk-1 in the cytoplasm (red) in confocal image and differential interference contrast images (A-B respectively). Figure C Dkk-1 Immunoblot of protein lysates from OA tissue show similar band of 39kDa in all patients.

Appendix 5:

| gene symbol | Gene Ref Seq | Description | Analys ed |
|--------------------|---------------------|--|------------------|
| AES | NM_001130 | Amino-terminal enhancer of split/ TLE/Groucho | Yes |
| APC | NM_000038 | Adenomatous polyposis coli | Yes |
| AXIN1 | NM_003502 | Axin 1 | Yes |
| AXIN2 | NM_004655 | Axin 2 | Yes |
| BCL9 | NM_004326 | B-cell CLL/lymphoma 9 | Yes |
| BTRC | NM_033637 | Beta-transducin repeat containing | Yes |
| CCND1 | NM_053056 | Cyclin D1 | Yes |
| CCND2 | NM_001759 | Cyclin D2 | Yes |
| CSNK1A1 | NM_001892 | Casein kinase 1, alpha 1 | Yes |
| CSNK2A1 | NM_001895 | Casein kinase 2, alpha 1 polypeptide | Yes |
| CTBP1 | NM_001328 | C-terminal binding protein 1 | Yes |
| CTNNB1 | NM_001904 | Catenin (cadherin-associated protein), beta 1, 88kDa | Yes |
| CTNNBIP1 | NM_020248 | Catenin, beta interacting protein 1 | Yes |
| CXXC4 | NM_025212 | CXXC finger protein 4 | Yes |
| DAAM1 | NM_014992 | Dishevelled associated activator of morphogenesis 1 | Yes |
| DAB2 | NM_001343 | Disabled homolog 2, mitogen-responsive phosphoprotein (Drosophila) | Yes |
| DIXDC1 | NM_033425 | DIX domain containing 1 | Yes |
| DKK-1 | NM_012242 | Dickkopf homolog 1 (Xenopus laevis) | Yes |
| Dkk2 | | Dickkopf homolog 2 | No |
| DKK3 | NM_015881 | Dickkopf homolog 3 (Xenopus laevis) | Yes |
| Dkk4 | | Dickkopf homolog 4 (Xenopus laevis) | No |
| DVL1 | NM_004421 | Dishevelled, dsh homolog 1 (Drosophila) | Yes |
| DVL2 | NM_004422 | Dishevelled, dsh homolog 2 (Drosophila) | Yes |
| EP300 | NM_001429 | E1A binding protein p300 | Yes |

| | | | |
|---------|--------------|--|-----|
| FBXW11 | NM_012300 | F-box and WD repeat domain containing 11 | Yes |
| FBXW4 | NM_022039 | F-box and WD repeat domain containing 4 | Yes |
| FGF4 | NM_002007 | Fibroblast growth factor 4 | Yes |
| FOSL1 | NM_005438 | FOS-like antigen 1 | Yes |
| FOXN1 | NM_003593 | Forkhead box N1 | Yes |
| FRAT1 | NM_005479 | Frequently rearranged in advanced T-cell lymphomas | Yes |
| FRZB | NM_001463 | Frizzled-related protein | Yes |
| FZD1 | NM_003505 | Frizzled family receptor 1 | Yes |
| FZD2 | NM_001466 | Frizzled family receptor 2 | Yes |
| FZD3 | NM_017412 | Frizzled family receptor 3 | Yes |
| FZD4 | NM_012193 | Frizzled family receptor 4 | Yes |
| FZD5 | NM_003468 | Frizzled family receptor 5 | Yes |
| FZD6 | NM_003506 | Frizzled family receptor 6 | Yes |
| FZD7 | NM_003507 | Frizzled family receptor 7 | Yes |
| FZD8 | NM_031866 | Frizzled family receptor 8 | Yes |
| FZD9 | NM_003508 | Frizzled family receptor 9 | Yes |
| GSK3A | NM_019884 | Glycogen synthase kinase 3 alpha | Yes |
| GSK3B | NM_002093 | Glycogen synthase kinase 3 beta | Yes |
| JUN | NM_002228 | Jun proto-oncogene | Yes |
| KREMEN1 | NM_001039570 | Kringle containing transmembrane protein 1 | Yes |
| LEF1 | NM_016269 | Lymphoid enhancer-binding factor 1 | Yes |
| LRP5 | NM_002335 | Low density lipoprotein receptor-related protein 5 | Yes |
| LRP6 | NM_002336 | Low density lipoprotein receptor-related protein 6 | Yes |
| MAPK8 | NM_002750 | Mitogen-activated protein kinase 8 | Yes |
| MMP7 | NM_002423 | Matrix metalloproteinase 7 (matrilysin, uterine) | Yes |
| MYC | NM_00246 | V-myc myelocytomatosis viral oncogene | Yes |

| | | | |
|----------|-----------|---|-----|
| | 7 | homolog (avian) | |
| NFATC1 | NM_172390 | Nuclear factor of activated T-cells, cytoplasmic, calcineurin-dependent 1 | Yes |
| NKD1 | NM_033119 | Naked cuticle homolog 1 (Drosophila) | Yes |
| NLK | NM_016231 | Nemo-like kinase | Yes |
| PITX2 | NM_000325 | Paired-like homeodomain 2 | Yes |
| PORCN | NM_022825 | Porcupine homolog (Drosophila) | Yes |
| PPARD | NM_006238 | Peroxisome proliferator-activated receptor delta | Yes |
| PRICKLE1 | NM_153026 | Prickle homolog 1 (Drosophila) | Yes |
| PYGO1 | NM_015617 | Pygopus homolog 1 (Drosophila) | Yes |
| RHOA | NM_001664 | Ras homolog gene family, member A | Yes |
| RHOU | NM_021205 | Ras homolog gene family, member U | Yes |
| RUVBL1 | NM_003707 | RuvB-like 1 (E. coli) | Yes |
| SFRP1 | NM_003012 | Secreted frizzled-related protein 1 | Yes |
| SFRP4 | NM_003014 | Secreted frizzled-related protein 4 | Yes |
| SOX17 | NM_022454 | SRY (sex determining region Y)-box 17 | Yes |
| TCF7 | NM_003202 | Transcription factor 7 (T-cell specific, HMG-box) | Yes |
| TCF7L1 | NM_031283 | Transcription factor 7-like 1 (T-cell specific, HMG-box) | Yes |
| TLE1 | NM_005077 | Transducin-like enhancer of split 1 (E(sp1) homolog, Drosophila) | Yes |
| VANGL2 | NM_020335 | Vang-like 2 (van gogh, Drosophila) | Yes |
| WIF1 | NM_007191 | WNT inhibitory factor 1 | Yes |
| WISP1 | NM_003882 | WNT1 inducible signaling pathway protein 1 | Yes |
| WNT1 | NM_005430 | Wingless-type MMTV integration site family, member 1 | Yes |
| WNT10A | NM_025216 | Wingless-type MMTV integration site family, member 10A | Yes |
| WNT11 | NM_004626 | Wingless-type MMTV integration site family, member 11 | Yes |
| WNT16 | NM_057168 | Wingless-type MMTV integration site family, member 16 | Yes |
| WNT2 | NM_003391 | Wingless-type MMTV integration site family member 2 | Yes |

| | | | |
|-------|-----------|---|-----|
| WNT2B | NM_004185 | Wingless-type MMTV integration site family, member 2B | Yes |
| WNT3 | NM_030753 | Wingless-type MMTV integration site family, member 3 | Yes |
| WNT3A | NM_033131 | Wingless-type MMTV integration site family, member 3A | Yes |
| WNT4 | NM_030761 | Wingless-type MMTV integration site family, member 4 | Yes |
| WNT5A | NM_003392 | Wingless-type MMTV integration site family, member 5A | Yes |
| WNT5B | NM_032642 | Wingless-type MMTV integration site family, member 5B | Yes |
| WNT6 | NM_006522 | Wingless-type MMTV integration site family, member 6 | Yes |
| WNT7A | NM_004625 | Wingless-type MMTV integration site family, member 7A | Yes |
| WNT7B | NM_058238 | Wingless-type MMTV integration site family, member 7B | Yes |
| WNT8A | NM_058244 | Wingless-type MMTV integration site family, member 8A | Yes |
| WNT9A | NM_003395 | Wingless-type MMTV integration site family, member 9A | Yes |
| ACTB | NM_001101 | Actin, beta | Yes |
| B2M | NM_004048 | Beta-2-microglobulin | Yes |
| GAPDH | NM_002046 | Glyceraldehyde-3-phosphate dehydrogenase | Yes |
| HPRT1 | NM_000194 | Hypoxanthine phosphoribosyltransferase 1 | Yes |
| RPLP0 | NM_001002 | Ribosomal protein, large, P0 | Yes |
| HGDC | SA_00105 | Human Genomic DNA Contamination | Yes |
| RTC | SA_00104 | Reverse Transcription Control | Yes |
| RTC | SA_00104 | Reverse Transcription Control | Yes |
| RTC | SA_00104 | Reverse Transcription Control | Yes |
| PPC | SA_00103 | Positive PCR Control | Yes |
| PPC | SA_00103 | Positive PCR Control | Yes |
| PPC | SA_00103 | Positive PCR Control | Yes |

Appendix 6:

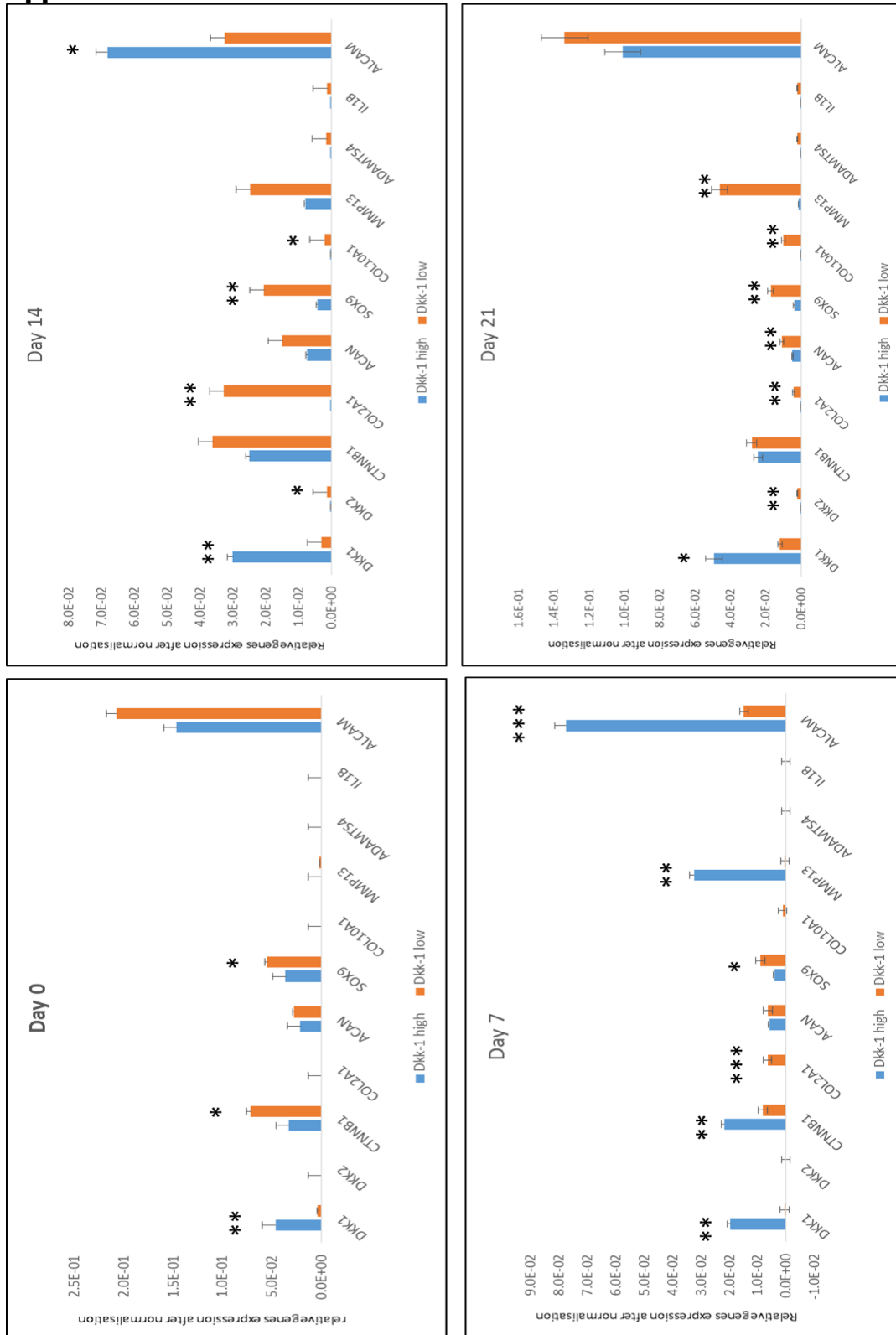
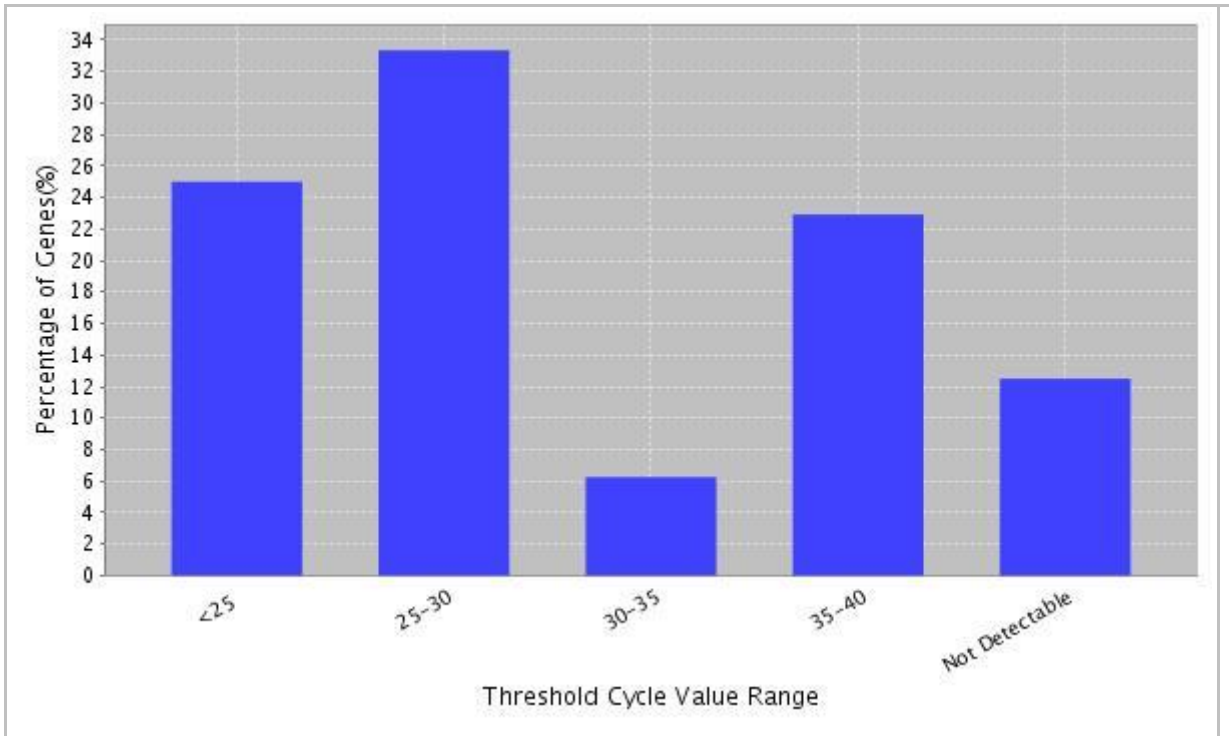


Figure 8. 4: Summary of CPC chondrogenic differentiation experiments at time points 0, 7, 14 & 21.

Appendix 7:

| Position | Gene Symbol | Control Gene | Control Group | | | Group 1 | | |
|--------------------------------|-------------|--------------|---------------|----------|----------|----------|----------|----------|
| | | | Sample 1 | Sample 2 | Sample 3 | Sample 4 | Sample 5 | Sample 6 |
| 12 | B2M | ✘ | 23.84 | 21.73 | 23.68 | 21.18 | 22.10 | 21.27 |
| 13 | GAPDH | ✘ | 22.54 | 21.88 | 22.95 | 22.11 | 22.02 | 22.23 |
| Arithmetic Mean | | | 22.54 | 21.88 | 22.95 | 22.11 | 22.02 | 22.23 |
| Avg. of Arithmetic Mean | | | 22.46 | | | 22.12 | | |
| Geometric Mean | | | 22.54 | 21.88 | 22.95 | 22.11 | 22.02 | 22.23 |
| Avg. of Geometric Mean | | | 22.46 | | | 22.12 | | |

| C _t Range | Distribution of C _t Values | | | Average | ST DEV |
|---|---------------------------------------|----------|----------|---------|--------|
| | Sample 4 | Sample 5 | Sample 6 | | |
| <25 | 4 | 4 | 4 | 4.00 | 0 |
| 25-30 | 5 | 6 | 5 | 5.33 | 0.5774 |
| 30-35 | 1 | 0 | 2 | 1.00 | 1.0000 |
| Absent Calls | 6 | 6 | 5 | 5.67 | 0.5774 |
| Percent Distribution of C _t Values | | | | | |
| <25 | 25.00% | 25.00% | 25.00% | 25.00% | 0 |
| 25-30 | 31.25% | 37.50% | 31.25% | 33.33% | 0.0361 |
| 30-35 | 6.25% | 0.00% | 12.50% | 6.25% | 0.0625 |
| Absent Calls | 37.50% | 37.50% | 31.25% | 35.42% | 0.0361 |



| Position | Gene Symbol | Average | ST DEV | Sample 4 | Sample 5 | Sample 6 |
|----------|-------------|---------|----------|----------|----------|----------|
| 1 | DKK1 | 27.79 | 0.904908 | 26.81 | 27.98 | 28.59 |
| 2 | DKK2 | 35.00 | 0 | 36.23 | 35.89 | 35.35 |
| 3 | CTNNB1 | 27.64 | 0.410099 | 27.99 | 27.74 | 27.19 |
| 4 | COL2A1 | 35.00 | 0 | 35.77 | No Ct | No Ct |
| 5 | ACAN | 29.54 | 1.771883 | 31.57 | 28.73 | 28.31 |
| 6 | SOX9 | 30.02 | 1.420408 | 28.75 | 29.75 | 31.55 |
| 7 | COL10A1 | 34.68 | 0.554256 | 35.80 | 35.46 | 34.04 |
| 8 | MMP13 | 27.07 | 1.691036 | 28.87 | 26.83 | 25.51 |
| 9 | ADAMTS4 | 35.00 | 0 | No Ct | 39.28 | 38.67 |
| 10 | IL1B | 35.00 | 0 | 37.34 | 37.38 | No Ct |
| 11 | ALCAM | 25.81 | 0.410406 | 26.18 | 25.37 | 25.89 |
| 12 | B2M | 21.52 | 0.507995 | 21.18 | 22.10 | 21.27 |
| 13 | GAPDH | 22.12 | 0.108543 | 22.11 | 22.02 | 22.23 |
| 14 | HIGX1A | 35.00 | 0 | 39.72 | No Ct | No Ct |
| 15 | RTC | 23.99 | 0.399291 | 24.16 | 23.53 | 24.27 |
| 16 | PPC | 20.01 | 0.147460 | 20.17 | 19.88 | 19.97 |

Select Group:

Standard RT² cDNA Synthesis Kit used

Standard RT² cDNA Synthesis Kit used with RT² Arrays Performed on Rotor-Gene Q

RT² PreAMP cDNA Synthesis Kit used with fresh/frozen samples*

RT² PreAMP cDNA Synthesis Kit used with fixed samples (FFPE)* 

*Note: The respective RT² PreAMP cDNA Synthesis Kit analysis settings also apply when the PreAMP kits are used with RT² Arrays performed on Rotor-Gene Q.

Quality Checks Performed

| Test Performed | Sample 4 | Sample 5 | Sample 6 |
|------------------------------|----------|----------|----------|
| 1. PCR Array Reproducibility | Pass | Pass | Pass |
| 2. RT Efficiency | Pass | Pass | Pass |
| 3. Genomic DNA Contamination | Pass | Pass | Pass |

- Remember to check each experimental group
- If 'Inquiry' is displayed then see the Troubleshooting Guide of the PCR Array User Manual/Handbook or Contact Technical Support at 888-503-3187.

Calculations Supporting Data Above

1. PCR Array Reproducibility:

| Array | Sample 4 | Sample 5 | Sample 6 | AVG | ST DEV |
|------------------|----------|----------|----------|-------|--------|
| Average Ct (PPC) | 20.17 | 19.88 | 19.97 | 20.01 | 0.15 |
| ST DEV Ct (PPC) | N/A | N/A | N/A | 0 | -- |
| Average Ct (RTC) | 24.16 | 23.53 | 24.27 | 23.99 | 0.4 |
| ST DEV Ct (RTC) | N/A | N/A | N/A | 0 | -- |

Criteria for the PCR Array Reproducibility: If the Average PPC C_t is 20±2 and no two arrays have Average PPC C_t are > 2 away from another then the sample and group Pass.

2. Reverse Transcription Control (RTC):

| Array | Sample 4 | Sample 5 | Sample 6 |
|------------------------------|----------|----------|----------|
| Delta Ct (AVG RTC - AVG PPC) | 3.99 | 3.65 | 4.3 |
| RT Efficiency | Pass | Pass | Pass |

Criteria: If Delta C_t (AVG RTC - AVG PPC) ≤ 5, RT Efficiency reports 'Pass'; otherwise, RT Efficiency reports 'Inquiry'. See the Troubleshooting Guide of the PCR Array User Manual or Contact Technical Support at 888-503-3187.

3. Genomic DNA Contamination (GDC):

| Array | Sample 4 | Sample 5 | Sample 6 |
|----------------------|----------|----------|----------|
| C _t (GDC) | N/A | N/A | N/A |
| Genomic DNA | N/A | N/A | N/A |

Criteria: If C_t(GDC) ≥ 35, then the GDC QC reports 'Pass'; if C_t(GDC) < 35, then the GDC QC reports 'Inquiry'. See the Troubleshooting Guide of the PCR Array User Manual or Contact Technical Support at 888-503-3187.

Appendix 8:

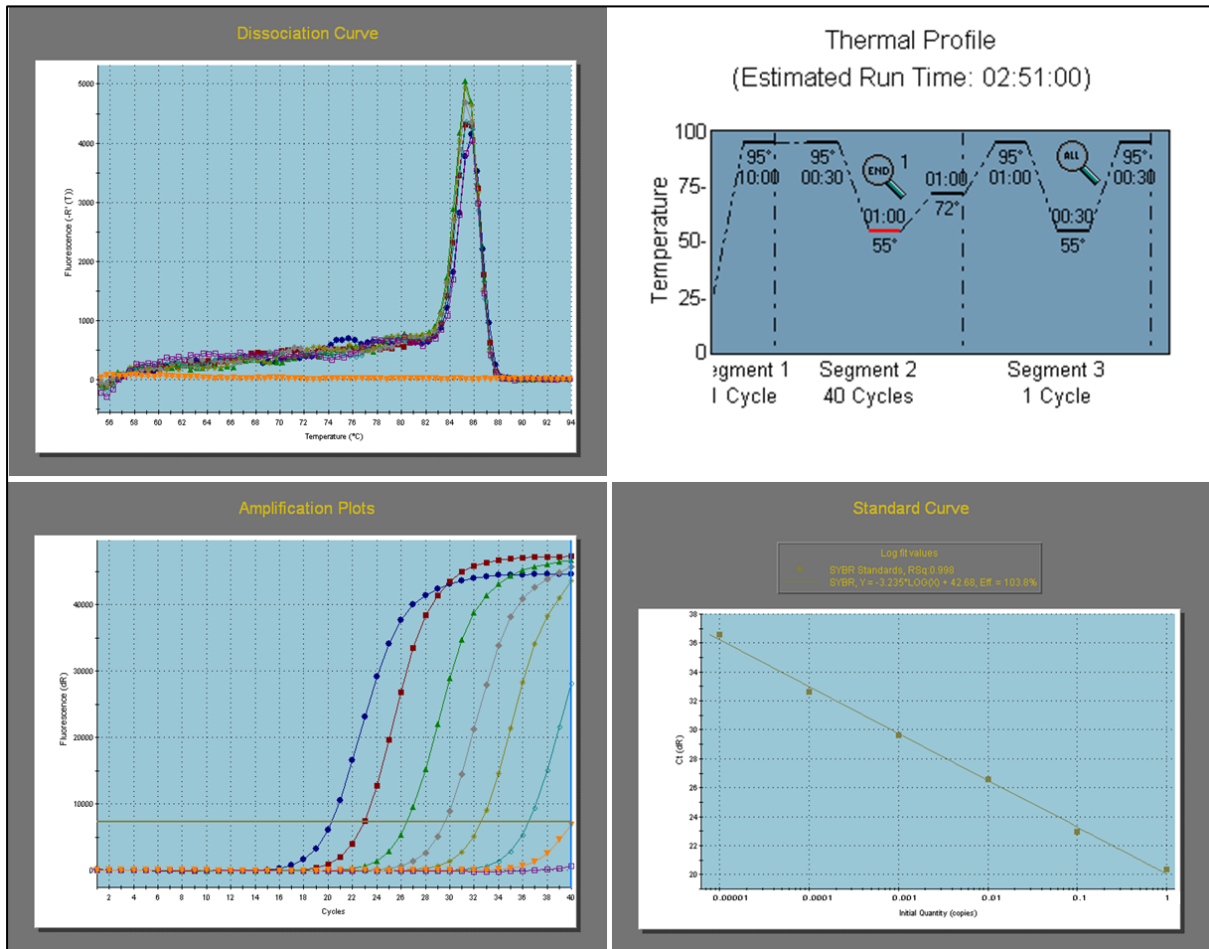


Figure 8. 5: Amplification, dissociation, thermal profile setup and standard curve of PCR reaction of GAPDH.

Appendix 9:

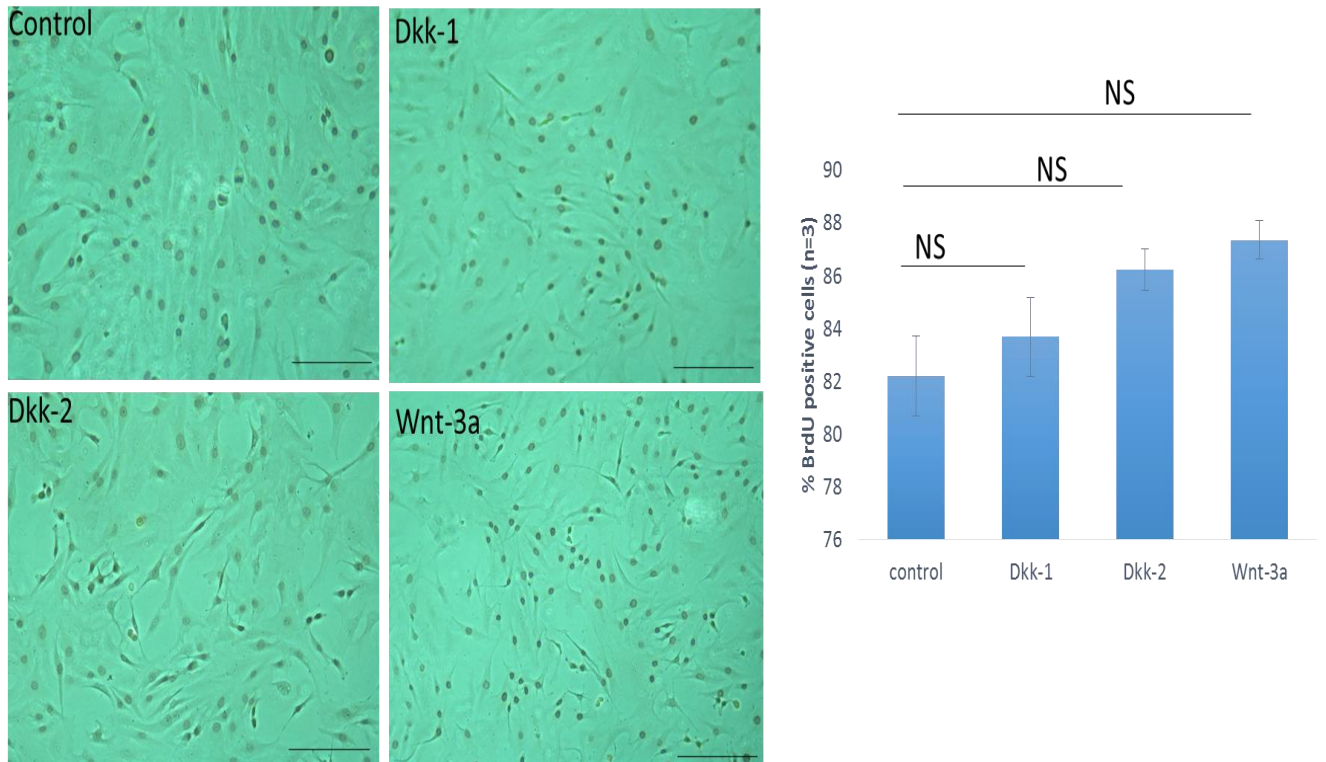


Figure 8. 6: BrdU-incorporated assay was used to determinate the cell proliferation after treatment with Wnt canonical modulators.

BrdU incorporation assay of CPC with different treatments of exogenous Wnt proteins modulators. Nuclear localisation of BrdU was examined in CPC treated with basal media \pm Dkk-1, Dkk-2, Wnt-3a all at 100ng/mL treatment for 48hrs. The percentage of positive stained cells was calculated (n=3) for each cell line and data are presented as mean \pm SEM. One-Way ANOVA to compare percentage BrdU incorporation of control with treated. NS=not significant.

References:

- AIGNER, T. & STOVE, J. 2003. COLLAGENS--MAJOR COMPONENT OF THE PHYSIOLOGICAL CARTILAGE MATRIX, MAJOR TARGET OF CARTILAGE DEGENERATION, MAJOR TOOL IN CARTILAGE REPAIR. *ADV DRUG DELIV REV*, 55, 1569-93.
- AKIRI, G., CHERIAN, M. M., VIJAYAKUMAR, S., LIU, G., BAFICO, A. & AARONSON, S. A. 2009. WNT PATHWAY ABERRATIONS INCLUDING AUTOCRINE WNT ACTIVATION OCCUR AT HIGH FREQUENCY IN HUMAN NON-SMALL-CELL LUNG CARCINOMA. *ONCOGENE*, 28, 2163-2172.
- AKIYAMA, H., LYONS, J. P., MORI-AKIYAMA, Y., YANG, X., ZHANG, R., ZHANG, Z., DENG, J. M., TAKETO, M. M., NAKAMURA, T., BEHRINGER, R. R., MCCREA, P. D. & DE CROMBRUGGHE, B. 2004. Interactions between Sox9 and beta-catenin control chondrocyte differentiation. *Genes Dev*, 18, 1072-87.
- AL-HAJJ, M., WICHA, M. S., BENITO-HERNANDEZ, A., MORRISON, S. J. & CLARKE, M. F. 2003. PROSPECTIVE IDENTIFICATION OF TUMORIGENIC BREAST CANCER CELLS. *PROCEEDINGS OF THE NATIONAL ACADEMY OF SCIENCES*, 100, 3983-3988.
- ALSALAMEH, S., AMIN, R., GEMBA, T. & LOTZ, M. 2004. Identification of mesenchymal progenitor cells in normal and osteoarthritic human articular cartilage. *Arthritis & Rheumatism*, 50, 1522-1532.
- ARCHER, C. W., DOWTHWAITE, G. P. & FRANCIS-WEST, P. 2003. DEVELOPMENT OF SYNOVIAL JOINTS. *Birth Defects Res C Embryo Today*, 69, 144-55.
- ARNAOUTOVA, I. & KLEINMAN, H. K. 2010. IN VITRO ANGIOGENESIS: ENDOTHELIAL CELL TUBE FORMATION ON GELLED BASEMENT MEMBRANE EXTRACT. *NAT. PROTOCOLS*, 5, 628-635.
- ARNER, E. C., HUGHES, C. E., DECICCO, C. P., CATERSON, B. & TORTORELLA, M. D. 1998. CYTOKINE-INDUCED CARTILAGE PROTEOGLYCAN DEGRADATION IS MEDIATED BY AGGRECANASE. *OSTEOARTHRITIS CARTILAGE*, 6, 214-28.
- ARTHRITIS AND MUSCULOSKELETAL ALLIANCE 2004. STANDARDS OF CARE FOR PEOPLE WITH OSTEOARTHRITIS. ARMA.

- ARTHRITIS RESEARCH UK. 2013. OSTEOARTHRITIS IN GENERAL PRACTICE DATA AND PERSPECTIVES [ONLINE].
- AYDELOTTE, M. B., RAISS, R. X., CATERSON, B. & KUETTNER, K. E. 1992. INFLUENCE OF INTERLEUKIN-1 ON THE MORPHOLOGY AND PROTEOGLYCAN METABOLISM OF CULTURED BOVINE ARTICULAR CHONDROCYTES. *CONNECT TISSUE RES*, 28, 143-59.
- BAFICO, A., LIU, G., YANIV, A., GAZIT, A. & AARONSON, S. A. 2001. NOVEL MECHANISM OF WNT SIGNALLING INHIBITION MEDIATED BY DICKKOPF-1 INTERACTION WITH LRP6/ARROW. *NAT CELL BIOL*, 3, 683-6.
- BAJADA, S., MARSHALL, M. J., WRIGHT, K. T., RICHARDSON, J. B. & JOHNSON, W. E. B. 2009. DECREASED OSTEOGENESIS, INCREASED CELL SENESCENCE AND ELEVATED DICKKOPF-1 SECRETION IN HUMAN FRACTURE NON UNION STROMAL CELLS. *BONE*, 45, 726-735.
- BALL, S. G., WORTHINGTON, J. J., CANFIELD, A. E., MERRY, C. L. & KIELTY, C. M. 2014. MESENCHYMAL STROMAL CELLS: INHIBITING PDGF RECEPTORS OR DEPLETING FIBRONECTIN INDUCES MESODERMAL PROGENITORS WITH ENDOTHELIAL POTENTIAL. *STEM CELLS*, 32, 694-705.
- BANFI, A., MURAGLIA, A., DOZIN, B., MASTROGIACOMO, M., CANCEDDA, R. & QUARTO, R. 2000. PROLIFERATION KINETICS AND DIFFERENTIATION POTENTIAL OF EX VIVO EXPANDED HUMAN BONE MARROW STROMAL CELLS: IMPLICATIONS FOR THEIR USE IN CELL THERAPY. *EXP HEMATOL*, 28, 707-15.
- BARA, J. J., JOHNSON, W. E., CATERSON, B. & ROBERTS, S. 2012. ARTICULAR CARTILAGE GLYCOSAMINOGLYCANS INHIBIT THE ADHESION OF ENDOTHELIAL CELLS. *CONNECT TISSUE RES*, 53, 220-8.
- BARKER, N., VAN ES, J. H., KUIPERS, J., KUJALA, P., VAN DEN BORN, M., COZIJNSEN, M., HAEGEBARTH, A. ET AL. (2007). IDENTIFICATION OF STEM CELLS IN SMALL INTESTINE AND COLON BY MARKER GENE LGR5. *NATURE*, 449:1003-1007.
- BERGERS, G. & BENJAMIN, L. E. 2003. TUMORIGENESIS AND THE ANGIOGENIC SWITCH. *NAT REV CANCER*, 3, 401-410.

- BERNARDO, B. C., BELLUOCIO, D., ROWLEY, L., LITTLE, C. B., HANSEN, U. & BATEMAN, J. F. 2011. CARTILAGE INTERMEDIATE LAYER PROTEIN 2 (CILP-2) IS EXPRESSED IN ARTICULAR AND MENISCAL CARTILAGE AND DOWN-REGULATED IN EXPERIMENTAL OSTEOARTHRITIS. *J BIOL CHEM*, 286, 37758-67.
- BIANCO, P., RIMINUCCI, M., GRONTHOS, S. & ROBEY, P. G. 2001. BONE MARROW STROMAL STEM CELLS: NATURE, BIOLOGY, AND POTENTIAL APPLICATIONS. *STEM CELLS*, 19, 180-92.
- BLAUWKAMP, T. A., NIGAM, S., ARDEHALI, R., WEISSMAN, I. L. & NUSSE, R. 2012. ENDOGENOUS WNT SIGNALLING IN HUMAN EMBRYONIC STEM CELLS GENERATES AN EQUILIBRIUM OF DISTINCT LINEAGE-SPECIFIED PROGENITORS. *NATURE COMMUNICATIONS*, 3, 1070.
- BLOM, A. B., BROCKBANK, S. M., VAN LENT, P. L., VAN BEUNINGEN, H. M., GEURTS, J., TAKAHASHI, N., VAN DER KRAAN, P. M. ET AL. (2009). INVOLVEMENT OF THE WNT SIGNALING PATHWAY IN EXPERIMENTAL AND HUMAN OSTEOARTHRITIS: PROMINENT ROLE OF WNT-INDUCED SIGNALING PROTEIN 1. *ARTHRITIS & RHEUMATISM*, 60:501-512.
- BONEWALD, L. F. & JOHNSON, M. L. 2008. OSTEOCYTES, MECHANOSENSING AND WNT SIGNALING. *BONE*, 42, 606-615.
- BONEWALD, L. F. & JOHNSON, M. L. 2008. Osteocytes, Mechanosensing and Wnt Signaling. *Bone*, 42, 606-615.
- BONEWALD, L. F. 2011. THE AMAZING OSTEOCYTE. *JOURNAL OF BONE AND MINERAL RESEARCH*, 26, 229-238.
- BONNET, C. S. & WALSH, D. A. 2005. OSTEOARTHRITIS, ANGIOGENESIS AND INFLAMMATION. *RHEUMATOLOGY (OXFORD)*, 44, 7-16.
- BONNET, C. S., WILLIAMS, A. S., GILBERT, S. J., HARVEY, A. K., EVANS, B. A. & MASON, D. J. 2013. AMPA/KAINATE GLUTAMATE RECEPTORS CONTRIBUTE TO INFLAMMATION, DEGENERATION AND PAIN RELATED BEHAVIOUR IN INFLAMMATORY STAGES OF ARTHRITIS. *ANN RHEUM DIS*.
- BOXALL, S. A. & JONES, E. 2012. MARKERS FOR CHARACTERIZATION OF BONE MARROW MULTIPOTENTIAL STROMAL CELLS. *STEM CELLS INTERNATIONAL*, 2012, 12.

- BRITTBERG, M., LINDAHL, A., NILSSON, A., OHLSSON, C., ISAKSSON, O. & PETERSON, L. 1994. TREATMENT OF DEEP CARTILAGE DEFECTS IN THE KNEE WITH AUTOLOGOUS CHONDROCYTE TRANSPLANTATION. *N ENGL J MED*, 331, 889-95.
- BRUNI-CARDOSO, A., JOHNSON, L. C., VESSELLA, R. L., PETERSON, T. E. & LYNCH, C. C. 2010. OSTEOCLAST DERIVED MATRIX METALLOPROTEINASE-9 DIRECTLY IMPACTS ANGIOGENESIS IN THE PROSTATE TUMOR-BONE MICROENVIRONMENT. *MOLECULAR CANCER RESEARCH*, 8, 459-470.
- BUCKWALTER, J. A. & MANKIN, H. J. 1998. ARTICULAR CARTILAGE: TISSUE DESIGN AND CHONDROCYTE-MATRIX INTERACTIONS. *INSTR COURSE LECT*, 47, 477-86.
- BUCKWALTER, J. A. H., E.B 1999. ARTICULAR CARTILAGE MORPHOLOGY AND BIOLOGY. IN: ARCHER, C. W. C., B (ED.) *BIOLOGY OF THE SYNOVIAL JOINT*. AMSTERDAM: HARWOOD ACADEMICS.
- CAKOWSKI, F. C., ANDERSON, J. L., PATRENE, K. D., CHOKSI, R. J., SHAPIRO, S. D., WINDLE, J. J., BLAIR, H. C. & ROODMAN, G. D. 2010. OSTEOCLASTS ARE IMPORTANT FOR BONE ANGIOGENESIS. *BLOOD*, 115, 140-9.
- CANO, A., PEREZ-MORENO, M. A., RODRIGO, I., LOCASCIO, A., BLANCO, M. J., DEL BARRIO, M. G., PORTILLO, F. ET AL. (2000). THE TRANSCRIPTION FACTOR SNAIL CONTROLS EPITHELIAL-MESENCHYMAL TRANSITIONS BY REPRESSING E-CADHERIN EXPRESSION. *NAT CELL BIOL*, 2:76-83.
- CARMON, K. S., LIN, Q., GONG, X., THOMAS, A. & LIU, Q. 2012. LGR5 INTERACTS AND COINTERNALIZES WITH WNT RECEPTORS TO MODULATE WNT/BETA-CATENIN SIGNALING. *MOL CELL BIOL*, 32, 2054-64.
- CHAN, B. Y., FULLER, E. S., RUSSELL, A. K., SMITH, S. M., SMITH, M. M., JACKSON, M. T., CAKE, M. A., READ, R. A., BATEMAN, J. F., SAMBROOK, P. N. & LITTLE, C. B. 2011. INCREASED CHONDROCYTE SCLEROSTIN MAY PROTECT AGAINST CARTILAGE DEGRADATION IN OSTEOARTHRITIS. *OSTEOARTHRITIS CARTILAGE*, 19, 874-85.
- CHEN, L., LI, M., LI, Q., WANG, C. J. & XIE, S. Q. 2013. DKK-1 PROMOTES HEPATOCELLULAR CARCINOMA CELL MIGRATION AND INVASION THROUGH BETA-CATENIN/MMP7 SIGNALING PATHWAY. *MOL CANCER*, 12, 157.

- CHENG, S.-L., SHAO, J.-S., BEHRMANN, A., KRCHMA, K. AND TOWLER, D. A. (2013). DKK-1 AND MSX2-WNT7B SIGNALING RECIPROCALLY REGULATE THE ENDOTHELIAL-MESENCHYMAL TRANSITION IN AORTIC ENDOTHELIAL CELLS. *ARTERIOSCLEROSIS, THROMBOSIS, AND VASCULAR BIOLOGY*, 33:10.1161-300647.
- CHRISTODOULIDES, C., LAUDES, M., CAWTHORN, W. P., SCHINNER, S., SOOS, M., O'RAHILLY, S., SETHI, J. K. & VIDAL-PUIG, A. 2006. THE WNT ANTAGONIST DICKKOPF-1 AND ITS RECEPTORS ARE COORDINATELY REGULATED DURING EARLY HUMAN ADIPOGENESIS. *J CELL SCI*, 119, 2613-20.
- CLARK, J. M. 1990. THE ORGANISATION OF COLLAGEN FIBRILS IN THE SUPERFICIAL ZONES OF ARTICULAR CARTILAGE. *J ANAT*, 171, 117-30.
- CLARKE, B. 2008. NORMAL BONE ANATOMY AND PHYSIOLOGY. *CLINICAL JOURNAL OF THE AMERICAN SOCIETY OF NEPHROLOGY*, 3, S131-S139.
- CLEVERS, H. AND NUSSE, R. 2012. WNT/BETA-CATENIN SIGNALING AND DISEASE. *CELL*, 149:1192-1205.
- CORNELIS, F. M., LUYTEN, F. P. AND LORIES, R. J., 2011. FUNCTIONAL EFFECTS OF SUSCEPTIBILITY GENES IN OSTEOARTHRITIS. *DISCOV MED* , 12,129–39.
- CUI, Y., NIZIOLEK, P. J., MACDONALD, B. T., ZYLSTRA, C. R., ALENINA, N., ROBINSON, D. R., ZHONG, Z. *ET AL.* (2011). LRP5 FUNCTIONS IN BONE TO REGULATE BONE MASS. *NAT MED*, 17:684-691.
- DAOUSSIS, D., LIOSSIS, S. N., SOLOMOU, E. E., TSANAKTSI, A., BOUNIA, K., KARAMPETSOU, M., YIANNOPOULOS, G. & ANDONOPOULOS, A. P. 2010. EVIDENCE THAT DKK-1 IS DYSFUNCTIONAL IN ANKYLOSING SPONDYLITIS. *ARTHRITIS & RHEUMATISM*, 62, 150-8.
- DE LAU, W. B., SNEL, B. & CLEVERS, H. C. 2012. THE R-SPONDIN PROTEIN FAMILY. *GENOME BIOL*, 13, 242.
- DE LAU, W., PENG, W. C., GROS, P. & CLEVERS, H. 2014. THE R-SPONDIN/LGR5/RNF43 MODULE: REGULATOR OF WNT SIGNAL STRENGTH. *GENES DEV*, 28, 305-16.
- DEANFIELD, J. E., HALCOX, J. P. & RABELINK, T. J. 2007. ENDOTHELIAL FUNCTION AND DYSFUNCTION: TESTING AND CLINICAL RELEVANCE. *CIRCULATION*, 115, 1285-1295.

- DEBACQ-CHAINIAUX, F., ERUSALIMSKY, J. D., CAMPISI, J. AND TOUSSAINT, O. (2009). PROTOCOLS TO DETECT SENESENCE-ASSOCIATED BETA-GALACTOSIDASE (SA-BETAGAL) ACTIVITY, A BIOMARKER OF SENESENCE CELLS IN CULTURE AND IN VIVO. NAT PROTOC, 4:1798-1806.
- DELISE, A. M., FISCHER, L. & TUAN, R. S. 2000. CELLULAR INTERACTIONS AND SIGNALING IN CARTILAGE DEVELOPMENT. OSTEOARTHRITIS CARTILAGE, 8, 309-34.
- DIARRA, D., STOLINA, M., POLZER, K., ZWERINA, J., OMINSKY, M. S., DWYER, D., KORB, A., SMOLEN, J., HOFFMANN, M., SCHEINECKER, C., VAN DER HEIDE, D., LANDEWE, R., LACEY, D., RICHARDS, W. G. & SCHETT, G. 2007. DICKKOPF-1 IS A MASTER REGULATOR OF JOINT REMODELING. NAT MED, 13, 156-63.
- DIARRA, D., STOLINA, M., POLZER, K., ZWERINA, J., OMINUTESKY, M. S., DWYER, D., KORB, A., SMOLEN, J., HOFFMANN, M., SCHEINECKER, C., VAN DER HEIDE, D., LANDEWE, R., LACEY, D., RICHARDS, W. G. & SCHETT, G. 2007. Dickkopf-1 is a master regulator of joint remodeling. Nat Med, 13, 156-63.
- DIAZ-ROMERO, J., GAILLARD, J. P., GROGAN, S. P., NESIC, D., TRUB, T. & MAINIL-VARLET, P. 2005. IMMUNOPHENOTYPIC ANALYSIS OF HUMAN ARTICULAR CHONDROCYTES: CHANGES IN SURFACE MARKERS ASSOCIATED WITH CELL EXPANSION IN MONOLAYER CULTURE. J CELL PHYSIOL, 202, 731-42.
- DIMRI, G. P., LEE, X., BASILE, G., ACOSTA, M., SCOTT, G., ROSKELLEY, C., MEDRANO, E. E., LINSKENS, M., RUBELJ, I., PEREIRA-SMITH, O. & ET AL. 1995. A BIOMARKER THAT IDENTIFIES SENESENCE HUMAN CELLS IN CULTURE AND IN AGING SKIN IN VIVO. PROC NATL ACAD SCI U S A, 92, 9363-7.
- DOMINICI, M., LE BLANC, K., MUELLER, I., SLAPER-CORTENBACH, I., MARINI, F., KRAUSE, D., DEANS, R., KEATING, A., PROCKOP, D. & HORWITZ, E. 2006. MINIMAL CRITERIA FOR DEFINING MULTIPOTENT MESENCHYMAL STROMAL CELLS. THE INTERNATIONAL SOCIETY FOR CELLULAR THERAPY POSITION STATEMENT. CYTOTHERAPY, 8, 315-7.

- DONG, Y. F., SOUNG DO, Y., SCHWARZ, E. M., O'KEEFE, R. J. & DRISSI, H. 2006. WNT INDUCTION OF CHONDROCYTE HYPERTROPHY THROUGH THE RUNX-2 TRANSCRIPTION FACTOR. *J CELL PHYSIOL*, 208, 77-86.
- DOWTHWAITE, G. P., BISHOP, J. C., REDMAN, S. N., KHAN, I. M., ROONEY, P., EVANS, D. J., HAUGHTON, L., BAYRAM, Z., BOYER, S., THOMSON, B., WOLFE, M. S. & ARCHER, C. W. 2004. THE SURFACE OF ARTICULAR CARTILAGE CONTAINS A PROGENITOR CELL POPULATION. *J CELL SCI*, 117, 889-97.
- DUANCE VC. VAUGHAN-THOMAS, A., WARDALE, RJ. WOTTON, SF. 1999. THE COLLAGENS OF ARTICULAR AND MENISCAL CARTILAGES. IN: ARCHER, C., CATERSON, B, BENJAMIN, M, RALPHS JR. (ED.) BIOLOGY OF THE SYNOVIAL JOINT. AMSTERDAM: HARWOOD ACADEMIC PUBLISHERS.
- DUDHIA, J. 2005. AGGREGAN, AGING AND ASSEMBLY IN ARTICULAR CARTILAGE. *CELL MOL LIFE SCI*, 62, 2241-56.
- DUERR, S., STREMME, S., SOEDER, S., BAU, B. & AIGNER, T. 2004. MMP-2/GELATINASE A IS A GENE PRODUCT OF HUMAN ADULT ARTICULAR CHONDROCYTES AND IS INCREASED IN OSTEOARTHRITIC CARTILAGE. *CLIN EXP RHEUMATOL*, 22, 603-8.
- EGEBLAD, M. & WERB, Z. 2002. NEW FUNCTIONS FOR THE MATRIX METALLOPROTEINASES IN CANCER PROGRESSION. *NAT REV CANCER*, 2, 161-74.
- ENOMOTO-IWAMOTO, M., KITAGAKI, J., KOYAMA, E., TAMAMURA, Y., WU, C., KANATANI, N., KOIKE, T., OKADA, H., KOMORI, T., YONEDA, T., CHURCH, V., FRANCIS-WEST, P. H., KURISU, K., NOHNO, T., PACIFICI, M. & IWAMOTO, M. 2002. THE WNT ANTAGONIST FRZB-1 REGULATES CHONDROCYTE MATURATION AND LONG BONE DEVELOPMENT DURING LIMB SKELETOGENESIS. *DEV BIOL*, 251, 142-56.
- EWAN, K., PAJAK, B., STUBBS, M., TODD, H., BARBEAU, O., QUEVEDO, C., BOTFIELD, H., YOUNG, R., RUDDLE, R., SAMUEL, L., BATTERSBY, A., RAYNAUD, F., ALLEN, N., WILSON, S., LATINKIC, B., WORKMAN, P., MCDONALD, E., BLAGG, J., AHERNE, W. & DALE, T. 2010. A USEFUL

- APPROACH TO IDENTIFY NOVEL SMALL-MOLECULE INHIBITORS OF WNT-DEPENDENT TRANSCRIPTION. *CANCER RES*, 70, 5963-73.
- EYRE, D. 2002. COLLAGEN OF ARTICULAR CARTILAGE. *ARTHRITIS RES*, 4, 30-5.
- EYRE, D. R. & WU, J. J. 1995. COLLAGEN STRUCTURE AND CARTILAGE MATRIX INTEGRITY. *J RHEUMATOL SUPPL*, 43, 82-5.
- FEDARKO, N. S., VETTER, U. K., WEINSTEIN, S. & ROBEY, P. G. 1992. AGE-RELATED CHANGES IN HYALURONAN, PROTEOGLYCAN, COLLAGEN, AND OSTEOLECTIN SYNTHESIS BY HUMAN BONE CELLS. *JOURNAL OF CELLULAR PHYSIOLOGY*, 151, 215-227.
- FEDARKO, N. S., VETTER, U. K., WEINSTEIN, S. AND ROBEY, P. G. (1992). AGE-RELATED CHANGES IN HYALURONAN, PROTEOGLYCAN, COLLAGEN, AND OSTEOLECTIN SYNTHESIS BY HUMAN BONE CELLS. *JOURNAL OF CELLULAR PHYSIOLOGY*, 151:215-227.
- FERNANDES, J. C., MARTEL-PELLETIER, J. & PELLETIER, J. P. 2002. THE ROLE OF CYTOKINES IN OSTEOARTHRITIS PATHOPHYSIOLOGY. *BIORHEOLOGY*, 39, 237-46.
- FICKERT, S., FIEDLER, J. & BRENNER, R. E. 2004. IDENTIFICATION OF SUBPOPULATIONS WITH CHARACTERISTICS OF MESENCHYMAL PROGENITOR CELLS FROM HUMAN OSTEOARTHRITIC CARTILAGE USING TRIPLE STAINING FOR CELL SURFACE MARKERS. *ARTHRITIS RES THER*, 6, R422-32.
- FLANNERY, C. R., HUGHES, C. E., SCHUMACHER, B. L., TUDOR, D., AYDELOTTE, M. B., KUETTNER, K. E. & CATERSON, B. 1999. ARTICULAR CARTILAGE SUPERFICIAL ZONE PROTEIN (SZP) IS HOMOLOGOUS TO MEGAKARYOCYTE STIMULATING FACTOR PRECURSOR AND IS A MULTIFUNCTIONAL PROTEOGLYCAN WITH POTENTIAL GROWTH-PROMOTING, CYTOPROTECTIVE, AND LUBRICATING PROPERTIES IN CARTILAGE METABOLISM. *BIOCHEM BIOPHYS RES COMMUN*, 254, 535-41.
- FUJIMORI, S., NOVAK, H., WEISSENBOCK, M., JUSSILA, M., GONCALVES, A., ZELLER, R., GALLOWAY, J., THESLEFF, I. & HARTMANN, C. 2010. WNT/BETA-CATENIN SIGNALING IN THE DENTAL MESENCHYME REGULATES INCISOR DEVELOPMENT BY REGULATING BMP4. *DEV BIOL*, 348, 97-106.

- FUNCK-BRENTANO, T. & COHEN-SOLAL, M. 2011. CROSSTALK BETWEEN CARTILAGE AND BONE: WHEN BONE CYTOKINES MATTER. *CYTOKINE & GROWTH FACTOR REVIEWS*, 22, 91-97.
- GANNON, J. M., WALKER, G., FISCHER, M., CARPENTER, R., THOMPSON, R. C., JR. & OEGEMA, T. R., JR. 1991. LOCALIZATION OF TYPE X COLLAGEN IN CANINE GROWTH PLATE AND ADULT CANINE ARTICULAR CARTILAGE. *J ORTHOP RES*, 9, 485-94.
- GAO, B., SONG, H., BISHOP, K., ELLIOT, G., GARRETT, L., ENGLISH, M. A., ANDRE, P., ROBINSON, J., SOOD, R., MINAMI, Y., ECONOMIDES, A. N. & YANG, Y. 2011. WNT SIGNALING GRADIENTS ESTABLISH PLANAR CELL POLARITY BY INDUCING VANGL2 PHOSPHORYLATION THROUGH ROR2. *DEV CELL*, 20, 163-76.
- GAO, W., SWEENEY, C., WALSH, C., ROONEY, P., MCCORMICK, J., VEALE, D. J. AND FEARON, U. (2013). NOTCH SIGNALLING PATHWAYS MEDIATE SYNOVIAL ANGIOGENESIS IN RESPONSE TO VASCULAR ENDOTHELIAL GROWTH FACTOR AND ANGIOPOIETIN 2. *ANN RHEUM DIS*, 72:1080-1088.
- GIORDANO, A., GALDERISI, U. & MARINO, I. R. 2007. FROM THE LABORATORY BENCH TO THE PATIENT'S BEDSIDE: AN UPDATE ON CLINICAL TRIALS WITH MESENCHYMAL STEM CELLS. *JOURNAL OF CELLULAR PHYSIOLOGY*, 211, 27-35.
- GOLDRING, M. B. 2000. THE ROLE OF THE CHONDROCYTE IN OSTEOARTHRITIS. *ARTHRITIS & RHEUMATISM*, 43, 1916-26.
- GOLDRING, M. B., TSUCHIMOCHI, K. & IJIRI, K. 2006. THE CONTROL OF CHONDROGENESIS. *J CELL BIOCHEM*, 97, 33-44.
- GOLDRING, S. R. & GOLDRING, M. B. 2004. THE ROLE OF CYTOKINES IN CARTILAGE MATRIX DEGENERATION IN OSTEOARTHRITIS. *CLIN ORTHOP RELAT RES*, S27-36.
- GOLDRING, S. R. & GOLDRING, M. B. 2007. EATING BONE OR ADDING IT: THE WNT PATHWAY DECIDES. *NAT MED*, 13, 133-134.
- GONG, Y., SLEE, R. B., FUKAI, N., RAWADI, G., ROMAN-ROMAN, S., REGINATO, A. M., WANG, H. *ET AL.* (2001). LDL RECEPTOR-RELATED PROTEIN 5 (LRP5) AFFECTS BONE ACCRUAL AND EYE DEVELOPMENT. *CELL* 107:513-523.

- GOODELL, M. A., NGUYEN, H. & SHROYER, N. 2015. SOMATIC STEM CELL HETEROGENEITY: DIVERSITY IN THE BLOOD, SKIN AND INTESTINAL STEM CELL COMPARTMENTS. *NAT REV MOL CELL BIOL*, 16, 299-309.
- GREGORY, C. A., GUNN, W. G., REYES, E., SMOLARZ, A. J., MUNOZ, J., SPEES, J. L. & PROCKOP, D. J. 2005. HOW WNT SIGNALING AFFECTS BONE REPAIR BY MESENCHYMAL STEM CELLS FROM THE BONE MARROW. *ANN N Y ACAD SCI*, 1049, 97-106.
- GROGAN, S. P., MIYAKI, S., ASAHARA, H., D'LIMA, D. D. & LOTZ, M. K. 2009. MESENCHYMAL PROGENITOR CELL MARKERS IN HUMAN ARTICULAR CARTILAGE: NORMAL DISTRIBUTION AND CHANGES IN OSTEOARTHRITIS. *ARTHRITIS RES THER*, 11, R85.
- GRYNPAS, M. D., ALPERT, B., KATZ, I., LIEBERMAN, I. AND PRITZKER, K. P. (1991). SUBCHONDRAL BONE IN OSTEOARTHRITIS. *CALCIF TISSUE INT* 49:20-26.
- GUO, X., DAY, T. F., JIANG, X., GARRETT-BEAL, L., TOPOL, L. & YANG, Y. 2004. WNT/BETA-CATENIN SIGNALING IS SUFFICIENT AND NECESSARY FOR SYNOVIAL JOINT FORMATION. *GENES DEV*, 18, 2404-17.
- GUSTAFSON, B. & SMITH, U. 2012. THE WNT INHIBITOR DICKKOPF 1 AND BONE MORPHOGENETIC PROTEIN 4 RESCUE ADIPOGENESIS IN HYPERTROPHIC OBESITY IN HUMANS. *DIABETES*, 61, 1217-24.
- HARTMANN, C. & TABIN, C. J. 2001. WNT-14 PLAYS A PIVOTAL ROLE IN INDUCING SYNOVIAL JOINT FORMATION IN THE DEVELOPING APPENDICULAR SKELETON. *CELL*, 104, 341-51.
- HARTMANN, C. 2002. WNT-SIGNALING AND SKELETOGENESIS. *J MUSCULOSKELET NEURONAL INTERACT*, 2, 274-6.
- HARTMANN, C. 2006. A WNT CANON ORCHESTRATING OSTEOBLASTOGENESIS. *TRENDS CELL BIOL*, 16, 151-8.
- HAYES, A. J., DOWTHWAITE, G. P., WEBSTER, S. V. & ARCHER, C. W. 2003. THE DISTRIBUTION OF NOTCH RECEPTORS AND THEIR LIGANDS DURING ARTICULAR CARTILAGE DEVELOPMENT. *J ANAT*, 202, 495-502.
- HAYES, A. J., MACPHERSON, S., MORRISON, H., DOWTHWAITE, G. & ARCHER, C. W. 2001. THE DEVELOPMENT OF ARTICULAR CARTILAGE: EVIDENCE FOR

- AN APPositionAL GROWTH MECHANISM. ANAT EMBRYOL (BERL), 203, 469-79.
- HAYES, A. J., TUDOR, D., NOWELL, M. A., CATERSON, B. & HUGHES, C. E. 2008. CHONDROITIN SULFATE SULFATION MOTIFS AS PUTATIVE BIOMARKERS FOR ISOLATION OF ARTICULAR CARTILAGE PROGENITOR CELLS. J HISTOCHEM CYTOCHEM, 56, 125-38.
- HIDAKA, C. & GOLDRING, M. B. 2008. REGULATORY MECHANISMS OF CHONDROGENESIS AND IMPLICATIONS FOR UNDERSTANDING ARTICULAR CARTILAGE HOMEOSTASIS. CURRENT RHEUMATOLOGY REVIEWS.
- HILLEN, F. & GRIFFIOEN, A. W. 2007. TUMOUR VASCULARIZATION: SPROUTING ANGIOGENESIS AND BEYOND. CANCER METASTASIS REV, 26, 489-502.
- HOLLANDER, A. P., DICKINSON, S. C. & KAFIENAH, W. 2010. STEM CELLS AND CARTILAGE DEVELOPMENT: COMPLEXITIES OF A SIMPLE TISSUE. STEM CELLS, 28, 1992-6.
- HSIEH, J. L., SHEN, P. C., SHIAU, A. L., JOU, I. M., LEE, C. H., WANG, C. R., TEO, M. L. & WU, C. L. 2010. INTRAARTICULAR GENE TRANSFER OF THROMBOSPONDIN-1 SUPPRESSES THE DISEASE PROGRESSION OF EXPERIMENTAL OSTEOARTHRITIS. J ORTHOP RES, 28, 1300-6.
- HUANG, H. C. & KLEIN, P. S. 2004. THE FRIZZLED FAMILY: RECEPTORS FOR MULTIPLE SIGNAL TRANSDUCTION PATHWAYS. GENOME BIOL, 5, 234.
- HUANG, K., MARUYAMA, T. & FAN, G. 2014. THE NAIVE STATE OF HUMAN PLURIPOTENT STEM CELLS: A SYNTHESIS OF STEM CELL AND PREIMPLANTATION EMBRYO TRANSCRIPTOME ANALYSES. CELL STEM CELL, 15, 410-415.
- HUNZIKER, E. B. 2002. ARTICULAR CARTILAGE REPAIR: BASIC SCIENCE AND CLINICAL PROGRESS. A REVIEW OF THE CURRENT STATUS AND PROSPECTS. OSTEOARTHRITIS CARTILAGE, 10, 432-63.
- IMAI, K., MORIKAWA, M., D'ARMIENTO, J., MATSUMOTO, H., KOMIYA, K. & OKADA, Y. 2006. DIFFERENTIAL EXPRESSION OF WNTS AND FRPS IN THE SYNOVIUM OF RHEUMATOID ARTHRITIS AND OSTEOARTHRITIS. BIOCHEM BIOPHYS RES COMMUN, 345, 1615-20.

- JANICH, P., PASCUAL, G., MERLOS-SUAREZ, A., BATLLE, E., RIPPERGER, J., ALBRECHT, U., CHENG, H.-Y. M., OBRIETAN, K., DI CROCE, L. & BENITAH, S. A. 2011. THE CIRCADIAN MOLECULAR CLOCK CREATES EPIDERMAL STEM CELL HETEROGENEITY. *NATURE*, 480, 209-214.
- JIN, H. J., BAE, Y. K., KIM, M., KWON, S.-J., JEON, H. B., CHOI, S. J., KIM, S. W., YANG, Y. S., OH, W. & CHANG, J. W. 2013. COMPARATIVE ANALYSIS OF HUMAN MESENCHYMAL STEM CELLS FROM BONE MARROW, ADIPOSE TISSUE, AND UMBILICAL CORD BLOOD AS SOURCES OF CELL THERAPY. *INTERNATIONAL JOURNAL OF MOLECULAR SCIENCES*, 14, 17986-18001.
- JONES, P. H. & WATT, F. M. 1993. SEPARATION OF HUMAN EPIDERMAL STEM CELLS FROM TRANSIT AMPLIFYING CELLS ON THE BASIS OF DIFFERENCES IN INTEGRIN FUNCTION AND EXPRESSION. *CELL*, 73, 713-24.
- KADLER, K. E., HOLMES, D. F., TROTTER, J. A. & CHAPMAN, J. A. 1996. COLLAGEN FIBRIL FORMATION. *BIOCHEM J*, 316 (PT 1), 1-11.
- KEENE, D. R., SAKAI, L. Y. & BURGESSON, R. E. 1991. HUMAN BONE CONTAINS TYPE III COLLAGEN, TYPE VI COLLAGEN, AND FIBRILLIN: TYPE III COLLAGEN IS PRESENT ON SPECIFIC FIBERS THAT MAY MEDIATE ATTACHMENT OF TENDONS, LIGAMENTS, AND PERIOSTEUM TO CALCIFIED BONE CORTEX. *J HISTOCHEM CYTOCHEM*, 39, 59-69.
- KERN, S., EICHLER, H., STOEVE, J., KLÜTER, H. & BIEBACK, K. 2006. COMPARATIVE ANALYSIS OF MESENCHYMAL STEM CELLS FROM BONE MARROW, UMBILICAL CORD BLOOD, OR ADIPOSE TISSUE. *STEM CELLS*, 24, 1294-1301.
- KHAN, I. M., BISHOP, J. C., GILBERT, S. & ARCHER, C. W. 2009. CLONAL CHONDROPROGENITORS MAINTAIN TELOMERASE ACTIVITY AND SOX9 EXPRESSION DURING EXTENDED MONOLAYER CULTURE AND RETAIN CHONDROGENIC POTENTIAL. *OSTEOARTHRITIS CARTILAGE*, 17, 518-28.
- KIM, K. S., CHOI, H. M., LEE, Y. A., CHOI, I. A., LEE, S. H., HONG, S. J., YANG, H. I. & YOO, M. C. 2011. EXPRESSION LEVELS AND ASSOCIATION OF GELATINASES MMP-2 AND MMP-9 AND COLLAGENASES MMP-1 AND MMP-13 WITH VEGF IN SYNOVIAL FLUID OF PATIENTS WITH ARTHRITIS. *RHEUMATOL INT*, 31, 543-7.

- KIRTON, J. P., CROFTS, N. J., GEORGE, S. J., BRENNAN, K. & CANFIELD, A. E. 2007. WNT/BETA-CATENIN SIGNALING STIMULATES CHONDROGENIC AND INHIBITS ADIPOGENIC DIFFERENTIATION OF PERICYTES: POTENTIAL RELEVANCE TO VASCULAR DISEASE? *CIRC RES*, 101, 581-9.
- KNUDSON, C. B. & KNUDSON, W. 2001. CARTILAGE PROTEOGLYCANS. *SEMIN CELL DEV BIOL*, 12, 69-78.
- KOBAYASHI, M., SQUIRES, G. R., MOUSA, A., TANZER, M., ZUKOR, D. J., ANTONIOU, J., FEIGE, U. & POOLE, A. R. 2005. ROLE OF INTERLEUKIN-1 AND TUMOR NECROSIS FACTOR ALPHA IN MATRIX DEGRADATION OF HUMAN OSTEOARTHRITIC CARTILAGE. *ARTHRITIS & RHEUMATISM*, 52, 128-35.
- KOELLING, S., KRUEGEL, J., IRMER, M., PATH, J. R., SADOWSKI, B., MIRO, X. & MIOSGE, N. 2009. MIGRATORY CHONDROGENIC PROGENITOR CELLS FROM REPAIR TISSUE DURING THE LATER STAGES OF HUMAN OSTEOARTHRITIS. *CELL STEM CELL*, 4, 324-35.
- KOVACIC, J. C., MERCADER, N., TORRES, M., BOEHM, M. & FUSTER, V. 2012. EPITHELIAL-TO-MESENCHYMAL AND ENDOTHELIAL-TO-MESENCHYMAL TRANSITION: FROM CARDIOVASCULAR DEVELOPMENT TO DISEASE. *CIRCULATION*, 125, 1795-808.
- KUHN, N. Z. & TUAN, R. S. 2010. REGULATION OF STEMNESS AND STEM CELL NICHE OF MESENCHYMAL STEM CELLS: IMPLICATIONS IN TUMORIGENESIS AND METASTASIS. *J CELL PHYSIOL*, 222, 268-77.
- KUMAR, R. M., CAHAN, P., SHALEK, A. K., SATIJA, R., JAY DALEYKEYSER, A., LI, H., ZHANG, J., PARDEE, K., GENNERT, D., TROMBETTA, J. J., FERRANTE, T. C., REGEV, A., DALEY, G. Q. & COLLINS, J. J. 2014. DECONSTRUCTING TRANSCRIPTIONAL HETEROGENEITY IN PLURIPOTENT STEM CELLS. *NATURE*, 516, 56-61.
- KURZ, D. J., DECARY, S., HONG, Y. & ERUSALIMSKY, J. D. 2000. SENESCENCE-ASSOCIATED (BETA)-GALACTOSIDASE REFLECTS AN INCREASE IN LYSOSOMAL MASS DURING REPLICATIVE AGEING OF HUMAN ENDOTHELIAL CELLS. *J CELL SCI*, 113 (PT 20), 3613-22.

- LAJEUNESSE, D., HILAL, G., PELLETIER, J. P. & MARTEL-PELLETIER, J. 1999. SUBCHONDRAL BONE MORPHOLOGICAL AND BIOCHEMICAL ALTERATIONS IN OSTEOARTHRITIS. *OSTEOARTHRITIS CARTILAGE*, 7, 321-2.
- LAJEUNESSE, D., MASSICOTTE, F., PELLETIER, J. P. & MARTEL-PELLETIER, J. 2003. SUBCHONDRAL BONE SCLEROSIS IN OSTEOARTHRITIS: NOT JUST AN INNOCENT BYSTANDER. *MOD RHEUMATOL*, 13, 7-14.
- LAMOUILLE, S., XU, J. & DERYNCK, R. 2014. MOLECULAR MECHANISMS OF EPITHELIAL-MESENCHYMAL TRANSITION. *NAT REV MOL CELL BIOL*, 15, 178-196.
- LANDER, A., KIMBLE, J., CLEVERS, H., FUCHS, E., MONTARRAS, D., BUCKINGHAM, M., CALOF, A., TRUMPP, A. & OSKARSSON, T. 2012. WHAT DOES THE CONCEPT OF THE STEM CELL NICHE REALLY MEAN TODAY. *BMC BIOLOGY*, 10, 19.
- LANE, N. E., NEVITT, M. C., LUI, L. Y., DE LEON, P., CORR, M. & STUDY OF OSTEOPOROTIC FRACTURES RESEARCH, G. 2007. WNT SIGNALING ANTAGONISTS ARE POTENTIAL PROGNOSTIC BIOMARKERS FOR THE PROGRESSION OF RADIOGRAPHIC HIP OSTEOARTHRITIS IN ELDERLY CAUCASIAN WOMEN. *ARTHRITIS RHEUM*, 56, 3319-25.
- LEIJTEN, J. C., EMONS, J., STICHT, C., VAN GOOL, S., DECKER, E., UITTERLINDEN, A., RAPPOLD, G., HOFMAN, A., RIVADENEIRA, F., SCHERJON, S., WIT, J. M., VAN MEURS, J., VAN BLITTERSWIJK, C. A. & KARPERIEN, M. 2012. GREMLIN 1, FRIZZLED-RELATED PROTEIN, AND DKK-1 ARE KEY REGULATORS OF HUMAN ARTICULAR CARTILAGE HOMEOSTASIS. *ARTHRITIS & RHEUMATISM*, 64, 3302-12.
- LEWIS, J. S., HEMBREE, W. C., FURMAN, B. D., TIPPETS, L., CATTEL, D., HUEBNER, J. L., LITTLE, D. *ET AL.* (2011). ACUTE JOINT PATHOLOGY AND SYNOVIAL INFLAMMATION IS ASSOCIATED WITH INCREASED INTRA-ARTICULAR FRACTURE SEVERITY IN THE MOUSE KNEE. *OSTEOARTHRITIS CARTILAGE* 19:864-873.
- LI, G., DICKSON, G. R., MARSH, D. R. & SIMPSON, H. 2003. RAPID NEW BONE TISSUE REMODELING DURING DISTRACTION OSTEOGENESIS IS ASSOCIATED WITH APOPTOSIS. *JOURNAL OF ORTHOPAEDIC RESEARCH*, 21, 28-35.

- LIVAK, K. J. AND SCHMITTGEN, T. D. (2001). ANALYSIS OF RELATIVE GENE EXPRESSION DATA USING REAL-TIME QUANTITATIVE PCR AND THE 2(-DELTA DELTA C(T)) METHOD. *METHODS* 25:402-408.
- LORENZO, P., AMAN, P., SOMMARIN, Y. & HEINEGARD, D. 1999. THE HUMAN CILP GENE: EXON/INTRON ORGANIZATION AND CHROMOSOMAL MAPPING. *MATRIX BIOL*, 18, 445-54.
- LORIES, R. J. U., PEETERS, J., BAKKER, A., TYLZANOWSKI, P., DERESE, I., SCHROOTEN, J., THOMAS, J. T. & LUYTEN, F. P. 2007B. ARTICULAR CARTILAGE AND BIOMECHANICAL PROPERTIES OF THE LONG BONES IN FRZB-KNOCKOUT MICE. *ARTHRITIS & RHEUMATISM*, 56, 4095-4103.
- LOUGHLIN, J., DOWLING, B., CHAPMAN, K., MARCELLINE, L., MUSTAFA, Z., SOUTHAM, L., FERREIRA, A., CIESIELSKI, C., CARSON, D. A. & CORR, M. 2004. FUNCTIONAL VARIANTS WITHIN THE SECRETED FRIZZLED-RELATED PROTEIN 3 GENE ARE ASSOCIATED WITH HIP OSTEOARTHRITIS IN FEMALES. *PROC NATL ACAD SCI U S A*, 101, 9757-62.
- LUYTEN, F. P., TYLZANOWSKI, P. & LORIES, R. J. 2009. WNT SIGNALING AND OSTEOARTHRITIS. *BONE*, 44, 522-7.
- LYASHENKO, N., WINTER, M., MIGLIORINI, D., BIECHELE, T., MOON, R. T. & HARTMANN, C. 2011. DIFFERENTIAL REQUIREMENT FOR THE DUAL FUNCTIONS OF BETA-CATENIN IN EMBRYONIC STEM CELL SELF-RENEWAL AND GERM LAYER FORMATION. *NAT CELL BIOL*, 13, 753-61.
- MACARTHUR, B. D., SEVILLA, A., LENZ, M., MÜLLER, F.-J., SCHULDT, B. M., SCHUPPERT, A. A., RIDDEN, S. J., STUMPF, P. S., FIDALGO, M., MA'AYAN, A., WANG, J. & LEMISCHKA, I. R. 2012. NANOG-DEPENDENT FEEDBACK LOOPS REGULATE MURINE EMBRYONIC STEM CELL HETEROGENEITY. *NAT CELL BIOL*, 14, 1139-1147.
- MACDONALD, B. T., TAMAI, K. & HE, X. 2009. WNT/BETA-CATENIN SIGNALING: COMPONENTS, MECHANISMS, AND DISEASES. *DEV CELL*, 17, 9-26.
- MANDELBOIM, O. 2006. TRANS-WELL MIGRATION ASSAY. *NATURE PROTOCOL EXCHANGE*. 10.1038
- MAO, B., WU, W., LI, Y., HOPPE, D., STANNEK, P., GLINKA, A. & NIEHRS, C. 2001. LDL-RECEPTOR-RELATED PROTEIN 6 IS A RECEPTOR FOR DICKKOPF PROTEINS. *NATURE*, 411, 321-5.

- MARIE, P., LOMRI, A., SABBAGH, A. & BASLE, M. 1989. CULTURE AND BEHAVIOR OF OSTEOBLASTIC CELLS ISOLATED FROM NORMAL TRABECULAR BONE SURFACES. *IN VITRO CELLULAR & DEVELOPMENTAL BIOLOGY*, 25, 373-380.
- MAROUDAS, A., BAYLISS, M. T., UCHITEL-KAUSHANSKY, N., SCHNEIDERMAN, R. & GILAV, E. 1998. AGGREGAN TURNOVER IN HUMAN ARTICULAR CARTILAGE: USE OF ASPARTIC ACID RACEMIZATION AS A MARKER OF MOLECULAR AGE. *ARCH BIOCHEM BIOPHYS*, 350, 61-71.
- MAROUDAS, A., PALLA, G. & GILAV, E. 1992. RACEMIZATION OF ASPARTIC ACID IN HUMAN ARTICULAR CARTILAGE. *CONNECT TISSUE RES*, 28, 161-9.
- MARTEL-PELLETIER, J. & PELLETIER, J. P. 2010. IS OSTEOARTHRITIS A DISEASE INVOLVING ONLY CARTILAGE OR OTHER ARTICULAR TISSUES. *EKLEM HASTALIK CERRAHISI*, 21, 2-14.
- MARTEL-PELLETIER, J., ALAAEDDINE, N. & PELLETIER, J. P. 1999. CYTOKINES AND THEIR ROLE IN THE PATHOPHYSIOLOGY OF OSTEOARTHRITIS. *FRONT BIOSCI*, 4, D694-703.
- MCCARTHY, H. E., BARA, J. J., BRAKSPEAR, K., SINGHRAO, S. K. & ARCHER, C. W. 2012. THE COMPARISON OF EQUINE ARTICULAR CARTILAGE PROGENITOR CELLS AND BONE MARROW-DERIVED STROMAL CELLS AS POTENTIAL CELL SOURCES FOR CARTILAGE REPAIR IN THE HORSE. *VET J*, 192, 345-51.
- MCKEE, M. D. & NANJI, A. 1996. OSTEOPONTIN: AN INTERFACIAL EXTRACELLULAR MATRIX PROTEIN IN MINERALIZED TISSUES. *CONNECT TISSUE RES*, 35, 197-205.
- MEDICI, D. 2015. ENDOTHELIAL-MESENCHYMAL TRANSITION AS A NOVEL MECHANISM FOR TISSUE REGENERATION. *THE FASEB JOURNAL*, 29.
- MEDICI, D., SHORE, E. M., LOUNEV, V. Y., KAPLAN, F. S., KALLURI, R. & OLSEN, B. R. 2010. CONVERSION OF VASCULAR ENDOTHELIAL CELLS INTO MULTIPOTENT STEM-LIKE CELLS. *NAT MED*, 16, 1400-6.
- MIAO, Z., JIN, J., CHEN, L., ZHU, J., HUANG, W., ZHAO, J., QIAN, H. & ZHANG, X. 2006. ISOLATION OF MESENCHYMAL STEM CELLS FROM HUMAN PLACENTA: COMPARISON WITH HUMAN BONE MARROW MESENCHYMAL STEM CELLS. *CELL BIOL INT*, 30, 681-7.

- MIN, J. K., PARK, H., CHOI, H. J., KIM, Y., PYUN, B. J., AGRAWAL, V., SONG, B. W., JEON, J., MAENG, Y. S., RHO, S. S., SHIM, S., CHAI, J. H., KOO, B. K., HONG, H. J., YUN, C. O., CHOI, C., KIM, Y. M., HWANG, K. C. & KWON, Y. G. 2011. THE WNT ANTAGONIST DICKKOPF2 PROMOTES ANGIOGENESIS IN RODENT AND HUMAN ENDOTHELIAL CELLS. *J CLIN INVEST*, 121, 1882-93.
- MIX, K. S., SPORN, M. B., BRINCKERHOFF, C. E., EYRE, D. & SCHURMAN, D. J. 2004. NOVEL INHIBITORS OF MATRIX METALLOPROTEINASE GENE EXPRESSION AS POTENTIAL THERAPIES FOR ARTHRITIS. *CLIN ORTHOP RELAT RES*, S129-37.
- NAGASE, H. & WOESSNER, J. F., JR. 1999. MATRIX METALLOPROTEINASES. *J BIOL CHEM*, 274, 21491-4.
- NATIONAL COLLABORATING CENTRE FOR CHRONIC CONDITIONS 2008. OSTEOARTHRITIS: NATIONAL CLINICAL GUIDELINE FOR CARE AND MANAGEMENT IN ADULTS. ROYAL COLLEGE OF PHYSICIANS.
- NELSON, L., MCCARTHY, H. E., FAIRCLOUGH, J., WILLIAMS, R. & ARCHER, C. W. 2014. EVIDENCE OF A VIABLE POOL OF STEM CELLS WITHIN HUMAN OSTEOARTHRITIC CARTILAGE. *CARTILAGE*, 5, 203-14.
- NIE, L., LYROS, O., MEDDA, R., JOVANOVIĆ, N., SCHMIDT, J. L., OTTERSON, M. F., JOHNSON, C. P., BEHMARAM, B., SHAKER, R. & RAFIEE, P. 2014. ENDOTHELIAL-MESENCHYMAL TRANSITION IN NORMAL HUMAN ESOPHAGEAL ENDOTHELIAL CELLS COCULTURED WITH ESOPHAGEAL ADENOCARCINOMA CELLS: ROLE OF IL-1B AND TGF-B2. *AMERICAN JOURNAL OF PHYSIOLOGY*. 2014, 307.C59-877.
- NIEHRS, C. 2006. FUNCTION AND BIOLOGICAL ROLES OF THE DICKKOPF FAMILY OF WNT MODULATORS. *ONCOGENE*, 25, 7469-81.
- NIEHRS, C. 2012. THE COMPLEX WORLD OF WNT RECEPTOR SIGNALLING. *NAT REV MOL CELL BIOL*, 13, 767-79.
- NOTH, U., STEINERT, A. F. & TUAN, R. S. 2008. TECHNOLOGY INSIGHT: ADULT MESENCHYMAL STEM CELLS FOR OSTEOARTHRITIS THERAPY. *NAT CLIN PRACT RHEUMATOL*, 4, 371-80.
- NUSSE, R. 2012. WNT SIGNALING. *COLD SPRING HARB PERSPECT BIOL*, 4.

- OEGEMA, T. R., JR., CARPENTER, R. J., HOFMEISTER, F. & THOMPSON, R. C., JR. 1997. THE INTERACTION OF THE ZONE OF CALCIFIED CARTILAGE AND SUBCHONDRAL BONE IN OSTEOARTHRITIS. *MICROSC RES TECH*, 37, 324-32.
- OH, H., CHUN, C. H. & CHUN, J. S. 2012B. DKK-1 EXPRESSION IN CHONDROCYTES INHIBITS EXPERIMENTAL OSTEOARTHRITIC CARTILAGE DESTRUCTION IN MICE. *ARTHRITIS & RHEUMATISM*, 64, 2568-78.
- OH, H., RYU, J. H., JEON, J., YANG, S., CHUN, C. H., PARK, H., KIM, H. J., KIM, W. S., KIM, H. H., KWON, Y. G. & CHUN, J. S. 2012C. MISEXPRESSION OF DICKKOPF-1 IN ENDOTHELIAL CELLS, BUT NOT IN CHONDROCYTES OR HYPERTROPHIC CHONDROCYTES, CAUSES DEFECTS IN ENDOCHONDRAL OSSIFICATION. *J BONE MINER RES*, 27, 1335-44.
- OSCELL. 2013. ASCOT TRIAL: AUTOLOGOUS STROMAL (MESENCHYMAL) STEM CELLS WITH CHONDROCYTES IN REPAIRING CARTILAGE IN THE KNEE. [ONLINE].OSWESTRY.AVAILABLE:
[HTTP://WWW.OSCELL.CO.UK/NEWS/ASCOT-TRIAL.HTML](http://www.oscell.co.uk/news/ascot-trial.html).
- OWEN, T. A., ARONOW, M., SHALHOUB, V., BARONE, L. M., WILMING, L., TASSINARI, M. S., KENNEDY, M. B. ET AL. (1990). PROGRESSIVE DEVELOPMENT OF THE RAT OSTEOBLAST PHENOTYPE IN VITRO: RECIPROCAL RELATIONSHIPS IN EXPRESSION OF GENES ASSOCIATED WITH OSTEOBLAST PROLIFERATION AND DIFFERENTIATION DURING FORMATION OF THE BONE EXTRACELLULAR MATRIX. *J CELL PHYSIOL* 143:420-430.
- PAPADIMITROPOULOS, A., PICCININI, E., BRACHAT, S., BRACCINI, A., WENDT, D., BARBERO, A., JACOBI, C. & MARTIN, I. 2014. EXPANSION OF HUMAN MESENCHYMAL STROMAL CELLS FROM FRESH BONE MARROW IN A 3D SCAFFOLD-BASED SYSTEM UNDER DIRECT PERFUSION. *PLOS ONE*, 9, E102359.
- PAPATHANASIOU, I., MALIZOS, K. N. & TSEZOU, A. 2010. LOW-DENSITY LIPOPROTEIN RECEPTOR-RELATED PROTEIN 5 (LRP5) EXPRESSION IN HUMAN OSTEOARTHRITIC CHONDROCYTES. *J ORTHOP RES*, 28, 348-53.

- PARK, J. R., JUNG, J. W., LEE, Y. S. & KANG, K. S. 2008. THE ROLES OF WNT ANTAGONISTS DKK-1 AND SFRP4 DURING ADIPOGENESIS OF HUMAN ADIPOSE TISSUE-DERIVED MESENCHYMAL STEM CELLS. *CELL PROLIF*, 41, 859-74.
- PATWARI, P., GAO, G., LEE, J. H., GRODZINSKY, A. J. & SANDY, J. D. 2005. ANALYSIS OF ADAMTS4 AND MT4-MMP INDICATES THAT BOTH ARE INVOLVED IN AGGREGANOLYSIS IN INTERLEUKIN-1-TREATED BOVINE CARTILAGE. *OSTEOARTHRITIS CARTILAGE*, 13, 269-77.
- PETERSSON, I. F., BOEGARD, T., SVENSSON, B., HEINEGARD, D. & SAXNE, T. 1998. Changes in cartilage and bone metabolism identified by serum markers in early osteoarthritis of the knee joint. *Br J Rheumatol*, 37, 46-50.
- PETRIE ARONIN, C. E. & TUAN, R. S. 2010. THERAPEUTIC POTENTIAL OF THE IMMUNOMODULATORY ACTIVITIES OF ADULT MESENCHYMAL STEM CELLS. *BIRTH DEFECTS RES C EMBRYO TODAY*, 90, 67-74.
- PFANDER, D., SWOBODA, B. & KIRSCH, T. 2001. EXPRESSION OF EARLY AND LATE DIFFERENTIATION MARKERS (PROLIFERATING CELL NUCLEAR ANTIGEN, SYNDECAN-3, ANNEXIN VI, AND ALKALINE PHOSPHATASE) BY HUMAN OSTEOARTHRITIC CHONDROCYTES. *AM J PATHOL*, 159, 1777-83.
- POOLE, C. A., AYAD, S. & GILBERT, R. T. 1992. CHONDRONS FROM ARTICULAR CARTILAGE. V. IMMUNOHISTOCHEMICAL EVALUATION OF TYPE VI COLLAGEN ORGANISATION IN ISOLATED CHONDRONS BY LIGHT, CONFOCAL AND ELECTRON MICROSCOPY. *J CELL SCI*, 103 (PT 4), 1101-10.
- POOLE, C. A., FLINT, M. H. & BEAUMONT, B. W. 1987. CHONDRONS IN CARTILAGE: ULTRASTRUCTURAL ANALYSIS OF THE PERICELLULAR MICROENVIRONMENT IN ADULT HUMAN ARTICULAR CARTILAGES. *J ORTHOP RES*, 5, 509-22.
- PRETZEL, D., LINSS, S., ROCHLER, S., ENDRES, M., KAPS, C., ALSALAMEH, S. AND KINNE, R. W. (2011). RELATIVE PERCENTAGE AND ZONAL DISTRIBUTION OF MESENCHYMAL PROGENITOR CELLS IN HUMAN OSTEOARTHRITIC AND NORMAL CARTILAGE. *ARTHRITIS RES THER*, 13:R64.
- PUISIEUX, A., BRABLETZ, T. AND CAMEL, J. (2014). ONCOGENIC ROLES OF EMT-INDUCING TRANSCRIPTION FACTORS. *NAT CELL BIOL*, 16:488-494.

- QUAIL, D. F. AND JOYCE, J. A. (2013). MICROENVIRONMENTAL REGULATION OF TUMOR PROGRESSION AND METASTASIS. *NATURE MED*, 19:1423-1437.
- QUASNICHKA, H. L., ANDERSON-MACKENZIE, J. M. AND BAILEY, A. J. (2006). SUBCHONDRAL BONE AND LIGAMENT CHANGES PRECEDE CARTILAGE DEGRADATION IN GUINEA PIG OSTEOARTHRITIS. *BIORHEOLOGY*, 43:389-397.
- RADIN, E. L. AND ROSE, R. M. ROLE OF SUBCHONDRAL BONE IN THE INITIATION AND PROGRESSION OF CARTILAGE DAMAGE. 1986. *CLIN ORTHOP RELAT RES* 34-40.
- RADIN, E. L., PAUL, I. L. AND TOLKOFF, M. J. SUBCHONDRAL BONE CHANGES IN PATIENTS WITH EARLY DEGENERATIVE JOINT DISEASE. 1970. *ARTHRITIS & RHEUMATISM* 13:400-405.
- RAGGATT, L. J. & PARTRIDGE, N. C. 2010. CELLULAR AND MOLECULAR MECHANISMS OF BONE REMODELING. *J BIOL CHEM*, 285, 25103-8.
- RAGGATT, L. J., JEFCOAT, S. C., JR., CHOUDHURY, I., WILLIAMS, S., TIKU, M. & PARTRIDGE, N. C. 2006. MATRIX METALLOPROTEINASE-13 INFLUENCES ERK SIGNALLING IN ARTICULAR RABBIT CHONDROCYTES. *OSTEOARTHRITIS CARTILAGE*, 14, 680-9.
- RATAJCZAK, M. Z. A NOVEL VIEW OF THE ADULT BONE MARROW STEM CELL HIERARCHY AND STEM CELL TRAFFICKING. 2015. *LEUKEMIA*, 29:776-782.
- REIS, M., CZUPALLA, C. J., ZIEGLER, N., DEVRAJ, K., ZINKE, J., SEIDEL, S., HECK, R., THOM, S., MACAS, J., BOCKAMP, E., FRUTTIGER, M., TAKETO, M. M., DIMMELER, S., PLATE, K. H. & LIEBNER, S. 2012. ENDOTHELIAL WNT/BETA-CATENIN SIGNALING INHIBITS GLIOMA ANGIOGENESIS AND NORMALIZES TUMOR BLOOD VESSELS BY INDUCING PDGF-B EXPRESSION. *J EXP MED*, 209, 1611-27.
- RIANCHO, J. A., OLMOS, J. M., PINEDA, B., GARCIA-IBARBIA, C., PEREZ-NUNEZ, M. I., NAN, D. N., VELASCO, J. *ET AL.* (2011). WNT RECEPTORS, BONE MASS, AND FRACTURES: GENE-WIDE ASSOCIATION ANALYSIS OF LRP5 AND LRP6 POLYMORPHISMS WITH REPLICATION. *EUR J ENDOCRINOL* 164:123-131.
- RICCI-VITIANI, L., LOMBARDI, D. G., PILOZZI, E., BIFFONI, M., TODARO, M., PESCHLE, C. AND DE MARIA, R. (2007). IDENTIFICATION AND EXPANSION OF HUMAN COLON-CANCER-INITIATING CELLS. *NATURE*, 445:111-115.

- RIESLE, J., HOLLANDER, A. P., LANGER, R., FREED, L. E. AND VUNJAK-NOVAKOVIC, G. (1998). COLLAGEN IN TISSUE-ENGINEERED CARTILAGE: TYPES, STRUCTURE, AND CROSSLINKS. *J CELL BIOCHEM*, 71:313-327.
- RODRIGUEZ-LOPEZ, J., POMBO-SUAREZ, M., LIZ, M., GOMEZ-REINO, J. J. AND GONZALEZ, A. (2007). FURTHER EVIDENCE OF THE ROLE OF FRIZZLED-RELATED PROTEIN GENE POLYMORPHISMS IN OSTEOARTHRITIS. *ANN RHEUM DIS*, 66:1052-1055.
- RUSSELL, K. C., PHINNEY, D. G., LACEY, M. R., BARRILLEAUX, B. L., MEYERTHOLEN, K. E. & O'CONNOR, K. C. 2010. IN VITRO HIGH-CAPACITY ASSAY TO QUANTIFY THE CLONAL HETEROGENEITY IN TRILINEAGE POTENTIAL OF MESENCHYMAL STEM CELLS REVEALS A COMPLEX HIERARCHY OF LINEAGE COMMITMENT. *STEM CELLS*, 28, 788-98.
- SAITO, T., FUKAI, A., MABUCHI, A., IKEDA, T., YANO, F., OHBA, S., NISHIDA, N., AKUNE, T., YOSHIMURA, N., NAKAGAWA, T., NAKAMURA, K., TOKUNAGA, K., CHUNG, U. I. & KAWAGUCHI, H. 2010. TRANSCRIPTIONAL REGULATION OF ENDOCHONDRAL OSSIFICATION BY HIF-2ALPHA DURING SKELETAL GROWTH AND OSTEOARTHRITIS DEVELOPMENT. *NAT MED*, 16, 678-86.
- SALTER, D. M., GODOLPHIN, J. L., GOURLAY, M. S., LAWSON, M. F., HUGHES, D. E. & DUNNE, E. 1996. ANALYSIS OF HUMAN ARTICULAR CHONDROCYTE CD44 ISOFORM EXPRESSION AND FUNCTION IN HEALTH AND DISEASE. *J PATHOL*, 179, 396-402.
- SALTER, D. M., HUGHES, D. E., SIMPSON, R. & GARDNER, D. L. 1992. INTEGRIN EXPRESSION BY HUMAN ARTICULAR CHONDROCYTES. *BR J RHEUMATOL*, 31, 231-4.
- SANDY, J. D., NEAME, P. J., BOYNTON, R. E. & FLANNERY, C. R. 1991. CATABOLISM OF AGGREGAN IN CARTILAGE EXPLANTS. IDENTIFICATION OF A MAJOR CLEAVAGE SITE WITHIN THE INTERGLOBULAR DOMAIN. *J BIOL CHEM*, 266, 8683-5.
- SATO, T., VRIES, R. G., SNIPPERT, H. J., VAN DE WETERING, M., BARKER, N., STANGE, D. E., VAN ES, J. H., ABO, A., KUJALA, P., PETERS, P. J. & CLEVERS, H. 2009. SINGLE LGR5 STEM CELLS BUILD CRYPT-VILLUS STRUCTURES IN VITRO WITHOUT A MESENCHYMAL NICHE. *NATURE*, 459, 262-5.

- SCHMID, T. M. & LINSENMAYER, T. F. 1985. DEVELOPMENTAL ACQUISITION OF TYPE X COLLAGEN IN THE EMBRYONIC CHICK TIBIOTARSUS. *DEV BIOL*, 107, 373-81.
- SCHUMACHER, B. L., BLOCK, J. A., SCHMID, T. M., AYDELOTTE, M. B. & KUETTNER, K. E. 1994. A NOVEL PROTEOGLYCAN SYNTHESIZED AND SECRETED BY CHONDROCYTES OF THE SUPERFICIAL ZONE OF ARTICULAR CARTILAGE. *ARCH BIOCHEM BIOPHYS*, 311, 144-52.
- SELTZER, J. L., ADAMS, S. A., GRANT, G. A. & EISEN, A. Z. 1981. PURIFICATION AND PROPERTIES OF A GELATIN-SPECIFIC NEUTRAL PROTEASE FROM HUMAN SKIN. *J BIOL CHEM*, 256, 4662-8.
- SHEN, J., LI, S. & CHEN, D. 2014. TGF-B SIGNALING AND THE DEVELOPMENT OF OSTEOARTHRITIS. *BONE RESEARCH*, 2, 14002.
- SIGURDSSON, V., HILMARSDOTTIR, B., SIGMUNSDOTTIR, H., FRIDRIKSDOTTIR, A. J. R., RINGNÉR, M., VILLADSEN, R., BORG, A., AGNARSSON, B. A., PETERSEN, O. W., MAGNUSSON, M. K. & GUDJONSSON, T. 2011. ENDOTHELIAL INDUCED EMT IN BREAST EPITHELIAL CELLS WITH STEM CELL PROPERTIES. *PLOS ONE*, 6, E23833.
- SINGH, A. M., HAMAZAKI, T., HANKOWSKI, K. E. AND TERADA, N. (2007). A HETEROGENEOUS EXPRESSION PATTERN FOR NANOG IN EMBRYONIC STEM CELLS. *STEM CELLS*, 25:2534-2542.
- SKILES, J. W., GONNELLA, N. C. & JENG, A. Y. 2004. THE DESIGN, STRUCTURE, AND CLINICAL UPDATE OF SMALL MOLECULAR WEIGHT MATRIX METALLOPROTEINASE INHIBITORS. *CURR MED CHEM*, 11, 2911-77.
- SLACK, J., MCMAHAN, C. J., WAUGH, S., SCHOOLEY, K., SPRIGGS, M. K., SIMS, J. E. & DOWER, S. K. 1993. INDEPENDENT BINDING OF INTERLEUKIN-1 ALPHA AND INTERLEUKIN-1 BETA TO TYPE I AND TYPE II INTERLEUKIN-1 RECEPTORS. *J BIOL CHEM*, 268, 2513-24.
- SMADJA, D. M., D'AUDIGIER, C., WEISWALD, L. B., BADOUAL, C., DANGLES-MARIE, V., MAUGE, L., EVRARD, S., LAURENDEAU, I., LALLEMAND, F., GERMAIN, S., GRELAC, F., DIZIER, B., VIDAUD, M., BIECHE, I. & GAUSSEM, P. 2010. THE WNT ANTAGONIST DICKKOPF-1 INCREASES ENDOTHELIAL PROGENITOR

- CELL ANGIOGENIC POTENTIAL. *ARTERIOSCLER THROMB VASC BIOL*, 30, 2544-52.
- SPATER, D., HILL, T. P., GRUBER, M. & HARTMANN, C. 2006. ROLE OF CANONICAL WNT-SIGNALING IN JOINT FORMATION. *EUR CELL MATER*, 12, 71-80.
- SPICER, A. P., JOO, A. & BOWLING, R. A., JR. 2003. A HYALURONAN BINDING LINK PROTEIN GENE FAMILY WHOSE MEMBERS ARE PHYSICALLY LINKED ADJACENT TO CHONDROITIN SULFATE PROTEOGLYCAN CORE PROTEIN GENES: THE MISSING LINKS. *J BIOL CHEM*, 278, 21083-91.
- STACKER, S. A., WILLIAMS, S. P., KARNEZIS, T., SHAYAN, R., FOX, S. B. & ACHEN, M. G. 2014. LYMPHANGIOGENESIS AND LYMPHATIC VESSEL REMODELLING IN CANCER. *NAT REV CANCER*, 14, 159-172.
- STAINES, K. A., MACRAE, V. E. & FARQUHARSON, C. 2012. CARTILAGE DEVELOPMENT AND DEGENERATION: A WNT WNT SITUATION. *CELL BIOCHEM FUNCT*, 30, 633-42.
- STOCKWELL, R. 1979. *BIOLOGY OF CARTILAGE CELLS*, CAMBRIDGE, CAMBRIDGE UNIVERSITY PRESS.
- STOCKWELL, R. A. 1978. CHONDROCYTES. *J CLIN PATHOL SUPPL (R COLL PATHOL)*, 12, 7-13.
- SURI, S. & WALSH, D. A. 2012. OSTEOCHONDRAL ALTERATIONS IN OSTEOARTHRITIS. *BONE*, 51, 204-211.
- SURMANN-SCHMITT, C., WIDMANN, N., DIETZ, U., SAEGER, B., EITZINGER, N., NAKAMURA, Y., RATTEL, M., LATHAM, R., HARTMANN, C., VON DER MARK, H., SCHEFF, G., VON DER MARK, K. & STOCK, M. 2009. WIF-1 IS EXPRESSED AT CARTILAGE-MESENCHYME INTERFACES AND IMPEDES WNT3A-MEDIATED INHIBITION OF CHONDROGENESIS. *J CELL SCI*, 122, 3627-37.
- SVENSSON, L., OLDBERG, A. AND HEINEGARD, D. (2001). COLLAGEN BINDING PROTEINS. *OSTEOARTHRITIS CARTILAGE*, 9 SUPPL A:S23-28.
- TAMAMURA, Y., OTANI, T., KANATANI, N., KOYAMA, E., KITAGAKI, J., KOMORI, T., YAMADA, Y., COSTANTINI, F., WAKISAKA, S., PACIFICI, M., IWAMOTO, M. & ENOMOTO-IWAMOTO, M. 2005. DEVELOPMENTAL REGULATION OF WNT/BETA-CATENIN SIGNALS IS REQUIRED FOR GROWTH PLATE

- ASSEMBLY, CARTILAGE INTEGRITY, AND ENDOCHONDRAL OSSIFICATION. J BIOL CHEM, 280, 19185-95.
- TAURIELLO, D. V., JORDENS, I., KIRCHNER, K., SLOOTSTRA, J. W., KRUITWAGEN, T., BOUWMAN, B. A., NOUTSOU, M., RUDIGER, S. G., SCHWAMBORN, K., SCHAMBONY, A. & MAURICE, M. M. 2012. WNT/BETA-CATENIN SIGNALING REQUIRES INTERACTION OF THE DISHEVELLED DEP DOMAIN AND C TERMINUS WITH A DISCONTINUOUS MOTIF IN FRIZZLED. PROC NATL ACAD SCI U S A, 109, E812-20.
- THORFVE, A., DEHNE, T., LINDAHL, A., BRITTBERG, M., PRUSS, A., RINGE, J., SITTINGER, M. & KARLSSON, C. 2012. CHARACTERISTIC MARKERS OF THE WNT SIGNALING PATHWAYS ARE DIFFERENTIALLY EXPRESSED IN OSTEOARTHRITIC CARTILAGE. CARTILAGE, 3, 43-57.
- THORFVE, A., DEHNE, T., LINDAHL, A., BRITTBERG, M., PRUSS, A., RINGE, J., SITTINGER, M. ET AL. (2012). CHARACTERISTIC MARKERS OF THE WNT SIGNALING PATHWAYS ARE DIFFERENTIALLY EXPRESSED IN OSTEOARTHRITIC CARTILAGE. CARTILAGE, 3:43-57.
- TOMINAGA, J., FUKUNAGA, Y., ABELARDO, E. & NAGAFUCHI, A. 2008. DEFINING THE FUNCTION OF BETA-CATENIN TYROSINE PHOSPHORYLATION IN CADHERIN-MEDIATED CELL-CELL ADHESION. GENES CELLS, 13, 67-77.
- TUAN, R. S., BOLAND, G. & TULI, R. 2003. ADULT MESENCHYMAL STEM CELLS AND CELL-BASED TISSUE ENGINEERING. ARTHRITIS RES THER, 5, 32-45.
- ULRICH-VINTHER, M., MALONEY, M. D., SCHWARZ, E. M., ROSIER, R. & O'KEEFE, R. J. 2003. ARTICULAR CARTILAGE BIOLOGY. J AM ACAD ORTHOP SURG, 11, 421-30.
- VAN DER KRAAN, P. M., BUMA, P., VAN KUPPEVELT, T. & VAN DEN BERG, W. B. 2002. INTERACTION OF CHONDROCYTES, EXTRACELLULAR MATRIX AND GROWTH FACTORS: RELEVANCE FOR ARTICULAR CARTILAGE TISSUE ENGINEERING. OSTEOARTHRITIS CARTILAGE, 10, 631-7.
- VEEMAN, M. T., SLUSARSKI, D. C., KAYKAS, A., LOUIE, S. H. & MOON, R. T. 2003. ZEBRAFISH PRICKLE, A MODULATOR OF NONCANONICAL WNT/FZ SIGNALING, REGULATES GASTRULATION MOVEMENTS. CURR BIOL, 13, 680-5.

- WALSH, D. A., BONNET, C. S., TURNER, E. L., WILSON, D., SITU, M. & MCWILLIAMS, D. F. 2007. ANGIOGENESIS IN THE SYNOVIUM AND AT THE OSTEOCHONDRAL JUNCTION IN OSTEOARTHRITIS. OSTEOARTHRITIS CARTILAGE, 15, 743-51.
- WARD, A. C., DOWTHWAITE, G. P. & PITSILLIDES, A. A. 1999. HYALURONAN IN JOINT CAVITATION. BIOCHEM SOC TRANS, 27, 128-35.
- WARE, C. B., NELSON, A. M., MECHAM, B., HESSON, J., ZHOU, W., JONLIN, E. C., JIMENEZ-CALIANI, A. J., DENG, X., CAVANAUGH, C., COOK, S., TESAR, P. J., OKADA, J., MARGARETHA, L., SPERBER, H., CHOI, M., BLAU, C. A., TREUTING, P. M., HAWKINS, R. D., CIRULLI, V. & RUOHOLA-BAKER, H. 2014. DERIVATION OF NAÏVE HUMAN EMBRYONIC STEM CELLS. PROCEEDINGS OF THE NATIONAL ACADEMY OF SCIENCES, 111, 4484-4489.
- WEIS, S. M. & CHERESH, D. A. 2011. TUMOR ANGIOGENESIS: MOLECULAR PATHWAYS AND THERAPEUTIC TARGETS. NAT MED, 17, 1359-1370.
- WEN, Y. A., LIU, D., XIAO, Y. Y., LUO, D., DONG, Y. F. & ZHANG, L. P. 2009. ENHANCED GLUCOSE SYNTHESIS IN THREE-DIMENSIONAL HEPATOCYTE COLLAGEN MATRIX. TOXICOL IN VITRO, 23, 744-7.
- WENG, L.-H., KO, J.-Y., WANG, C.-J., SUN, Y.-C. & WANG, F.-S. 2012. DKK-1 PROMOTES ANGIOGENIC RESPONSES AND CARTILAGE MATRIX PROTEINASE SECRETION IN SYNOVIAL FIBROBLASTS FROM OSTEOARTHRITIC JOINTS. ARTHRITIS & RHEUMATISM, 64, 3267-3277.
- WENG, L.-H., WANG, C.-J., KO, J.-Y., SUN, Y.-C. & WANG, F.-S. 2010. CONTROL OF DKK-1 AMELIORATES CHONDROCYTE APOPTOSIS, CARTILAGE DESTRUCTION, AND SUBCHONDRAL BONE DETERIORATION IN OSTEOARTHRITIC KNEES. ARTHRITIS & RHEUMATISM, 62, 1393-1402.
- WIELAND, H. A., MICHAELIS, M., KIRSCHBAUM, B. J. & RUDOLPHI, K. A. 2005. OSTEOARTHRITIS - AN UNTREATABLE DISEASE. NAT REV DRUG DISCOV, 4, 331-44.
- WILLIAMS, R., KHAN, I. M., RICHARDSON, K., NELSON, L., MCCARTHY, H. E., ANALBELSI, T., SINGHRAO, S. K. ET AL. (2010). IDENTIFICATION AND CLONAL CHARACTERISATION OF A PROGENITOR CELL SUB-POPULATION IN NORMAL HUMAN ARTICULAR CARTILAGE. PLOS ONE 5:E13246.

- XU, Y. K. & NUSSE, R. 1998. THE FRIZZLED CRD DOMAIN IS CONSERVED IN DIVERSE PROTEINS INCLUDING SEVERAL RECEPTOR TYROSINE KINASES. *CURR BIOL*, 8, R405-6.
- YAMAMOTO, H., SAKANE, H., YAMAMOTO, H., MICHIEUE, T. & KIKUCHI, A. 2008. WNT3A AND DKK-1 REGULATE DISTINCT INTERNALIZATION PATHWAYS OF LRP6 TO TUNE THE ACTIVATION OF BETA-CATENIN SIGNALING. *DEV CELL*, 15, 37-48.
- YAMASHITA, A., NISHIKAWA, S. & RANCOURT, D. E. 2010. IDENTIFICATION OF FIVE DEVELOPMENTAL PROCESSES DURING CHONDROGENIC DIFFERENTIATION OF EMBRYONIC STEM CELLS. *PLOS ONE*, 5, E10998.
- YAN, H. & YU, C. 2007. REPAIR OF FULL-THICKNESS CARTILAGE DEFECTS WITH CELLS OF DIFFERENT ORIGIN IN A RABBIT MODEL. *ARTHROSCOPY*, 23, 178-87.
- YAN, K. S., CHIA, L. A., LI, X., OOTANI, A., SU, J., LEE, J. Y., SU, N. ET AL. (2012). THE INTESTINAL STEM CELL MARKERS BMI1 AND LGR5 IDENTIFY TWO FUNCTIONALLY DISTINCT POPULATIONS. *PROC NATL ACAD SCI U S A*. 109, 466-471.
- YANG, H. S., LA, W. G., BHANG, S. H., KIM, H. J., IM, G. I., LEE, H., PARK, J. H. & KIM, B. S. 2011. HYALINE CARTILAGE REGENERATION BY COMBINED THERAPY OF MICROFRACTURE AND LONG-TERM BONE MORPHOGENETIC PROTEIN-2 DELIVERY. *TISSUE ENG PART A*, 17, 1809-18.
- YANG, S., KIM, J., RYU, J. H., OH, H., CHUN, C. H., KIM, B. J., MIN, B. H. & CHUN, J. S. 2010. HYPOXIA-INDUCIBLE FACTOR-2ALPHA IS A CATABOLIC REGULATOR OF OSTEOARTHRITIC CARTILAGE DESTRUCTION. *NAT MED*, 16, 687-93.
- YOUNG, R. D., LAWRENCE, P. A., DUANCE, V. C., AIGNER, T. & MONAGHAN, P. 2000. IMMUNOLocalIZATION OF COLLAGEN TYPES II AND III IN SINGLE FIBRILS OF HUMAN ARTICULAR CARTILAGE. *J HISTOCHEM CYTOCHEM*, 48, 423-32.
- YUAN, X. L., MENG, H. Y., WANG, Y. C., PENG, J., GUO, Q. Y., WANG, A. Y. & LU, S. B. 2014. BONE-CARTILAGE INTERFACE CROSSTALK IN OSTEOARTHRITIS:

POTENTIAL PATHWAYS AND FUTURE THERAPEUTIC STRATEGIES. OSTEOARTHRITIS AND CARTILAGE. 8, 1077–1089.

ZAMLI, Z., ROBSON BROWN, K., TARLTON, J. F., ADAMS, M. A., TORLOT, G. E., CARTWRIGHT, C., COOK, W. A. ET AL. (2014). SUBCHONDRAL BONE PLATE THICKENING PRECEDES CHONDROCYTE APOPTOSIS AND CARTILAGE DEGRADATION IN SPONTANEOUS ANIMAL MODELS OF OSTEOARTHRITIS. BIOMED RES INT 2014:606870.

ZHEN, G., WEN, C., JIA, X., LI, Y., CRANE, J. L., MEARS, S. C., ASKIN, F. B., FRASSICA, F. J., CHANG, W., YAO, J., CARRINO, J. A., COSGAREA, A., ARTEMOV, D., CHEN, Q., ZHAO, Z., ZHOU, X., RILEY, L., SPONSELLER, P., WAN, M., LU, W. W. & CAO, X. 2013. INHIBITION OF TGF-[BETA] SIGNALING IN MESENCHYMAL STEM CELLS OF SUBCHONDRAL BONE ATTENUATES OSTEOARTHRITIS. NAT MED, 19, 704-712.

ZHU, M., TANG, D., WU, Q., HAO, S., CHEN, M., XIE, C., ROSIER, R. N., O'KEEFE, R. J., ZUSCIK, M. & CHEN, D. 2009A. ACTIVATION OF BETA-CATENIN SIGNALING IN ARTICULAR CHONDROCYTES LEADS TO OSTEOARTHRITIS-LIKE PHENOTYPE IN ADULT BETA-CATENIN CONDITIONAL ACTIVATION MICE. J BONE MINER RES, 24, 12-21.

ZHU, Y., SUN, Z., HAN, Q., LIAO, L., WANG, J., BIAN, C., LI, J., YAN, X., LIU, Y., SHAO, C. & ZHAO, R. C. 2009B. HUMAN MESENCHYMAL STEM CELLS INHIBIT CANCER CELL PROLIFERATION BY SECRETING DKK-1. LEUKEMIA, 23, 925-33.